# Electronic structure and thermochemistry of $Si_n$ clusters(n=2-11)

Gabriel Freire Sanzovo Fernandes[1*], Luiz Fernando de Araujo Ferrão[1], Francisco Bolivar Correto Machado[1].

[1]*Instituto Tecnológico de Aeronáutica, São José dos Campos, SP 12228-900, Brazil.*

**Abstract:** *Agglomerates and nanostructured materials containing a few atoms (in the order of magnitude of $10^0$-$10^2$ units) present potential in the development of new materials in several technological areas crucial for human society in the 21st century, such as electronics*[1□3]*, catalysis, chemical resistors and X-rays. Due to their low dimensionality, these clusters make it possible to create new routes for some processes and increase the efficiency of devices*[1,2]*. Also, the miniaturization of electronic components in processors crossed the line between the microscopic systems governed by classical mechanics and sub-microscopic systems governed by quantum mechanics. In 2016, commercial transistor processing technology is 14 nm*[4]*, that is, on the order of 100 atoms in length, with 10 nm transistors expected to be produced on an industrial scale by 2018. On a laboratory scale, transistors with technology of 7 nm are under development.*

*In this work, we focused in characterize the "magic numbers" of $Si_n$ (n=2-11) series through DFT method within M06 approximation combined with 6-311++G(3df,3pd) atomic basis set. The stability analysis was carried out with the Hartree-Fock orbitals energy diagram and on the atomization Free Gibbs Energy and atomization Enthalpy evaluation. The results obtained in the present work, shows $Si_6$ and $Si_{10}$ as "magic numbers" in agreement with previously theoretical and experimental works.*

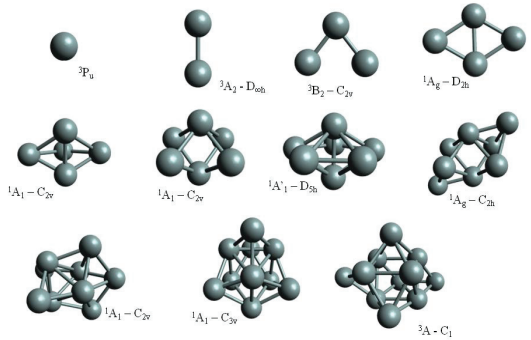


**Figure 1.** Growth pattern of the $Si_n$ clusters, n=1-11, through the M06/6-311++G(3df,3pd) methodology.

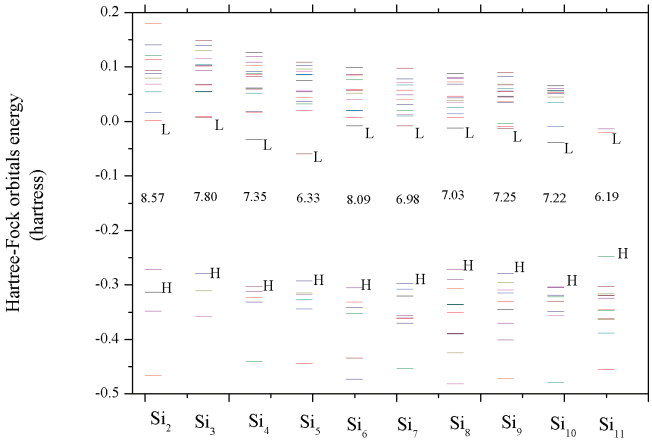


**Figure 2.** Hartree-Fock orbitals energy diagram of the $Si_n$ clusters, n=2 - 11, through the HF/6-311++G(3df,3pd) methodology.

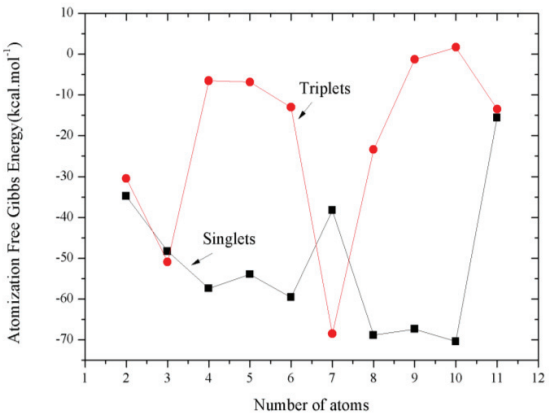


**ɡure 3.** Atomization Free Gibbs Energy of the $Si_n$ clusters at singlet and triplet spin multiplicity, n=2 - 11, through the M06/6-311++G(3df,3pd) methodology.

**y-words**: *nanomaterials, electronic structure, thermochemistry, silicon clusters.*
**ɒpport:** *ITA*

**ferences:**

G. Schön, U. Simon, A fascinating new field in colloid science: small ligand-stabilized metal clusters and their possible application in microelectronics - Part II: Future directions, Colloid Polym. Sci. 273 (1995) 202□218. doi:10.1007/BF00657826.

L. Brus, Electronic wave functions in semiconductor clusters: experiment and theory, J. Phys. Chem. 90 (1986) 2555□2560. doi:10.1021/j100403a003.

G.S. Anagnostatos, Magic numbers in semiconductor microclusters, Phys. Lett. A. 143 (1990) 332□336. doi:10.1016/0375-9601(90)90349-S.

Intel, 14 nm Transistor Explained□ Following the Path of Moore□s Law, (2016).

# High Performance Collision Cross Section Calculation - HPCCS

Gabriel Heerdt[a], Leandro N. Zanotto[a,b], Paulo C. T. Souza[a,c], Guido C. S. Araujo[b], Munir S. Skaf[a]

[a]*Institute of Chemistry, University of Campinas, Barão Geraldo, 13083-852, Campinas - São Paulo, Brazil.*

[b]*Institute of Computing, University of Campinas, Barão Geraldo, 13083-970, Campinas - São Paulo, Brazil.*

[c]*Faculty of Mathematics and Natural Sciences, University of Groningen, Groningen 9747, AG, The Netherlands.*

Ion Mobility Spectrometry (IMS) is a widely used and 'well-known' technique of ion separation in the gaseous phase, based on the differences in ion shape and charge. Despite IMS is a fairly rapid experiment, the data interpretation is still a challenge and depends on accurate theoretical estimates of the molecule Collision Cross Section (CCS).

The *Mobcal* software [1-3], developed in 1996 by Jarrold et al., is the most widely used program for theoretical CCS calculations. *Mobcal* uses three different algorithms to calculate CCS: Projection Approximation (PA), Exact Hard Sphere Scattering (EHSS) and Trajectory Method (TM). TM is the most accurate one, being the best choice for CCS estimates, especially for highly-charged macromolecules as proteins.[4] As demonstrated in Fig. 1 (B), the orientationally averaged collision integral ($\Omega_{avg}^{(1,1)}$) can be calculated by integrating over all scattering angles ($\chi$). However, such estimates involve performing thousands molecular dynamics simulations per analyzed molecule (Fig. 1 (A)), with a very high computational cost.

Since the original Mobcal were written for serial execution with Fortran language, it is not prepared for the technology we have today. Herein, we present a new software to High Performance Collision Cross Section Calculation (HPCCS). Our software, focused only in Trajectory Method, was totally rewritten in C++ language, improved with new features and increased the performance using High Performance Computing (HPC) techniques.

On the first release, the code rewrite and CPU parallelization and vectorization [5] were completed. Large biomolecules can be simulated in a short time, within high accuracy, which helps the interpretation of experimental IM-MS data. As can be seen in Fig. 1 (C), the theoretical CCS results, performed with the TM by our program, are in good agreement with experimental data.

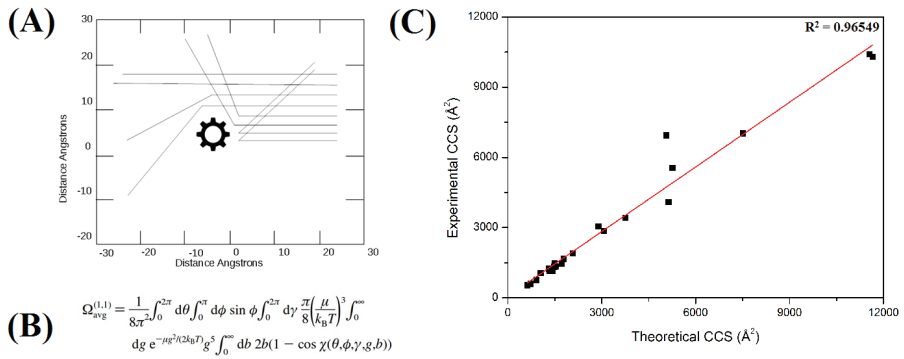


**Figure 1**: Actually, the accurate estimation of CCS (Ω in the formula**)** requires the calculation of the all possible collision angles (χ, indicated at (B)) between a buffer gas and a target molecule, as shown in (A). Such angles can be generated by individual MD simulations, they depend on the relative orientation of the molecule, size, shape and interaction with the gas. (C) Experimental versus Theoretical Collision Cross Section, $Å^2$.

As for the computational time, for the largest simulated protein complex, which contains approximately 32,000 atoms, the total time considering 32 threads was about 4 hours. This means that for a common user it is perfectly possible to simulate on your desktop, usually with 2 - 4 threads, CCSs for proteins and their complexes in a viable time. The IM-MS experiments combined with appropriate simulations are an excellent tool to obtain biomolecule structure information.

**Key-words**: Ion Mobility, Mass Spectrometry, Collision Cross Section, Trajectory Method, High Performance Computing
**Support:** This work has been supported by FAPESP: 2016/04963-6, 2013/08293-7.
**References:**
[1] A. A. Shvartsburg, M. F. Jarrold, *Chem. Phys. Lett.*, 261, 86 (1996).
[2] M. F. Mesleh, J. M. Hunter, A. A. Shvartsburg, G. C. Schatz, M. F. Jarrold, *J. Phys. Chem.,* 100, 16082 (1996).
[3] A. A. Shvartsburg, G. C. Schatz, M. F. Jarrold, *J. Chem. Phys.*, 108, 2416 (1998).
[4] F. Lanucara, S. W. Holman, C. J. Gray, C. E. Eyers, *Nat. Chem.,* 6, 281 (2014).
[5] J. Jeffers, J. Reinders, "Intel Xeon Phi coprocessor high performance programming" (2013), Elsevier, Newnes.

# Estudo das Propriedades Físico-Químicas do Líquido Iônico 1-Butil-3-Metil-Imidazólio Bis(Trifluormetanosulfonil)Imida ([BMIm][$Tf_2N$]) Puro e em Solução Aquosa

Gabriel J. C. Araujo (PG), Tuanan da Costa Lourenço (PG), Luciano T. Costa (PQ)

*Instituto de Química, Universidade Federal Fluminense. R. São João Batista, 2-188 - Centro, Niterói - RJ*

**Abstract:** Líquidos Iônicos (LIs) são uma classe de materiais compostos por cátion e ânion que em sua maioria possuem ponto de fusão inferior a 100°C. Devido a possibilidade de apresentar propriedades físico-químicas diferenciadas (criadas a partir de simples modificações em sua estrutura química) como, baixa pressão de vapor, baixa flamabilidade, grande solubilidade de compostos orgânicos e inorgânicas, estabilidade térmica e química, seu espectro de aplicação torna-se amplo, desde aplicações biológicas [1] a materiais para captura e separação de gases [2]. Para se obter uma melhor performance destas aplicações é necessário o entendimento das interações entre os solventes envolvidos no processo. Sabe-se que a água é um solvente amplamente utilizado industrialmente e, portanto, é altamente relevante entender como se dá a interação entre os líquidos e os efeitos destas interações sobre suas propriedades físico-químicas. Devido à facilidade de se correlacionar efeitos estruturais e propriedades termodinâmicas, a dinâmica molecular (DM) tem sido amplamente utilizada para este tipo de estudo. Porém, para que os resultados obtidos da simulação computacional sejam consistentes com as propriedades medidas experimentalmente, é fundamental o desenvolvimento de um campo de força que reproduza de maneira correta as interações entre as espécies químicas do sistema. No caso de LIs o procedimento é um pouco mais complexo que para compostos moleculares, já que além das interações eletrostáticas a dispersão de carga confere propriedades como baixa pressão de vapor, boa condutividade iônica, entre outras [3]. Dois efeitos devem ser levados em conta: a polarização e a transferência de carga entre os íons. Isso ocorre devido ao grande número e diferentes tipos de interações entre cátion e ânion, reduzindo as cargas efetivas dos íons para menores do que um inteiro em fase condensada [4]. Nos últimos anos modelos de campo de força polarizáveis e não-polarizáveis têm sido desenvolvidos com o intuito de reproduzir esses efeitos [5]. Os campos não-polarizáveis possuem como vantagem um menor custo computacional, possibilitando estudar sistemas maiores e mais complexos. Por outro lado, à medida que o LI interage com outro solvente, os íons são dissociados e é razoável considerar suas cargas como

inteiras, segundo Köddermann *et al.* [6]. No presente trabalho, estudos por simulação de dinâmica molecular (DM) das propriedades físico-químicas, estruturais e dinâmicas do Líquido Iônico [BMIm][$Tf_2N$] puro e em sistemas aquosos com diferentes frações de água (5%, 10%, 20%, 50%, 90% e 95%) têm sido realizados. Densidade, coeficientes de difusividade, função de distribuição radial (RDF) e tensão superficial são os parâmetros calculados de modo a avaliar os efeitos produzidos pela mistura de água e LI. Para isso, foram utilizados dois campos de força [6,7] de forma comparativa para assim propormos uma re-parametrização. Um deles, campo de força não-polarizável desenvolvido por Zhong *et. al.*, no qual as cargas totais dos íons foram escaladas por um fator de 0,8 de modo a reproduzir a transferência de carga entre íons e as propriedades termodinâmicas do LI puro [BMIm][$Tf_2N$] em fase condensada. No outro campo de força, desenvolvido por Köddermann *et. al*., para LIs do tipo [$C_n$MIm][$Tf_2N$], as cargas foram mantidas inteiras e os parâmetros intermoleculares (interações de Lennard-Jones) ajustados de maneira empírica a fim de se reproduzir dados experimentais, como densidade e coeficientes de difusão, obtidos por espectroscopia de NMR. O campo de força usado para simular a molécula de água foi o do tipo TIP4P [8]. Os resultados obtidos têm sido comparados com os valores experimentais disponíveis na literatura [9,10] de modo a se avaliar tanto a reprodutibilidade dos dados resultantes de cada campo de força no sistema de LI puro e em mistura aquosa, como também esclarecer os fenômenos provenientes da interação da água com o LI a nível molecular.

**Key-words**: Líquido Iônico, Água, Dinâmica Molecular, Campo de Força
**Support:** Os autores gostariam de agradecer ao suporte financeiro dado pela CAPES, CNPQ e FAPERJ e ao PPGQ-UFF.

**References:**

[1] T. L. Greaves, C. J. Drummond, Chem. Rev., 108, 206−237, (2008).
[2] E. D. Bates, R. D. Mayton, I. Ntai, J. H. Davis Jr., J. Am. Chem. Soc., 124 (6), 926–927, (2002).
[3] Y. Zhang, E. J. Maginn, J. Phys. Chem. B, 116, 10036-10048, (2012).
[4] C. Schröder, Phys. Chem. Chem. Phys., 14, 3089, (2012).
[5] F. Dommert, L. Delle Site, C. Holm et al., ChemPhysChem, 13, 1625 – 1637, (2012).
[6] T. Köddermann, D. Paschek, R. Ludwig, ChemPhysChem, 14, 3368 – 3374, (2013).
[7] X. Zhong, Z. Liu, D. Cao, J. Phys. Chem. B, 115, 10027–10040, (2011).
[8] W. Jorgensen, J. Chandrasekhar, J. Madura, R. Impey, M. Klein, J. Chem. Phys., 79, 926, (1983).
[9] H. Tokuda, K. Hayamizu, K. Ishii, M. A. B. H. Susan, M. Watanabe, J. Phys. Chem. B, 109, 6103, (2005).
[10] A-LP. Rollet, M. Porion, M. Vaultier, et al., J. Phys. Chem. B, 111, 11888–11891 (2007).

# Theoretically understanding the exchange of NO and the nature of the Ru-NO bond in ruthenium-nitrosyl metallic complexes.

Gabriel L. S. Rodrigues, Willian R. Rocha

*LQC-MM (Laboratório de Química Computacional e Modelagem Molecular) Departamento de Química, ICEx, Universidade Federal de Minas Gerais, Belo Horizonte 31270-901, MG, Brazil*

**Abstract:** Specially after its discovery as a signaling molecule in the cardiovascular system[1], which led to the 1998 Nobel Prize in Physiology, nitric oxide (NO) has been shown to be involved in numerous other physiological functions such as modulation of the immune and endocrine response, cardiovascular control, neurotransmission, induction of apoptosis, among others[2-4]. Therefore, NO has been the focus of various studies in the past decades, many of them aiming at developing compounds capable of controlling NO's concentration in the body. As example, ruthenium-NO complexes have shown promising results for this purpose and thus, they are subject of great study in the literature [5-7]. However, despite the progress in synthesis, characterization and biological studies, there are much to be understood about the release of NO by metallic complexes, such as the reaction mechanism, the oxidation forms of the released NO and how it stays in the body after dissociation. Regarding these objectives, in this work density functional theory was used to investigate the electronic structure, reduction potentials and nitric oxide ligand exchange reactions in a series of ruthenium-nitrosyl model complexes of form $[Ru^{II/III}(X)(L)(NO)]$(X = salen or $NH_3$; L = Cl-, $NH_3$, pyridine, $P(OEt)_3$, OH, $H_2O$). For instance, Natural Bond Orbital and Charge Decomposition Analysis studies revealed the key influence of the axial ligand in the electronic population of nitrosyl and $NO^+/NO^0$ character, as well as in the strength and electronic donation/backdonation of the Ru-NO interaction. As an example, strong π receptors in the axial position, trans to the NO, tend to weaken the Ru-NO backdonation and thus, weakening the Ru-NO bond. General aspects from the aqueous solvation of the complexes were also investigated through Monte Carlo statistical mechanical simulations. They showed that the complexes may be involved in strong hydrogen bonds with water, in particular the amino-complexes, which can form H-bonds with average energies up to -22.4 ± 0.4 kcal $mol^{-1}$. Calculations also show that while $Ru^{II}$ complexes have only one thermically accessible spin state, $Ru^{III}$ complexes may have excited spin states lying very close to the ground state (less than 30 kcal $mol^{-1}$) depending on the ligands coordinated to the metallic center, suggesting that the mechanism of NO ligand exchange, which is a spin-forbidden reaction, may vary across the different complexes. To investigate these observations, we constructed Potential Energy Surfaces (PES) for reactions of exchanging NO. The PESs showed the presence of one or multiples Minimum Energy Crossing Points (MECP) between the singlet and

triplet species of the $Ru^{III}$-NO complexes. For instance, the NO release for the $[Ru(NH_3)_5NO]^{3+}$ is more favorable in the triplet state, with activation barriers seven times smaller (~6 kcal $mol^{-1}$) than in the singlet state[8]. High level Complete Active Space Self Consistent Field (CASSCF) calculations were also done in located MECPs geometries, revealing in some complexes the presence of strong spin-orbit coupling, with coupling constants larger than 500 $cm^{-1}$.

**Key-words**: nitric oxide, ruthenium, coordination complexes, dft, spin-forbidden reactions, cda, nbo.
**Support:** This work has been supported by CAPES, FAPEMIG, CNPq, INCT-Catálise
**References:**
[1] L. J. Ignarro, in Journal of Physiology and Pharmacology; **2002**,DOI: 10.1111/j.1742-6723.2010.01285.x
[2] Z. J. Tonzetich, L. E. McQuade, S. J. Lippard, *Inorg. Chem.*, **2010**, DOI:10.1021/ic9022757.
[3] C. Bogdan, *Nat. Immunol.*, **2001**, DOI:10.1038/ni1001-907.
[4] F. Ignarro, L. J.; Murad, in Nitric Oxide: Biochemistry, Molecular Biology and Therapeutic Implications; A. Press, Ed.; California, **1995**.
[5] J. C. Toledo, H. A. S. Silva, M. Scarpellini, V. Mori, A. J. Camargo, M. Bertotti, D. W. Franco, *Eur. J. Inorg. Chem.*, **2004**, DOI:10.1002/ejic.200300683.
[6] G. F. Caramori, A. O. Ortolan, R. L. T. Parreira, E. H. da Silva, *J. Organomet. Chem.*, **2015**, DOI:10.1016/j.jorganchem.2015.08.018.
[7] L. Freitag, S. Knecht, S. F. Keller, M. G. Delcey, F. Aquilante, C. Thomas Bondo Pedersen, R. Lindh, M. Reiher, L. Gonzá lez, *Phys. Chem. Chem. Phys. Phys. Chem. Chem. Phys*, **2015**, DOI:10.1039/c4cp05278a.
[8] G. L. S. Rodrigues, W. R. Rocha, J. Phys. Chem. B, **2016**, DOI:10.1021/acs.jpcb.6b08813

# Charge Transfer descriptors application: TD-DFT protocol for analysis on DMABN transitions and push-pull effect on D-π-A dyes.

Gabriel M. Zanotto(PG), Josene M. Toldo(PG), Paulo F. B. Gonçalves(PQ)

gabriel.zanotto@ufrgs.br

*Universidade Federal do Rio Grande do Sul, Instituto de Química, Grupo de Química Teórica. Av. Bento Gonçalves, 9500, Porto Alegre-RS*

## INTRODUCTION

Charge transfer (CT) involving excited state is a phenomenon that arouses the interest of different research groups, not only because it is useful for the development of electronic devices and solar cells, but also because quantifying the magnitude of this effect is still a challenge. The great interest in this phenomenon moves the scientific community towards the development of ways to identify the different types of electronic transitions and, in particular, quantify transitions with charge transfer character.

In this sense, this work aimed the comparison of three descriptive tools, Δr, $D_{CT}$ and Φs, based on TD-DFT calculations, to study the character of electronic transitions. To evaluate the performance of these charge-transfer descriptors, we adopted two aspects: sensitivity against geometries changes and solvent effect, and donor/acceptor group strength in D-π-A (Donor-π bridge-Acceptor) molecules. For the first study, we used the molecule 4-(dimethyl amino) benzonitrile (DMABN) (Figure 1-a), as a model, since it is a well-known example of a molecule that presents state inversion with dimethylamine rotation, and electronic excitations of determined character. For the second study, we applied in a series of push-pull molecules, some recently synthetized, characterized by our group (Figure 1-b) and a third part, similar to those proposed as a new structure, in order to check if the descriptors can describe properly the character of the main electronic transitions, according to the increase in the push-pull effect.

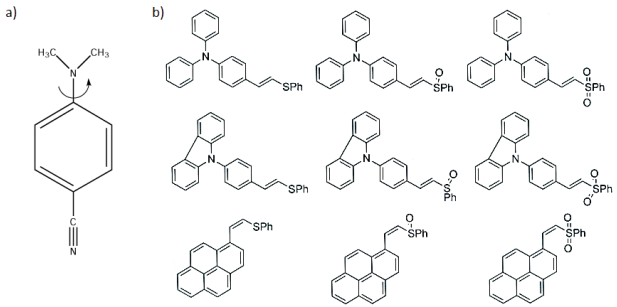


*Figure 1: a)DMABN structure b)D-π-A dyes structures*

## METHODOLOGY

Time-Dependent Density Functional Theory (TD-DFT) calculations were carried out at CAM-B3LYP/cc-pVDZ level for geometry optimization and CAM-B3LYP/jun-cc-pVTZ level for the transition analysis in gas phase and acetonitrile (using Polarizable Continuum Model). Descriptors analyses were carried out with proper software: MULTIWFN for $\Delta r$ and $D_{CT}$, and NancyEx for $\Phi s$.

## RESULTS AND DISCUSSION

The analysis with D-π-A dyes aimed at the validation in the influence of the donor/acceptor group for the constitution of the push-pull effect strength. Variations of the donor group (from pyrene to triphenylamine and later to carbazole) and of the acceptor group (from sulfide to sulfoxide and later to sulfones), showed great increase in the charge transfer character, which have been described in a satisfactorily way with all descriptors.

The analysis with DMABN molecule aimed at the evaluation of the descriptors, against changes of conformation and addition of solvent. The overall performance for the conformation changes were satisfactorily, however, regarding the addition of the solvent effect (acetonitrile), $\Phi_S$ descriptor presented difficulties to describe the $S_1/S_2$ inversion, a characteristic well known of DMABN, most likely because of the theoretical approach used.

As an overall analysis, $D_{CT}$ index present in its analysis a goroup of auxiliary quantitative indexes that can be of great help when considering charge-transfer related properties. In particular, $q_{CT}$, which is an indication of the amount of charge that has been transferred should be considered as the great differential of this index.

## CONCLUSIONS

The objective has been fully accomplished by $D_{CT}$ and $\Delta r$ descriptors. Both have presented results consistent with the proposed changes. $\Phi_S$ showed difficulties in describing the solvent effect, which is crucial for understanding DMABN states behavior and important for material applications. It has been shown that charge transfer description tools can be an efficient way in determining the character of electronic transitions. As a strong charge-transfer character is of extreme importance for technological applications, the use of descriptor tools along with calculations, for research groups aiming the development of efficient D-π-A dye-based materials, should be encouraged.

**Keywords**: **TD-DFT, DSSC, DMABN, charge-transfer**

**Support:** This work has been supported by CAPES and CNPQ.

# Conformational Analysis of Alanine, its Radical Cation and Anion.

Gabriel S. S. Brites, Diego Nascimento de Jesus, Neubi F. Xavier Junior, Glauco F. Bauerfeldt

*Departamento de Química, Instituto de Ciências Exatas, Universidade Federal Rural do Rio de Janeiro, Rodovia Br km 7, Seropédica, RJ, Brasil*

More than 70 amino acids have been identified in meteorites collected in Earth coming from interstellar medium (ISM) and alanine [$CH_3CH(NH_2)CO_2H$] is one of the most abundant among them [1]. In the ISM, amino acids are found in solid phase, covered by icy mantle and the presence of water molecules seems to be essential for their survival [2]. However, due to some high energy phenomena of the hostile ISM, amino acids may undergo to gas phase, not only in their neutral form but also as radical cations and anions. These desorbed (transient) specie may produce characteristic fragments, which are commonly detected in the ISM [2]. This work aims to the conformational analysis of alanine, in its neutral, cationic and anionic forms ($CH_3CH(NH_2)CO_2H$, $[CH_3CH(NH_2)CO_2H]^{+}$ and $[CH_3CH(NH_2)CO_2H]^{-}$) described as an isolated system, and also in its neutral and zwitterionic ($[CH_3CH(^{+}NH_3)CO_2^{-}]$) forms, in aqueous solution. The collection of the geometries corresponding to the possible stationary points will be useful for simulating the high energy phenomena in space and evaluating the possible decomposition and formation paths of alanine in the ISM and in its way to Earth. The conformational analysis is extended to its radical cation and anionic forms. Theoretical calculation have been performed at the B3LYP/6-311++G(2d,2p) level for optimizations and additional single-point calculations have been performed at the CCSD(T)/6-311++G(2d,2p) level in order to achieve more accurate electronic energies. Results suggest the location of 12 conformers for alanine as R stereoisomers, and, consequently, 12 S stereoisomers, in neutral form, in gas phase. Here, the conformers have been denominated following their dihedrals angles. The dihedral angles of the lowest energy conformers (031) are D(HOCO)=-178.4º, D(OCCN)=-13.9º and D(CCNH)=-94.4º. These conformers can be seen in Figure 1. The population of the most stable conformer have been calculated as 58.6%, at 300K, while the second (112) and third (011) have been predicted as 16.5% and 10.5% respectively. Other conformers account for approximately 15%. CPCM calculations, simulating the icy mantle in which amino acids are frequently found in ISM, have been performed using the Pauling atomic radii for building up the molecular cavity and explicitly including the solute cavitation energy and solute-solvent dispersion and repulsion interaction energies in the total energies. Eleven conformers (in S stereochemistry) have been located and characterized as local and global minima. Among those geometries, the 112 has been observed as the most stable in aqueous solution, showing a population of 96%. In aqueous phase,

however, the zwitterionic form is predominant and the predicted tautomerization Gibbs free energy (112 → ZW) is -5.00 kcal $mol^{-1}$.

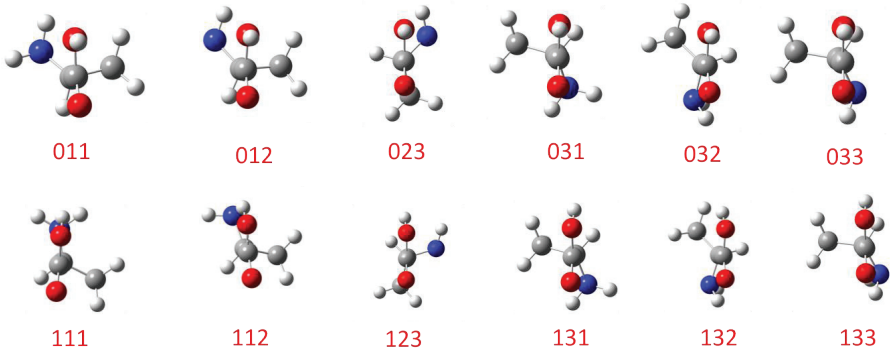


**Figure 1.** Conformational spectrum of neutral alanine in gas phase, calculated in B3LYP/6-311++G(2d,2p) level of theory.

A conformational spectrum for cation radical form reveals 6 conformers. The lowest energy geometry shows dihedral angles of D(HOCO)=-1.5º; D(OCCN)=35.5º and D(CCNH)=-69.2º and account for a population of 73.2% at 300K, while the second lowest energy conformer accounts for 26.2% (population of the other conformers is less than 1%, at 300K). Adiabatic ionization energy (including the vibrational zero-point .energy corrections) is predicted as 8.74 eV, in agreement with experimental data, 8.88 eV [3]. The possibility of electron capture due to the ISM phenomena is not rare, and encouraged the search for possible geometries for the corresponding anions. Five conformers for $[CH_3CH(NH_2)CO_2H]^-$ have been characterized. The characterization of geometries in different forms, in gas and aqueous phase, for alanine, indicates that the lowest energy conformer represents a first contribution for this amino acid behavior in interstellar medium.

**Key-words**: alanine, B3LYP, interstellar, astrochemistry, amino acid
**Support:** This work has been supported by CAPES
**References:**
[1] C. Engel & S. Macko, Nature, **389**, 265–268 (1997)
[2] A. Pernet, J. Pilmé, F. Pauzat *et al*, Astronomy & Astrophysics, 552, A100 (2013)
[3] NIST Chemistry Webbook (http://webbook.nist.gov/chemistry)

# Molecular Modelling of Polyol Electro-Oxidation Reaction on Pt Surfaces

Authors: Gabriela Volpini Soffiati[1], Pablo Sebastián Fernandez[1], Miguel Angel San Miguel Barrera[1], Edison Zacarias da Silva[2]

*Address:* [1]*Institute of Chemistry, University of Campinas, Campinas, SP, Brazil*
[2] *'Gleb Wataghin' Institute of Physics, University of Campinas, Campinas, SP, Brazil*

**Abstract:** The Biomass is the most abundant renewable resource and an alternative to reduce the world dependence of Diesel Oil.[1,2] Brazil has 18% energy supply originated by sugar cane and it is one of the largest producers and consumers of Biodiesel in the world[3]; for these reasons, the efficient use of polyol, derivative from Biomass, like Glycerol, Erythritol, Xylitol, Arabitol, Sorbitol, and others, is essential.

The Polyol Electrooxidation Reaction (REOP) is an alternative because, through electrochemical techniques, products with higher value can be obtained from these Biomass derivatives. Prof. Pablo Fernández, with his electrocatalysis group, from Unicamp's Institute of Chemistry, has explored this reaction using a four carbons polyol, Erythritol, a common compound used as sweetener by the Food Industry.

There is a great lack of knowledge regarding the intermediates from REOP and studies aimed to understand the reaction mechanisms are necessary. The present work applies computational simulations based on Density Functional Theory (DFT), using the software VASP, to explore the interaction of multiple Erytritol intermediates with different platinum surfaces. The modeling helps to elucidate the details from the mechanisms and contributes to the understanding of the electrochemical results obtained.

First principles calculations based on periodic DFT have been performed to gain insight into the structural, energetic and electronic structure of five intermediates with two dehydrogenations, on three different platinum surfaces. Based on adsorption energy calculations, the intermediates were compared and the understanding of the abundance of intermediates and products on REOP was possible.

Intermediates with surface bonds through adjacent carbons were more unstable and disadvantaged; the fact was justified by the great tension created in the bonds and the lesser degree of freedom. The most favorable adsorption energies were found to those intermediates having bonds with two non-adjacent carbons; the possibility of a stronger interaction between the molecular chain and the surfaces was a favorable point for the systems stabilities.

The analysis of Electron Charge Differences showed a charge rearrangement between the dehydrogenated carbons and the Pt atoms, indicating bond between these atoms; with the PDOS analysis, the electronic nature of the bonds was explored. The

interactions occurred mainly between the Pt ‘d’ states and the C ‘p’ states. Further analyses were performed to understand the interactions between the hydroxyls and the surfaces; the PDOS profile showed stronger interactions between the same energy states as the carbons.

**Key-words**: Polyol Electro-oxidation, DFT, Simulation, Modelling, Adsorption Study.
**Support:** This work has been supported by CNPq – The Brazilian Council for Research and Scientific Development (www.cnpq.br).

**References:**

[1] García-Muelas, R.; López, N.; J. *Phys. Chem. C.*, **2014**, 118, 17531-17537.
[2] Ragauskasm, A. J.; Williams, C. K.; Davison, B. H.; Britovsek, G.; Cairney, J.; Eckert, C. A.; Frederick, W. J.; Hallett, J. P.; Leak, D. J.; Liotta, C. L.; et al. *Science* **2006**, 311, 484-489.
[3] Site da ANP - Agencia Nacional do Petróleo (http://www.anp.gov.br/).
[4] Dzade, N., Roldan, A., Leeuw, N., *Environ. Sci. Technol.*, **2017**, 51, 3461-3470.
[5] Chang, C., Liu, C., Wu, S., Tsai, M., *Phys. Chem. Chem. Phys.*, **2017**, 19, 4989-4996.
[6] Garcia, A. C.; Kolb, M. J.; Nierop y Sanchez C.; Vos, J.; Birdja, Y. Y.; Kwon, Y.; Tremiliosi-Filho, G.; Koper, M. T. M.; ACS Catal., **2016**, 6, 4491-4500
[7] Kwon, Y., de Jong, Ed., van der Waal, J.K., Koper, M.T.M., *ChemEletroChem*, accepted.

# Aplicação do método RM1 em complexos de $Eu^{3+}$, $Gd^{3+}$ e $Tb^{3+}$ contendo ligantes com anéis Porfirina.

Higo Lima Bezerra Cavalcanti[a] (PG), Gerd Bruno Rocha[b] (PQ)

[a]*Instituto Federal de Educação, Ciência e Tecnologia Campus Sousa, Jardim Sorrilândia, Sousa PB*
[b]*Departamento de Química Universidade Federal da Paraíba, Campus I, João Pessoa - PB*

A porfina é um macrociclo constituído de quatro anéis pirrólicos ligados por "pontes" metínicas (ligações –CH– ), figura 1a. Quaisquer substituições nas posições *meso* e/ou β-pirrólicas do anel de porfina (figura 1b), dá origem às chamadas porfirinas (nomeadas aqui simplesmente de P), que ao sofrerem metalação, processo no qual um átomo ou íon metálico coordena-se na posição central do anel porfirínico geram as chamadas metaloporfirinas (MP). A metalação ocorre mediante substituição dos dois átomos de hidrogênio centrais (resultando no íon porfirinato, de carga –2*e*), e tendo os átomos de nitrogênio atuando como doadores de pares eletrônicos.

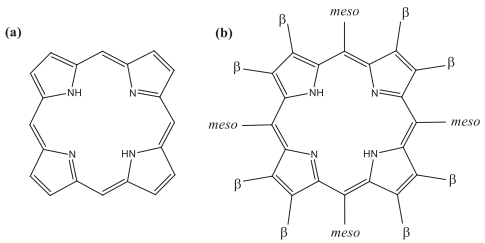


**Figura 1.** (a) Porfina, (b) Posições meso e β-pirrólicas no anel da porfina.

Nesse trabalho nosso objetivo foi a realização de testes de validação para o novo conjunto de parâmetro para $Eu^{3+}$, $Gd^{3+}$ e $Tb^{3+}$ no método RM1[1], direcionado para complexos contendo ligantes derivados do anel porfirina $Ln^{3+}P$, onde $Ln^{3+}$ é um desses cátions. Os complexos avaliados nesses estudo são provenientes do banco de dados CSD versão 5.38[2] através de uma busca combinando-se os termos "*Porphyrin* e "Gd, Eu, Tb". O resultado dessa busca foi 10 moléculas cujos códigos são: ACIXIU, DEGDUQ, EJUTOT, EJUTUZ, GAPRUK, GAWBEL, IHOBEO, OBUJIE, VEDZOU e ZUNJID. Todos os cálculos usaram como critério de convergência do SCF o valor de $1x10^{-8}$ kcal $mol^{-1}$ e para a otimização de geometria um critério na norma do gradiente de 0.25 kcal $mol^{-1}$ $Å^{-1}$. Também foi realizado o cálculo das frequências vibracionais a fim de garantir que as geometrias obtidas correspondiam a geometrias de mínimo de energia. Os cálculos foram realizados em fase gasosa. Toda esta metodologia foi aplicada utilizando uma versão modificada do programa MOPAC2012[3,4]. Para realizar a avaliação do poder preditivo do método RM1 aplicados em complexos do tipo $Ln^{3+}P$, primeiramente realizamos uma superposição das duas estruturas, a de referência (cristalográfica) e a otimizada com o método RM1. Após concluídas todas as

superposições, realizou-se comparações das distâncias dos átomos que compõe o poliedro de coordenação de cada um dos complexos estudados. Para isso usou-se duas métricas, a média dos valores absolutos dos desvios das distâncias entre o íon central e os átomos a ele ligados ($UME_{(Ln-L)}$) e a mesma média agora tomada entre as distâncias atômicas correspondentes entre todos os átomos do poliedro de coordenação ($UME_{poly}$). Os valores para essas métricas de comparação estão na Tabela 1, bem como os valores de RMSD para as superposições.

Tabela 1. Comparações entre as geometrias preditas pelo método RM1 e as correspondentes geometrias cristalográficas. O complexo de código CSD DEGDUQ possui dois poliedros de coordenação, assim, os dados marcados com * são para o poliedro 1 e os com $ são para o poliedro 2.

| Complexo | RMSD (Å) | $UME_{Ln-L}$ (Å) | $UME_{poly}$ (Å) |
|---|---|---|---|
| **ACIXIU** | 1,059 | 0,020 | 0,052 |
| **DEGDUQ*** | 0,828 | 0,061* | 0,083* |
| **DEGDUQ$** | | 0,058$ | 0,082$ |
| **EJUTOT** | 0,331 | 0,182 | 0,230 |
| **EJUTUZ** | 0,404 | 0,149 | 0,158 |
| **GAPRUK** | 0,344 | 0,038 | 0,066 |
| **GAWBEL** | 0,829 | 0,034 | 0,069 |
| **IHOBEO** | 0,455 | 0,013 | 0,053 |
| **OBUJIE** | 0,966 | 0,024 | 0,054 |
| **VEDZOU** | 1,706 | 0,017 | 0,063 |
| **ZUNJID** | 0,591 | 0,037 | 0,081 |

Pelos resultados obtidos observa-se que os valores de RMSD das superposições foram na sua maioria abaixo de 1,000Å, o que é um ótimo resultado. A comparação dos valores de $UME_{poly}$ e $UME_{Ln-L}$ para os complexos estudados nessa seção da tese e os respectivos valores médios obtidos quando foram avaliados com os complexos dos conjuntos de testes durante a parametrização dos cátions $Eu^{3+}$, $Gd^{3+}$ e $Tb^{3+}$ revelou que a maioria dos valores de $UME_{poly}$ e $UME_{Ln-L}$ estão abaixo do correspondente obtido para o conjunto de testes da parametrização. Assim, como conclusão tem-se que a parametrização do RM1 para os cátions Eu(III), Gd(III) e Tb(III)[1] possui um bom poder preditivo em reproduzir a geometria do estado fundamental desses tipos de complexos. Esse comentário é reforçado pelo fato de que alguns desses complexos possuem longos grupos ramificados ou grupos e anéis com rotações livres (ex. ACIXIU, DEGDUQ e VEDZOU), o que dificulta a predição da geometria correta.

**Palavras-chave**: RM1, Métodos semiempíricos, complexos de lantanídeos, porfirina
**Apoio:** Agradecimentos ao CNPq e CAPES pelo apoio financeiro a esse trabalho.

**Referências:**

(1) Filho, M. A. M.; Dutra, J. D. L.; Cavalcanti, H. L. B.; Rocha, G. B.; Simas, A. M.; Freire, R. O., J. Chem. Theory Comput. 2014, 10, 3031–3037.
(2) Groom, C. R.; Bruno, I. J.; Lightfoot, M. P.; Ward, S. C., Acta Crystallogr. Sect. B Struct. Sci. Cryst. Eng. Mater. 2016, 72, 171–179.
(3) Stewart, J. J. P. MOPAC web site openmopac.net.
(4) Maia, J. D. C.; Urquiza Carvalho, G. A.; Mangueira, C. P.; Santana, S. R.; Cabral, L. A. F.; Rocha, G. B., J. Chem. Theory Comput. 2012, 8, 3072–3081.

# Assessing Dunning's basis set along with the G3(MP2)//B3 theory for ionization energies

Gerlane Bezerra da Silva, [a] Régis Casimiro Leal, [a, b]

[a] *Instituto Federal de Educação, Ciência e Tecnologia do Rio Grande do Norte (IFRN), 59215-000, Nova Cruz, Rio Grande do Norte - RN, Brasil*
[b] *Instituto de Química, Universidade Estadual de Campinas (UNICAMP), 13084-970, Campinas, São Paulo - SP, Brasil*

**Abstract:** Combinations of ab initio calculations at distinct levels to produce accurate results are known as composite methods. Its use has been often made to estimate different properties with high accuracy, mainly controlling basis functions and electron correlation effects [1]. Among these methods, Gaussian-n (n = 1, 2, 3, 4) developed by Pople, Curtiss et al [2] stands out in the literature. Different versions of the G3 theory with reduced computational costs have been developed more recently as for example: G3(MP2)//B3 [3] e G3(MP2)//B3-CEP [1]. In all Gaussian-n composite methods the use of Pople basis functions is predominant. In this work, we evaluated the effectiveness of Dunning basis sets, cc-pVnZ and aug-cc-pVnZ with n = 2, 3, 4 and 5, in the reduced order theory G3(MP2)//B3 for ionization energy calculations of atoms from the 1st, 2nd and 3rd period of the periodic table. The original version uses the 6-31G(d) double-zeta basis sets for the optimization of geometry, harmonic frequencies, both at the B3LYP level, and electronic correlation effects at QCSID(T). For the purpose of comparison, the mean absolute error (MAD) and standard deviations (Std.) were used. All calculations were performed with Gaussian software 09W [4].
From the calculation of first ionization energies it was observed a reduction of MAD from 1.6 kcal $mol^{-1}$ to 0.8 kcal $mol^{-1}$ when the cc-pVdZ and cc-pV5Z basis set were used along with G3(MP2)//B3. The results with the largest basis set show that the modified G3(MP2)//B3 achieves lower MAD than the original method (MAD = 1.7 kcal $mol^{-1}$) and the respective version using pseudopotential, G3(MP2)//B3-CEP (MAD = 2.3 kcal $mol^{-1}$). The inclusion of diffuse functions reduces the error from 1.4 kcal $mol^{-1}$ to 1.0 kcal.$mol^{-1}$.
Therefore, the results show that the search for better accuracy in calculations involving ionization energy and the G3(MP2)//B3 composite method is convenient to consider the correlation-consistent basis set instead of the traditional Pople's bases.

**Key-words**: ionization energy, compound methods, Dunning basis set.
**Support:** IFRN by the research grant awarded to G. B. Silva, Edital 04/2017

**References:**

[1] C. M. R. Rocha, D. H. Pereira, N. H. Morgon, R. Custodio. J. Chem. Phys. 139, 184108, (2013).
[2] L. A. Curtiss, P. C. Redfern, K. Raghavachari. WIREs Comput. Mol. Sci. 1, 810, (2011).

[3] A. G. Baboul, L. A. Curtiss, P. C. Redfern, K. Raghavachari. J. Chem. Phys. 110, 7650, (1999).
[4] M. J. Frisch, G. W. Trucks, H. B. Schlegel, G. E. Scuseria, M. A. Robb, J. R. Cheeseman, G. Scalmani, V. Barone, B. Mennucci, G. A. Petersson, H. Nakatsuji, M. Caricato, X. Li, H. P. Hratchian, A. F. Izmaylov, J. Bloino, G. Zheng, J. L. Sonnenberg, M. Hada, M. Ehara, K. Toyota, R. Fukuda, J. Hasegawa, M. Ishida, T. Nakajima, Y. Honda, O. Kitao, H. Nakai, T. Vreven, J. A. Montgomery, Jr., J. E. Peralta, F. Ogliaro, M. Bearpark, J. J. Heyd, E. Brothers, K. N. Kudin, V. N. Staroverov, T. Keith, R. Kobayashi, J. Normand, K. Raghavachari, A. Rendell, J. C. Burant, S. S. Iyengar, J. Tomasi, M. Cossi, N. Rega, J. M. Millam, M. Klene, J. E. Knox, J. B. Cross, V. Bakken, C. Adamo, J. Jaramillo, R. Gomperts, R. E. Stratmann, O. Yazyev, A. J. Austin, R. Cammi, C. Pomelli, J. W. Ochterski, R. L. Martin, K. Morokuma, V. G. Zakrzewski, G. A. Voth, P. Salvador, J. J. Dannenberg, S. Dapprich, A. D. Daniels, O. Farkas, J. B. Foresman, J. V. Ortiz, J. Cioslowski, and D. J. Fox, Gaussian 09, Revision B.01, Gaussian, Inc., Wallingford CT, (2010).

**Calculations of the electronic state TICT of the diphenyl polyenes P,P'- and O,O'-di-substituted using the functional density theory**

**Gisele Franco de Castro (PG), Helene Lopes Lima (IC), Alberto dos Santos Marques**

*Universidade Federal do Amazonas, Laboratório de Tecnologia com Moléculas Bioativas, LTMB, Departamento de Química, Av. General Rodrigo Otavio, 6200, Coroado I, CEP: 69077-000, Manaus, AM.*
*marquesalbertods@gmail.com*
*Keywords: excited electronic state TICT, semiconductors, diphenyl polyenes.*

The polymers of type "pull-push" as diphenyl-polyenes, must present large optical nonlinearity, which can be incremented with increasing the size of the conjugation, (hence the delocalization of electrons), strength of donor groups and electron acceptors and the resultant flatness of the overlap of the orbital $2p_z$. The limiting factors can be affected by at least three points: (i) the types and positions of donor substituents and / or electron acceptors, (ii) the length of polyenic chain. (iii) the photophysical properties and dynamics of excited electronic states. Here were analyzed some diphenyl-disubstituted polyenes, for a series of polymers derived from D - Ph - (CH = CH) n - Ph - A, type P, P 'and O, O'-disubstituted 1,6-diphenyl-1,3,5-hexatrienos, (refered as D, A-DPH), where D and A are free internal rotation group (IRG) ($OCH_3$, CN) and groups with restricted internal rotation (RIR) [- N $(CH_3)_2$ and (-$NO_2$)], where P, P '(para-substituted) and O, O' (ortho-substituted), and (n) and (2, 3, or 4), with purpose of determining the low-lying electronic singlet state, $S_1$, a intramolecular charge-transfer state caracterized as resultant from a twisted molecular conformation (i. e., TICT state), the hyperpolarizability second order and β values and the dipole moment.

AM1 and Hartree-Fock methods were used with basis function 6-31 + G *, for the geometry optimization calculations and second-order hyperpolarizability β values. For the calculation of excitation energies were used the Functional Density Time dependent theory (TD-DFT), using the B3LYP functional and function base 6-31 + G *.

Two series of polymers were formed: series (a) p, p'sibstituintes; (1) [N $(CH_3)_2$], ($NO_2$); (2) ($OCH_3$), ($OCH_3$); (3) [$N(CH_3)_2$], (CN); (4) ($NO_2$), ($NO_2$); (5) (CN), (CN); (6) ($OCH_3$), (CN); (7) [$N(CH_3)_2$], [$N(CH_3)_2$]; (8) (CN), ($NO_2$); (9) [$N(CH_3)_2$], ($OCH_3$) and (10) ($NO_2$), ($OCH_3$); and the series (b), O, O'-substituents (1) [$N(CH_3)_2$], ($NO_2$); (2) ($OCH_3$), ($OCH_3$); (3) [$N(CH_3)_2$], ($OCH_3$); (4) (CN), (CN). Calculations of excitation energies showed that all molecules with twisted conformation has increased dipole moment and the presence of groups (RIR) D and A, both polymers produces the electronic state $S_1$, it is assigned as TICT (n, π *), involving a transition from the n orbital of D to the π * orbital of group A, for example, . the polymer (1), with n = 2,3 and 4, shows a state TICT with the following energies: 2.03 eV; 1.82 eV and 1.54 eV respectively. On the other hand, the polymer (2) where D and A are groups (NIR) with n = 2.3 and 4, does not produces the TICT state. The β values increase in the polymer

n = 2.3 and 4, does not produces the TICT state. The β values increase in the polymer (a) (1) where n = 2,3 and 4, respectively: (55, 48, 38) $48x10^{-30}$ seu, while for the polymer (DPH) without substituents the values are (0.032, 0.006 and 0.104) $x10^{-30}$ esu. The theoretical methods used here are good tools for: (i) the determination of the non-linearity of these optical polymers; (Ii) detection of TICT origin and the most important factors for produção a strong TICT state in each polymer: the substituent (RIR) or (RIL); or molecular geometry, planar or non-planar or both.

The authors would like to thank FAPEAM and CNPq for the support.

References

[1]Lin,C.T., Guan,H.W., Marques,A.D.S., Lee,H.Y., Laser Spectroscopy 1989, IX, 255-257..

[2]Lin,C.T., Guan,H.W, McKoy, R.K.,Splangler, C.W., J. Phys. Chem. 93, 39, 1989.

# Effect of microsolvation in low-energy positron collisions with formaldehyde-water complexes.

Authors: Giseli Maria Moreira, Márcio Henrique Franco Bettega

*Address: Departamento de Física, Universidade Federal do Paraná, Caixa Postal 19044, 81531-990 Curitiba, Paraná, Brazil*

**Abstract:** The microsolvation's effect in formaldehyde water have been studied in scattering of electrons [1]. In this work, we report the integral cross sections for elastic collisions of low energy positrons with the $CH_2O...H_2O$ complex. In the scattering cross sections calculations we employed the Schwinger Multichannel Method (SMC) [2,3] in the static plus polarization (SP) approximation for energies from 0.1 to 10 eV. We also include the contribution of the permanent electric dipole moment of molecule through the *Born closure*. In this work, we considered four different hydrogen-bonded structures for the $CH_2O...H_2O$ complex that were generated by classical Monte Carlo simulation of formaldehyde in water environment at room temperature [4]. We also optimized the geometry of the four formaldehyde complexes, after the optimization we need to consider only one systems since all four complexes have the same optimized geometry. We also showed a comparison of the integral cross section for this optimized structure with the results for the other four structures. The aim of this work is to investigate the influence of microsolvation on the cross section of formaldehyde. The scattering of positrons by formaldehyde in gas phase ($CH_2O$) has been studied before [5] and we compared our results for $CH_2O$ molecule with this previous experimental results in the literature.

**Key-words**: microsolvation, scattering, positrons

**Support:** G. M. M. and M. H. F. B. acknowledges support from CNPq and acknowledge computational support from Professor Carlos M. de Carvalho at Dfis-UFPR.

**References:**

[1] T. C. Freitas, M. A. P. Lima, S. Canuto, and M. H. F. Bettega, *Phys. Rev. A* **80**, 062710 (2009);

[2] K. Tkatsuka and V. McKoy, *Phys. Rev. A* **24**, 2473 (1981); **30**, 1734 (1984);

[3] M. A. P. Lima, L. M. Brescansin, A. J. R. da Silva, C. Winstead, and V. McKoy, *Phys. Rev. A* **41**, 327 (1990);

[4] K. Coutinho and S. Canuto, *J. Chem. Phys.*, **113,** 9132 (2000).

[5] A. Zecca, E. Trainotti, L. Chiari, G. García, F. Blanco, M. H. F. Bettega, M. T. do N. Varella, M. A. P. Lima, and M. J. Brunger , *J. Phys. B: At. Mol. Opt. Phys.* **44** (2011).

# Estudo da reação entre wustita e água durante o processo de loop químico utilizando a teoria do funcional de densidade

Giuliano de Mesquita Cordeiro, Márcio Soares Pereira, Clarissa Oliveira da Silva*

*Universidade Federal Rural do Rio de Janeiro, Instituto de Ciências Exatas, Departamento de Química, BR 465, Km 47, CEP:23.897-000, Seropédica, RJ.*

**clarissa-dq@ufrrj.br*

**Abstract:** Um fornecimento confiável de energia é uma questão chave para o desenvolvimento e crescimento econômico mundial. Atualmente, grande parte da energia global é produzida a partir de combustíveis fósseis, constituindo uma escolha ambiental inadequada e uma aposta questionável em um futuro à médio e longo prazo. Neste contexto, a adoção do hidrogênio como uma nova matriz energética surge como uma alternativa promissora para diminuir as emissões de gases que colaborem para o efeito estufa e, consequentemente, acarretem em mudanças climáticas[1]. A reação de reforma em loop químico oferece um esquema de oxi-redução eficaz e versátil que pode converter combustíveis à base de carbono, em hidrogênio e outros produtos químicos valiosos, ao mesmo tempo em que fornece captação de $CO_2$ à um baixo custo[2]. O processo de reforma em loop químico consiste em dois reatores interconectados, um de combustível e outro de ar, pelos quais circula um fluxo de carreadores de oxigênio. O carreador de oxigênio é oxidado no reator de ar produzindo uma corrente pura de $H_2$. Após a oxidação, o carreador é transportado ao reator de combustível onde é regenerado, podendo ser aplicado novamente na etapa de oxidação. O esquema da reação é ilustrado abaixo, utilizando óxido de ferro como carreador de oxigênio e metano como combustíve1:

Oxidação: $12FeO + 4H_2O = 4Fe_3O4 + 4H_2$

Redução: $CH_4 + 4Fe_3O_4 = CO_2 + 2H_2O + 12FeO$

O fato de que o oxidante gasoso e o combustível nunca estão diretamente em contato, resulta em uma corrente de hidrogênio pura, eliminando a necessidade de purificação do mesmo[3]. O conhecimento a respeito das reações envolvendo óxidos de ferro e água é de grande importância no planejamento de processos de reação em loop químico, e muitos trabalhos experimentais têm sido realizados sobre a reatividade destas espécies químicas [4,5]. Entretanto, ainda falta uma compreensão detalhada do mecanismo de reação entre óxidos de ferro e água por uma abordagem teórica. Isto posto, o trabalho tem como objetivo apresentar um estudo utilizando a teoria do funcional de densidade (DFT) para modelar a reação da etapa de oxidação do processo de reforma em loop químico, com a wustita como carreador de oxigênio e a água como agente oxidante. Tal análise consiste em cálculos de estrutura eletrônica para os reagentes, produtos e estados de transição envolvidos na reação, empregando a abordagem de cluster. O

modelo de cluster se justifica pela pequena dimensão que as partículas dos carreadores de oxigênio devem ter (nanopartículas) para que sejam eficientes nas reações que compõem a reforma em loop químico [3]. Uma questão importante em pesquisas utilizando estruturas de dimensão de cluster é investigar o tamanho mínimo no qual o cluster começa a mimetizar o comportamento do sólido [6]. Portanto, foi imprescindível a avaliação do número mínimo de átomos de ferro e oxigênio do óxido empregado. Em nossas análises foi possível observar que clusters que continham um número baixo de átomos, por exemplo $Fe_4O_4$, apresentaram considerável deformação de modo a perder completamente a estrutura característica do sólido. Assim sendo, foi possível chegar a um número ótimo de 12 átomos de ferro e 12 átomos de oxigênio. Quanto a investigação da reação, foi de extrema importância a consideração dos distintos processos quimissortivos possíveis para a molécula de água, nos diferentes sítios do óxido. A partir desta análise foi possível inferir que a molécula de água adsorve preferencialmente sobre o átomo de ferro, de modo que um dos átomos de hidrogênio da molécula de água esteja apontado para um átomo de oxigênio do cluster. O resultado obtido foi uma conformação onde o grupo hidroxila proveniente da água está posicionado em ponte, entre os átomos de ferro do óxido. O átomo de hidrogênio remanescente permanece adsorvido sobre o átomo de oxigênio do cluster. A etapa de dessorção do $H_2$ ainda está em estudo.

**Key-words**: Produção de hidrogênio molecular; Reação de reforma em loop químico; Teoria do funcional de densidade.
**Support:** CAPES.

**References:**

[1] J. Plou *et al.*, Fuel 118 (2014) 100-106.
[2] L. Huang *et al.*, Applied Energy 159 (2015) 132-144.
[3] S. Bhavsar *et al.*, Catalysis Today 228(2014) 96-105.
[4] C. Trevisanut *et al.*, International Journal of Hydrogen Energy 40 (2015) 5264-5271.
[5] C. Trevisanut *et al.*, Top Catal 59 (2016) 1600-1613.
[6] N. O. Jones *et. al*, Physical Review B 72 (2005) 165411.

# Kinetic Analysis of Acetone Combustion Reactions

Gladson de Souza Machado, Rodrigo Rangel Vasquez Castro, João Claudio Avila Fonseca, Glauco Favilla Bauerfeldt

*Departamento de Química, Instituto de Ciências Exatas, UFRuralRJ*

**Abstract:** Acetone is an important intermediate specie in several combustion mechanisms and is a potential candidate fuel. It is also a by-product in the biomass fermentation [1,2]. Hence it is crucial to develop a consistent kinetic mechanism of combustion of this biofuel, in order to better understand its process of combustion. A combustion mechanism has already been proposed by Sarathy et al [3]. In this context, this work aims to investigate some uni- e bimolecular reactions, which are of great importance to the initiation phase of the acetone combustion process, predict new kinetic parameters and then improve the former combustion mechanism. The reactions are: (R1) $CH_3COCH_3 \rightarrow CH_3 + CH_3CO$; (R2) $CH_3COCH_3 \rightarrow CH_4 + CH_2CO$; (R3) $CH_3COCH_3 \rightarrow H_2 + CH_3COCH$; (R4) $CH_3COCH_3 \rightarrow CH_3C(OH)CH_2$; (R5) $CH_3COCH_3 + O_2 \rightarrow HO_2 + CH_3COCH_2$. Therefore, calculations of geometry optimization, frequency and reaction paths have been performed at M06-2X/cc-pVDZ and M06-2X/aug-cc-pVTZ levels of calculation. Moreover, single points calculations have been performed at the CCSD(T)/aug-cc-pVTZ level. Rate coefficients of reactions R2 – R5 have been calculated by canonical transition state theory in a range of temperature of 500 – 2000 K. For reaction (R1), microcanonical rate coefficients (RRKM) have been calculated and the temperature and pressure dependence has been investigated through the solution of Master Equation, adopting the weak collision model. Rate coefficients have been determined in the range 500 – 2000 K and 10 – 38000 torr. Concerning the geometry optimizations, the improvement of the basis set quality did not yield significant differences on the bond lengths and angle values, except for the $CH_3COCH$ specie, in which the $C_{(CH)}CO$ angle decreases as the quality of the basis set increases. Barrier heights and reaction energy differences calculated at the DFT level with either DZ or TZ basis set are very close, exception is noted for (R4), in which the TZ result for the reaction energy difference is 4.7 kcal $mol^{-1}$ smaller than the DZ result. The single point calculations have also not significantly changed the former energy differences. The barrier heights determined at the CCSD(T)/aug-cc-pVTZ level were (in kcal $mol^{-1}$): 87.5 (R2), 102.2 (R3), 65.2 (R4) and 47.2 and 47.7 (R5). The larger deviation observed for the CCSD(T) and M06-2X barrier heights was 3.2 kcal $mol^{-1}$ (for reaction R4), and the mean value was 1.7 kcal $mol^{-1}$, indicating that the single point calculations have only slightly improved the results. All of these reactions were found to be endothermic, with CCSD(T)/ aug-cc-pVTZ reaction energy differences (in kcal $mol^{-1}$): 81.0 (R1), 21.7 (R2), 101.4 (R3), 12.0 (R4) and 47.2 (R5). For reaction (R1), Troe parameters have been estimate, with low pressure Arrhenius parameters of $8.34x10^{-5}$ $cm^3$ $molec^{-1}$ $s^{-1}$ and 62.30 kcal $mol^{-1}$, high pressure of $6.54x10^{17}$ $s^{-1}$ and 85.91 kcal $mol^{-1}$, and parameters P1,

P2, P3 and P4 respectively: 1.05, $3.29x10^{10}$, $7.20x10^{2}$ and $2.08x10^{9}$. This fit has shown an excellent agreement with some experimental results [4,5] and also provides reliable rate coefficients at higher pressures. For the other reactions, the Arrhenius expression at CCSD(T) level of calculation were (units: kcal $mol^{-1}$ and $s^{-1}$ or $cm^3$ $molec^{-1}$ $s^{-1}$): $k_2(T) = 4.43\ x10^{13}\ exp(-89.23/RT)$; $k_3(T) = 3.07\ x10^{15}\ exp(-106.16/RT)$; $k_4(T) = 3.89\ x10^{13}\ exp(-66.42/RT)$ and $k_5(T) = 1.82\ x10^{-10}\ exp(-52.56/RT)$. For the unimolecular reactions, the branching ratios have demonstrated that the reaction (R1) is the most important for temperature values above 1000 K, while for lower temperatures, reaction (R4) prevails. On the other hand, it is well known that the hydrogen abstraction by $O_2$ molecules is the dominant step in the initiation phase of low temperature combustion reactions (lower than 1000 K). Hence, a competition between the reactions (R4) and (R5) is expected. Ignition delay times have finally been calculated for the acetone combustion at high and low temperature regimes using the original mechanism [3]. Experimental results [6] obtained in the range from 1346 to 1633 K have compared to our predicted results. The calculated ignition delay times obtained from the original model [3] were higher than the experimental data [6] with an average error of 81%. After optimization of the combustion model (achieved by including our suggested kinetic parameters), the calculated errors are lower, decreasing to 24%. Therefore, in this work it has been shown that, for these reactions, our DFT calculations yields good molecular properties to be applied on chemical kinetics, comparable to high level *ab initio* calculations. Moreover, rate coefficients have been calculated, providing reliable and more accurate Arrhenius parameters for acetone combustion mechanism.

**Key-words**: Transition State Theory, Rate coefficients, Troe Parameters.
**Support:** This work has been supported by CAPES.

**References:**

[1] Y. Wu et al., Fuel, 185, 577 (2016).
[2] V. M. Babu et al., Renew. Sustainable Energy Rev., 78, 1068 (2017).
[3] S.M. Sarathy, et al. Combust Flame, 159, 6, 2028 (2012).
[4] D. F. Davidson et al., J. Phys. Chem. A, 119, 7257 (2015).
[5] S. Saxena, J. H. Kiefer, S. J. Klippenstein, Proc. Combust. Inst., 32, 123 (2009).
[6] K. Sato, Y. Hidaka. Combust Flame. 122, 3, 291 (2000).

# Calculations of Rate Coefficients for the Uni and Bimolecular Reactions of Dimethyl Ether and Improvement of its Combustion Mechanism

Rodrigo Rangel Vasquez Castro, Vinicius Nunes da Rocha, Gladson de Souza Machado, Glauco Favilla Bauerfeldt

*Departamento de Química □Universidade Federal Rural do Rio de Janeiro*

**Abstract:** Great attention has been given to dimethyl ether (DME) since it has been indicated as potential candidate fuel for compression ignition engines. It shows high cetane number ( > 55) and favorable C/O ratio for combustion. [1] Moreover, it has been shown that DME is smokeless when it burns, causing lower CO and particulate emission [2], the latter observation justified by the lack of carbon-carbon bonds, resulting in low soot formation. From the economical appeal, DME can be cheaply produced from syngas (CO, $H_2$), also from coal, natural gas, biomass, and blends of these. Previous studies on the combustion properties highlight the importance of the unimolecular reactions (DME $\rightarrow$ products) for the initiation of the combustion mechanism at the high temperature range. DME shows six unimolecular steps, namely: dissociation ($CH_3OCH_3 \rightarrow CH_3O + CH_3$ (R1) and $CH_3OCH_3 \rightarrow CH_3OCH_2 + H$ (R2)), $H_2$ elimination (E11, $CH_3OCH_3 \rightarrow CH_3OCH + H_2$ (R3) and E12, $CH_3OCH_3 \rightarrow CH_2OCH_2 + H_2$ (R4)) and decomposition ($CH_3OCH_3 \rightarrow CH_2O + CH_4$ (R5) and $CH_3OCH_3 \rightarrow CH_3OH + CH_2$ (R6)). In turn, bimolecular reactions (DME + X $\rightarrow$ $CH_3OCH_2$ + HX, X = OH (R7), O (R8), $CH_3$ (R9), $HO_2$ (R10), $O_2$ (R11) and H (R12)) are important channels for the mechanism propagation. In special, reaction R11 prevails in the initiation phase, in the low temperature combustion. Despite the relevance of the combustion models for the decision about the implementation of a candidate fuel, the kinetic parameters for the abovementioned reactions have only been crudely estimated. In this work, a contribution for this issue is proposed by the determination of the rate coefficients for these most important reactions, based on a quantum mechanical description at the M06-2X/aug-cc-pVTZ level (with *a posteriori* improvement of the electronic energies from single point calculations at the CCSD(T)/aug-cc-pVTZ level) and variational transition state theory calculations. The reassessment of the combustion mechanism represents another goal of our work. Here, a numerical analysis of the improved combustion mechanism has been simulated using kintecus®, adopting the DVODE numerical method to integrate the coupled ordinary differential equations. The improved mechanism has been proposed adopting the combustion model by Yasunaga and co-workers [3] as a starting point and including our calculated rate parameters. The R1 and R2 unimolecular reactions are barrierless, with dissociation limits predicted as 80.33 and 93.73 kcal $mol^{-1}$. Barrier heights for the unimolecular reactions R2 – R6 are 84.78, 79.31, 88.49 and 83.20 kcal $mol^{-1}$, respectively. The bimolecular, DME + OH

reaction (R7), is also shown to be important for the consumption of the fuel and proceeds by a hydrogen abstraction mechanism, leading to methoxymethyl radical and $H_2O$. For such reaction, theoretical calculations have also been performed at the M06-2X/aug-cc-pVTZ level. Concerning the available literature on this bimolecular reaction, new stationary points have been located and connected to reactants and products via reaction paths, whose contribution to the global kinetics has been proved significant. Pre-barrier complexes have been located, stabilized by 0.76, 4.81 and 5.05 kcal $mol^{-1}$. These intermediates are connected to corresponding saddle points, which lie 0.29, -0.34 and 1.57 kcal $mol^{-1}$, respectively, also with respect to reactants. For the other bimolecular reactions the predicted barrier heights at the M06-2X/aug-cc-pVTZ level are (in kcal $mol^{-1}$): 0.4 (R8), 11.6 and 14.1 (R9a and R9b), 14.3 and 13.4 (R10a and R10b), 40.8 and 41.1 (R11a and R11b) and 8.0 (R12). Canonical variational rate coefficients have been calculated for all reaction paths in the range from 500 – 2000 K. For the reactions showing more than one saddle point, individual rate coefficients have been summed up to predict the global rate coefficients. Some kinetic parameters (R7 and R9-R12) have been compared to literature data, showing very good agreement with the previous results. These reactions have finally been included in the DME combustion model and the agreement of the predicted ignition delay times have been improved, as compared to the original combustion model. The proposed kinetic data finally represent a great contribution to the literature, concerning the combustion chemistry of dimethyl ether.

**Key-words**: combustion chemistry, ether combustion, rate coefficients
**Support:** This work has been supported by CNPq and CAPES
**References:**
[1] C. Bänsch *et al.* J. Phys. Chem. A 117, 8343−8351 (2013).
[2] R. Sivaramakrishnan *et al.* Combustion and Flame 158, 618–632 (2011).
[3] K. Yasunaga *et al.* Combustion and Flame 158, 1032–1036 (2011).

# Estudo de Adsorção de Água em Wustita para Aplicação Catalítica na Produção de $H_2$ Combustível

Gabriela N. Pereira,[a] Glauco F. Silva,[a] Marcelo Marques,[b] Lara K. Teles,[b] Antônio M. Da Silva Jr.[a]

*a: Universidade Federal Rural do Rio de Janeiro, Departamento de Química-ICE, BR 465, Km 7, 23.897-000, Seropédica-RJ, Brazil.*
*antonio.msj1@gmail.com*
*b: Grupo de Materiais Semicondutores e Nanotecnologia, Instituto Tecnológico de Aeronáutica, DCTA, 12228-900 São José dos Campos, Brazil.*

**Resumo:** Observando o quadro energético global atual, existem várias evidências de que este encontra-se em processo de transformação. Com o crescimento da demanda energética, se torna preocupante a utilização majoritária de combustíveis de origem fóssil. Desta forma, tem-se buscado a implementação de fontes alternativas limpas e que sejam economicamente viáveis. Um forte candidato a este papel é o hidrogênio molecular, por ser renovável, sustentável e apresentar menor impacto ambiental[2]. Um dos métodos para a produção de $H_2$ é o processo chamado *chemical looping combustion*[1]. Este é caracterizado por duas reações químicas paralelas e fisicamente separadas, sendo uma de oxidação de um catalisador óxido metálico: $12FeO + 4H_2O = 4Fe_3O_4 + 4H_2$; e outra de oxidação de um composto hidrogenado orgânico: $CH_4 + 4Fe_3O_4 = CO_2 + 2H_2O + 12FeO$. Somadas, as duas equações resultam em: $CH_4 + 2H_2O = CO_2 + 4H_2$. A produção em duas etapas separadas é a grande vantagem desse processo, pois evita a necessidade de subsequentes estágios de purificação e remoção de subprodutos. Alguns catalisadores diferentes podem ser utilizados, sendo que os constituídos a base de Fe são comparativamente baratos, disponíveis em grandes quantidades e são pouco agressivos ao meio ambiente. No presente trabalho, tem-se interesse particular no processo oxidativo do catalisador, devido a questões, a nível molecular, ainda em aberto na literatura[3]. Estão sendo simulados mecanismos de transferência de oxigênio da água para duas superfícies (111) da wustita, contendo terminações de O e Fe. O formalismo empregado é a DFT+U, utilizando condições periódicas de contorno, como implementado no pacote computacional VASP. Tem-se, como objetivo inicial, o estudo topológico da adsorção molecular da água na superfície, bem como suas decorrentes barreiras energéticas para a obtenção do produto oxidado, segundo cálculos empregando a metodologia *Nudged Elastic Band* (NEB).

**Palavras-chave**: Hidrogênio Combustível, Chemical Looping, DFT, Wustita.

**Referências:**

[1] S. Bhavsar *et al.,* Catalysis Today **228**, 96 (2014).
[2] T. S.Veras *et al*., Int. J. Hydrogen Energy **42**, 2018 (2017).
[3] J. L. Daschbach *et al.*, J. Phys. Chem. B **109**, 10362 (2005).

# Estudo de Adsorção de Água em Wustita para Aplicação Catalítica na Produção de $H_2$ Combustível

Gabriela N. Pereira,[a] Glauco F. Silva,[a] Marcelo Marques,[b] Lara K. Teles,[b] Antônio M. Da Silva Jr.[a]

*a: Universidade Federal Rural do Rio de Janeiro, Departamento de Química-ICE, BR 465, Km 7, 23.897-000, Seropédica-RJ, Brazil.*
*antonio.msj1@gmail.com*
*b: Grupo de Materiais Semicondutores e Nanotecnologia, Instituto Tecnológico de Aeronáutica, DCTA, 12228-900 São José dos Campos, Brazil.*

**Resumo:** Observando o quadro energético global atual, existem várias evidências de que este encontra-se em processo de transformação. Com o crescimento da demanda energética, se torna preocupante a utilização majoritária de combustíveis de origem fóssil. Desta forma, tem-se buscado a implementação de fontes alternativas limpas e que sejam economicamente viáveis. Um forte candidato a este papel é o hidrogênio molecular, por ser renovável, sustentável e apresentar menor impacto ambiental[2]. Um dos métodos para a produção de $H_2$ é o processo chamado *chemical looping combustion*[1]. Este é caracterizado por duas reações químicas paralelas e fisicamente separadas, sendo uma de oxidação de um catalisador óxido metálico: $12FeO + 4H_2O = 4Fe_3O_4 + 4H_2$; e outra de oxidação de um composto hidrogenado orgânico: $CH_4 + 4Fe_3O_4 = CO_2 + 2H_2O + 12FeO$. Somadas, as duas equações resultam em: $CH_4 + 2H_2O = CO_2 + 4H_2$. A produção em duas etapas separadas é a grande vantagem desse processo, pois evita a necessidade de subsequentes estágios de purificação e remoção de subprodutos. Alguns catalisadores diferentes podem ser utilizados, sendo que os constituídos a base de Fe são comparativamente baratos, disponíveis em grandes quantidades e são pouco agressivos ao meio ambiente. No presente trabalho, tem-se interesse particular no processo oxidativo do catalisador, devido a questões, a nível molecular, ainda em aberto na literatura[3]. Estão sendo simulados mecanismos de transferência de oxigênio da água para duas superfícies (111) da wustita, contendo terminações de O e Fe. O formalismo empregado é a DFT+U, utilizando condições periódicas de contorno, como implementado no pacote computacional VASP. Tem-se, como objetivo inicial, o estudo topológico da adsorção molecular da água na superfície, bem como suas decorrentes barreiras energéticas para a obtenção do produto oxidado, segundo cálculos empregando a metodologia *Nudged Elastic Band* (NEB).

**Palavras-chave**: Hidrogênio Combustível, Chemical Looping, DFT, Wustita.

**Referências:**

[1] S. Bhavsar *et al.,* Catalysis Today **228**, 96 (2014).
[2] T. S.Veras *et al*., Int. J. Hydrogen Energy **42**, 2018 (2017).
[3] J. L. Daschbach *et al.*, J. Phys. Chem. B **109**, 10362 (2005).

# Title: Entanglement in disordered systems via DFT calculations

Authors: Guilherme Arantes Canella[a] (PG), Vivian Vanessa França Henn[b] (PQ)

*Address: Instituto de Química de Araraquara, Universidade Estadual Paulista*
*[a]guycanella@gmail.com, [b]vvfranca@iq.unesp.br*

**Abstract:** It is well known that spatial inhomogeneities can affect electrical, magnetic, entanglement properties among others. Since entanglement is the key ingredient of quantum information theory, it is of great importance to understand the influence of these inhomogeneities. However, obtaining exact results in strongly correlated systems is a very complex task, even in homogeneous systems, since all particle-particle interactions should be considered. For inhomogeneous systems, this is even worse [1]. The Density Functional Theory (DFT) makes this task easier as it considers the ground-state entanglement as a functional of the density. Moreover, to obtain a good description of the interaction in many-body systems, the one-dimensional Hubbard model can be used. This model has shown interesting results in the understading of entanglement in solids [2–4], mainly when the analytical expression of the functional is known [5]. Most of the studies of the impact of disorder to now has concentrated to repulsive systems. In the present work, we investigate the influence of it on the entanglement properties of systems, which is for example the regime where the model describes BCS superconductivity, Bose-Einstein condensation and exotic superfluidity.

**Key-words:** Entanglement, disordered systems, Hubbard model, Density Functional Theory

## References

[1] V. V. França and K. Capelle, "Entanglement in spatially inhomogeneous many-fermion systems," *Phys. Rev. Lett.*, vol. 100, p. 070403, Feb 2008.

[2] S.-J. Gu, S.-S. Deng, Y.-Q. Li, and H.-Q. Lin, "Entanglement and quantum phase transition in the extended hubbard model," *Phys. Rev. Lett.*, vol. 93, p. 086402, Aug 2004.

[3] J. P. Coe, V. V. França, and I. D'Amico, "Feasibility of approximating spatial and local entanglement in long-range interacting systems using the extended hubbard model," *EPL (Europhysics Letters)*, vol. 93, no. 1, p. 10001, 2011.

[4] J. P. Coe, V. V. França, and I. D'Amico, "Hubbard model as an approximation to the entanglement in nanostructures," *Phys. Rev. A*, vol. 81, p. 052321, May 2010.

[5] V. V. França and I. D'Amico, "Entanglement from density measurements: Analytical density functional for the entanglement of strongly correlated fermions," *Phys. Rev. A*, vol. 83, p. 042311, Apr 2011.

# Competition for βCD cavity on inclusion complex of antihypertensive drugs and Excipient

Guilherme Augusto B. Soares(PG)[1], Homero Bonomini(G)[1],Larissa Helena Da Rocha Meira(PG)[2],Frederico Barros De Sousa(PQ)[2], Juliana FedoceLopes(PQ)[1]

[1]*Laboratório de Química Computacional -LaQC,* [2]*Laboratório de Sistemas Poliméricos e Supramoleculares-LSPS, IFQ -Instituto de Física e Química, Universidade Federal de Itajubá-UNIFEI, Av. BPS, 1303, Bairro Pinheirinho, Itajubá-MG CEP: 37500-903*

**Abstract:** Excipients, as Sodium Dodecyl Sulfate (SDS), are often present in drug compositions and they can improve the active molecule stability as well as modulate its pharmacological properties. Atenolol (ATE) and Losartan (LOS) are antihypertensive drugs, and in this work the competition between them and SDS for the β-cyclodextrin (βCD) cavity is evaluated. Molecular Dynamics were performed using GROMACS[1] for binary systems as control: ATE:βCD, LOS:βCD and SDS:βCD. Topology files were obtained from *The Automated Topology Builder (ATB) and Repository*[2], as βCD ID= 23854, ATEID= 36896, LOS ID=4615 and SDS ID=20332; geometries were all optimized with Gaussian 09[3] by DFT-M062X[4] and 6-31+g(d,p)[5]. The local minima were assured by vibrational analysis. To properly use GROMACS with ATB files, gromos53a6[6] force field was updated before MD run. Virtual boxes (7,0nm x 5,0nm x 5,0nm) were defined and filled with 5631 water molecules each, using the SCP216 force field[7]. For all systems, a 20ps NPT equilibration step, using a modified Berendsen thermostat denominated V-rescale[8], as well as a pressure coupling with Berendsen barostate[9]. The simulation stage was done during 10 ns at NPT ensemble at 300K and1.01325 bar. For all simulations, bonds were constrained by LINCS[10] and long range interactions were described by PME method[11]. The inclusion competition along MD simulation is represented in the Figure 1.

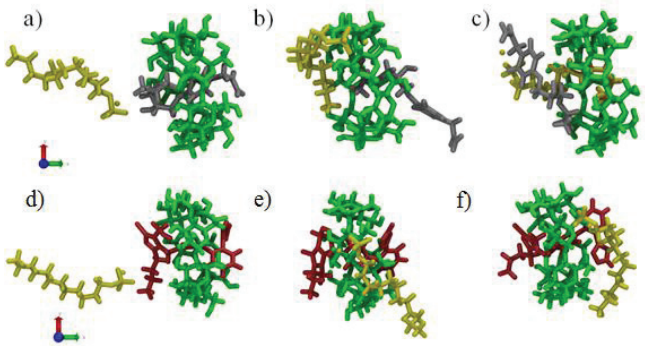


Figure 1 – Molecular dynamics frames for: First row ATE:βCD:SDS. a)t=0.00ns; b)t=5.19ns and c)t=9.35ns; second row LOS: βCD:SDS. d)t=0.00ns; e)t=2.16ns and f)t=9.46ns.Watermolecules representations were neglected. ATE:grey; SDS:yellow, BCD:green and LOS:red.

In reference system SDS:βCD Center of Masses (CoM...CoM) distances varies approximately between 1,5-6Å along the simulation. In ATE:βCD:SDS system, SDS-βCD d(CoM...CoM) decreases to values close to those verified for the binary system (2-5,5Å), while ATE:βCD d(CoM...CoM) arises along the simulation. This result means that excipient would win the competition, being held inside cavity. In LOS:βCD:SDS system, SDS:βCD d(CoM...CoM) varies (13,8-7,5Å), but distance does not reach binary system levels, indicates that LOS does not allow SDS to get into βCD. Distances between hydrogen atoms of guests and βCD were estimated using the software ILIAAD - Import and List Individual or Average Atomic Distances, developed by us for this purpose, aiming to help the ROESY experimental data analysis. Using a 5Å distance as cutoff, correlation maps similar to NMR 2D were obtained and are presented in Figure 2. The circles diameters were settled to indicate the occurrence frequency while the color scale refers to the average of hydrogen atoms distance.

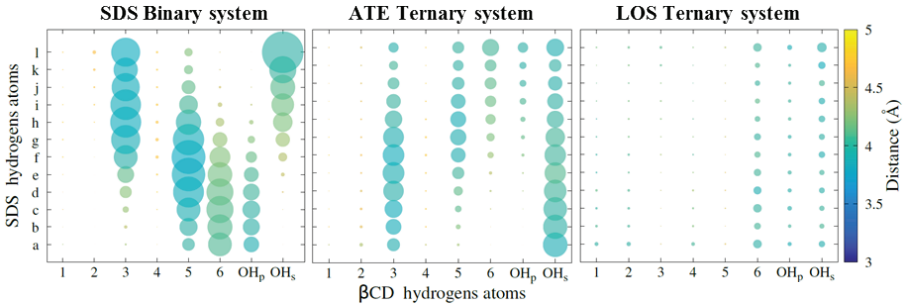


Figure 2 – Correlation Maps between SDS andβCD hydrogen atomson three systems types.

ATE:βCD:SDS system, shows a pattern distribution similar to the reference βCD:SDS system. Also, the inner βCD hydrogen atoms are statistically correlated with the guest ones, while for LOS:βCD:SDS system, there are no these correlations types. This result illustrates the competition for the βCD cavity through the molecular dynamics which was also experimentally observed by our coworkers on ITC as well as NMR experiments.

**Key-words**: Molecular dynamics, Losartan, Atenolol, Cyclodextrin, Inclusion complex
**Support:** This work has been supported by CAPES, CNPQ e FAPEMIG.

**References:**

[1] Spoel, D. Van Der; et al. **Journal of Computational Chemistry**, v. 26, n. 16, p. 1701–1718 (2005).
[2] Malde, A.K.; et al.**Journal of Chemical Theory and Computation**,v.7, n.12, p.4026–4037 (2011).
[3] Caricato, M.; et al.**Gaussian 09**(2013).
[4] Zhao, Y.; Truhlar, D.G. **Theoretical Chemistry Accounts**, v. 120, n. 1–3, p. 215–241 (2008).
[5] Ditchfield, R.; et al. **The Journal of Chemical Physics**, v. 54, n. 2, p. 724–728 (1971).
[6] Oostenbrink, C.; Soares, T.A.; et al. **European Biophysics Journal**, v. 34, n. 4, p. 273–284 (2005).
[7] Berendsen, H.J.C., et al. **Intermolecular Forces**. Reidel, Dordrecht, Holland. 1981, p. 331–342.
[8] Bussi, G.; et al. **The Journal of Chemical Physics**, v. 126, n. 1, p. 14101 (2007).
[9] Berendsen, H.J.C.; et al. **The Journal of Chemical Physics**, v. 81, n. 8, p. 3684–3690 (1984).
[10] Hess, B.; et al. LINCS: **Journal of Computational Chemistry**, v. 18, n. 12, p. 1463–1472( 1997).
[11] Darden, T.; York, D.; et al. **The Journal of Chemical Physics**, v. 98, n. 12, p. 10089 (1993).

# POLYCARBONITRILE: A DFT INVESTIGATION OF STRUCTURAL STABILITY

**Authors:** Guilherme de Souza Tavares de Morais[a] and Rogério Custodio[b]

**Address:** *Universidade Estadual de Campinas, Instituto de Química, Depto. Físico-Química, 13083-970 Campinas, São Paulo, Brazil*
*email: a) guilherme.morais@iqm.unicamp.br; b)* rogerct@g.unicamp.br

## INTRODUCTION

The fact that polyacetylene (PA) $[C_2H_2]_\infty$ is isoelectronic with polycarbonitrile (PCN) $[CHNH]_\infty$ has caused many theoretical studies to investigate the later compound in diverse levels of theories, but using a fully trans structure [1], since this is the most stable structure for PA. More recent studies of the structural and thermodynamic stability using PCN in fully trans, cis-transoidal, and trans-cisoidal configurations have indicated that the cis-transoidal structure is more stable than a fully trans [2] showing that the use of the fully trans configuration of the PCN can generate errors, as for example the study polarizability and hyperpolarizability of this polymer [3].

In this work the structural stability of polyacetylene with different number of monomeric units was evaluated by substituting carbon atoms by nitrogen, but maintaining nitrogens always separated by at least one carbon atom.

## METHODS

Different structures in the ground state was analyzed at the density functional theory (DFT) level with different functionals such as: B3LYP, CAM-B3LYP and M06-2X and aug-cc-pVDZ basic functions. Maximum and minimum points were also analyzed by using ab initio calculations at the CCSD(T) and QCISD levels. All calculations were performed using the Gaussian09 program.

## RESULTS AND DISCUSSION

A total of 34 isomers were analyzed by fixing the central dihedral angle of the structure every 5 degrees and optimizing all other geometric parameters. The conformational energy of pure PA is confirmed to be the fully trans planar as the most stable structure. The substitution of 2 alternating carbons by 2 nitrogens in trans configuration still shows to be the most stable. However, in these cases, a most stable conformation between the cis structure and the trans structure was observed presenting a stability of the order of 1.7 kcal $mol^{-1}$ relative to the trans configuration (see Fig.1 as example).

For tetramers, the structure of the PA in trans conformation has a difference between cis and trans of 3.4 kcal $mol^{-1}$. The rotational barrier for the cis-trans interconversion is of the order of 8.2 kcal $mol^{-1}$. The substitution of 2 carbons alternated by 2 nitrogens reduces this difference to 1.9 kcal $mol^{-1}$. The difference between the structures in of tetramers in which nitrogens are not alternating, the rotational barrier is of the order of 6.0 kcal $mol^{-1}$. The substitution of 3 alternate carbons leads to a more stable intermediary

conformation with an equilibrium dihedral angle of 40° and a difference of 1.3 kcal $mol^{-1}$ concerning trans configuration and 1.4 kcal $mol^{-1}$ for the cis configuration. The rotational barrier from trans to cis is of the order of 2.5 kcal $mol^{-1}$. Polymers with 3 carbon with no alternating nitrogen present the trans conformation as most stable by 6.8 kcal $mol^{-1}$ with respect to cis, while with 2 alternating nitrogens the difference is 6.1 kcal $mol^{-1}$.

The relative conformational energy curve of the polymer with the 4 alternating carbons replaced by nitrogen is shown in Figure 1. One of the most stable structures is shown in Figure 2.

## CONCLUSIONS

Our results indicate that PCN or similar compounds are unlikely to be planar as suggested previously in an exploratory work [3]. The PA modifications replacing carbons by nitrogens and increasing the chain has produced non-planar stable structures with equilibrium dihedral angles between ±40° and ±60°. These non-planar structures differ from those used in literature to study optical properties of PCN. Most likely, significant changes in the calculated optical and electronic properties of PCN will be observed with respect to the literature [4]. Calculations in this sense are in progress and will be presented in the meeting.

**Key-words**: Polycarbonitrile, Conformational analysis, Density functional theory, Electronic properties

**Support:** The authors would like to thank the financial support from: FAPESP – CEPID, CNPq, FAEPEX– UNICAMP and CENAPAD-SP.

## References

[1] Karfen, A.; *Chemical Physics Letters*, **1979**, 64, 299.
[2] Abdurahman, A., Shukla A., Dolg M.; *Chem. Phys.*, **2000**, 257, 301.
[3] Del Nero, J.; Laks, B.; Custodio, R.; *Synth. Met.*, **1997**, 85, 1127
[4] Bonabi, F., Pedersen, T.G.; *J. Phys.: Condens. Matter,* **2017,** 29, 165702.

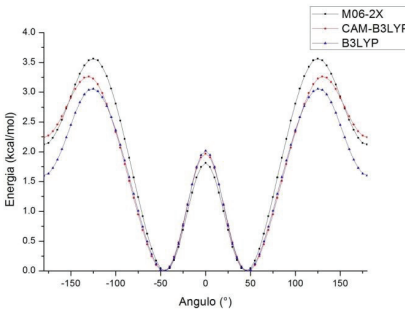


**Figure 1**. Relative conformational energy curve as a function of the dead center of the single central bond of the compound HN=CH-N=CH-N=CH-N=$CH_2$.

| Átomos | Ângulo de Diedro |
|---|---|
| 5C-11N-8C-10N | 176.080° |
| 8C-10N-1C-12N | 45° |
| 1C-12N-3C-13N | 177.048° |

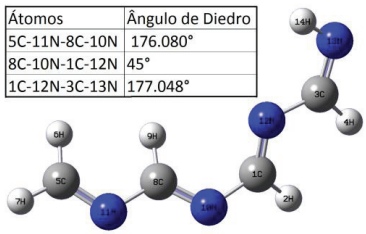


**Figure 2**. More stable conformation of the compound HN=CH-N=CH-N=CH-N=$CH_2$ and dihedral.

# CBS-QB3 Composite Method Along with Pseudopotential for the Calculation of Standard Enthalpy of Formation

**Authors:** Guilherme Luiz Chinini[a], Rogério Custodio[b]

***Address:*** *Universidade Estadual de Campinas, Instituto de Química, Depto. Físico-Química, 13083-970 Campinas, São Paulo, Brazil a. guilherme@iqm.unicamp.br, b. roger@iqm.unicamp.br.*

**Abstract:** Composite methods currently represent the one of the best choices for the calculation of electronic and thermochemical properties due to the reasonable computational cost and applicability to chemical systems with up to 100 electrons. One of the best alternative of this class of methods was introduced by Petersson et al. [1] known as CBS (Complete Basis Set). These methods incorporate additive corrections to the order of electronic correlation and considers extrapolation techniques to a complete basis set. CBS presents similar accuracy with the Gn methods [2]. However, they can seldom be applied to systems containing many electrons due to the high number of integrals appearing in CCSD(T) and QCISD(T). In this sense, the use of pseudopotential reduces the computational cost and extends the applicability of the method to larger systems preserving its accuracy. In the present paper the authors report the development of a composite method based on the implementation of pseudopotential in the CBS-QB3 (Eq.1) methodology [3]. The calculation of the electronic energy of a hypothetical system according to the CBS-QB3 method is described as follows:

$$E_e = E(MP2) + \Delta E\big(MP4(SDQ)\big) + \Delta E\big(CCSD(T)\big) + \Delta E(CBS) + \Delta E(NaCorr) + \\ + \Delta E(emp) + \Delta E(Spin) + \Delta E(SO) \qquad (Eq.1)$$

The method, referred to as CBS-QB3//CEP-31G(d)/CEP, uses calculations at MP2(fc)/CEP-CBSB3 as reference energy. The basis set was optimized according to the variational principle within the boundary conditions of the reference energy. The cutoff of the basis set (6-311G(2df,2p) H-Ne and 6-311G(3d2f) for Na-Ar) to be used with the pseudopotential was defined from the Hartree-Fock density matrix maps [4]. For the optimization of the equilibrium structure, frequency calculation (ZPE correction) and ΔE(CCSD(T)) (E(CCSD(T)) □E(MP4(SDQ))) the CEP-31G(d) basis set was used. The MP4 calculation and ΔE(NaCorr) were discarded. The latter correction was used only for species containing sodium atoms. The other steps were maintained, whereas the parameters for empirical correction and ΔE(Spin), due to spin contamination, were adapted to the set of 234 enthalpies of formation. The expression for CBS-QB3//CEP-31G(d)/CEP is then defined as follows:

$$E_e = E(MP2/CEP - CBSB3) + \Delta E(CCSD(T)/CEP - 31G(d)) + \Delta E(CBS) + \quad (Eq.2)$$
$$+ \Delta E(emp) + \Delta E(Spin) + \Delta E(SO)$$

This method was applied to the calculation of 234 standard enthalpies of formation taken from the G3/05 test set for validation. **Figure 1** shows the histogram containing the error between theoretical enthalpy (CBS-QB3//CEP-31G(d)/CEP) with respect to the experimental data and comparison of mean absolute error of the proposed method with other methods [5-6].

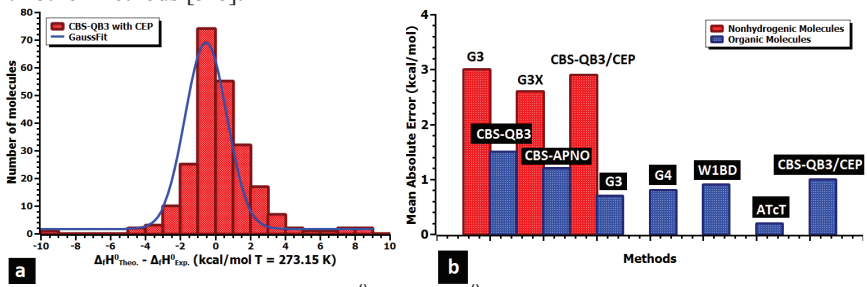


**Figure1.** (a) Histogram for 234 $\Delta_fH^0_{Theo.}$ - $\Delta_fH^0_{Exp.}$ calculated with CBS-QB3 (red bar) and Gaussian Fit. (b) Bar chart containing the comparison between the mean absolute error of various methods [5-6].

When compared to other composite methods, a mean absolute error of 2.1 kcalmol-1 is achieved against 2.0 kcalmol$^{-1}$ for G3 and 2.6 kcalmol$^{-1}$ for G3X (for a set of 19 nonhydrogenic molecules) and 1.0 kcalmol$^{-1}$ (our method) against 1.5 kcalmol$^{-1}$ CBS-QB3 (original) 1.2 kcalmol$^{-1}$ CBS-APNO; 0.7 kcalmol$^{-1}$ G3; 0.8 kcalmol$^{-1}$ G4; 0.9 kcalmol$^{-1}$ W1BD and 0.2 kcalmol$^{-1}$ ATcT for a set of 20 organic molecules [5-6]. With these previous results, it is notable that the implementation of pseudopotential in CBS-QB3 shows to be an efficient strategy for the calculation of enthalpy of formation.

**Key-words**: Pseudopotential, Composite Methods, Complete Basis Set.

**Support:** The authors are grateful for the support provided by FAPESP-CEPID, CNPq, CAPES and FPE-Unipinhal.

**References:**

[1] Jr., J. A. M.; Ochterski, J. W.; Petersson, G. A. J. Chem Phys. 101, 5900 (1994).
[2] Curtiss, L. A.; Raghavachari, K.; Redefern, P. C.; Rassolov, V.; Pople, J. A. J. Chem. Phys. 109, 7764 (1998).
[3] Jr., J. A. M.; Frisch, M. J.; Ochterski, J. W.; Petersson, G. A. J. Chem. Phys. 110, 2822 (1999).
[4] Silva, C. S.; Pereira, D. H.; Custodio, R. J. Chem. Phys. 144, 204118 (2016).
[5] DeYonker, N. J.; Cundari, T. R.; Wilson, A. K. J. Chem. Phys. 124, 114104 (2006).
[6] Curtiss, L. A.; Redfern, P. C.; Raghavachari, K. J. Chem. Phys. 123, 124107 (2005).

# Estudo Teórico do Mecanismo e da Cinética da Reação Atmosférica $HF + OH \rightarrow H_2O + F$

Gustavo Gomes de Sousa*, Flávio O. Sanches-Neto, Hugo Gontijo, Valter Henrique Carvalho-Silva

*Grupo de Química Teórica e Estrutural de Anápolis, Ciências Exatas e Tecnológicas. Universidade Estadual de Goiás, CP 459, 75001-970 Anápolis, GO Brazil.*

**Abstract:** Este resumo analisa as informações obtidas nas simulações computacionais da reação química HF + OH → F + $H_2O$ [1]. Esta reação pertence a uma classe de reações atmosféricas que liberam espécies livres de halogênios as quais apresentam um papel fundamental na química atmosférica, pois são capazes de alterar o equilíbrio natural de formação e destruição de ozônio. Com o conhecimento atual da literatura não há disponibilidade de dados experimentais ou teóricos da constante cinética para esta reação. Dentro deste contexto, este trabalho tem como objetivo a determinação dos dados das constantes cinéticas em função da temperatura da reação HF + OH → F + $H_2O$. Para isso foi realizado cálculos teóricos de estrutura eletrônica utilizando vários níveis de cálculos (DFT e pós-HF) caracterizando os paramentos geométricos e as energias dos reagentes, produtos e da estrutura de transição. A partir dos dados geométricos e energéticos dos estados estacionários foi possível estimar constante cinética via Teoria do Estado de Transição com correção Deformada (*d*-TST) [2] e de Bell. Deste modo observa-se que a reação HF + OH → F + $H_2O$ é endotérmica e apresenta uma alta barreira energética. Esse trabalho possibilitou a obtenção dos dados cinéticos da reação HF + OH → F + $H_2O$ podendo concluir assim os dados teóricos apresentados para as series de reações de haletos de hidrogênio com o radical hidroxil [3] observando assim o comportamento dessa importantes reações atmosféricas.

**Key-words**: sub-Arrhenius, tunelamento, correção de Bell, *d*-TST

**Support:** Gustavo Gomes de Sousa agradece a PrP/UEG. Valter Henrique Carvalho Silva agradece à PrP / UEG e à FAPEG. Nayara Dantas Coutinho agradece FAPDF e CAPES. Vincenzo Aquilanti agradece ao Ministério italiano da Educação, Universidade e Pesquisa, MIUR, pelo apoio financeiro.

**References:**

[1] Song, H. & Guo, H. Mode specificity in bond selective reactions F + HOD ??? HF + OD and DF + OH. *J. Chem. Phys.* **142,** 1–8 (2015).

[2] Carvalho-Silva, V. H., Aquilanti, V., Oliveira, H. C. B. de & Mundim, K. C. Deformed Transition-State Theory: Deviation from Arrhenius Behavior and

Application to Bimolecular Hydrogen Transfer Reaction Rates in the Tunneling Regime. *J. Comput. Chem.* **38,** 178–188 (2017).
[3] Aquilanti, V., Coutinho, N. D. & Carvalho-Silva, V. H. Kinetics of Low-Temperature Transitions and Reaction Rate Theory from Non-Equilibrium Distributions. *Philos. Trans. R. Soc. London A* **375,** 20160204 (2017).

# Fully Anharmonic Resonance Raman Spectra of Diatomic Systems Through Variation Quantum Monte Carlo Simulations

Authors: Gustavo J. Costa[a], Antonio C. Borin[b], Pedro A. M. Vazquez[c], Rogério Custodio[c], Luciano N. Vidal[a]

*Address: [a]Chemistry and Biology Department, UTFPR/Curitiba; [b]Department of Fundamental Chemistry, Institute of Chemistry; [c]Chemistry Institute, Unicamp/Campinas.*

**Abstract:** In this work, the time independent framework of the Resonance Raman (RR) effect was used to obtain pure vibrational (RR) spectra of diatomic systems within the Born-Oppenheimer approximation. The anharmonic correction was introduced by the vibrational Modified Variation Quantum Monte Carlo (MVQMC) method [1]. In order to improve the performance the method, three Random Numbers Generators (RNG) were accessed (MT19937, RANLUX 4 and the native RNG of GNU F77 compiler, version 4.8) for the calculations of the six low lying vibrational states of $X^1\sum^+_g$ and $B^1\sum^+_u$ electronic states of $H_2$. We found that the most cost effective RNG was the MT19937, which was adopted in the subsequent calculations, followed by the GNU F77 RNG. The Potential Energy Curves of the ground and excited states and the Electric Dipole Transition Moment Curve were computed at the CASSCF(124,2)/d-aug-cc-pVQZ level. In general, we found that the CASSCF/MVQMC vibrational energies of low-lying states are very accurate compared to experimental data [2] (**Figure 1**). **Figure 2** shows harmonic intensities significantly higher than anharmonic ones and that the inclusion of Herzberg-Teller vibronic coupling correction increases the RR intensities relative to the Franck-Condon level. We found that aharmonic and vibronic corrections are elevant for other systems as well (e.g. $O_2$, not shown here), where the relative RR intensities changes with the inclusion of these corrections.

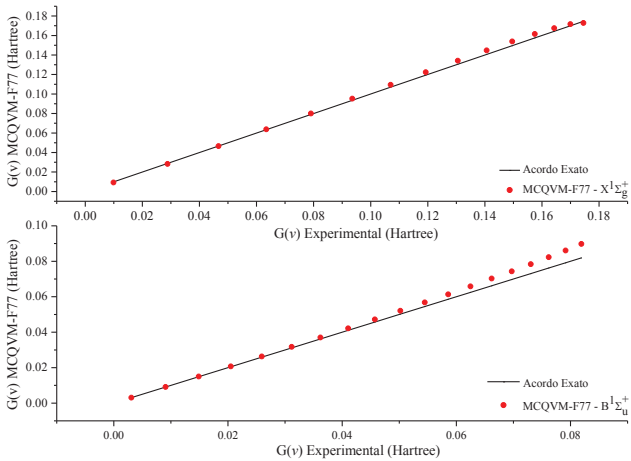


**Figure 1:** $H_2$ vibrational energies of states $X^1\sum^+_g$ e $B^1\sum^+_u$.

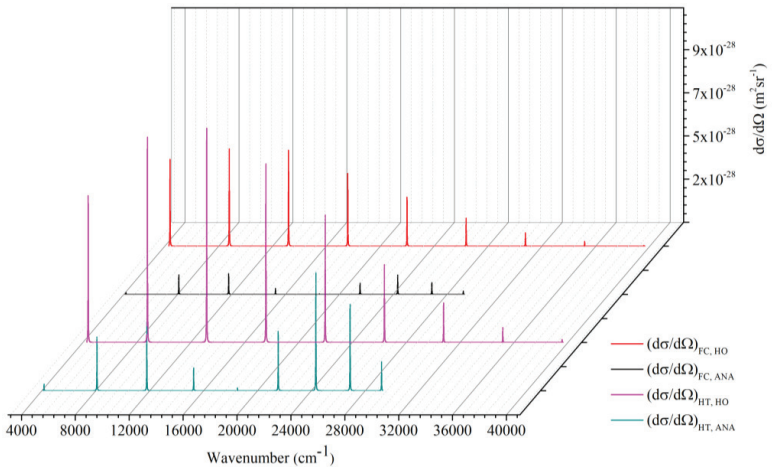


**Figure 2:** Franck-Condon (FC) and Herzberg-Teller (FC+HT) RR spectra of $H_2$ from harmonic (HO) and fully anharmonic (ANA) wavefunctions.

**Key-words**: Resonance Raman Spectroscopy; Variation Quantum Monte Carlo; Anharmonicity; *Ab initio* methods.
**Support:** This work has been supported by CNPq.

**References:**

[1] Angelotti, W. F. D., Fonseca, A. L. D., Torres, G. B., & Custodio, R., Quím. Nova. 2, 433 (2008).
[2] Huber, K. P. (2013). Molecular spectra and molecular structure: IV. Constants of diatomic molecules. Springer Science & Business Media.

# Reaction Rate of $H_2CO = H_2+CO$

H. O. Euclides, P. R. P. Barreto

*Instituto Nacional de Pesquisas Espaciais (INPE/MCT), Laboratório Associado de Plasma (LAP), São José dos Campos, SP, CEP 12247-970, CP515, Brasil*

**Abstract:** In this work, we study the dissociation of formaldehyde, $H_2CO$, which is a stable molecule in the singlet carbenes [1]. There is two possible pathways, the first one the dissociation reaction to $H_2$+CO:

$$H_2CO \rightleftarrows H_2+CO \quad (R1)$$

and second one, via the isomerization of hydroxycarbene, HCOH [2]:

$$\begin{aligned} H_2CO &\rightleftarrows^{k_1}_{k_{-1}} trans-HCOH \\ trans-HCOH &\rightleftarrows^{k_2}_{k_{-2}} cis-HCOH \\ cis-HCOH &\rightarrow^{k_3} H_2+CO \end{aligned} \quad (R2)$$

According to the mechanism the global rate is given by:

$$k = \frac{k_1 k_2 k_3}{k_{-1}k_{-2}+k_{-1}k_3+k_2 k_3} \quad (1)$$

The optimize the geometry and frequencies where determine at B3LYP/6-311g(2d,d,p) internal to CBS-QB3 methods, calculated using GAUSSIAN09 program. The reaction rate are determined using the APUAMA code [3], applying the tunneling correction of Wigner, Eckart and small curvature transmission coefficient [4,5], which is presented in the Arrhenius' form. Figure 1 below shows the rate for the dissociation reaction, and figure 2 the rate according equation (1).

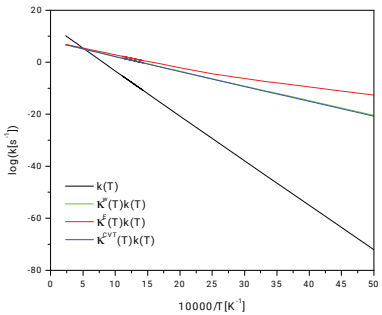


Fig.1 Dissociation reaction path

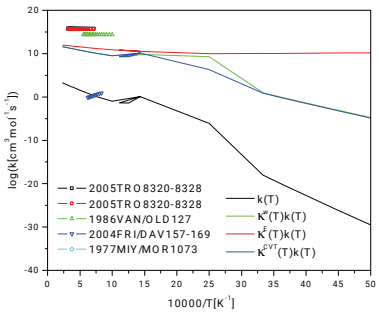


Fig. 2: Isomerization reaction path

**Key-words**: Rate constant; Quantum chemistry; Thermodynamic properties, H2CC

**Support:** This work has been supported by CAPES.

**References:**

[1] Nufida Dwi Aisyah et al., Procedia Engineering, 170, 119 (2017).
[2] M. Elango, G. S. Maciel, A. Lombardi, S. Cavalli, V. Aquilanti, Int. J. Qua Chem., 111, 1784 (2011).
[3] H.O. Euclides, P.R.P. Barreto, J Mol Model, 23, 176 (2017).
[4] Gonzalez-Lafont A., Truong T. N., Truhlar D. G., J. Chem. Phys. 95, 8875 (199
[5] Duncan W. T., Bell R. L., Truong T. N. J. Comput. Chem. 19, 1038 (1998).

# Implementation of Configurational Bias Monte Carlo Method to Sample Flexible Solute in Solvent Media

Henrique M. Cezar, Sylvio Canuto, Kaline Coutinho

*Institute of Physics, University of São Paulo, São Paulo, Brazil*

**Abstract:** The molecular structure has an important role in several processes in chemistry, physics and biology. In computer simulations, structures are usually sampled through either Monte Carlo (MC) or Molecular Dynamics (MD). The method of choice, usually depends on the system and the properties one is interested in investigating. To study flexible molecules usually MD is applied, since several efficient implementations are available and MC lacks a standard and established method to sample the molecular internal degrees of freedom of a molecule. This problem arises since the standard atomic displacements usually applied within MC are very inefficient to generate new configurations with large conformational changes. In this work we implemented and improved a Configurational Bias Monte Carlo (CBMC) method used to sample molecular conformations in solvent. Based on the work of Shah and Maginn [1,2] we implemented in the DICE package [3] a CBMC strategy that separates hard and soft degrees of freedom within a fragment scheme. By enforcing the detailed balance while obtaining the acceptance criterion, we guarantee that the correct ensemble is sampled. We checked and benchmarked our implementation [4] by using it to sample octane and 1,2-dicholoroethane in different solvents. The trans and gauche populations were compared with experimental data and results from MD simulations. In both cases the results had an excellent agreement. We observe that at least for those systems, the correct population is achieved faster with our CBMC implementation than with MD. The CBMC also has a lower autocorrelation time, and is less likely to get trapped in local minima.

**Key-words**: Sampling, Configurational Bias, Monte Carlo, solute, solvent.
**Support:** This work has been supported by the National Council for Scientific and Technological Development (CNPq)

**References:**

[1] J. K. Shah, E. J. Maginn J. Chem. Phys. 2011, 135(13), 134121.
[2] J. K. Shah, E. Marin-Rimoldi, R. G. Mullen, B. P. Keene, S. Khan, A. S. Paluch, N. Rai, L. L. Romanielo, T. W. Rosch, B. Yoo, E. J. Maginn. J. Comput. Chem. 2017, 38(19), 1727.
[3] K. Coutinho, S. Canuto, *DICE: A Monte Carlo Program for Molecular Liquid Simulation*, v: 2.9; University of São Paulo: Brazil, 2011.
[4] H. M. Cezar, S. Canuto, K. Coutinho (manuscript in preparation)

# Ground State Energy for Confined Hydrogen Molecule

Hugo de Oliveira Batael*, Elso Drigo Filho

*Universidade Estadual Paulista □J lio de Mesquita Filho□, Campus S□o Jos□do Rio Preto, Instituto de Biociências, Letras e Ciências Exatas*
**email:hugobatelll@gmail.com*

**Abstract:** The ground state energy for the confined $H_2$ molecule is computed by the Variational Method [1]. The approach proposed here uses the wave function molecular of the type Valence Bond (VB) [2], written as the sum of the covalent term with ionic term, for last term is given a weight different in relation the first term. The molecule is confined in impenetrable prolate spheroidal boxes. The atomic orbitals are built from previous suggestion inspired from the factorization of Schrödinger equation [3]. The aim of this work is to propose a simple wave function for confined hydrogen molecule, compared with wave functions found in literature [4]. The results obtained are in agreement with other results presents in the literature.

**Key-words**: **Molecular Confinement, Hydrogen Molecule, Variational Method.**
**Support:** This work has been supported by CAPES and FAPESP

**References:**

[1] Schiff, L. I.; Quantum Mechanics. 3. ed. New York: Mcgraw-hill, 1968
[2] Levine, I. N.; Quantum Chemistry, Prentice Hall, New York, USA, 1991.
[3] Drigo Filho, E.; Ricotta, R. M.; Phys. Lett. A 2002, 299, 137.
[4] Colín-Rodríguez, R.; Cruz, S. A.; J. Phys. B: At. Mol. Opt. Phys. 2010, 43, 235102.

# Homochiral salt of S-Fluoxetine Oxalate: Theoretical Insights on Preferential Crystallization of RS-Fluoxetine Antidepreessant

Hugo Gontijo Machado[1*], Paulo Sousa Carvalho Jr.[2], Valter Henrique Carvalho-Silva[1]

[1]*Grupo de Química Teórica e Estrutural de Anápolis, Ciências Exatas e Tecnológicas. Universidade Estadual de Goiás, CP 459, 75001-970 Anápolis, GO Brazil.*
[2]*Universidade de São Paulo, Instituto de Física de São Carlos, CP 369, 13560-970 – São Carlos, Brazil*

**Abstract:** Fluoxetine (FLX) is a beta-blockers antidepressant drug [1] currently marketed as a racemic salt (RS-FLX). However, due to higher potency of their metabolites, the S-FLX has a higher duration of action than R-FLX [2]. In the present study, S-FLX oxalate was separated by the preferential crystallization of the molecule with oxalic acid on the racemic mixture, and its structure determined by X-ray diffraction. Despite its importance, the chiral recognition mechanism of S-FLX is not sufficiently understood. In order to determine the motives that led to the preferential crystallization of S-FLX, an approximation for the R-FLX oxalate was performed by reversing the configuration of the S-form for the comparative effect of theoretical calculations. All the static calculations were performed using the Density Functional Theory (DFT) with the M062X/6-311G(d, p) level. The estimated lattice energy did not show significant differences for each enantiomer. The rigid potential energy surface (PES) scan of the dihedral angles of FLX (for solution enantiomers) have shown that the S-form has a higher conformational freedom than the approximate R-form. These results suggest that the mechanism leading to the preferential crystallization of the S-FLX probably occurs in crystal formation due to the differences between properties of the enantiomers in solution. With this in mind, another static calculations and Molecular Dynamics (CPMD) simulations was proposed in order to determine the behaviour of the enantiomers in solution with solvent effect.

**Key-words**: S-fluoxetine, RS-fluoxetine, preferential crystallization, potential energy surface

**Support:** The authors thanks PrP/UEG, FAPEG and CAPES for financial support.

**References:**

[1] C. Hiemke, S. Härtter, Pharmacology & therapeutics. 85(1), 11. (2000)

[2] D.T. Wong, F. P. Bymaster, L. R. Reid, Neuro. Psyc. Pharm., 8(4), 337, (1993)

# Molecular Modeling of Azo-Enaminone Derivatives in Solvent Medium: Investigation of the Nonlinear Optical Properties

Igo, T. Lima[1], Morgana, C. S. Santos[1], Demétrio A. S. Filho[2], Antonio, R. Cunha[1]

[1]*Universidade Federal do Maranhão, Campus Balsas, 65800-000, Balsas-MA, Brasil*
[2]*Universidade de Brasília, Campus Universitário Darcy Ribeiro, 70910-900, Brasília-DF, Brasil*

**Abstract:** Azo dyes are the most fundamental and representative class of commercial synthetic organic dyes [1]. These dyes have the azo group −N=N− in its molecular structures and are well-known by its applications like pigments, photoelectronics, optical storage technology, analytical chemistry and printing systems. In this work, we investigate the solvent effects in the nonlinear optical properties of the azo-enaminone derivative shown in the Figure below. We performed quantum chemical calculations and molecular dynamics simulations with different models considering the polarization for solute due to the presence of the solvent. Namely, the tetrahydrofuran, ethanol, water and dimethyl sulfoxide were included using both the implicit and explicit solvation models. Molecular Dynamics (MD) simulations, using the GROMCAS software were carried out with the azo-enaminone in aqueous solution. Quantum Chemical calculations using Gaussian 09 [2] package were performed to access the nonlinear optical properties, with the solvent described by both polarizable continuum model (PCM), [3] and point charges model [4]. Our results were compared to reported work of Machado, D.F.S. et al [5], which solvent medium was included only by PCM model.

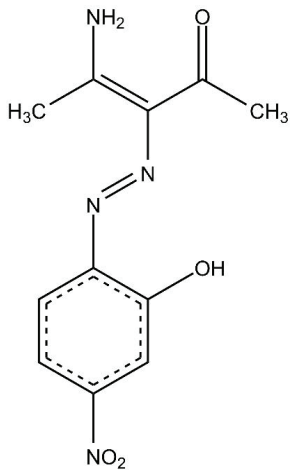

**Key-words**: Azo-enaminone, PCM, Molecular Dynamics.
**Support:** D.A.S.F. gratefully acknowledges the financial support from CNPq, grants 304020/2016-8 and 407682/2013-9, and FAP-DF grants 0193.001.062/2015 and 193.001.284/2016.

**References:**

[1] L. Zhang, J. M. Cole and X. Liu. J. Phys. Chem. C, 117, 26316, (2013).
[2] M. J. Frisch, et al. Gaussian 09, Revision D.01, Gaussian, Inc., (2009).
[3] S. Miertus, E. Scrocco and J. Tomasi. Chem Phys. 55, 117, (1981).
[4] M.J. Field, P. A.Bash and M. Karplus, J. Comput. Chem., 11, 700, (1900).
[5] D. F. S. Machado, T. O. Lopes, I. T. Lima, D. A. da Silva Filho, H. C. B. de Oliveira, J. Phys. Chem. C, 120, 17660, (2016).

# Metastability of the low-lying electronic states of $CBr^{2+}$: A CASSCF/MRCI Study

Igor Araujo Lins[1], Antonio Ricardo Belinassi[2], Fernando Rei Ornellas[2], Tiago Vinicius Alves[1]

[1]*Departamento de Físico-Química, Instituto de Química, Universidade Federal da Bahia, Salvador, Bahia, 40170-115, Brazil*

[2]*Departamento de Química Fundamental, Instituto de Química, Universidade de São Paulo, São Paulo, São Paulo, 05508-900, Brazil*

**Abstract:** Spectroscopic data for the low-lying electronic states of the doubly ionized cation, $CBr^{2+}$, are scarce due to the inherent difficulties related to the preparation and detection of this highly reactive ion. To the best of our knowledge, the only experimental evidence of this dication was reported in 1982 by Proctor et al. [1], who demonstrated by charge stripping mass spectrometry the existence of this species. In this context, the aim of this work is to present a reliable characterization of the metastability, structure, and spectroscopy of the low-lying electronic states of $CBr^{2+}$ thus extending our present knowledge of the halocarbon dications. For this purpose, the low-lying electronic states of $CBr^{2+}$ correlating with the two lowest dissociation channels was investigated at a high level theoretical approach, SA-CASSCF/MRCI. Spin-orbit interaction changes substantially the profile of the potential energy curves, specially for the ground ($X\ ^2\Sigma^+$) and first excited ($1\ ^2\Pi$) states. The second adiabatic ionization energies are also determined and show an excellent agreement with the experimental derived values. Tunneling widths computed for the Ω bound states show that the lowest vibrational levels of components 1/2 are stable against tunneling.

**Key-words**: Spectroscopic, Metastability, MRCI
**Support:** This work has been supported by CNPq, and FAPESB.
**References:**
[1] C. Proctor, C. Porter, T. Ast, J. Beynon Int. J. Mass Spectrom. 41, 251 (1982).

# Study of Local Reactivity of Ricin Toxic A chain Based on Conceptual Density Functional Theory

Igor Barden Grillo (PG), Gerd Bruno Rocha (PQ)

*Departamento de Química, Universidade Federal da Paraíba, João Pessoa, PB*

**Abstract:** The Ricin Toxic A chain RTA is a subunity of Ricin protein, which is a ribossome inactivator very toxic for humans. This protein is found in castor plant that is raw material for several valuable products. Hence, it is plenty interest in inactivation of RTA toxicity activity to insure industry biosafety[1]. The field computational molecular modeling provide useful tools to explore drug design, one of them that is growing for biological systems is the Reactivity Descriptors (RDs) developed by Hard and Soft Acid Base Theory, and Fukui's Frontier Molecular Orbital. The Conceptual Density Functional Theory rises in the process of establishing correspondence between the RDs and coefficients of the fundamental differential equation of DFT[2]. These descriptions cover global molecule's trends of charge transfer, polarization and electrostatic long range interactions[3]. Also, local reactivity trends derived from electron density changes as electron number vary[4]. Such descriptors are well established for small molecules, currently being applied for reaction rationalization[5], QSAR[6] and regioselectivity[4] studies. For large/biological system the application of RDs can be exemplified in the literature as: protonation state determination[7]; docking ligand score functions and evaluation of residue interactions[8]. Although, these studies relies on quantum mechanical methods with lack of electron correlation or without computing properly the protein and solvent environment effects on active sites. However, it is difficult to demand full ab initio treatment for such large systems as proteins. In the present work, we propose the use of Fragment Molecular Orbital (FMO)[9] method for efficient ab initio calculation to obtain local reactivity descriptors of RTA. FMO is a fragmentation scheme for quantum mechanical (QM) calculations that divides a large system in several monomers[9]. The FMO does not depend on empirical fitted parameters and are reported for providing accurate energies, orbital and densities for large system when compared with full ab initio calculations[10]. Then, we use the frontier molecular orbitals densities of RTA obtained with FMO to calculate the Fukui indices in order to describe local reactivity. The first calculations were performed using the 2-nbody FMO method[11] in GAMESS program, at HF/STO-3G level of theory without counting the solvent effect. The fragmentation was carried out using two protein residues by monomer. The Fukui indices for the electrophilic attack susceptibility from the electron density of a neutral charge state of RTA and a negatively charged. The results show that there is a spatial concentration of that descriptor, which is shown in Figure 1 by the rendered scalar field volume around the protein atoms. That region could indicate an active site for a electrophile ligand to react or dock. The FMO method allow us to calculate the descriptors using ab-initio or DFT treatment for a molecule containing more than 4000 atoms, accounting the electronic structure of the entire protein.

# Theoretical and Computational Description of Equivalent Chemical Bonds

Isabella D. M. S. Rosado (IC)[1], Juliana A. B. Silva (PQ)[2], Renaldo T. Moura Jr. (PQ)[3], Ricardo L. Longo (PQ)[1]

*[1]Universidade Federal de Pernambuco, Departamento de Química Fundamental, Recife, PE, Brazil. [2]Universidade Federal de Pernambuco, Centro Acadêmico do Agreste, Caruaru, PE, Brazil. [3]Universidade Federal da Paraíba, Departamento de Química e Física, Areia, PB, Brazil. email: isabella.msrosado2@ufpe.br*

**Abstract:** The chemical bond is a unifying concept that is widely employed in explaining and rationalizing many aspects related to the reactivity, selectivity and characterization of the different physical and chemical properties of molecules, substances and materials[1]. However, because it is not an observable it has been the source of debates and disputes, remaining a challenge to theoretical and computational chemistry[1]. One source of problems has been the approximations employed in the description of the chemical bond, particularly the orbital model or independent (quasi-)particle approximation. This leads to some apparent contradictions when applied to molecular spectroscopy of symmetric molecules such as angular $AH_2$ and tetrahedral $AH_4$. In these molecules, the A−H bonds are equivalent with the lengths, strengths and energies (degenerate), which lead to difficulties when describing the symmetric and antisymmetric stretches in their vibrational spectra as well as the presence of two peaks in the valence region of their photoelectron spectra. These have caused several erroneous conclusions and misconceptions regarding approximate theories and models used to describe the chemical bonds in these molecules. We propose to include the interactions between these equivalent bonds as a step towards solving these conceptual problems and allowing qualitative and quantitative interpretation of spectroscopic data. These interactions are treated as perturbations and the solution of the secular determinant within first-order perturbation theory for degenerate states provides the (partial) removal of degeneracy of the bond energies. In addition, this separation between the states is proportional to the strength of the perturbation, which can be related to chemical properties such as the bond pair-bond pair interaction. As result, the photoelectron and vibrational spectra of symmetric molecules can be explained within the scope of interacting equivalent and independent bonds.

In the vibrational spectra, the perturbation strength is proportional to the frequency difference between the symmetric and antisymmetric normal modes, which can be related to the coupling between the oscillators due to the removal of translational and rotational degrees of freedom. Thus, the perturbation represents the requirement for the center of mass of the molecule to remain unchanged during a vibration. Whereas, the peak separations in the valence region of photoelectron spectra represent the strengths of the interactions between the electron pairs in each chemical bond. Thus, this

approach may provide quantitative data for the valence shell electron pair repulsion (VSEPR) theory.

Quantum chemical methods (MP2 and DFT) were used to calculate the vibrational frequencies of symmetric molecules with different isotopes in order to correlate the reduced masses with the difference between the antisymmetric and symmetric wavenumbers $\Delta_{as}$. For methane ($CH_4$) a linear relationship between $\Delta_{as}$ and the inverse of the square-root of the carbon isotope mass was found, where the slope depends upon the hydrogen isotope mass employed. This analysis is being extended to other symmetric angular, pyramidal and tetrahedral molecules and a theoretical foundation for this relationship is being developed.

The valence ionization energies (IEs) of molecules with equivalent bonds were calculated with electron propagator methods and provided the difference between the IEs, $\Delta_{IE}$, which should be related to the bond-bond electron repulsion. The chemical bond overlap model (BOM) has been generalized and implemented with localized molecular orbitals, allowing the efficient treatment of polyatomic molecules[2]. BOM provides the overlap contributions for several properties of each chemical bond in a molecule such as charge density ($\rho_{OP}$) and polarizability ($\alpha_{OP}$). In addition, numerical integration yields the Coulomb repulsion ($J_{inter}$) between the overlap charge densities of each pair of bonds. Some trends were observed between $\Delta_{IE}$ and overlap properties ($\rho_{OP}$, $J_{inter}$) and preliminary analyses show (semi-)quantitative correlations. However, the calculations of $\Delta_{IE}$ need to be improved, because the comparisons with available experimental $\Delta_{IE}$´s indicate large non-systematic errors.

The proposed model based on perturbation theory for degenerate states is simple and can provide a unifying description of chemical bonds as well as yield quantitative results for important chemical properties or descriptors.

**Key-words**: chemical bond; perturbation theory; equivalent; interacting bonds.

**Support:** This work has been supported by CNPq, CAPES, FACEPE, PRONEX, PET-Química, UFPE and dQF.

**References:**

[1] (a) L. Pauling, The Nature of the Chemical Bond, 3rd edition, Cornell University Press, Ithaca, 1960; (b) R. J. Gillespie, P. L. A. Popelier, Chemical Bonding and Molecular Geometry: From Lewis to Electron Densities, Oxford University Press, New York, 2001; (c) F. Weinhold, C. R. Landis, Valency and Bonding: A Natural Bond Orbital Donor-Acceptor Perspective, Cambridge University Press, Cambridge, 2005.

[2] (a) R. T. Moura Jr., A. N. Carneiro Neto, R. L. Longo, O. L. Malta, J. Lumin. 170 (2016) 420; (b) R. T. Moura Jr., G. C. S. Duarte, T. E. da Silva, O. L. Malta, R. L. Longo, Phys. Chem. Chem. Phys. 17 (2015) 7731; (c) R. T. Moura Jr., O. L. Malta, R. L. Longo, Inter. J. Quantum Chem. 111 (2011) 1626; (d) O. L. Malta, R. T. Moura Jr., R. L. Longo, J. Braz. Chem. Soc. 21 (2010) 476.

# Ensemble docking studies of interaction between pesticides and acetylcholinesterase of mosquito and homo sapiens

I. A. Guerra(1)* and A. S. Gonçalves(1)

* *i.auroraguerra@gmail.com*

**Abstract:** In Brazil agrochemicals are consumed uncontrollably with a consumption of 725.6 thousand tons of pesticides, quantity would correspond to an average of 3.7 kilograms of agrochemicals per inhabitant [1]. An important position in this scenario are the agricultural activities in various regions of the country. The principal motivation of this work was to propose pesticides less toxic for the human health based at little difference between mosquito and human enzyme at the position 286, where in the human acetylcholinesterese (HuAChE) active site there is a tryptophan and at the mosquito acetylcholinesterase (MosAChE) a cysteine [2]. In this work was employed editing technical of three-dimensional molecules and structure optimization using current semi-empirical methods, homology-modelling, molecular docking and molecular dynamics to predicted in silic interaction energies between known and planning pesticides, with human acetylcholinesterase (HuAChE) and mosquito acetylcholinesterase (MosAChE). To analyze the structures generated after molecular dynamics and molecular docking calculations, the programs VMD, PyMOL and Autodock Tolls were used. Root mean square deviation (RMSD), total energy and root mean square fluctuation (RMSF) were analyzed using the XMGRACE program. With molecular docking was possible to predict interaction modes besides polar contact between receptors (HuAChE and MosAChE) and known pesticides. In this way, in the end of this work it is intended to obtain potential information so that future research groups can synthesize pesticides less harmful to human health.

**Key-words**: Ensemble docking, pesticides, acetylcholinesterase, mosquito.
**Support:** This work has been supported by IFES and FAPES, notice 006/2014 - process 67648479 by the financial support.

**References:**

[1] RIGOTTO, M.R. Agrotóxicos. Observatório de Conflitos Ambientais - Universidade Federal de Minas. 2014.

[2] Dou, D. et al. Novel Selective and Irreversible Mosquito Acetylcholinesterase Inhibitors for Controlling Malaria and Other Mosquito-Borne Diseases. Sci. Rep. 3, 1068; DOI:10.1038/srep01068 (2013).

# Evaluation of α-lapchones Reduction Sites through DFT and QTAIM calculations

Italo Curvelo Anjos[1], Yen Galdino de Paiva[2], Marília Oliveira Fonseca Goulart[2], Eufrânio Nunes da Silva Júnior[3], Gerd Bruno Rocha[1]

[1]*Departamento de Química, Universidade Federal da Paraíba*
[2]*Instituto de Química e Biotecnologia, Universidade Federal de Alagoas*
[3]*Departamento de Química, Universidade Federal da Minas Gerais*

**Abstract:** Quinones are a class of organic compounds which participate on a wide range of vital biochemical processes.[1] They have also been studied for their anticancer, anti-inflammatory, trypanocidal, and antimicrobial activity.[2] The ease of reduction is an important feature in the chemistry of quinones, and in some cases their redox potential correlates with the biological activity.[3,4] Thus, a molecular description of the reduction mechanism of quinones may prove useful to understand their role on many biochemical processes. In a recent study, two α-lapachone isomers (01 and 02, Figure 1) have been synthesized and their electrochemical properties have been evaluated.[5] Analysis of compound 01 electrogram suggests that the reduction site for the first and third reduction happen at the quinone moiety while the second reduction takes place at the nitro group. Although 01 and 02 differ only by the position of nitro group, they exhibited very different electrograms, and the reduction mechanism for 02 is still unclear. In this work, we study the reduction mechanism of compounds 01 and 02 by calculating the first three reduction intermediates and assessing the reduction site in each reduction. Full optimization and frequency calculations were performed for the neutral, -1, -2 and -3 anionic forms of compounds 01 and 02. Calculations were carried out using DFT and QTAIM approaches at M11-L/6-31+g(d,p) level and DMF as implicit solvent using PCM model. Both singlet and triplet states have been calculated for -2 forms, and both duplet and quartet for -3 forms. It has been found that singlet and duplet were the most stable states for -2 and -3 forms respectively. QTAIM charges points the quinone moiety as the first reduction site for both 01 and 02, as shown by the net charge difference between the neutral and -1 forms. In addition, $NO_2$ group and the quinone moiety are likely to be the second and third sites respectively for compound 01. Compound 02, on the other side, shows a similar change in the net charge over the quinone and nitro regions of about -0,3 for the second reduction. Therefore, the electron density change on going from -1 to -2 form is highly delocalized. It is unclear either the reduction site is spread along the structure or the anion undergoes an intramolecular charge transfer following the second reduction. Finally, the third reduction of compound 02 seems well localized at the quinone moiety. Results agree with experimental evidence of quinone and nitro groups being the most likely electroactive groups for these compounds and the reduction mechanism for compound 01. It also suggests that compound 02 dianion is partially stabilized by charge delocalization.


***Figure 1*** *$\alpha$-lapachones isomers 01 and 02*

**Keywords**: Quinones, Redox Potential, Density Functional Theory, Quantum Theory of Atoms in Molecules
**Support:** CENAPAD-SP, CAPES, CNPq

**References:**

[1] M. N. Silva, V. F. Ferreira, M. C. B. V. Souza, Quim. Nova, 26, 3, 407 (2003)
[2] F. C. Silva, S. B. Ferreira, C. R. Kaiser, A. C. Pinto, V. F. Ferreira, J. Braz. Chem. Soc., 20, 8, 1478 (2009)
[3] J. Koyama, I. Morita, N. Kobayashi, T. Osakai, H, Cancer Lett. (Shannon, Irel.) 212, 1 (2004)
[4] A-S Pan, H. Gonzalez, Mol. Pharmacol., 37, 966 (1990)
[5] E. F. G. Cruz, C. M. B. Hussene, G. G. Dias, E. B. T. Diogo, I. M. M. Melo, B. L. Rodrigues, M. G. Silva, W. O. Valença, C. A. Camara, R. N. Oliveira, Y. G. Paiva, M. O. F. Goulart, B. C. Cavalcanti, C. Pessoa, E. N. Silva Júnior, Bioorg. Med. Chem. 22, 1608 (2014)

# CORRELATION BETWEEN MOLECULAR ELETRONIC STRUCTURE, SENSITIVY TO EXPLOSION AND CHEMICAL STABILITY OF ENERGETIC MATERIALS: NITRAMINES

Marco Aurélio Souza de Oliveira, Itamar Borges Jr.

*Departamento de Química, Instituto Militar de Engenharia- Pça Gen Tibúrcio, 80, Urca, 22290-270, Rio de Janeiro-RJ, Brasil*

**Abstract:** Military explosives have extreme mechanical demands hence must withstand impact without initiating their detonation / deflagration. They also must have chemical stability during storage to resist to deterioration resulting from temperature variations and humidity. Among the different types of explosives, nitramines are a promising class of energetic materials for military used due to its great insensitivity and high energy content; e.g., nitroguanidine is a member of the class already in use. In this work, 21 nitramines molecules were investigated. Their geometries were optimized using the DFT/B3LYP//6-311+G(d) method and the Gaussian 09 program. Their molecular electronic densities were decomposed using two different atom-centered partition methods, the distributed multipole analysis (DMA) and the deformed atoms in molecules (DAM). From the partitioned electronic densities, mathematical relations were found between molecular properties and sensitivity to explosion of the nitramines following the approaches developed in our group for nitroaromatics [1,2]. Chemical stability employing this approach was also investigated. The results will be presented at the conference.

**Key-words**: Nitramines, electronic structure, impact sensitivity, chemical stability.

**Support:** Capes, CNPq, Faperj, Departamento de Ciência e Tecnologia (DCT) of the Brazilian Army.

**References:**

[1] Anders, G.; Borges Jr., I. The Journal of Physical Chemistry A 115, 9055 (2011).
[2] Giannerini, T.; Borges Jr., I. Journal of the Brazilian Chemical Society, v. 26, vol. 5, p. 851-859 (2015).

# A comparative DFT study on antioxidant-related properties of myricetin

Iuri N. Soares[1], Shawan K. C. Almeida[1], and Gabriel L. C. de Souza[1]

[1]*Departamento de Química, Universidade Federal de Mato Grosso, 78060-900 Cuiabá, Brazil*

**Abstract:** It is well known that the antioxidant potential of a given substance can be probed through its capability to scavenge free radicals [1]. The mechanisms related to the referred activity are (mainly): i) hydrogen-atom transfer (HAT), and ii) single electron transfer (SET) [2,3]. For the HAT mechanism, it is established that the weaker the O-H bond, the higher is the antioxidant activity. The bond dissociation enthalpy (BDE) is determined as the difference in the heat of formation between the molecule and corresponding radical, and thus corresponds to the O-H bond-breaking energy. In the SET mechanism, one electron is transferred from the neutral molecule to the free radical: the lower the ionization potential (IP), the easier is the electron abstraction. Hence, probing the bond dissociation energies (BDEs) and ionization potentials (IPs) of flavonols can aid in the identification of compounds that can be applied as phytotherapeutics. In order to compute the referred properties, the density functional theory (DFT) combined with several exchange-correlation functionals have been widely used.

In a very recent study, La Rocca *et al.* [4] benchmarked twenty-one (21) commonly used exchange-correlation functionals for the determination of the BDEs and IPs for two selected molecules that are well known to present antioxidant activity: quercetin and edaravone. The conclusion was that M05-2X [5], M06-2X [6], and LC-ωPBE [7] were the preferred functionals to compute the antioxidant behavior. Hence, in the present work, we decided to apply one of Minnesota family functionals (M06-2X), LC-ωPBE and the widely used B3LYP [8] to investigate the differences among BDEs and IPs determined using these three functionals in the case of another molecule known to be antioxidant: myricetin (chemical structure is shown in Figure 1).

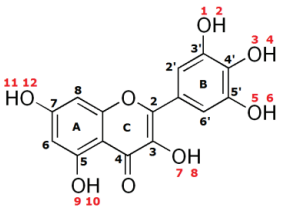


**Figure 1.** Representation of the chemical structure of myricetin.

Geometry optimizations, vibrational frequencies and energetics of the neutral molecule and their radicals were carried out using the B3LYP, M06-2X, and LC-ωPBE (UB3LYP, UM06-2X, ULC-ωPBE for the open-shell species) exchange-correlation

functionals with the 6-311G(d,p) basis set [9]. Solvent effects (for *n*-hexane, ethanol, methanol, and water) were included using the integral equation formalism polarizable continuum model. The Gaussian 09 software suite [10] was the software utilized.

The smallest BDE among the six OH groups of myricetin was determined to be the $O_3$-$H_4$ for all the three funcionals (in the gas phase or any solvent environment). The values obtained for the referred OH group are shown in Table 1 (IPs are also included).

| | BDE | | | IP | | |
|---|---|---|---|---|---|---|
| | **M06-2X** | **LC- ωPBE** | **B3LYP** | **M06-2X** | **LC- ωPBE** | **B3LYP** |
| gas phase | 69.89 | 65.00 | 63.43 | 167.21 | 167.79 | 157.98 |
| water | 73.75 | 68.56 | 67.15 | 137.17 | 134.03 | 108.31 |
| methanol | 73.25 | 68.84 | 66.67 | 135.10 | 134.68 | 126.08 |
| ethanol | 73.19 | 68.98 | 66.47 | 135.41 | 135.01 | 126.36 |
| *n*-hexane | 70.97 | 74.65 | 64.43 | 151.40 | 151.52 | 142.17 |

**Table 2.** BDEs and IPs for myricetin. The values are given in kcal.mol$^{-1}$ and were determined using the 6-311G(d,p) basis set.

It is possible to notice that BDEs values are much lower than IPs and, thus, the HAT will play a major role over the SET mechanism in the antioxidant activity of myricetin.

In a qualitative perspective, B3LYP and M06-2X present the same order for computed BDEs (gas phase<*n*-hexane<ethanol<methanol<water) while this trend is not observed for the results determined with the LC-ωPBE (which presents: gas phase<water<methanol<ethanol<*n*-hexane). On the quantitative point of view, the B3LYP and the M06-2X BDEs differ up to 6.7 kcal.mol$^{-1}$ (10.0 %). In comparison to the BDEs obtained with the LC-ωPBE, B3LYP results show good agreement with differences up to 2.9 %, except for the results probed in *n*-hexane (which differ in 15.8 %). However, the referred discrepancy can be neglected since the BDEs in water are most relevant for biological antioxidant activity. Therefore, B3LYP can be considered a decent choice in terms of functional for probing the antioxidant potential of myricetin. More results will be presented in the Conference.

**Key-words**: Antioxidant activity, myricetin, bond dissociation energy, ionization potential, density functional theory

**Support:** This work has been supported by CNPq.

**References:**

[1] I. Fernandez-Pastor *et al.*, J. Nat. Prod. 79, 1737 (2016).
[2] J. S. Wright *et al.*, J. Am. Chem. Soc. 123, 1173 (2001)
[3] M. Leopoldini *et al.*, J. Phys. Chem. A 108, 4916 (2004).
[4] La Rocca *et al.*, J. Mol. Model. 22, 250 (2016).
[5] Y. Zhao and D. G. Truhlar, J. Chem. Theo. Comp. 2, 364 (2006).
[6] Y. Zhao and D. G. Truhlar, Theor. Chem. Account. 120, 215 (2006).
[7] O. A. Vydrov and G. E. Scuseria, J. Chem. Phys. 125, 234109 (2006).
[8] A. D. Becke, J. Chem. Phys. 98, 5648 (1993).
[9] M. J. Frisch, J. A. Pople and J. S. Binkley, J. Chem. Phys. 80, 3265 (1984).
[10] M. J. Frisch *et al.*, Gaussian Inc., Wallingford CT, G09, Revision D.01 (2009).

# Estudo comparativo de diferentes métodos de ensemble generalizado em simulações computacionais de polímeros de pequenos comprimentos

J.C.O. Guerra

*Insituto de Física, Universidade Federal de Uberlândia*

**Resumo: Proteínas são os blocos construtores e as unidades funcionais de todos os sistemas biológicos, desempenhando funções as mais importantes. Há 20 aminoácidos naturais que a natureza usa para "fabricar" proteínas, os quais diferem-se entre si quanto ao tamanho e outras propriedades físicas e químicas. Mas, a diferença mais importante entre eles, no que diz respeito à determinação da estrutura da proteína, é sua hidrofobicidade. Uma cadeia de proteína aberta, sob condições fisiológicas, se dobrará em uma configuração tridimensional para desenvolver sua função, a qual é chamada de o estado nativo. Para proteínas globulares de domínio simples, o comprimento da cadeia é da ordem de 100 aminoácidos. A maioria das proteínas globulares de domínio simples solúvel em água é muito compacta, com uma forma aproximadamente arredondada. Um dos principais objetivos do problema de dobramento de proteínas é predizer a estrutura dobrada tridimensional para uma dada sequência de aminoácidos. É claro que parâmetros ambientes de caráter físico ou físico-químico (como a temperatura e o pH) irão definir se uma dada proteína estará dobrada ou desdobrada. Contudo, a força hidrofóbica é a força diretora essencial no processo de dobramento terciário [1]. A estrutura dobrada de uma proteína funcional é termodinamicamente estável sob condições fisiológicas. Entretanto, mesmo uma pequena mudança das condições ambientes, tais como, temperatura e pH, poderá desestabilizar a fase dobrada. A desestabilização efetivamente torna a contribuição entrópica à energia livre dominante relativamente à contribuição energética levando ao decaimento do seu núcleo hidrofóbico. Isso não necessariamente significa um desdobramento globular da proteína de imediato. Uma fase conformacional intermediária compacta poderá permanecer estável. Veremos em seguida que o estudo e a compreensão do comportamento estrutural e as transições conformacionais experimentadas por polímeros e proteínas têm atraído cada vez mais atenção da comunidade científica nas últimas décadas, pela sua relevância científica e tecnológica. Tomemos o caso relevante de polímeros de pequenos comprimentos [2, 3]. Com a introdução e consequente disponibilização de técnicas experimentais de alta resolução e a demanda pela nanofabricação de aplicações moleculares, a investigação das propriedades estruturais de peptídeos sintéticos quando ancorados em substratos (metálicos ou semicondutores) tem permitido o projeto e aplicação de nanodispositivos híbridos [2]. Outro campo fascinante diz respeito ao estudo de fases conformacionais induzidas por nanofios ultra-finos atrativos, isto é, substratos com topologia unidimensional [3]. Em todos os casos,**

**contudo, modelos simplificados de polímeros ou proteínas são utilizados. Os chamados modelos de granulação grosseira (coarsed-grained models) são empregados desde que transições conformacionais acompanhando processos de estruturação molecular exibem similaridades com transições de fase termodinâmicas e, com isso, deve ser possível caracterizá-las por meio de um conjunto fortemente reduzido de graus de liberdade efetivos. Uma vez que a caracterização de macroestados conformacionais por espaços de parâmetros de baixíssima dimensão é possível, são introduzidas subestruturas de granulação grosseira. Nos tratamentos mais simples, apenas dois tipos de aminoácidos são intoduzidos: resíduos hidrofóbicos e resíduos polares. Simulações de Monte Carlo têm sido empregadas a heteropolímeros hidrofóbico-polar de modo a investigar transições conformacionais [4] e de modo a obter-se o diagrama de fases estruturais do polímero sob diferentes condições [2, 3]. Simulações de Monte Carlo-Metropolis simplesmente não são algoritmicamente eficientes para se obter uma amostragem abrangente do espaço configuracional. Logo, técnicas de ensemble generalizado, como, por exemplo, temperamento paralelo, abordagem multicanônica, e Wang-Landau têm sido extensivamente usadas com esse propósito. Neste trabalho, pretende-se discutir e aplicar esses diferentes métodos com o objetivo de se comparar sua eficiência. Para isso, aplicaremos os diferentes métodos de ensemble generalizado a um homopolímero de granulação grosseira de diferentes comprimentos. Um parâmetro para medir a eficiência da amostragem será introduzido, o qual levará em consideração tanto o espaço configuracional varrido durante a simulação quanto o tempo de computação. Em todos os casos, quantidades de flutuação, como o calor específico, serão plotadas contra a temperatura, pois sinalizam relevantes transições conformacionais experimentadas pelo polímero. Um tal estudo é extremamente importante devido ao fato de que simulações computacionais de sistemas poliméricos possuem um custo simulacional não trivial, mesmo levando em conta um aumento das capacidades computacionais ano após ano. Assim, determinar a eficiência dos diferentes métodos de ensemble generalizados atualmente disponíveis permite à comunidade científica discernir entre os melhores métodos simulacionais presentes e, possivelmente, atuar como catalizador para que novos e mais eficientes métodos possam vir a ser projetados.**

**Palavras-Chave**: Mecânica Estatística de Polímeros, Dobramento de Proteínas, Transição de fase, Simulações de Monte Carlo, Métodos de ensemble generalizado

**Suporte:** Este trabalho foi suportado pela Fapemig

**Referências:**

[1] M. Bachmann, W. Janke, Proceedings of the Conference “Path Integrals – New Trends and Perspectives”, 531 (2008).
[2] M. Bachmann, W. Janke, Physical Review Letters, 95, 058102 (2005).
[3] T. Vogel, M. Bachmann, Physical Review Letters, 104, 198302 (2010).
[4] M. Bachmann, Physics Procedia, 3, 1387 (2010).

# Molecular dynamics simulations of *Plasmodium falciparum* Fe-superoxide dismutase

Janay Stefany C. Araújo[1], David B. Costa Júnior[1], Larissa de M. Oliveira[1], Pedro Sousa Lacerda[2], Manoelito C. Santos Junior[1], Franco Henrique A. Leite[1]

[1]Programa de Pós-graduação em Ciências Farmacêuticas, Universidade Estadual de Feira de Santana; [2] Serviço Social da Indústria – BA;
*janay@hotmail.com.br*

**Abstract:** Malaria is a parasite disease caused by *Plasmodium* spp. that affects 214 million people, with more than 400,000 deaths per year [1]. Among the protozoan species, *P. falciparum* is responsible for almost severe form, cerebral malaria and deaths due to malaria. Despite of epidemiological data, drugs available for its treatment have limited efficacy and safety profile [2]. Aiming at circumvents this dilemma, key enzymes of the parasite can be targeted to identify new promisse drugs. Fe-superoxide dismutase from *P. falciparum* (*Pf*Fe-SOD) plays a crucial role against reactive oxygen species (ROS) that are likely formed during intraerytrocitic stage due to haemoglobin breakdown and can be lethal for parasites. Thus, this target is considered a promising target for drug development. However, it would appear difficult to inhibit *Pf*Fe-SOD using classical 'active-site directed' approaches, because the orthosteric site can acommodade just two atoms (e.g. superoxide). Thus, molecular dynamics (MD) simulations on GROMACS 5.1.2 program [3] were employed to predict potential allosteric site. The AMBER99SB-ILDN force field [4] was adapted to support $Fe^{+2}$ cations on a non-bonded model [5]. The interactions were described by a potential with Coulombic and Lennard-Jones terms obtained through various particle mesh Ewald (PME) simulations and chosen to minimize the error the experimenttal values of hydration free energy (HFE) and distance between the ion and the oxygen of the first solvation shell (ion-oxygen distante, IOD). The selected water model was single point charge extended (SPC/E) because it had the fewest error for $Fe^{2+}$ [5]. The MD simulations (70 ns) were performed with a periodic boundary in the NPT (T = 298 K, P=1 atm). We used a time step of 2 ps and a short range interaction cuttof radius of 1.4 nm. The convergence parameters from MD (Fig. 1) suggest stability after 35 ns (RMSD = 0.16 ± 0.03 nm) with normal fluctuations from c-alpha (RMSF < 0.11 ± 0.04 nm; except for loops regions). The most representative structure was selected by the GROMOS clustering algorithm with a 0.25 nm cut-off then submitted to AlloSite 2.0 to predict allosteric sites [6]. The covariance matrix (Fig. 2; maximum: 0.0671; minium: -0.0168) suggests some correlation between a predicted site and the active one. A maximum inter-site value of 0.005 between the pairs HIS26B/TYR27B, and minimum intersite value of -0.005 between the pairs HIS161/TYR9B, HIS161A/PRO82B, HIS26A/PRO82B and HIS26A/CYS84B. This possible allosteric site will be use for virtual screening campaings to indetify promise allosteric *Pf*Fe-SOD drugs against malaria.

**Figure 1: Convergence parameters from MD simulations:** RMSD (C-alpha) (a) and RMSF (C-alpha) (b) of PfFe-SOD during the DM simulations. The highlighted areas in RMSD and RMSF graphics correspond to productive phase and loops regions respectively.

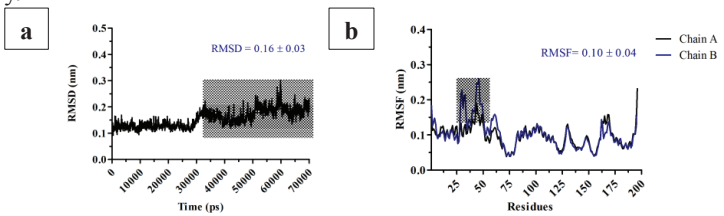


**Figure 2: Correlation matrix reduced to show only the predicted allosteric site by the active site:** the active site (vertical axis) by the predicted allosteric site (horizontal axis) correlation. The red surface on the structure represents the allosteric prediction.

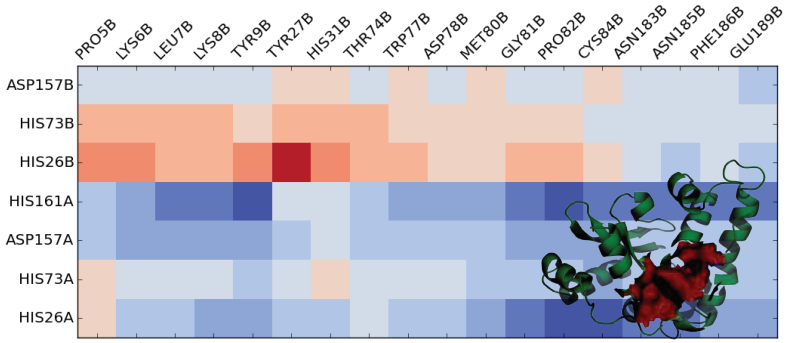


**Keywords:** Allosteric site, malaria, molecular dynamics, superoxide dismutase.

**Support:** State University of Feira de Santana and CAPES.

**References:**

[1] World Healthy Organization (WHO), World Malaria Report (2016), Geneva.
[2] F. H. Leite, A. L. Fonseca, R. R. Nunes, M. Comar Junior, F. P. Varotti, A. G. Taranto, Biochemistry and Biotechnology Reports, 2, 4 (2014).
[3] D. Van der Spoel, E. Lindahl, B. Hess, G. Groenhof, A. E. Mark, H. J. Berendsen, Journal of Computational Chemistry, 26, 16 (2005).
[4] K. Lindorff-Larsen, S. Piana, K. Palmo, P. Maragakis, J. L. Klepeis, R. O. Dror, D. E. Shaw, Proteins, 78 (2010).
[5] P. Li, B. P. Roberts, D. K. Chakravorty D. K., Merz Jr K. M., Journal of chemical theory and computation, 9, 6 (2013).
[6] W. Huang, S. Lu, Z. Huang, X. Liu, L. Mou, Y. Luo, Y. Zhao, Y. Liu, Z. Chen. T. Hou, J. Zhang, Bioinformatics, 29, 18 (2013).

# Global and local reactivity descriptors based on quadratic and linear energy models in α, β-unsaturated systems

Javier Oller, Esteban Vöhringer-Martinez
*Departament of Physical Chemistry, Faculty of Chemistry, University of Concepción; Chile.*
*ollerjavier@gmail.com*

**Abstract:** Global and local descriptors of chemical reactivity can be derived from conceptual density functional theory. Their explicit form, however, depends on how the energy is defined as a function of the number of electrons. Here, within the existing interpolation models the quadratic energy and the linear model were used to derive global descriptors as the electrophilicity (defined by Parr) and nucleophilicity (defined as the negative of the ionization potential), and local descriptors employing either the corresponding condensed fukui function in the linear model or the local response of the global descriptor in the quadratic model [1,2].
As test systems alpha, beta-unsaturated organic molecules have been studied, varying the heteroatom, resulting in alpha, beta-unsaturated thioesters, esters and amides. Specifically, the reduction of the neutral systems and following electrophilic attack by carbon dioxide reactions have been studied. These reactions represent the rate limiting steps in carboxylation reactions of thioesters under enzymatic environment studied experimentally by Erb et al. [3].
The respective descriptors for each molecule were calculated in the gas and solvent phase (water), using wB97X-D3 / 6-311G (d,p) level of theory. The calculation of the respective condensed fukui functions to derive the local descriptors was performed within the FMO (frontier molecular orbitals) approach using the Hirshfeld-I partitioning method [4].
Our results identify correctly the most reactive atom in each molecule for each reaction and show a correlation between the global descriptors and the local descriptors for the same energy model (quadratic, linear). The obtained descriptors agree with the reported experimental reactivity and present therefore a valuable tool to predict reactivity in heterogeneous environments.

**Key-words**: Conceptual DFT, condensed fukui function, global and local reactivity descriptors.

**Support:** This work has been supported by Beca Doctorado Nacional 2015 CONICYT folio #21150596.

**References:**

[1] F. Heidar-Zadeh, R. A. Miranda-Quintana, T. Verstraelen, P. Bultinck, and P. W. Ayers., J. Chem. Theory. Comput. 12, 5777 (2016).
[2] F. Heidar-Zadeh, S. Fias, E. Vohringer-Martinez, T. Verstraelen, and P. W. Ayers., Theor. Chem. Acc. 136, 19 (2017).
[3] T. J. Erb, et.al., Proc. Nati. Acad. Sci. USA. 106, 8871.(2009)
[4] Bultinck et al., J. Chem. Phys, 126, 144111.(2007)

# Electronic structure and spectroscopic properties of the scandium monosulfide, ScS

João Gabriel Farias Romeu, Antonio Ricardo Belinassi, Fernando R. Ornellas

*Departamento de Química Fundamental, Instituto de Química, Universidade de São Paulo, Av. Prof. Lineu Prestes, 748, São Paulo, São Paulo, 05508-000, Brazil*

**Abstract:** Scandium, with a single d-electron, has a referential role in understanding and studying the electronic structure and reactivity of systems involving transition metals atoms. Diatomic systems containing transition metals atoms, such as monoxides and monosulfides, besides their intrinsic chemical relevance, are also important in astrophysical studies, since there are detections of some oxides and sulfides in variable stars [1,2]. Nevertheless, in the case of scandium monosulfide, ScS, there are very few spectroscopic data available in the literature, including those determined through experimental and theoretical studies. Moreover, the high density of electronic states relatively close to the lowest-lying states hinders its analysis and characterization, making the investigation of diatomic systems containing transition metals elements much more challenging comparatively to other diatomic molecules.

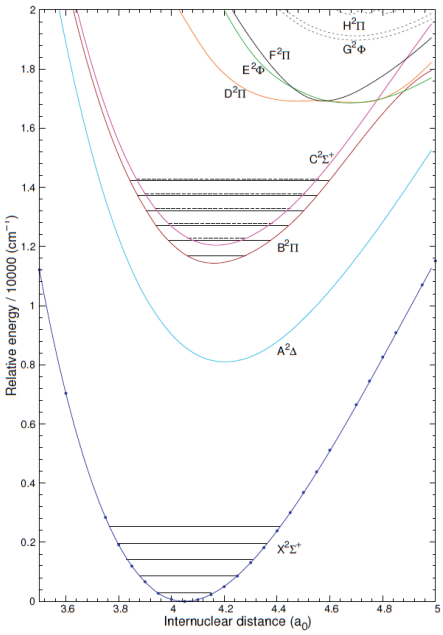


Fig. 1. PEC associated to the lowest-lying states near equilibrium region.

Our theoretical approach to describe the electronic states makes use of the state-averaged complete active space self-consistent field (SA-CASSCF) [3, 4] and the multireference configuration interaction (MRCI) [5, 6] methods, both implemented in the Molpro suite of programs [7], and a cc-pV5Z basis set [8, 9]; all doublet states associated to the two lowest-lying dissociation channels were calculated.

In the present work, a characterization of the doublet electronic states of the ScS molecule associated with the lowest-lying dissociation channels is presented via potential energy curves (PEC) from the equilibrium region to the dissociation limit and the associated set of spectroscopic parameters. The closeness of the second and the third dissociation channels gives rise to difficulties in describing the electronic states at higher energies, but does not influence the description of the major states investigated in this study, which are shown in Fig. 1, including their associated vibrational levels. For the ground

state, X $^2\Sigma^+$, the prediction of $\omega_e$ equal to 569.8 $cm^{-1}$ shows a very good agreement with the experimental one, 565.2 $cm^{-1}$ [10], a significant improvement relative to the theoretical ones of 608 $cm^{-1}$ and 503 $cm^{-1}$, using single and double excitation configuration interaction (SDCI), and coupled-pair functional (CPF) approaches, respectively. For the C $^2\Sigma^+$ state, the set of constants ($R_e$, $\omega_e$, $T_e$) of (4.169 $a_0$, 503 $cm^{-1}$, 12 040 $cm^{-1}$) is also quite concordant with those obtained experimentally (4.1596 $a_0$, 488.74 $cm^{-1}$, 12 455.77 $cm^{-1}$) [11]. For the new $^2\Delta$ state, predicted theoretically [12], with values of $T_e$ and $\omega_e$ varying from 6803 to 8996 $cm^{-1}$ and from 488 to 513 $cm^{-1}$, respectively, according to the methodology employed, are also well described; for the $T_e$ and $\omega_e$ parameters, are values of 8086 $cm^{-1}$ and 504 $cm^{-1}$, respectively, are expected to be much more reliable than existing ones. All the four states studied are very polar, showing an increasing polarity in the order X $^2\Sigma^+$ < C $^2\Sigma^+$ < B $^2\Pi$ < A $^2\Delta$. Besides the electronic transitions for the systems, B $^2\Pi$ – X $^2\Sigma^+$, C $^2\Sigma^+$ – X $^2\Sigma^+$, we also report the one for the B $^2\Pi$ – A $^2\Delta$ transition. With the transition moment functions, we also evaluated transition probabilities and radiative lifetimes, thus improving significantly the characterization of this system.

Considering the reliability of the results obtained in this study in describing experimentally known states and the new ones, it is expected that this investigation can guide and motivate additional experimental and theoretical investigations involving this molecule and related systems in the future, by providing new data and new tools to approach similar diatomic molecules calculations.

**Key-words**: Spectroscopy, ab initio methods, electronic states, scandium monosulfide, CASSCF/MRCI.

**Support:** This work has been supported by Fundação de Amparo à Pesquisa do Estado de São Paulo (FAPESP) and by Conselho Nacional de Desenvolvimento Científico e Tecnológico (CNPq).

**References:**

[1] J. Jonsson, O. Launila, B. Lindren, Mon. Not. R. Astron. Soc., **258**, 49 (1992).
[2] J. Jonsson, B. Lindren, A. G. Taklif, Astron. Astrophys., **246**, L67 (1991).
[3] P. J. Knowles and H. -J. Werner, J. Chem. Phys. **82**, 5053 (1985).
[4] H. -J. Werner and P. J. Knowles, Chem. Phys. Lett. **115**, 259 (1985).
[5] P. J. Knowles and H. -J. Werner, Chem. Phys. Lett. **145**, 514 (1988).
[6] H. -J. Werner and P. J. Knowles, J. Chem. Phys. **89**, 5083 (1988).
[7] MOLPRO is a package of *ab initio* programs written by H. -J. Werner, P. J. Knowles, with contributions of A. Almlöf, D. Amos, A. Berning, *et alli*.
[8] N. B. Balabanov and K. A. Peterson, J. Chem. Phys., **123**, 064107 (2005).
[9] D. E. Woon and T. H. Dunning, Jr., J. Chem. Phys., **98**, 1358 (1993).
[10] R. Stringat and B. Fenot, Can. J. Phys., **54**, 2293 (1976).
[11] J. Gengler, J. Chen, T. C. Steimle, R. S. Ram, and P. F. Bernath, J. Mol. Spectrosc., **237**, 36 (2006).
[12] C. W. Bauschlicher, Jr. and S. R. Langhoff, J. Chem. Phys., **85**, 5936 (1986).

# A new approach for sampling descriptors in 4D-QSAR methodology using computational geometry

Authors: João Vitor Soares Tenório[1], Loïc Pascal Gilles Cerf[1], João Paulo Ataide Martins[2]

*(1) Computer Science Department, Federal University of Minas Gerais*
*(2) Chemistry Department, Federal University of Minas Gerais*

**Abstract:** The quantitative structure-activity relationship (QSAR) is an important research field in theoretical medicinal chemistry, which deals with the prediction of the biological activities of new compounds using mathematical relationships based on structural, physicochemical and conformational properties of previously tested potential agents [1]. A recently developed 4D-QSAR approach named LQTA-QSAR [2], is based on the generation of a conformational ensemble profile, CEP, for each compound followed by the the calculation of 3D descriptors for a set of compounds. This methodology explores jointly the main features of CoMFA [3] and Hopfinger's 4D-QSAR [4] paradigms. LQTA-QSAR makes use of the GROMACS free package to run the molecular dynamics, MD, simulations. The CEPs generated by the MD simulations are aligned and put into a virtual 3D box or grid, which acts like a virtual receptor, and different types of atoms, ions or functional groups, called probes, are used to compute the energy values for the interactions that the selected probe experiences in a respective position of the regular 3D lattice using LQTAgrid program.

One problem observed with the approach described above is that the probe crosses the CEP of the compound and some descriptors presents unrealistic values when the probe falls into or close to an atom of the CEP. Besides, as the 3D lattice plays the role of the receptor, points inside the CEP cannot be associated to a portion of the receptor interacting with the ligand.

This work presents a new approach to generate the 3D region that plays the role of the virtual receptor. Our method takes into account the shape of the CEP using computational geometry algorithms to prevent the probe passes through the points inside the CEP. First, the region which envelop the CEP of each compound in 3D lattice is estimated by generating a convex hull, that is the smallest convex polyhedron containing the atoms of the CEP [6].

After the convex hull generation, the points of the path that the probe must travel are sampled in polar coordinates, to explore the shape of the convex hull efficiently. First, the proposed method requires three parameters:  , which is the variation of each angle of the spherical coordinates in each step, $\Delta r$ which is the radius variation of the coordinate, and $N$, which is the number of times the radius will be varied in a step

equals to $\Delta r$. For each angle step, the initial radius value is defined as the intersection of the angle with the convex hull incremented with the predefined distance equals to 1.5 Å. Then, that point is collected and the remaining $N$-1 points varying up the radius with step equals to $\Delta r$. In this way, the points are sampled respecting a minimum distance of 1.5 Å and the maximum distance of 1,5 Å+(N-1)*$\Delta r$ from a point to the convex hull. In the present work, these parameters were empirically defined as $\Delta\theta$=3, $\Delta r$=1 e $N$=7.

In order to validate this new approach two data sets of compounds were investigated and QSAR models were built. The first data set (data set 1) is formed by 49 compounds used as target of study in the development of new drugs against prostate cancer. The second data set (data set 2) is formed by 48 compounds with antimalarial activity. After a variable selection with OPS algorithm [5] a PLS model was built for each data set and the results are presented in Table 1.

**Table1:** Statistical parameters for QSAR models obtained

| Data set | Nº of variables | Nº of latent variables | $R^2$ | RMSEC | $Q^2$ | RMSECV |
|---|---|---|---|---|---|---|
| 1 | 10 | 3 | 0.58 | 0.46 | 0.51 | 0.50 |
| 2 | 16 | 8 | 0.87 | 0.24 | 0.73 | 0.35 |

These results are very promising, since no models with $Q^2$ superior to 0.50 were obtained with descriptors generated with the original approach and the descriptors generated with this new approach are more physically meaningful.

In order to obtain better results other regression methods will be tested. Besides, an external validation will be performed.

**Key-words**: LQTA-QSAR, Molecular dynamics, Convex hull, Computational Geometry

**Support:** This work has been supported by FAPEMIG and CAPES

**References:**

[1] M. M. C. Ferreira, J. Braz. Chem. Soc., 13, 742 (2002).
[2] J. P. A. Martins, E. G. Barbosa, K. F. M. Pasqualoto, M. M. C. Ferreira, J. Chem. Inf. Model., 49, 1428 (2009).
[3] R. D. Cramer, D. E. Patterson, J. D. Bunce, J. Am. Chem. Soc., 110, 5959 (1988).
[4] A. J. Hopfinger, S. Wang, J. S. Tokarski, B. Jin, M. Albuquerque, P. J. Madhav, C. Duraiswami, J. Am. Chem. Soc., 119, 10509 (1997).
[5] R. F. Teófilo, J. P. A. Martins, M. M. C. Ferreira, J. Chemom., 23, 32 (2009).
[6] M. Berg, O. Cheong, M. Kreveld "Computational Geometry: Algorithms and Applications." (2008), Springer-Verlag TELOS, Santa Clara, CA, USA, 3rd edition.

# Vibrational and Electronic Properties of Carbon Dioxide Absorbed in Graphene Nanosheets

João Paulo Cascudo Rodrigues, Wiliam Ferreira da Cunha, Pedro Henrique de Oliveira Neto, Ricardo Gargano

*Institute of Physics, University of Brasília – UnB, Brasília, Brazil*

**Abstract:** Graphene has turned into a key material in chemistry, condensed matter physics, and materials science in view of their unique structural features[1]. Acting as a platform for anchoring catalyst, photodetectors, solar cells, and battery devices, graphene systems have already found various applications[2]. In this work, we investigated the electronic and vibrational properties of multi-layers graphene sheets interacting with a CO2 molecule. Electronic structure calculations were performed by means of density functional theory (DFT). The possible equilibrium geometries and binding energies were evaluated using Gaussian09 at the B3LYP level using the 6-31G** basis set. In order to evaluate the potential energy curves, we performed several single points DFT calculations for varying distances between the Carbon-dioxide molecule and the graphene sheet, as in ref[3]. Using an extended Rydberg function[4], we fit the potential energy curve, thus obtaining an analytical expression. Following, through the application of the DVR methodology[5], we used the analytical expression in the solution of the Schrodinger nuclear equation in order to obtain rovibrational energies. The results presented here may provide guidance to the understanding of the underlying science of Carbon-dioxide absorption in graphene nanosheets.

**Key-words**: carbon dioxide absorption, potential energy curve, density functional theory

**Support:** This work has been supported by the Brazilian Research Councils CNPq, CAPES, and FAPDF.

**References:**

[1] W. F. Cunha, P. H. O. Neto, A. Terai, G.M. Silva Phys. Rev B. 94, 014301 (2016)
[2] A. Zurutuza, C. Marinelli Nat. Nanotechnology 9, 730 (2014)
[3] P. E. Costa, W. F. Cunha, P. H. O. Neto, G.M. Silva, J. B. Martins, R. Gargano, J. Phys. Chem. A, 117, 2854, 2013.
[4] J. N. Murrel, S. Carter, S. C. Farantos, P. Huxley, A. Varandas, A. "Molecular Potential Energy Functions" (1984), Wiley, Chinchester, U.K., 1984.
[5] J. J. Neto, L. S Costa, Braz. J. Phys. 28, 111 (1998)

# Simulation of the AHAS-imazaquin system by Molecular Dynamics to design an enzyme-based AFM nanobiosensor

João Vitor Afonso Borges(IC) ,Renan Faria Guerra(PG)*, Eduardo de Faria Franca(PQ)

*Laboratory of Crystallography and Computational Chemistry, Chemistry Institute, Federal University of Uberlândia – *renanfg@ufu.br*

**Abstract:** The monitoring of herbicides in the environment is extremely important to prevent and control contamination. The development of nanobiosensors is a powerful alternative because of the speed and accuracy of analysis [1-4]. In this study, our goal was develop and describe a molecular model of the enzyme-inhibiting interaction, which can be used for an optimized projection of an Atomic Force Microscope (AFM) nanobiosensor to detect pesticides molecules used in agriculture, in order to evaluate its accordance with limit levels stipulated in valid legislation for its use. Molecular Dynamics were performed to study the system Acetohydroxiacid Synthase (AHAS) and an herbicide inhibitor of its activity, imazaquin (IQ) – a typical member of imidazolinone family [5] (Figure 1).

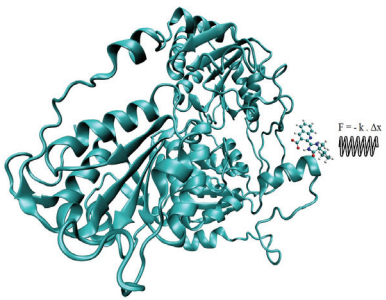


**Figure 1:** Possible unbinding pathway imazaquin from the AHAS active site.

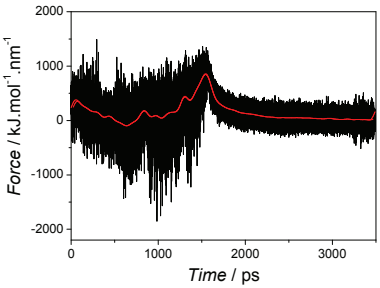


**Figure 2:** SMD force-extension profil between IQ and AHAS active site.

In order to study the system AHAS-IQ (PDB-1Z8N) in the presence of FAD and TPP cofactors, a Molecular Dynamic was carried for 20 ns with 42169 *tip3p* water molecules. After that, a Steered Molecular Dynamics (SMD) was carried for 3.5 ns in vacuum applying to the distance constraints between the IQ and active site of AHAS-TPP with a force constant of 367 $kJ.mol^{-1}.nm^{-1}$ and a constant velocity of 0.001 $nm.ps^{-1}$. Molecular dynamics simulations were performed using GROMACS 4.6.5 program in an NVT ensemble (298K) with CHARMM27 force field [6].

The total energy for the enzymatic system (Figure 1) is almost constant along the 20 ns of simulation (- 1,413 x $10^6$ kJ.mol$^{-1}$). Conformational stability of enzyme was showed calculating the Radius of Gyration (2,595 ± 0,029 nm) and RMSD (0,235 ± 0,006 nm), which confirm a small systematic fluctuation of protein in aqueous solution. The initial and final structures were compared using the Ramachandran plotting and results obtained shown no eligible differences $\varphi$ and $\psi$ dihedral angles from the initial and final structure after 20 ns of MD trajectory. The Figure 2 shows the force-extension profiles of the interaction between IQ and AHAS active site with the presence of FAD and TPP substrates. It is observed that the maximum of force necessary required to remove the herbicide from active site occurs at about 500 kJ.mol$^{-1}$.nm$^{-1}$, around 100 ps, from the start of the simulation, which can be attributed to the moment of rupture of the main interactions between residues of active site of the enzyme with the IQ. Another maximum peak can be observed around 1500 ps associated to the complete separation of the IQ molecule and the external amino acids residues of enzyme.

Experimental data of adhesion force using functionalized AFM tip with the enzyme ALS on three different substrates contaminated with the herbicide imazaquin (K = 0.20 N.m$^{-1}$) obtained an average of 40 (±4) nN [7]. The average force was calculated in the time interval from $t_i$ = 0 to $t_f$ = 65 ps and an average force of 0.39 (±0.2) nN per enzyme was obtained. Considering the standard deviation of the analysis of mean force obtained from SMD curve is a multiple of the experimental data. Therefore, the theoretical results validated the AHAS-IQ system proposed and are useful to predict optimized conditions for the fabrication of AFM nanobiosensors with high sensitivity.

**Key-words**: Nanobiosensor, Atomic Force Microscopy, Imazaquin, Molecular Dynamics.

**Support:** This work has been supported by FAPEMIG (CEX-APQ-02176-11), CNPq, FAPEMIG (2015-EXA052), and Rede Mineira de Química (RQ-MG).

**References:**

[1] J. Ding, et al., Sensors and Actuators, B: Chemical, 199, 284–290 (2014).
[2] M. A. Espinoza, et al., Analytical Biochemistry, 457, 85–90 (2014).
[3] T. M. H. Lee, Sensors, 8, 5535–5559 (2008).
[4] G. C. Oliveira, et al., Talanta, 98, 130–136 (2012).
[5] M. F. Oliveira, et al., Pesquisa Agropecuária Brasileira, 39, 787–793 (2004).
[6] A. D. Mackerell, et al., The Journal of Physical Chemistry B, 102, 18 (1998).
[7] D. K. Deda, et al., Materials Research 16(3), 683–687 (2013).

# Theoretical Study of ion mobility of isomers in different drift gases

Jorge Leonardo O. Santos[1], José Diogo L. Dutra[1], Priscila M. Lalli[2], Marcos N. Eberlin[2] and Ricardo O. Freire[1]

[1]*Pople Computational Chemistry Laboratory, Department of Chemistry, UFS.*
[2]*ThoMSon Mass Spectrometry Laboratory, Institute of Chemistry, UNICAMP.*

**Abstract:** A new dimension for ion analysis has been added to Mass Spectrometry, via its coupling with ion mobility spectrometry (IMS), where the separation of isomers occurs while the ions migrate through a drift gas. The use of other gases in place of helium has allowed the separation of isomeric species in a much more efficient way. In this work, we study isomeric systems aiming to understand, from the molecular point of view, the separation in different drift gases [1-2]. The chosen system was the *ortho*, *meta* and *para* isomers of the chlorophenyl piperazine. The collision cross sections were calculated by using three different methods: trajectory method (TM), exact hard-sphere scattering approximation (EHSS) and projection approximation (PA). To take account all configurations of an isomer when it is moving through the gas, we have performed a conformational analysis by varying the angle between the two aromatic rings by 10 degrees in the interval from 0 to 180º. The calculations were performed by using the RM1 semiempirical model and the DFT methodology with B3LYP/6-31G(d,p). Then we had performed the calculation of population distributions seeking to estimate the contribution of cross sections calculated for each conformer. The results showed that the final cross sections (weighted average) obtained for each isomer by RM1 and DFT methodology were very similar. The calculation of the collision cross sections using $N_2$ or $CO_2$ as drift gas through the EHSS and PA approximation showed a good agreement with experimental data. According to these data the crescent order of the ionic mobility was: *ortho* > *para* > *meta*. However, when TM method was carried out, we observed an order inversion of the results regarding from the experimental data. In the case of the results for $N_2$, as gas drift, the order found was: *para* (178.59Å$^2$) > *meta* (177.33Å$^2$) > *ortho* (175.82Å$^2$). The ortho compound has a larger theoretical cross section, in contrast with experimental data. When $CO_2$ was used as drift gas the results found for TM method was: *para* (294.15Å$^2$)> *ortho* (292.83Å$^2$) > *meta* (290.50Å$^2$). These discrepancies can be explained due to ε and σ parameters of Lennard-Jones potential, which were not optimized in the TM method for this kind of system.

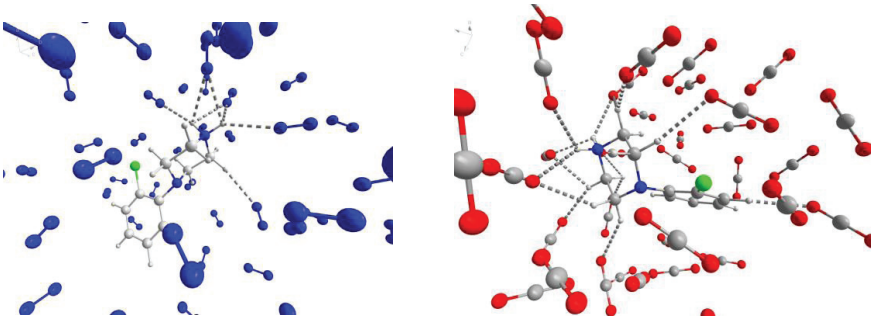

(A) (B)

Figure 1. Hydrogen bonds between the ortho - chlorophenyl piperazine isomer with (A) $N_2$ and (B) $CO_2$ as drift gas.

To explain why the drift time is longer when $CO_2$ is used as drift gas, calculations were performed for each isomer. As Figure 1(A) shows, when $N_2$ was used as a drift gas, the formation of seven hydrogen bonds between the isomer specie and $N_2$ gas molecules were observed. The Figure 1(B) shows the formation, on average, of 13 hydrogen bonds between the $CO_2$ molecules and the isomeric species. The larger number of interactions when $CO_2$ was used as a drift gas explains why experimentally the drift time increases by approximately 1.5 ms when $CO_2$ is used instead of $N_2$.

**Key-words**: Ion Mobility Spectrometry, Isomers, Drift Gas
**Support:** This work has been supported by CNPq, CAPES, FAPITEC-SE and FACEPE
**References:**
[1] L. W. Beegle, I. Kanik, L. Matz, H. H. Hill, Int. J. Mass Spectrom. 216, 257, (2002).
[2] A. B. Kanu, M. M.; Gribb, H. H. Hill, *Anal. Chem*. 80, 6610 (2008).

# Development of Models for the Calculation of Collision Cross Section

José Diogo L. Dutra, Jorge Leonardo O. Santos, and Ricardo O. Freire

*Pople Computational Chemistry Laboratory, Department of Chemistry, UFS*

**Abstract:** Ion mobility spectrometry (IMS) consists of an analytical technique that can separate gas phase ions based on their size, shape and polarizability [1]. In turn, the mobility can be used to determine the collision cross section (Ω), which is a measure of an ion's conformation in the gas phase. As the number of collisions is dependent on the conformations of an analyte, ions of identical composition with different conformations may be separated by using IMS. When Ω is utilized in conjunction with computational modeling, comparisons between theoretical and experimental data can be used to deduce the gas phase structures of analyte ions. Hence, various simulation methods have been applied to generate low-energy structures for correlating with experimentally determined collision cross section (CCS) [2]. The computational procedure follows the steps: i) calculation of molecular structure in gas phase, ii) application of an approximate method for calculating theoretical Ω by using the projection approximation (PA), the exact hard-sphere scattering approximation (EHSS), or the trajectory method (TM). In the PA approximation, the ion is modeled by a collection of overlapping hard spheres with radii equal to hard sphere collision distances. Differently of the PA approximation, in the EHSS approximation the orientationally-averaged momentum transfer cross section is calculated by determining the scattering angles between the incoming buffer gas atom trajectory and the departing buffer gas atom trajectory. The trajectory method treats the ion as a collection of atoms, each one represented by a 12-6-4 potential. In theory, the experimental drift time should be correlate well with the theoretical cross section. However, many tests carried out by our research group showed that this trend is not always obeyed. This way, the main of this work is to develop models based on the PA, EHSS, and TM method, which is implemented into the MOBCAL code [3], to improve the correlation between structure and theoretical cross section. The database that was used in the development procedure of our models consisted of values of the experimental collision cross sections reported by Campuzano et al [4]. Due to the limited number of compounds, we have decided to include all them as training set. Moreover, at the first moment, the helium was used as the drift gas. The geometry of each considered compound was then optimized with DFT method by using B3LYP/6-311++G(d,p). The atomic charges used in the TM method were the Mulliken charges calculated with the same DFT method. We have decided re-written the Fortran 77 code of MOBAL for the Fortran 90 standard with the intention of allowing further implementations. Consequently, this new code was applied in the parametrization process. For now, we have only considered compounds containing the H, C, O, and N atoms. For the PA and EHSS approximations the atomic radii were treated as parameters; whereas for the parametrization of the model based on the TM method the ε

and σ parameters of the Lennard-Jones potential, regarding to each atom, were treated as adjustable parameter in the development of the model. The results obtained after months of parametrization using the GSA algorithm are shown in the below table. The mean relative percentage errors for the PA, EHSS, and TM method are 1.3%, 2.3%, and 2.3%, respectively, regarding the experimental results. It is worth highlighting that a difference of 1% for a mean relative percentage error suggests that all three models developed by us have satisfactory quality for general purpose.

Table 1. Experimental and theoretical collision cross sections calculated by using the models developed by us.

| | $\Omega_{EXP}$ (Å$^2$) | $\Omega_{PA}$ (Å$^2$) | $\Omega_{EHSS}$ (Å$^2$) | $\Omega_{TM}$ (Å$^2$) |
|---|---|---|---|---|
| N-ethylaniline | 63.0 | 62.2 | 60.8 | 61.3 |
| acetaminophen | 67.0 | 67.0 | 67.0 | 67.0 |
| alprenolol | 96.9 | 100.7 | 104.1 | 105.3 |
| tetramethylammonium | 48.5 | 47.0 | 46.0 | 47.6 |
| tetraethylammonium | 65.9 | 64.5 | 64.5 | 65.7 |
| tetrapropylammonium | 88.9 | 87.5 | 89.2 | 89.6 |
| tetrapentylammonium | 133.5 | 132.2 | 136.9 | 139.2 |
| tetrahexylammonium | 154.9 | 154.9 | 161.5 | 162.5 |
| tetraheptylammonium | 174.5 | 178.3 | 185.6 | 192.5 |
| naphthalene | 59.4 | 59.9 | 58.7 | 59.2 |
| anthracene | 73.9 | 74.0 | 73.0 | 73.1 |
| phenanthrene | 71.9 | 73.1 | 72.4 | 71.7 |
| pyrene | 76.4 | 76.7 | 75.8 | 76.4 |
| triphenylene | 83.8 | 85.5 | 84.9 | 84.8 |
| C60 | 122.6 | 122.6 | 122.6 | 122.6 |
| C70 | 135.0 | 134.4 | 134.7 | 135.0 |

**Key-words**: Ion mobility spectrometry. Collision cross section. Development of models.
**Support:** This work has been supported by CNPq. CAPES, FAPITEC-SE, and FACEPE.

**References:**

[1] R. Cumeras, E. Figueras, C. E. Davis, J. I. Baumbach, I. Gracia, Analyst, 140, 1376 (2015).
[2] N. L. Zakharova, C. L. Crawford, B. C. Hauck, J. K. Quinton, W. F. Seims, H. H. Hill Jr, A. E. Clark, J. Am. Soc. Mass Spectrom., 23, 792 (2012).
[3] M. F. Mesleh, J. M. Hunter, A. A. Shvartsburg, G. C. Schatz, M. F. Jarrold, J. Phys. Chem., 100, 16082 (1996).
[4] I. D. G. Campuzano, M. F. Bush, C. V. Robinson, C. Beaumont, K. Richardson, H. Kim, H. I. Kim, Anal. Chem., 84, 1026 (2012).

# Cluster Expansion Method for Solvation Free Energy Calculations: Theoretical Development

Josefredo R. Pliego Jr. (PQ)

*Departamento de Ciências Naturais, Universidade Federal de São João del-Rei, 36301-160 São João del-Rei-MG, Brazil*

**Abstract:** The cluster expansion approach was used by McMillan and Mayer in the forties for the development of imperfect gas theory [1]. An interesting advantage of the method is that configurational integrals are relevant only in regions where the gas molecules are close. Considering the possibility of taking advantage of this property, a cluster-like expansion method for computation of the solvation free energy difference was developed in this work. Based on pairwise potentials, a Mayer-like function involving variation in the solute-solvent potential energy was used. Thus, considering solute-solvent initial potential energy $U^0$ and a new potential energy $U^1$, the related solvation free energies of the solute "S" are given by:

$$\Delta G^1_{solv}(S) = \Delta G^0_{solv}(S) - kTln[1 + \rho\bar{B}_2 + \rho^2\bar{B}_3 + \cdots] \qquad (1)$$

In this proposal, the series expansion remains inside the logarithm and is a finite series. The first correction term, $\bar{B}_2$, is given by:

$$\bar{B}_2 = \int f_{s,1} e^{-\beta\Delta W^0(\boldsymbol{r_1})} \boldsymbol{dr_1} \qquad (2)$$

The $f_{s,1}$ is the Mayer-like function, using the difference in the potential energy, and the $\Delta W^o$ is the potential of mean force for the position of the solvent molecule around the solute. The integral in equation (2) is meaningful only for configurations of the solvent close to the solute. The method can be applied for improving hybrid QM/MM calculations. In this case, the reference potential is classical and the new potential is calculated by quantum mechanics. Thus, equations (1) and (2) can be applied in the case that classical solvent molecules are transformed in quantum molecules. Further manipulation of equation (2) can be done for application in hybrid discrete/continuum approach.[2]

**Key-words**: free energy perturbation, cluster-continuum, single ions solvation, continuum method

**Support:** This work has been supported by CNPq and FAPEMIG.

**References:**

[1] W. G. McMillan Jr. and J. E. Mayer, J. Chem. Phys. **13**, 276 (1945).

[2] J. R. Pliego Jr, J. Chem. Phys. **147**, 034104 (2017).

# New insights on Photo-Fries rearrangement: a model for photodegradation of carbamate pesticides

Authors: Josene Toldo,[a,b] Mario Barbatti,[b] Paulo F. B. Gonçalves[a]

*Address: [a]Institute of Chemistry, Universidade Federal do Rio Grande do Sul, Porto Alegre-RS, Brazil,[b]Aix Marseille Univ, CNRS, ICR, Marseille, France*

Photo-Fries rearrangement (PFR) is a photochemical conversion of aryl esters to *ortho*- and *para*-hydroxyphenones.[1] This reaction is a key step in the synthesis of a large number of compounds and plays an important role in the design of functional polymers and in the photodegradation of drugs and an important class of carbamate pesticides. Although there are a large number of experimental studies about the mechanism of PFR, the last theoretical work is from 1992 and some points of PFR reaction are still under debate. Given the knowledge gap between theory and the most recent experimental works,[2] our aim has been to provide a comprehensive picture of PFR, based on high-level multiconfigurational theoretical methods.

In this work, we present a three-state model for the Photo-Fries rearrangement (PFR) based on CASSCF(14,12)/CASPT2(14,12) calculations.[3] It provides a comprehensive mechanistic picture of all steps of the reaction, from the photoabsorption to the final tautomerization, as shown in Figure 1.

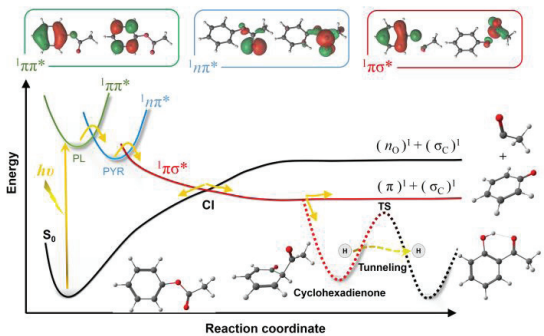


**Figure 1:** Schematic overview of the three-state model for Photo-Fries rearrangement applied to phenyl acetate.

The three states participating in the PFR are an aromatic $^1\pi\pi^*$, which absorbs the radiation; a pre-dissociative $^1n\pi^*$, which transfers the energy to the dissociative region; and a $^1\pi\sigma^*$, along which dissociation occurs. The transfer from $^1\pi\pi^*$ to $^1n\pi^*$ involves

pyramidalization of the carbonyl carbon, while transfer from $^1n\pi^*$ to $^1\pi\sigma^*$ takes place through CO stretching. Different products are available after a conical intersection with the ground state. Among them, a recombined radical intermediate, which can yield *ortho*-PFR products after an intramolecular 1,3-Hydrogen tunneling. The three-state model is developed for phenyl acetate, the basic prototype for PFR, and it reconciles theory with a series of observations from time-resolved spectroscopy. It also delivers a rational way to optimize PFR yields since diverse substituents can change the energetic order of the $^1\pi\pi^*$ and $^1n\pi^*$ states, preventing or enhancing PFR.

Calculations for the $S_1$ minima show that changing the methyl by an amino group inverts the energetic order of the planar ($^1\pi\pi^*$) and pyramidal ($^1n\pi^*$) minima (Figure 2). While with the methyl group, the $^1n\pi^*$ state is more stable by 0.1 eV, with the amino group, the $^1\pi\pi^*$ becomes the most stable by 0.2 eV in **b** and by 0.4 eV in **c** and **d.** We can rationalize this effect based on the resonance structures that characterize the amino substituted molecules, stabilizing the lone pairs and increasing the energies of the $^1n\pi^*$ state.

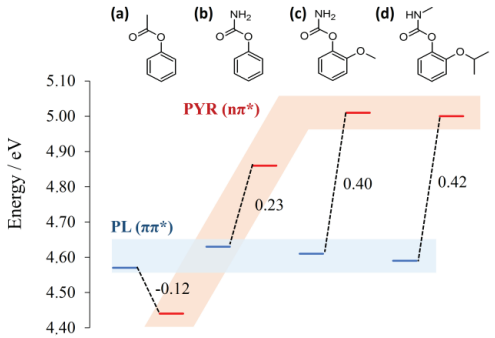


**Figure 2:** Energies of the planar ($^1\pi\pi^*$) and pyramidal ($^1n\pi^*$) $S_1$ minima of (a) phenyl acetate, (b) phenyl carbamate, (c) ortho-methoxyphenyl carbamate, and (d) 2-isopropoxyphenyl N-methylcarbamate (Propoxur) in the gas phase.

**Key-words**: Photo-Fries Rearrangement, Multiconfigurational, Photochemistry.
**Support:** This work has been supported by CAPES/PDSE and CNPq.

**References:**

[1] Anderson, J. C.; Reese, C. B., *Proc. Chem. Soc.* **217** (1960)
[2] a) S. Lochbrunner, M. Zissler, J. Piel, E. Riedle, A. Spiegel and T. Bach, *J. Chem. Phys.* **120**, 11634 (2004). b) S. J. Harris, D. Murdock, M. P. Grubb, G. M. Greetham, I. P. Clark, M. Towrie and M. N. R. Ashfold, *Chem. Sci.* **5**, 707 (2014). c) S. Grimme, *Chem. Phys.* **163**, 313 (1992).
[3] Toldo, J.; Barbatti, M.; Gonçalves, P.F.B., ***A three-state model for the Photo-Fries rearrangement***, *Phys. Chem. Chem. Phys*. **2017**, 19, 19103-19108.

# Different ways to compute the ground state of electronic energy of ion hydrogen molecule confined via variational method

Josimar Fernando da Silva*, Elso Drigo Filho

*Instituto de Biociências, Letras e Ciências Exatas – Universidade Estadual Paulista "Júlio de Mesquita Filho", josimarfsilva@sjrp.unesp.br*

**Abstract:** The electronic energy can be calculated by two ways [1,2]. We want to compare two methods of calculate the ground state of electronic energy of $H_2^+$ confined in impenetrable cavities. One way is using the mean value of the electronic energy of the atomic orbital [1] and the other way is computing the atomic electronic energy [2]. There is a discussion about this subject in literature [3,4]. We conclude that both methods are appropriated to describe confined molecules. But, the method that uses the mean value of the atomic orbital affords energy eigenvalues less than the energy eigenvalues of the other method.

**Key-words**: ground state, electronic energy, ion hydrogen molecule, confined system, variational method.

**Support:** This work has been supported by Capes and Fapesp.

**References:**

[1] J. F. da Silva, F. Ramos Silva, E. Drigo Filho. Int. J. Quantum Chem. 2016, 116, 497–503. DOI: 10.1002/ qua.25084

[2] S. A. Cruz, R. Colín Rodríguez. Int. J. Quantum Chem. 2009, 109, 3041–3054. DOI: 10.1002/ qua.22257

[3] S. A. Cruz, H. Olivares-Pilon Int. J. Quantum Chem. 2016, 00: 000–000. DOI: 10.1002/qua.25298

[4] J. Fernando da Silva, F. Ramos Silva, E. Drigo Filho. Int. J. Quantum Chem. 2016, 116, 1894–1897. DOI: 10.1002/qua.25297

# Conformational Dependence of the Hydrophobicity of Fluorine-containing Agrochemicals

Authors: Daniela Rodrigues Silva, Matheus Puggina de Freitas, Joyce Karoline Daré

*Universidade Federal de Lavras, Lavras-MG*

**Abstract:**

Fluorine-containing compounds are an important subclass of bioactive organic molecules being present in around 20% [1] of current pharmaceuticals and 30% of agrochemical candidates [2]. For agrochemicals, hydrophobicity is a relevant parameter to be analyzed because some important environmental properties can be estimated from the octano/water partition coefficient (logP), such as soil sorption and bioconcentration. This primary measurement along with the pH-dependent distribution coefficient ($logD_{ph}$) have been exhaustively used to explore the structure-property relationships of bioactive molecules, which gives insights about their solubility and interaction with physiologically relevant macromolecules and environments [3].

The controversial influence of fluorine in logP has caught attention of many researchers in the last years, mainly, because flaws were found in the generalization that a change of a hydrogen with a fluorine substituent on a carbon atom always results in a lipophilicity increment [4]. Therefore, the present project aims to determine the conformational isomerism of some fluorine-containing agrochemicals (Pyroxsulam, Penoxsulam, Trifluralin, Ethalfluarin e Flumioxazin) and correlate their molecular dipole moment with the respective logP data, in order to show the subtle dependence of the hydrophobicity with the molecular conformation. Thus, compounds with and without rotamers originated from the rotation around the C-C(F) bonds will be taken into account. Those whose C-C(F) rotation yields different rotamers have dependence of the molecular dipole moment (and, therefore, of logP) with the rotation around this bond.

Therefore, to guarantee uniformity in the experimental measurements used, the logP values for the whole set of molecules were selected from a unique producer (Safety Data Sheet available in the website of **The Dow Chemical Company**). Next, the molecular dipole moment values for the agrochemical molecules were obtained from their optimization using the computational method ωB97X-D/6-31g(d,p) available in the *Gaussian 09* software. Finally, a correlation plot was built (dipole moment *vs.* logP) including each relevant conformation of Penoxsulam and a tendency line was added, according to Figure 1.

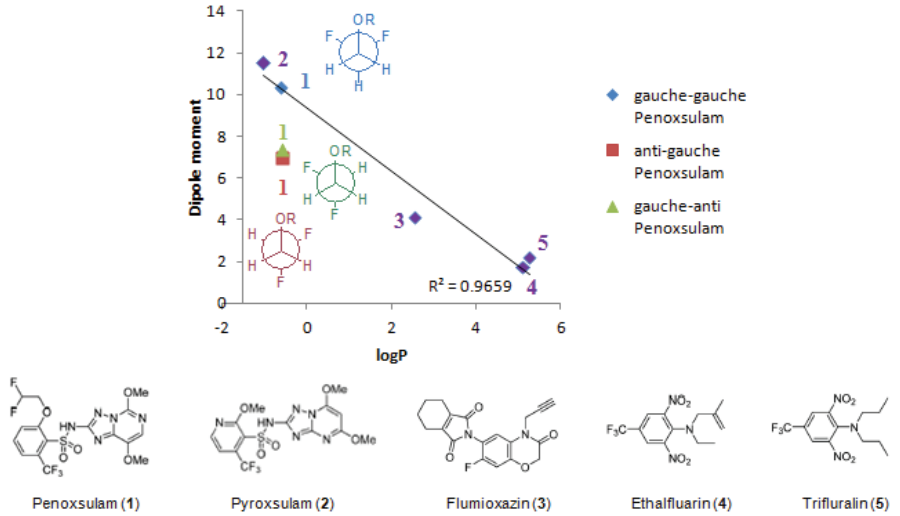


**Figure 1.** Plot of experimental logP *vs* calculated dipole moment (Db).

Based on the graph above, the *gauche-gauche* conformation of Penoxsulam is the only matching the linear correlation with the other compounds. This finding can be rationalized by the dominant conformation, which is stabilized by a double gauche effect owing to $\sigma_{CH} \rightarrow \sigma^*_{CF}$ and by $\sigma_{CH} \rightarrow \sigma^*_{CO}$ hyperconjugative interactions. Thus, subtle structural changes describe accurately the lipophilicity of fluorine-containing agrochemicals. Now, we aim to increase the number of fluorine-containing compounds in order to feed the model and make the correlation more reliable.

**Key-words**: Fluorine-containing agrochemicals, logP, molecular dipole moment.
**Support: Coordenação de Aperfeiçoamento de Pessoal de Nível Superior (CAPES) e Conselho Nacional de Desenvolvimento Científico e Tecnológico (CNPq)**

**References:**

[1] E. P. Gillis, K. J. Eastman, M. D. Hill, D. J. Donnely, N. A. Meanwell, "Application of Fluorine in Medicinal Chemistry" (2015), J. Med. Chem. V. 58, p. 8315–8359.

[2] T. Fujiwara, D. O'Hagan, " Successful fluorine-containing herbicide agrochemicals" (2014), J. Fluorine Chem. V. 167, p. 16– 29.

[3] D. O'Hagan, R. Young, "Accurate Lipophilicity (LogP) Measurements Inform on Subtle Stereoeletronic Effects in Fluorine Chemistry" (2016), Wiley-VCH, Weinheim, Germany. V. 55, p. 3858 – 3860.

[4] K. Mîller, C. Faeh, F. Diederich, "Fluorine in pharmaceuticals: looking beyond intuition" (2007), Science. V. 317, p. 1881–1886.

# Hierarchical virtual screening for identification of *Leishmania braziliensis N*-myristoyltraferase inhibitors

GALLO, J.C.C.[1*]; OLIVEIRA, L. M.[1]; SANTOS JUNIOR, M. C.[1]
*Laboratório de Modelagem Molecular, Universidade Estadual de Feira de Santana-BA*[1]
**julianaccgallo@gmail.com*

**Abstract:** Leishmaniasis is considered a neglected tropical disease with a limited therapeutic arsenal [1]. In order to overcome this problem, the enzyme N-myristoyltransferase of *Leishmania braziliensis* (*Lb*NMT) has been chosen as a molecular target, by catalyzing the transference of fatty acids, important in the constitution of parasite's cellular membrane [2]. Here, we report a combination of ligand- and structure-based screening approaches in finding *Lb*NMT inhibitors. Based on the published literatures, we collected five inhibitors as training set to generate pharmacophore models (PM), and six inhibitors as a test set to validate the PM. The test set were utilized for generating decoys in the DUD-E [3]. The PM were constructed in GALAHAD (SYBYL-X 2.0) [4]. 10 PM were generated and these were aligned to the test set and decoys, and then the Receiver Operating Characteristic Curve (ROC curve) was constructed in SigmaPlot 12.0 [5]. The PM01 showed the highest rate of recovery of active molecules, with AUC =1.0, indicating that PM distinguish between the molecules groups (true positives and false positives). This pharmacophore model show four hydrophobic centers, one positive nitrogen center and four hydrogen bond acceptor (Fig.1). The Biogenic Bank from Zinc15 [6] database was submitted to flexible alignment with PM01. 220 molecules were aligned to the PM01, the pharmacophoric match (QFIT) these molecules ranged from 6.0 to 47.9, these molecules were submitted to molecular docking approaches. Molecular docking was performed in DOCK 6.8 [7] program, using PDB [8] ID 5A27 receptor. Docking success was considered when the top scoring pose is within 2Å heavy atom Root-Mean-Square Deviation (RMSD) of the crystal ligand and AUC $> 0.8$ in ROC curve. 1.12Å RMSD is acceptable value, indicating that the pose generated by the DOCK 6.8 is close to that obtained by the crystallographic ligand**.** The AUC = 0.93 show perfect separation of the true positives/negatives molecules showing that Grid Score from DOCK 6.8 to be an effective score function. The molecules selected for the ligand-based method were submitted to molecular docking using Grid Score function. The top ranked molecules with their respective energy values (Kcal/mol) were ZINC85629024 (-105.79), ZINC85630510 (-98.04) and ZINC85630554 (-96.00). The ZINC85629024 forms hydrogen bonds acceptor with Tyr84, Met369 and Glu74, hydrogen bonds donor with Tyr209, Met369, Met412, Gly197 and π-stacking T-shaped with Tyr337 (Fig. 2). The combination of ligand and structure-based virtual screening allowed the identification of potential inhibitors of *Lb*NMT.

Figure 1. Hydrophobic Centers: cyan, Positive Nitrogen Center: red and Hydrogen Bonds Acceptors: green. The distance between the spheres was measured in Å.

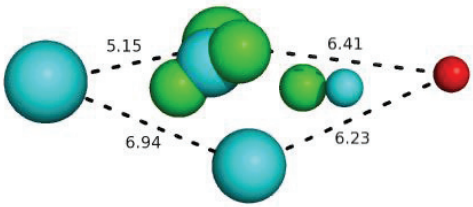


Figure 2. Intermolecular interactions between *Lb*NMT and the ZINC85629024 molecule. Hydrogen bonds (solid blue line) and π-stacking T-shaped (dashed yellow line).

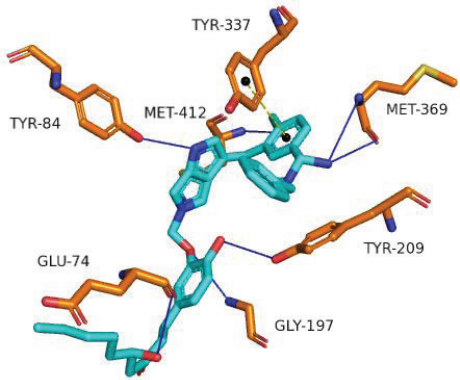


**Key-words**: Pharmacophore model. Molecular docking. NMT. *Leishmania braziliensis.* Natural products.

**Support:** FAPESB, PPGCF-UEFS and Prof. Dr. Marcelo Castilho (UFBA) for giving licence of SYBYL-X 2.0 software.

**References:**

[1] VELÁSQUEZ, A. M. A.et al. Efficacy of a Binuclear Cyclopalladated Compound Therapy for cutaneous leishmaniasis in the murine model of infection with *Leishmania amazonensis* and its inhibitory effect on Topoisomerase 1B. **Antimicrob. Agents Chemother**, 2017.
[2] BOWYER, P. W. et al. N-myristoyltransferase: a prospective drug target for protozoan parasites. **ChemMedChem**, 2008.
[3] MYSINGER, M. M. et al. DUD-Enhanced – better ligands and decoys for better benchmarking. **Journal of Medicinal Chemistry**, 2012.
[4] TRIPOS. **SYBYL-X 2.0**, St Louis, MO, USA, 2010.
[5] SIGMA PLOT 12.0. **San Jose: Systat Software**, 2014.
[6] IRWIN et al. ZINC15. J. **Chem. Inf. Model**, 2012.
[7] ALLEN et al. DOCK 6.8 Users Manual. **Regents of the University of California**, 2017.
[8] BERMAN, H. M. et al. The Protein Data Banking. **Nucleid Acids Research,** 2000.

# Azoles molecules as potential corrosion inhibitors: A DFT study.

Juliana O. Mendes, Marco Antonio Chaer Nascimento

*Instituto de Química, Universidade Federal do Rio de Janeiro, Brazil*

**Abstract:** Corrosion is an undesirable process that affects several areas of industrial activity, especially the oil industry, resulting in huge economic losses. Although it is not possible to completely avoid the corrosion process there are ways to inhibit it. Organic heterocyclic compounds containing nitrogen atoms are commonly used as corrosion inhibitors. Those inhibitors can adhere to a metal surface to form a protective film against corrosive agents in the environment [1]. Azoles and particularly their derivatives are known as efficient corrosion inhibitors [2].

With the advances in computational chemistry and the development of new algorithms, theoretical methods have been used to investigate the inhibition mechanism and to design new and environment friendly molecules with potential to corrosion inhibition. Most of the theoretical calculations try to correlate structural properties with the inhibition efficiency of an isolated molecule. Since the interaction with the metallic surface is not taken into account, these calculations do not provide a full picture of the inhibition mechanism. Some recent studies considered the adsorption of the inhibitor on a metallic surface by performing calculations within the framework of the density functional theory (DFT) under periodic boundary conditions providing significant understanding about the corrosion inhibition mechanism [3,4].The aim of the present study is to analyze the nature of the interaction of four azole molecules – imidazole, imidazoline, imidazolidine and pyrrolidine – with the (001) iron surface in gas phase, in order to verify whether these molecules are potential corrosion inhibitors and how the inhibition process takes place.

The calculations were performed using DFT under periodic boundary conditions with a plane wave basis set and ultrasoft pseudopotentials. We used the Generalized Gradient Approximation (GGA) functional of Perdew, Burke and Ernzerhof (PBE) [5] implemented in the PWSCF code of the Quantum Espresso suite of programs [6]. Several initial orientations of the molecules relative to the surface, parallel,

perpendicular and tilted, as well as the binding sites, *hollow* and *top*, have been considered.

In their neutral forms pyrrolidine and imidazole exhibit good potential as corrosion inhibitors, pyrrolidine being more strongly adsorbed than imidazole, imidazoline and imidazolidine on the Fe(001) surface. Considering all the possible orientations, the four molecules showed preference to interact with a *top* iron atom of the surface, with pyrrolidine and imidazole interacting preferably with an iron atom of the surface through the *pyridine-like* nitrogen atom, while imidazoline and imidazolidine molecules adsorb tilted to the surface to interact with two iron atoms. The process of adsorption of the molecules showed to be quite different and clearly ditacted by the molecular structure of the azole. Also, the differences in the strength of interaction of the molecules with the surface, are directly related to the way that they bind to the surface.

**Key-words**: Corrosion inhibition, azoles, iron surface, periodic DFT calculations

**Support:** This work has been supported by CNPq, FAPERJ, INOMAT

**References:**

[1] Z. Zhang, S. Chen, Y. Li, S. Li, L. Wang, Corros. Sci. 51, 291 (2009).
[2] Y. I. Kuznetsov, L. P. Kazansky, Russian Chemical Reviews 77, 219 (2008).
[3] J. O. Mendes, A. B. Rocha, E. C da Silva, Corrosion Science 57, 254 (2012).
[4] N. Kovačević, A. Kokalj, Corros. Sci. 73, 7 (2013).
[5] J. Perdew, K. Burke, M. Ernzerhof, Phys. Rev. Lett. 77, 3865 (1996).
[6] P. Giannozzi, S. Baroni, N. Bonini, M. Calandra, R. Car, C. Cavazzoni, et al., J. Phys. Condens. Matter. 21, 395502 (2009).

# Olefins Hydroformylation Reaction Catalyzed by Rhodium Complexes of the Type $HRh(P\cap P)(CO)_2$: A DFT and *ab initio* Study

Daniel H. C. Neto (IC),[a] Júlio C. S. da Silva (PQ),[b] Willian R. Rocha (PQ)[c] and Roberta P. Dias (PQ)[a]

[a] *Núcleo Interdisciplinar de Ciências Exatas e Inovação Tecnológica (NICIT), Universidade Federal de Pernambuco (UFPE), Campus Agreste, Caruaru, PE, 55002-970, Brasil.*

[b] *Instituto de Química e Biotecnologia, Universidade Federal de Alagoas (UFAL), Campus A.C. Simões, Maceió, AL, 57072-900, Brasil.*

[c] *Departamento de Química, Instituto de Ciências Exatas (ICEx), Universidade Federal de Minas Gerais (UFMG), Campus Universitário Pampulha, Belo Horizonte, MG, 31270-901, Brasil.*

**Abstract:** Homogeneous hydroformylation of olefins (convention of alkenes to aldehydes in the presence of $CO_2$ and $H_2$) catalyzed by transition metals compounds represents a versatile route for the production of commercially important aldehydes and alcohols, which are difficult to be obtained via conventional synthetic routes. [1] Several organometallic complexes have been used as catalyst for this reaction. Nevertheless, mainly regarding to selectivity of this reaction, catalysts containing phosphines ligands have occupied a central role. [2,3] Studies have showed that coordinating phosphines ligands plays an important role on control of metal´s catalytic activity and selectivity by influencing its electronic and spatial properties. [2,3] Despite the very attractive properties of organometallic compounds with phosphines in the catalysis of the olefins hydroformylation reaction some fundamental questions are not yet fully understood. Specially, concerning to complexes containing phosphines coordinated to metal centers through of bidentate mode, as for instance, the ligands BISBI and DPPE.

In this work, we studied the catalytic cycle of the hydroformylation of propene catalyzed by $HRh(BISI)(CO)_2$ complex. All intermediates and transition states located along the reaction coordinate were obtained at the B3LYP-D2/BS1 of theory. (BS1:Relativistic effective core potential and valence double-ξ basis set of Hay and Wadt was used for Rh atom. The atoms of the ligands were described by using the 6-311G(d) basis set.

Our results show that the propene insertion (first step of catalytic cycle) is the rate-determining step on regioselectivity of the reaction with an activation energy around 22.0 $kcal.mol^{-1}$ for the pathway that leaves to branched product and around 13.0

kcal.mol$^{-1}$ for route that generates the linear aldehyde. Single point energy calculations using several exchange-correlation functional of different approximations (GGA, meta-GGA, Hybrid, double-hybrid and with inclusion of dispersion effects) and the explicitly correlated version of the Möller-Plesset and coupled cluster theories MP2-F12 [4] and CCSD(T)-F12, [5] respectively, were carried out to refine the energetics. The results of this ab initio study as well the details about the DFT calculations will be presented and discussed during the conference.

**Key-words**: DFT, MP2-F12, CCD(T)-F12, phosphines ligands, hydroformylation

**Support:** FACEPE, CNPq, INCT-Catálise

**References:**

[1] R. Franke, D. Selent and A. Börner, Chem, Rev. 112, 5675(2012).
[2] R. Martin and S. L. Buchwald, Acc. Chem. Res., 41, 1461 (2008).
[3] J. A. Gillespie, P. C. J. Kramer and P. W. N. M. van Leeuwen, "Phosphorus Ligand Efects in Homogeneous Catalysis and Rational Catalyst Design" (2012), Wiley-VCH, Weinheim, Germany.
[4] H. J. Werner, T. B. Adler and F. R. Manby, J. Chem. Phys. 126, 164102 (2007).
[5] T. B. Adler, G. Knizia and H. J. Werner, J. Chem. Phys. 127, 221106 (2009).

# π-π Stacking Interactions between Asphaltene and Aggregation Inhibitors: A Study by Density Functional Theory.

Alexandre N. M. Carauta[a,c] (PQ), Fernanda B. Silva[c] (PQ), Kelly F. Pessôa[b,c], Julio C. C. Guedes[c] (PQ), Peter R. Seidl[b] (PQ)

*Address: [a]Fundação Técnico-Educacional Souza Marques. Rio de Janeiro- RJ. Brazil*
*[b] Departamento de Processos Orgânicos, Escola de Química, Universidade Federal do Rio de Janeiro - UFRJ. Rio de Janeiro – RJ. Brazil.*
*[c]Centro de Tecnologia Mineral – CETEM. Rio de Janeiro- RJ. Brazil*

Solid deposition is one of the most serious problems that arise in oil production. The tendency of certain oils to flocculate and form deposits is attributed to asphaltenes and their respective molecular interactions. One of the most effective methods of preventing the precipitation and deposition of these compounds is the use of inhibitors and since understanding the mechanism of inhibition is of great practical relevance, numerous studies have been performed to investigate the factors that affect the efficiency of inhibitors. It is known that π-π stacking interactions are responsible for the aggregation of asphaltenes and resins [1]. Molecular modeling can play an important role in the investigation of association phenomena of asphaltenes but most of the standard semiempirical, density functional theory (DFT) and ab initio methods do not properly account for the dispersion term. π-π stacking interactions have proven to be sensitive to the methodology that is employed and are very dependent on the size of the basis set used in calculations being subject to large basis-set superposition errors (BSSE). The goal of this study is investigate π-π interactions between asphaltene and aggregation inhibitors using selected exchange-correlation functionals to overcome the well-known problems related to the use of DFT to correctly describe the dispersion interactions which constitute one of the main components of π-π stacking interactions [2]..

An average structure of an asphaltene and three potential inhibitor molecules, p-nonylphenol, p-nonylaniline and cardanol were used for computational simulations by.standard methods adopted by our group: Conformational analysis was done by molecular dynamics using the COMPASS force field for both asphaltene and inhibitor structures. Docking between the most stable structures of the asphaltene molecule and each inhibitor molecule was adjusted manually and conformational analysis of asphaltene-inhibitor structures was carried out by molecular dynamics using the same force field. Then only the structure involved in the interaction between the asphaltene and p-nonylaniline was used to test some functionals with a 6-31G(d,p). basis set. Results for the energies that were calculated are given in Table 1:

Table 1 – Interaction energies calculated by MPW91, PW91 and B3LYP functionals

| Functional 6-31G(d,p) | pnonylaniline | Asphaltene | Asphaltene-pnonylaniline | ΔE (hartree) | ΔE(kcal/mol) |
|---|---|---|---|---|---|
| MPW91 | -641,431805 | -2053,01985 | -2694,434391 | 0,017263 | 10,83 |
| PW91 | -641,257690 | -2052,49620 | -2693,750908 | 0,002983 | 1,87 |
| B3LYP | -641,562238 | -2053,34581 | -2694,888824 | 0,019222 | 12,06 |

Only the interaction energy calculated by the SVWN funcional, shown in Table 2, gave a negative value. Thus calculations for the other asphaltene-inhibitor systems were carried out with the SVWN functional and the 6-31G(d,p) basis set adjusted for BSSE – Basis-Set Superposition Error.

Table 2 - Interaction energies (kcal.mol$^{-1}$) (ΔE, corrected for BSSE) for Inhibitor-asphaltene systems calculated by SVWN functional and the 6-31G(d,p) basis set.

| Inhibitor | Energy | Asphaltene | Inhibitor - asphaltene | ΔE | $\Delta E_{corrected}$ |
|---|---|---|---|---|---|
| p-nonylaniline | -637,88 | -2041,47 | -2679,38 | -23,21 | -20,72 |
| p-nonylphenol | -657,66 | -2041,47 | -2699,17 | -24,53 | -22,04 |
| cardanol | -888,52 | -2041,47 | -2930,04 | -35,34 | -29,11 |

Calculations with the ωB97X-D functional that has atom-atom dispersion corrections are being run with 6-31G(d,p), 6-31+G(d,p) e 6-31++G(d,p) basis sets.

**Key-words**: π-π stacking, asphaltenes, inhibitors, DFT

**Support: CNPq and PCI/CETEM**.

**References:**

[1] Chavez-Miyauchi, T. E.; Zamudio-Rivera, L. S.; Barba-Lopez, V.; Buenrostro-Gonzalez, E.; Martinez-Magadan, J. M., **Fuel**,110, 302–309, 2013.
[2] Swart, M.; Wijst, T.; Guerra, C. F.; Bickelhaupt, F. M., J. Mol. Model., 2007, 13, pp 1245-1257.

# The Perlin Effect in terms of molecular orbitals

Kahlil Schwanka Salome, Cláudio Francisco Tormena

*Institute of Chemistry □University of Campinas*

**Abstract:** Many studies have shown the importance of scalar spin-spin coupling constants (SSCCs) obtained by NMR spectroscopy in conformational analysis of molecules, in cyclohexane derivatives SSCCs are used to determine conformation and relative stereochemistry [1]. For instance, in 1,3-dioxane (**1**, figure 1) the $^{1}J_{C1\text{-}Hax}$ is smaller than $^{1}J_{C1\text{-}Heq}$ and in 1,3-dithiane (**2**, figure 1) the $^{1}J_{C1\text{-}Hax}$ is larger than $^{1}J_{C1\text{-}Heq}$. This differences are known as Perlin and reverse-Perlin effect respectively and are usually interpreted in terms of hyperconjugation effects such as $LP_O \rightarrow \sigma^*_{C1\text{-}Hax}$ and $\sigma_{C\text{-}S} \rightarrow \sigma^*_{C1\text{-}Heq}$, which are reflected in the bond length of the $C_1$-$H_{ax}$ and $C_1$-$H_{eq}$ [2]. Although these interpretations seem reasonable, it is not compatible with computational results. In both compounds, not only for **1**, the calculated bond length and hyperconjugation effects are larger for $C_1$-$H_{ax}$ than $C_1$-$H_{eq}$, so, considering only the classical explanation of Perlin effect, both $^{1}J_{C1\text{-}Hax}$ should be larger than $^{1}J_{C1\text{-}Heq}$, but this is not what experimental results show (table 1). Also, when comparing both molecules, one can clearly see the small difference in $^{1}J_{C1\text{-}Hax}$ and the large difference in $^{1}J_{C1\text{-}Heq}$ between both molecules. Therefore, the aim of this work is to study the origins of Perlin effect for **1** and **2**. In order to do that, the structures were optimized and the SSCCs were calculated and decomposed using the ADF 2017 program with several levels of theory. To understand the effects responsible for these SSCCs, the *J*-couplings were analyzed in terms of molecular orbitals (MO) and its natural bond orbitals (NBO) contributions. Both $^{1}J_{C1\text{-}Hax}$ are similar, and this decomposition revealed that the MOs relevant for *J*-coupling are constituted of analogous NBOs, resulting in close values of SSCC, and surprisingly, the LP (2) has a very small contribution for **1** and **2** in these MOs. In fact, LP (1) showed a greater contribution than LP (2) for both cases. For the $^{1}J_{C1\text{-}Heq}$, the decomposition showed more delocalized MOs in **2**, meaning that more NBOs contribute to the total SSCC in **2** than in **1**. Moreover, the MOs which contributes the most to the SSCC presented a decrease in the contribution of $\sigma_{C1\text{-}Heq}$ and an increase of adjacent NBOs. Decreasing the $\sigma_{C1\text{-}Heq}$ contribution, lowers the total value of $^{1}J_{C1\text{-}Heq}$ and at the same time, increasing adjacent NBOs contributions to MOs, also lowers the $^{1}J_{C1\text{-}Heq}$ since the contribution of these orbitals to $^{1}J_{C1\text{-}Heq}$ is negative (table 2), as stated in the literature [3,4]. With this work, we were able to identify the origin of Perlin effect in **1** and **2** and attribute it to contributions of MOs, mainly to the $\sigma_{C1\text{-}Heq}$.

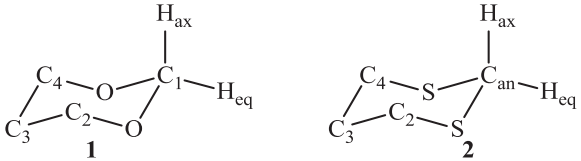


Figure 1: compounds studied in this work

Table 1: $^{1}J_{C1\text{-}H}$ and bond length values of **1** and **2**.

| Molecule/bond | Bond length (theor)[a] | $^{1}J_{Can\text{-}H}$ (expt)[b] | $^{1}J_{Can\text{-}H}$ (theor)[c] |
|---|---|---|---|
| **1**/$C_1$-$H_{ax}$ | 1.102 | 158.6 | 154.3 |
| **1**/$C_1$-$H_{eq}$ | 1.085 | 167.5 | 168.6 |
| **2**/$C_1$-$H_{ax}$ | 1.902 | 154.2 | 157.0 |
| **2**/$C_1$-$H_{eq}$ | 1.089 | 146.2 | 145.8 |

[a]optimized with MP2/aug-cc-pvdz. [b]obtained at -80ºC in $CD_2Cl_2$. [c]calculated with pbe0/jcpl

Table 2: contributions of selected MOs to SSCC and its NBOs.

| **1**, C-Heq | | | **2**, C-Heq | | |
|---|---|---|---|---|---|
| MO | Contribution to SSCC (Hz) | Main NBO contribution to MO | MO | Contribution to SSCC (Hz) | Main NBO contribution to MO |
| 3 | -10.4 | CR (1) O (99%) | 3 | -10.6 | CR (1) S (99%) |
| 7 | 10.9 | $C_1$-O (44%) | 15 | 16.8 | $C_{2/4}$-$C_3$ (26%) |
| 9 | 16.9 | $C_{2/4}$-$C_3$ (46%) | 16 | 47.4 | $C_{2/4}$-$C_3$ (28%) |
| 11 | 80.3 | $C_1$-Heq (17%) | 18 | 56.9 | $C_1$-Heq (15%) |
| 12 | 12.8 | $C_1$-Hax (21%) | 20 | 22.9 | $C_{2/4}$-Hax (34%) |
| 13 | 16.1 | $C_1$-Heq (26%) | 21 | 10.4 | $C_{2/4}$-Heq (53%) |
| 15 | -1.1 | $C_1$-Hax (37%) | 22 | -5.2 | $C_1$-Hax (31%) |
| 16 | 23.1 | $C_3$-Heq (47%) | 23 | 16.2 | $C_3$-Heq (39%) |
| 18 | -8.7 | $C_1$-Heq (24%) | 26 | -20.2 | $C_1$-S (36%) |
| 21 | 28.8 | $C_1$-Heq (17%) | 30 | 11.2 | $C_{2/4}$-S (38%) |
| Total | 168.6 | | Total | 145.8 | |

**Key-words**: Perlin effect, *J*-coupling decomposition, molecular orbitals.

**Support:** This work has been supported by CAPES, CNPq, FAPESP

**References:**

[1] Tormena, C. F., Prog. Nuc. Mag. Reson. Spec. 96, 73 (2016).
[2] Juaristi, E. and Cuevas, G., Acc. Chem. Res. 40, 961 (2007).
[3] Neto, A. et. al. The J. Phys. Chem. A. 112, 11956 (2008).
[4] Contreras, R. et. al. Int. J. of Quant. Chem. 110, 532 (2010).

# Study of the interaction between resins and albite by MM/QM methods.

Kelly F.Pessôa, Fernanda B. da Silva, Júlio C.G.Correia[a], Alexandre N.M.Carauta[a,b]

*Address: [a]Centro de Tecnologia Mineral – CETEM/MCTI. Rio de Janeiro-RJ. Brasil*
*[b]Fundação Técnico-Educacional Souza Marques. Rio de Janeiro-RJ. Brasil*

**Abstract:** The resin process of ornamental stones is crucial in the treatment of this type of stone, because, besides conferring an esthetic beauty, it protects against the action of physical, chemical and biological inclement weather increasing the mineral durability. However, the epoxy resin, which is the most used in this process, it presents toxicity, besides of not being biodegradable, thus creating an important environmental liability and contributes to the interest in finding alternatives in renewable sources[1]. The present work studies, through molecular modeling techniques, the interaction of epoxy resin and two possible active principles of biodegradable resins, cardanol [2] and ricinoleic acid [3], with the mineral albite which is representative of granitic stone, in order to better understand the adsorption process and the energies involved, in order to investigate a renewable alternative to the epoxy resin. A conformational analysis, using mechanical and molecular dynamics techniques, with the COMPASS force field, it was carried out for each of the representative molecules of the resins. The most stable structures obtained were submitted to a geometric optimization with frequency calculation by semi-empirical PM6-DH + [3] methodology, in order to obtain the minimum energy structure and ensure that they were in the ground state. Obtained the minimum structure, geometric optimization calculations with the PM6-DH+ method [4] were performed for successive approximations and in different orientations of each resin in relation to the albite structure constructed from crystallographic data. The maximum distance between the resin and the albite so that the method used admits that there is an interaction was 5Å. Above this value, the optimizations did not evolve into an interaction and the two structures have separated. In all cases, the resins assumed a position very close of the albite indicating the formation of chemical bonds. This seems to indicate that phenomena of chemisorption are expected. The figure 1 shows the results for the adsorption energy of the three systems studied and it indicates that the interaction with ricinoleic acid is the strongest, followed by the epoxy and finally by the resin the cardanol.

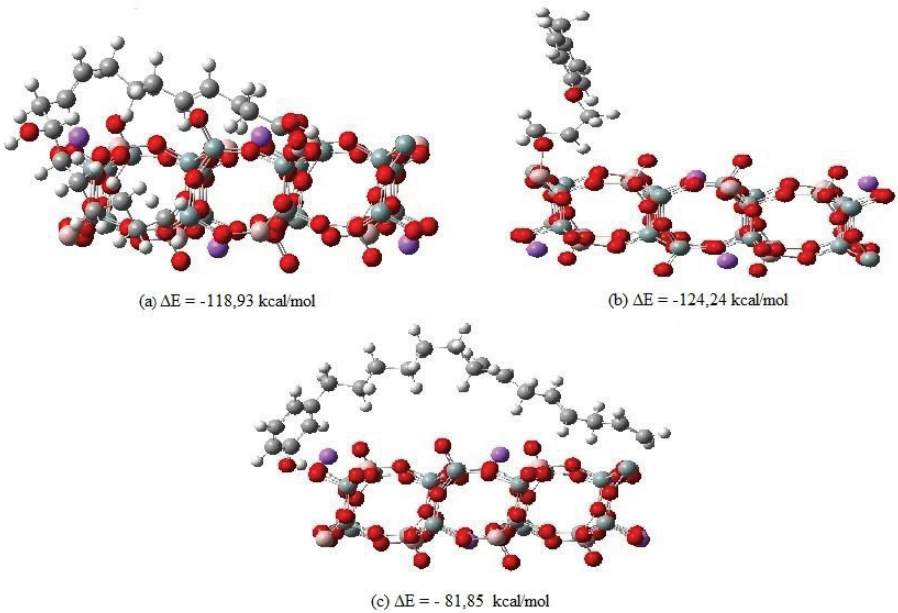


Figure 1 – Resin-Albite structures and respective adsorption energies: (a) Ricinoleic Acid-Albite; (b) Epoxy-Albite; (c) Cardanol-Albite.

**Key-words**: Ornamental Stones, Resins, Compass force field, PM6-DH+

**Support:** The authors acknowledge support from CNPq and PCI/CETEM and LABMOL collaborators. The authors thanks Prof. Prof. Peter Seidl by the Accelerys Inc. package license.

**References:**

[1] Silva, B. B. R.; Santana, R. M. C., Forte, M, M. C., International Journal of Adhesion & Adhesives, 2010, 30, pp 559–565.
[2] Mazzetto, S. E.; Lomonaco, D.; Mele, G., Química Nova, 2009, 32 (3), pp 732-741.
[3] Dalen, M. B.; Ibrahim, A. Q.; Adamu, H. M., British Journal of Applied Science & Technology 4(18): 2661-2683, 2014
[4] M. Korth, J. Chem. Theory Comput., 2010, 6 (12), pp 3808–3816.

# Pharmacophore and docking-based hierarchical virtual screening to identify *Leishmania major* farnesyl pyrophosphate synthase inhibitors

Larissa de Mattos Oliveira[1], David B. Costa Jr.[1], Janay Stefany C. Araújo[1], Raquel G. Benevides[2], Franco Henrique A. Leite[1,2], Manoelito C. dos Santos Jr.[1,2]
[1]Programa de Pós-graduação em Ciências Farmacêuticas, Universidade Estadual de Feira de Santana; [2]Programa de Pós-graduação em Biotecnologia, Universidade Estadual de Feira de Santana
*lare_oliveira@yahoo.com.br*

**Abstract:** Cutaneous leishmaniasis caused by *L. major* is the most important clinical form of leishmaniasis. The available therapeutic arsenal for its treatment is limited and has low efficacy and safety profile [1]. Aiming at circumvent this dilemma *Leishmania major* farnesyl pyrophosphate synthase (LmFPPS) (E.C. 2.5.1.10) has been targeted because it catalyzes the rate-limiting step of isoprenoid biosynthetic pathway [2]. The aim of the study was to identify potential LmFPPS inhibitors by pharmacophore and docking-based virtual screening at natural products catalogs from ZINC15 database (http://zinc15.docking.org/). A set of 76 inhibitors was retrieved from literature [3,4] and split into training (n = 8; Ki < 1 μM) and test (n = 68; 0.011 < Ki < 7.30 μM) sets for evaluation. Hence, 8 inhibitors were employed to build 10 pharmacophore models, using GALAHAD default parameters. 6 models with low steric strain (< 100 kcal/mol) were probed their ability to recover 68 actives among 6,300 decoys, built within DUD-E server, as available in UNITY-3D module. Among pharmacophore models, one of them was selected due to higher AUC (0.88) and BEDROC (0.99) values. This pharmacophore model has two charged centers and six hydrogen bond donors (HBD) (Fig. 1). These features are found in all bisphosphonates inhibitors, thus are essential for biological properties. This model was used as template to filtering approximately 85,000 compounds from natural products database and after submitted for docking routine on DOCK 6.8 software (PDB: 4JZX). The redocking was carried out to guarantee that default parameters were enough to find acceptable poses (RMSD<2Å) from the crystallographic ligand. Once the top scoring pose has a RMSD=0.17Å, only the best ranking pose of selected molecules was considered further. After, these parameters were probed for their ability to recover actives among decoys (similar to pharmacophore model protocol). This analysis showed adequate enrichment rate (AUC=0.99 and BEDROC=0.87) for default docking parameters. 148 compounds previously filtered by pharmacophore model (2.88 ≤ QFIT ≥ 52.91) were then docked into the FPPS active site. Finally, 2-top ranked in both methods was evaluated by intermolecular interaction profile (Fig. 2). HBond interactions occur between ZINC000001529189 and Arg50, Lys263 and Lys206. Interactions between the phosphate group of the molecule and ions $Ca^{2+}$ are present. The complex of the molecule ZINC000039031116 with the LmFPPS shows HBond interactions with Asp97, Arg106, Lys206 and Lys263. There is one interaction between $Ca^{2+}$ and the

oxygen of the molecule and the aliphatic chain and heterocyclic ring of the molecule forms hydrophobic interactions with Phe93, Thr163 and Gln166. The interactions with the divalent ions ($Ca^{2+}$) occur through the interaction of these with aspartic acid residues from the sequence motif DDXXD ($D^{98}$, $D^{102}$ and $D^{250}$) and seem to be crucial for LmFPPS inhibition [5]. This approach selected two compounds as potential LmFPPS inhibitors from the natural products ZINC database, that can be evaluated by enzymatic assays.

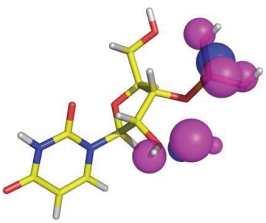

**Fig.1** Superposimg of top-ranked (ZINC000001529189) on pharmacophore model 3 (blue spheres: charged centers and magenta: hydrogen bonding donor sites). The molecule is in stick model and colored per atom (carbon: yellow, nitrogen: blue, oxygen: red, phosphorus: orange).

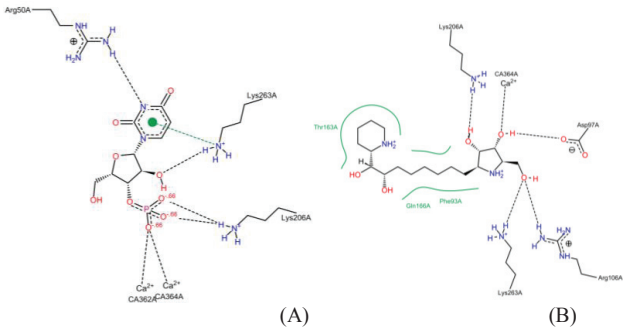


**Fig.2** Interaction maps between the 2-top ranked molecules: ZINC000001529189 (A) and ZINC000039031116 (B) and LmFPPS. (Hbonds: black dotted lines, hydrophobic interactions: green lines and electrostatic interactions: green dotted lines).

**Keywords**: Virtual screening, farnesyl pyrophosphate synthase, leishmaniases.

**Support:** The PPGCF-UEFS and FAPESB was financial support this work. The authors would like to acknowledge Prof. Dr. Marcelo S. Castilho (UFBA) for giving SYBYL-X 2.0 software.

**References:**

[1] Pan American Health Organization. Leishmaniasis Report, 5 (2017).
[2] M. K. Dhar, A. Koul, S. Kaul, New Biotechnology, 30, 2 (2013).
[3] J.M. Sanders, A.O. Go´Mez, J. Mao, G.A. Meints, E.M.V. Brussel, A. Burzynska, P. Kafarski, D. Gonza´Lez-Pacanowska, E. Oldfield, Journal of Medicinal Chemistry, 46 (2003).
[4] J.M. Sanders, Y. Song, J.M.W Chan, Y. Zhang, S. Jennings, T. Kosztowski, S. Odeh, R. Flessner, C. Schwerdtfeger, E. Kotsikorou, G.A. Meints, A.O. Go´Mez, D. Gonza´Lez-Pacanowska, A.M. Raker, H. Wang, E.R. Van Beek, S.E. Papapoulos, C.T. Morita, E. Oldfield, Journal of Medicinal Chemistry, 48 (2005).
[5] S.B. Gabelli, J.S. McLellan, A. Montalvetti, E. Oldfield, R. Docampo, L.M. Amzel, Proteins: Structure, Function, and Bioinformatics, 62 (2006).

# Computational study of glycerol/guanidine associative system for $CO_2$ capture

Larissa F. Vasconcelos, Rodolfo G. Fiorot, José Walkimar de M. Carneiro

*Instituto de Química, Programa de Pós-gradução em Química, Universidade Federal Fluminense. Outeiro de São João Batista s/n, 24020-141 Niterói, RJ, Brasil*

The excess of atmospheric $CO_2$ is a problem that has been causing harsh climatic changes, needing the urgent control of its emission and capture. To that purpose, the chemical absorption with alcohols and amines has been largely in use [1]. According to experimental [1] and theoretical [2] works, guanidine, a strong base, is a promising $CO_2$ scavenger. Alternatively, biofuels – produced from vegetable oils - is also a way to reduce its atmospheric concentration through photosynthesis. [3] However the byproduct, glycerol (propanetriol), has low industrial application [4]. Towards this problematic and knowing that the associative use of strong bases with polyols has been studied for $CO_2$ capture [5], the present work aims to investigate the possible pathways and energetic profiles involved in the $CO_2$ scavenging. Three possible systems were identified, which are shown in **Figure 1**.

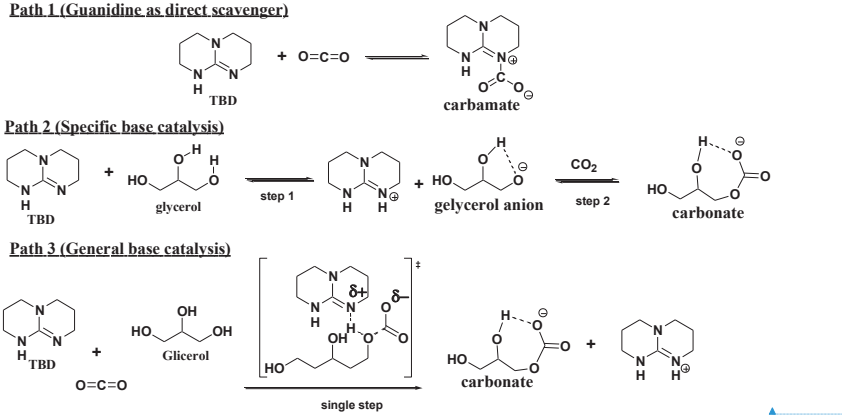


**Figure 1.** Possible paths to $CO_2$ capture with the system guanidine-glycerol.

DFT CAM-B3LYP/6-311++g(2d,2p) method was selected after trial with different functionals compared to reference methods a similar system [2]. Polar media was

simulated with IEFPCM, using water as solvent. In **path 1**, different guanidines were investigated to identify the molecular properties important for the capture. Among them, **TBD** showed the best energetic profile, suggesting that intramolecular hydrogen bond (IHB) is more important than possible π-electron delocalization (**Figure 2**). However, although $CO_2$ concentration is reduced by guanidines, the carbamate intermediate may not be isolated, probably due to decomposition *in situ*.

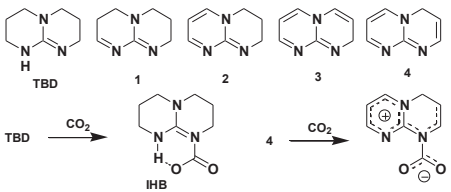


| Guanidine | $\Delta G^{\square}$ [kcal mol$^{-1}$] | $\Delta G$ [kcal mol$^{-1}$] |
|---|---|---|
| **TBD** | 10.13 | - 11.36 |
| **1** | 6.43 | 1.19 |
| **2** | 5.71 | 1.04 |
| **3** | 8.33 | 4.46 |
| **4** | 8.30 | 4.90 |

**Figure 2.** Energetic data to $CO_2$ capture with different guanidines at 298 K

In **path 2**, the conformational analysis of glycerol and its anions indicated that deprotonation of primary hydroxyl is energetically preferred, with the anion establishing two IHBs. In **step 1**, a positive Gibbs free energy change was observed ($\Delta G^{298}$ = 7,69 kcal mol$^{-1}$). In **step 2**, $CO_2$ is spontaneously captured by glycerol anion ($\Delta G^{298}$ = -12,73 kcal mol$^{-1}$) with no activation barrier.

Calculations are still being made to find the concerted transition state of single step (**Path 3**).

**Key-words**: Carbon dioxide, capture, glycerol, DFT.
**Support:** This work has been supported by FAPERJ and Cap.

**References:**

[1] Pereira, F.S. et al. *Tetrahedron.* **2008**, 64, 10097-10106
[2] Orestes, E.; Ronconi,C.M.; Carneiro, J. W. M. C. *Phys. Chem. Chem. Phys.* **2014**, 16, 17213-17219.
[3] Costa, O. A.; Oliveira, L. B.; Silva, A. C. M.; Araujo, M. S. M.; Jr. Pereira, A. O.; Rosa, L. P. *Renew. Sustain. Energy Rev.,* **2013,** 27, 407-412.
[4] Heider, M. K.; Dummer, N. F.; Knight, D. W.; Jenkins, R. L.; Howard, M.; Moulijn, J.; Taylor, S. H.; Hutchings, G. J. Nature Chemistry, **2015**, 7, 1028-1032.
[5] Zhang, S.; He, L.-N. *Aust. J. Chem*. **2014**, *67(7)*, 980.

# Structural and thermodynamic analysis of the compound $\{[Zn(2,5\text{-pdc})(H_2O)_2].\ H_2O\}_n$ and its dehydrated and delaminated forms.

Larissa Lavorato Lima*, Leonã da Silva Flores, Sérgio Rodrigues Tavares, Gustavo Senra Gonçalves de Carvalho, Charlane Cimini Corrêa, Alexandre Amaral Leitão.

*Universidade Federal de Juiz de Fora, Juiz de Fora, Minas Gerais, Brazil.*

**e-mail: larissa.lavorato@ice.ufjf.br*

**Abstract:** In recent decades, a new class of porous solids was reported, the Metal-Organic Frameworks (MOFs), and it is known as a subclass of the coordination polymers. These solids bring together the selective function of the pore modulation with the electronic properties. In general, they typically have crystalline structure formed by coordination of primary organic units and inorganic construction and thus generate infinitely extended structures with different dimensions: 1D (chains), 2D (layers) or 3D (networks) [1]. In particular, the 2D functional materials attracted much attention for the development of a new generation of electronic and optoelectronic devices due to their high surface area and synthetic approach robustness [2]. The two dimensional MOF studied in this work was the network $\{[Zn(2,5\text{-pdc})(H_2O)_2].H_2O\}_n$ (2,5-pdc = 2,5-pyridinedicarboxylate), ZnPDC2D. The MOF 2D was synthesized [3] and characterized by different experimental techniques and was also studied by computer simulation. Two optimized ZnPDC2D structures were obtained by distinct methods (PBE and PBE-D2) with a good agreement of their parameters. The structure obtained from the simulation of the dehydration process suggest the formation of three new phases (d1-ZnPDC2D, d2-ZnPDC2D and d3-ZnPDC2D). The temperature at which ZnPDC2D undergoes amorphization was determined by X-ray powder diffraction measurement with in situ temperature rise and it could be inferred that the amorphous phase undergoes a reversible transformation after being exposed to the environment. The thermodynamics of the first stage of dehydration shows that the PBE functional is adequate to describe the minimum temperature at which this process is spontaneous (142 °C to PBE and 227 °C to PBE-D2). The experimental results from TGA (termogravimetric analysis) show that the ZnPDC2D has a endothermic peak in the range of 130-250 °C. These work also reports the simulation of the monofilm by the PBE and PBE-D2 methods. The analyses

of electronic properties for all the cited structures were performed and discussed according to the processes and changes involved. The elimination of the water molecules caused a change of the geometry especially for the metal center and also a decrease of the band gap energy for the totally dehydrated structure. The monofilm formation energy was obtained and the DOS calculations showed that the band gap energy increased.

**Key-words**: Metal-organic frameworks. Two-dimensional metal-organic frameworks. Structural transformation. DFT.

**Support:** This work has been supported by CAPES, CNPq, FAPEMIG, Brazilian agencies and the enterprise Petrobras S/A (CENPES). We also acknowledge the CENAPAD-SP computational center.

**References:**

[1] G. Férey, Chem. Soc. Rev. 37, 191 (2008).
[2] V. Stavila, A. A. Talin, M. D. Allendorf, Chem. Soc. Rev. 43, 16, 5994 (2014).
[3] J. Jin, X. Han, Q. Meng, D. Li, Y. X. Chi, S. Y. Niu, Journal of Solid State Chemistry 197, 92 (2013).

# DockThor 2.0: a Free Web Server for Protein-Ligand Virtual Screening

Isabella A. Guedes[1], Eduardo Krempser[2], Laurent E. Dardenne[1]

[1] Laboratório Nacional de Computação Científica – LNCC/MCTI, Av. Getúlio Vargas, 333, Petrópolis – RJ, Brazil
[2] Fundação Oswaldo Cruz – Fiocruz – Rio de Janeiro – RJ - Brazil

**Abstract: INTRODUCTION.** Receptor-ligand molecular docking is a structure-based approach widely used by the scientific community in Medicinal Chemistry. The main objective is to assist the process of drug discovery, searching for new lead compounds against relevant therapeutic targets with known three-dimensional structures [1]. The program DockThor [2,3], developed by the group GMMSB/LNCC, has obtained promising results in comparative studies with other well-established docking programs for predicting experimental binding modes, considering several molecular targets and chemical classes of ligands. The first version of the DockThor portal was firstly available for binding mode prediction and was strict to the docking of a single ligand at a time. Despite useful for pose prediction, the scoring function implemented in the first version of the DockThor portal was not suitable for predicting binding affinities, which is crucial for virtual screening studies. Recently, our research group developed new empirical scoring functions to predict protein-ligand binding affinities that demonstrated to be competitive with the best scoring functions reported in the literature [4]. Such encouraging results motivated the development of a new version of the Web server for virtual screening. The DockThor 2.0 portal utilizes the computational facilities provided by the SINAPAD Brazilian high-performance platform (www.lncc.br/sinapad) and the Santos Dumont supercomputer.
**MATERIALS AND METHODS.** The DockThor program has implemented a grid-based method that employs a steady-state genetic algorithm for multiple solutions as the search engine and the MMFF94S force field as the scoring function for pose evaluation. The web server provides the major steps of ligand and protein preparation, being possible to change the residues protonation states and to define the degree of flexibility of the ligand. It is possible to perform virtual screening experiments with a maximum of 100 compounds as a guest user or 1000 compounds for registered users with an approved project. The main parameters of the grid box and the genetic algorithm can also be customized. We recently developed general and specific scoring functions for target-classes, the last to account for binding characteristics associated with a target class of interest, focusing on proteases, kinases and protein-protein interactions complexes (PPIs). The scoring functions were derived using linear regression (MLR) and more sophisticated machine learning techniques for nonlinear problems using the PDBbind refined set 2013 (N = 2959) for training and testing. We also trained and evaluated general scoring functions using docking results obtained with DockThor.
**DISCUSSION AND RESULTS.** The DockThor program has obtained very satisfactory results in redocking experiments using benchmarking datasets considering diverse RMSD values as success criterion, achieving performances of 78%, 83.33% and 78%

in the Astext diverse (N = 85), Iridium-HT (N = 120) and PDBbind 2013 core set (N = 195), respectively, for the top-ranked energy pose. Furthermore, our scoring functions obtained promising performances when evaluated in both experimental and docking structures, indicating that they are reliable to be applied in both cases, with the best one achieving a high correlation with measured binding data (R = 0.705) from the PDBbind core set v2013. In the DockThor portal, docking results are automatically clustered and ordered by an internal analyses tool. The parameters of the analysis step may also be customized by the user, as the number of different binding modes and compare them with a reference conformation of the ligand through the RMSD calculation. Compounds docked in virtual screening studies are ranked according to the score provided by the general and linear scoring function developed by our research group specifically for the DockThor program. Such scoring function was also validated for virtual screening using the DUD-E dataset for several protein targets with active and decoy compounds. For example, the scoring function developed for the DockThor program obtained an AUC = 0.722 when evaluated on a set of 976 active and 25980 inactive compounds for the protease Trypsin [5].

**CONCLUSION.** The new version of the DockThor Portal is a free Web server for protein-ligand docking and virtual screening experiments available for the scientific community at the address www.dockthor.lncc.br/v2.

**Key-words:** virtual screening, protein-ligand docking, drug design.

**Support:** This work has been supported by FAPERJ, CNPq and CAPES.

**References:**

[1] I. A. Guedes, C. S. de Magalhães, and L. E. Dardenne, "Receptor–ligand molecular docking," Biophys. Rev., vol. 6, no. 1, pp. 75–87, Mar. 2014.

[2] C. S. de Magalhães, H. J. C. Barbosa, and L. E. Dardenne, "Selection-Insertion Schemes in Genetic Algorithms for the Flexible Ligand Docking Problem," in Genetic and Evolutionary Computation – GECCO 2004, vol. 3102, K. Deb, Ed. Berlin, Heidelberg: Springer Berlin Heidelberg, 2004, pp. 368–379.

[3] C. S. de Magalhães, D. M. Almeida, H. J. C. Barbosa, and L. E. Dardenne, "A dynamic niching genetic algorithm strategy for docking highly flexible ligands," Inf. Sci., vol. 289, pp. 206–224, Dec. 2014.

[4] I. A. Guedes, A. M. S. Barreto, M. A. Miteva, and L. E. Dardenne, "Development of Empirical Scoring Functions for Predicting Protein-Ligand Binding Affinity," Laboratório Nacional de Computação Científica, Petrópolis - RJ, 2016.

[5] F. S. S. Pereira, I. A. Guedes, and L. E. Dardenne, "Avaliação de Funções Empíricas de Scoring em Experimentos de Triagem Virtual em Larga Escala," 2017.

# Photophysics and Thermoquemistry of 1-8-Naphthalimide in solvents

Franco, L. R., Coutinho, K.

*Instituto de Física, Universidade de São Paulo, Cidade Universitária 05508-090, São Paulo, SP, Brazil*

**Abstract:** In the scope of a Sequential QM-MM approximation [1], we investigated the solvent effect on the conformational and electronic structure of 1-8-Naphthalimide in both ground and excited states. We obtained the optimized structure of 1-8-Naphthalimide in acetonitrile, ethanol and water, in ground and in the first excited state. Then we computed the absorption and fluorescence spectra using CASPT2 and TD-DFT approximations. Our absorption results show a solvatocromic deviation of the first absorption band from acetonitrile (331nm) to water phase (343nm) of 12 nm, that is in good agreement with experimental results [2]. In the excited state we tested two different hypothesis for the lifetime of the excitation: (a) a short lifetime, when the solute goes to excited state and the solvent does not have time to relax; (b) a long lifetime, when solute and solvent are both relaxed in the excited state. We found a good agreement between the computed emission energies and experimental results in the first hypothesis for acetonitrile and ethanol, and in the second hypothesis for water. This is reasonable since it was recently revealed by experimentalists [2] that the excited state of 1-8-Naphthalimide has a short lifetime in acetonitrile and ethanol, and a long lifetime in water (2.3ps). Especially in water, it is found in literature an interesting contradiction. Manna A. and Chakravorti S. (2009) [2] disagreed from Samanta et al. (1996) [3] about the protonation state of 1-8-Naphthalimide. Both are experimental results, and there is no theoretical study about this case in literature. In this context we also studied the unprotonated form of 1-8-Naphthalimide in water. From theoretical spectroscopy we found that is not possible to differentiate between neutral and unprotonated form, both has similar absorption and emission spectra. Otherwise we calculate the standard deprotonation free energy of 1-8-Naphthalimide in water and the pKa in ground and first excited states, with Free Energy Perturbation theory in Monte Carlo simulations. We obtained a pKa=9.17±1.0Kcal/mol for ground state and pka=-3.84±1.4Kcal/mol for excited state. This means that 1-8-Naphthalimide is probably neutral in ground state and unprotonated in first excited state. Now we are doing some spectroscopic experiments in different ph to validate our theoretical results. All quantum mechanics calculations was carried out in Molcas 8.0 and Gaussian g09, and the Monte Carlo simulations was performed in Dice program [4].

**Key-words**: 1-8-Naphthalimide, Photophysics, Thermoquemistry, QM/MM.

**Support:** This work has been supported by CAPES agency.

of electronic properties for all the cited structures were performed and discussed according to the processes and changes involved. The elimination of the water molecules caused a change of the geometry especially for the metal center and also a decrease of the band gap energy for the totally dehydrated structure. The monofilm formation energy was obtained and the DOS calculations showed that the band gap energy increased.

**Key-words**: Metal-organic frameworks. Two-dimensional metal-organic frameworks. Structural transformation. DFT.

**Support:** This work has been supported by CAPES, CNPq, FAPEMIG, Brazilian agencies and the enterprise Petrobras S/A (CENPES). We also acknowledge the CENAPAD-SP computational center.

**References:**

[1] G. Férey, Chem. Soc. Rev. 37, 191 (2008).
[2] V. Stavila, A. A. Talin, M. D. Allendorf, Chem. Soc. Rev. 43, 16, 5994 (2014).
[3] J. Jin, X. Han, Q. Meng, D. Li, Y. X. Chi, S. Y. Niu, Journal of Solid State Chemistry 197, 92 (2013).

# DFT calculations of spectroscopic properties of drug delivery systems formed by oxidized carbon nanostructures

Leonardo A. De Souza[a], Diego Paschoal[b], Hélio F. Dos Santos[b], Luciano T. Costa[c], Wagner B. De Almeida[a]

*[a] LQC, Departamento de Química Inorgânica; [c]MOLMOD-CS, Departamento de Físico-Química, Instituto de Química, Universidade Federal Fluminense, Campus do Valonguinho, Centro, Niterói, RJ 24020-141, Brazil.*
*[b]NEQC, Departamento de Química, ICE, Universidade Federal de Juiz de Fora, Campus Universitário, Martelos, Juiz de Fora, MG 36036-330, Brazil.*

**Abstract:** Drug delivery systems (DDS) formed by oxidized carbon nanostructures are attractive systems and require specific studies of the inclusion compounds formation, interaction type, stability and spectroscopic characterization [1,2]. In the present study, DFT methods were used to study inclusion complexes formed between cisplatin and busulfan antitumor drugs (AD) with oxidized carbon nanotube (CNTox) and nanocone (CNCox) molecules (Figure 1). Gauge-Independent Atomic Orbital (GIAO) method was used for the calculation of $^{1}H$ and $^{195}Pt$ (protocol proposed by Paschoal et. al. [3] to cisplatin) magnetic shielding constants. Solvent effects on the calculation of NMR chemical shifts was evaluated using PCM and water solvent. The B3LYP/6-31G complexes geometries were used for calculations of vibrational modes of IR and Raman spectra. All calculations were performed with the Gaussian 09 package. Molecular modeling studies reported in this work can assist the experimentalists in the spectroscopic characterization of DDS formed by AD and carbon nanostructures.

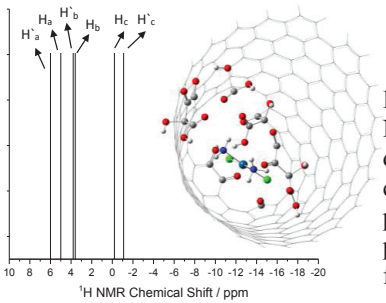


**Figure 1.** B3LYP/6-31G(d,p)-PCM($H_2O$) $^{1}H$ NMR spectrum shows that the experimental detection of the inclusion complexes formed by cisplatin and oxidized carbon nanocone can be promptly attained. It was observed variations of -6 ppm due to the formation complex compared to the free cisplatin.

**Key-words**:DDS, Oxidized carbon nanostructures, DFT calculations, $^{1}H$ and $^{195}Pt$ RMN
**Support:** This work has been supported by CAPES and CNPQ.

**References:**

[1] L. A. De Souza, C. A.S. Nogueira et al, Inorg. Chim. Acta, 447, 38 (2016).
[2] L. A. De Souza, A. M. Da Silva Jr et al, RSC Adv., 7, 13212 (2017).
[3] D. Paschoal, C. F. Guerra et al., J. Comput. Chem., 37, 2360 (2016).

# Estudo da Dissociação de Espécies Aniônicas e Catiônicas do Metano e Sua relação com a Irradiação de Gelos Astrofísicos

Authors: Leonardo Baptista[1], Enio Frota da Silveira[2]

*Address: [1]Universidade do Estado do Rio de Janeiro, Faculdade de Tecnologia,*

*Departamento de Química e Ambiental,*
*[2]Pontifícia Universidade Católica do Rio de Janeiro, Departamento de Física*

**Resumo:** No meio interestelar (ISM), cometas meteoritos e superfícies planetárias são constantemente bombardeadas por radiação e vento solar. É sabido que este processo de irradiação leva à erosão de sólidos e à síntese de novas moléculas. A molécula de metano é encontrada em diversos corpos congelados de nosso sistema solar, como nas nuvens de gelo de planetas Jovianos, em Titã e na superfície de plutão. Por meio de experimentos pode-se constatar que o bombardeio de metano sólido por íons pesados de alta energia leva à síntese de hidrocarbonetos. Após irradiação, foram observados como produtos majoritários: etano, eteno, etino e propano[1]. A partir dos dados experimentais surge a questão: Qual o mecanismo que leva ao crescimento da cadeia carbônica após impacto dos íons? Este trabalho tem como objetivos de longo prazo descrever os caminhos de dissociação do metano após ionização[2] e captura de elétrons e, finalmente, relacionar estes processos a síntese de novas moléculas em gelos astrofísicos. Neste momento será apresentada a descrição quanto-mecânica da dissociação do $CH_4$ e $CH_4^-$. Todo o estudo de dissociação foi realizado em nível multiconfiguracional (CASSFC e NEVPT2) com espaço ativo de nove elétrons e oito orbitais, no caso do ânion, oito elétrons e oito orbitais para molécula neutra, e base 6-311++G(d,p). Os caminhos de dissociação foram descritos e, quando possível, são propostas geometrias para as estruturas de transição envolvidas nestes caminhos. A investigação da contribuição dos estados eletrônicos excitados do metano para dissociação e captura de elétrons foi investigada em nível MRCISD. Inicialmente os resultados dos coeficientes de velocidade microcanônicos, calculados via teoria RRKM e dados de estrutura eletrônica obtidos em nível NEVPT2(9,8)/6-311++G(d,p), foram comparados com as seções de choque de dissociação induzida por captura de elétrons do metano (Figura 1)[3]. Qualitativamente observa-se um bom acordo entre as k(E) calculadas e a seção de choque experimental. Ambos os dados indicam que após a captura de elétrons o caminho de dissociação majoritário é a formação de $CH_3$ e $H^-$. Comparações entre as curvas de dissociação do metano neutro e metano aniônico estão sendo realizadas a fim de se entender como a captura de elétrons afeta o processo de dissociação e como tais processos se relacionam com a irradiação de gelos astrofísicos.

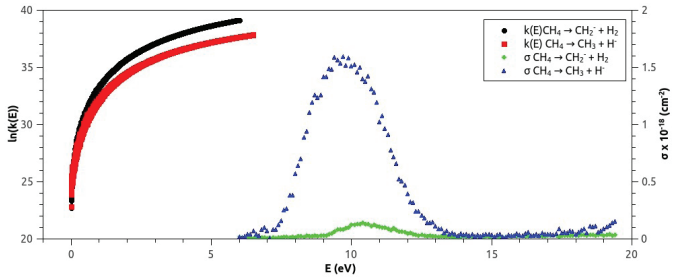


Figura 1: Comparação da seção de choque para dissociação induzida por captura de elétrons[3] e k(E) calculada via teoria RRKM e propriedades eletrônicas e estruturais calculadas em nível NEVPT2(9,8)/6-311++G(d,p).

**Key-words**: dissociação do metano, métodos multiconfiguracionais, astroquímica, teoria RRKM
**Support:** FAPERJ e CNPq
**References:**
[1] A. L. F. de Barros et al. A&A 531, A160 (2011)
[2] L. Baptista, E. F. da Silveira, Phys. Chem. Chem. Phys., 16, 21867, (2014)
[3] M. Song et. al., J. Phys. Chem. Ref. Data, 44, 023101-1, (2015)

# Efficient molecular design of nanoporus mebranes: the role of intermolecular interactions

Leonardo A. Cunha, Max Pinheiro Jr., Luiz F. A. Ferrão, Francisco B. C. Machado

*Departamento de Química, Instituto Tecnológico de Aeronáutica*
*São José dos Campos – 12.228-900 – São Paulo/Brasil*

**Abstract**: Gas separation is a subject of relevance for several strategic industrial and chemical processes, encompassing oil refinery and waste gas purification [1,2]. Despite the availability of a wide range of porous membrane structures based on organic polymeric aggregates or silicon derivatives, their efficiency is usually compromised due to their thickness [3]. In this context, graphene-based nanoporous membranes play an important role. While several theoretical studies have already been reported discussing the use of different graphene-based porous structures for the separation of gas molecules [4-7], the interplay between the pore selectivity and specific intermolecular interactions with the approaching system remains to be understood.

The aforementioned question is addressed in the present work by analyzing the diffusion barrier of several gas molecules passing through two carbon-based pores which differs on size and chemical affinity. The potential energy surface (PES) for the interaction is computed by means of the Density Functional Theory, applying various dispersion-corrected exchange-correlation functionals. We were able to verify the importance of the dispersion interaction in order to explain the diffusion barrier and the existence of a minimum well on the PES. A deeper evaluation of the total interaction energy unfolding into its physically meaningful components (electrostatics, exchange, induction and dispersion) is obtained at the Symmetry-Adapted Perturbation Theory [8] level. Our results suggest that, despite the dominance of the exchange interaction due to the steric hindrance, electrostatics and dispersion are key components that could be tuned by chemical modification of the pore structure, leading to an enhancement of the efficiency and selectivity of permeable membranes for gas-separation purposes. Finally, the influence of intermolecular charge-transfer towards the prediction of the diffusion barrier is assessed through the behavior of the induction component and by a detailed analysis of the frontier orbitals of the dimer complex.

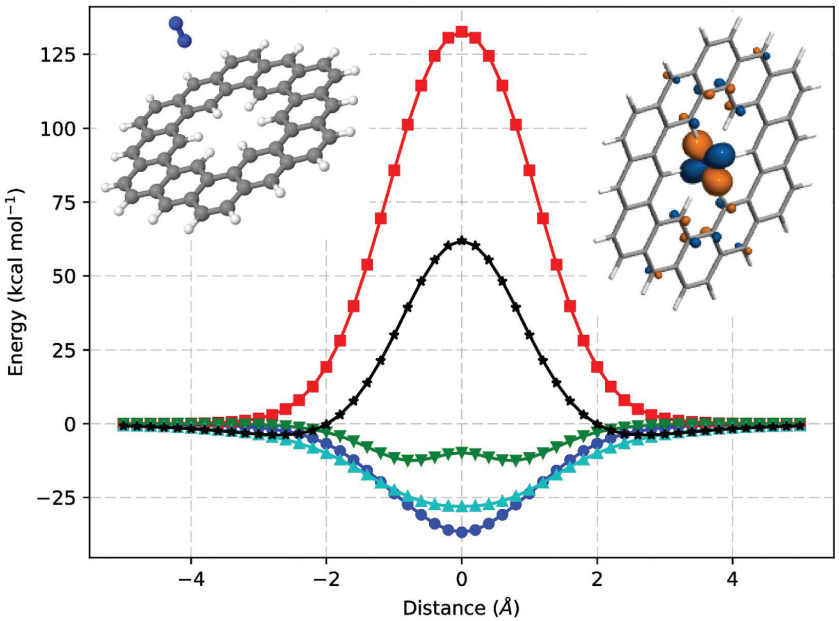


**Key-words**: gas separation, graphene, SAPT, intermolecular interactions.
**Support**: This work has been supported by CAPES, CNPQ and FAPESP.

**References**:

[1] L. Wang, M.S.H. Boutilier, P.R. Kidambi, D. Jang, N.G. Hadjiconstantinou, R. Karnik, Nat. Nanotechnol. **12**, 509 (2017).
[2] A. Ambrosetti, P.L. Silvestrelli, J. Phys. Chem. C **118**, 19172 (2014).
[3] S. Oyama, D. Lee, P. Hacarlioglu, R. Saraf J. Memb. Sci. **244**, 45 (2004).
[4] Y. Wang, Q. Yang, C. Zhong, J. Li, Appl. Surf. Sci. **407**, 532 (2017).
[5] Y. Tao, Q. Xue, Z. Liu, M. Shan, C. Ling, T. Wu, X. Li, ACS Appl. Mater. Interfaces **6**, 8048 (2014).
[6] L. Zhu, Q. Xue, X. Li, Y. Jin, H. Zheng, T. Wu, Q. Guo, ACS Appl. Mater. Interfaces **7**, 28502 (2015).
[7] L. Zhu, Q. Xue, X. Li, T. Wu, Y. Jin, W. Xing, J. Mater. Chem. A **3**, 21351 (2015).
[8] B. Jeziorski, R. Moszynski, K. Szalewicz, Chem. Rev. **94**, 1887 (1994).

# Electronic structure calculations for the study of polyfuran-based chemical sensors: evaluation of local reactivities

Leonardo Gois Lascane, Augusto Batagin-Neto

*leonardo.gois@grad.itapeva.unesp.br*

**Abstract:** Organic polymers are promising materials for active layers of chemical sensors. In this context, polyfurane (PF) derivatives have not been extensively investigated due to typical stability problems and low electrical response of these compounds. A recent work have demonstrate that some of these typical drawbacks can be overcome by an appropriate choice of lateral substituents, which could allow the application of PF derivatires in varied areas, including as chemical sensors [1]. In order to better evaluate possible sensory features of these materials, in this report we employed electronic structure calculations to identify and analyze reactive site on the main chain of eight polyfurane derivatives with distinct side ramifications (R). Oligomeric structures with 9 units were fully optimized *in vacuo* in a Hartree-Fock approach by using the PM6 hamiltonian [2] implemented in the MOPAC2016 computational package [3,4]. The identification of more susceptible sites for analytes adsorption was performed via Condensed-to-atoms Fukui indexes (CAFI) [5] calculated in the Density Functional Theory framework, employing the B3LYP exchange-correlation functional and 6-31G basis set for all the atoms. CAFI calculations were performed with the aid of Gaussian 09 computational package [6]. Hirshfeld partition method was employed for the evaluation of electronic populations in order to avoid negative CAFI values [7,8]. The obtained results indicate the derivatives PF-C≡CH and PF-$NO_2$ as the most promising materials for the development of chemical sensors. These compounds present high reactivity in the lateral ramifications (more accessible sites for analyte adsorption) and more stability to oxidation in relation to PF. Adsorption studies guided by the reactivity results are currently in progress.

**Key-words**: polyfuran, Condensed-to-atoms Fukui indexes, chemical sensors, electronic structure calculations.

**Support:** This work was supported by FAPESP (Proc. 2016/11358-1), CNPq (Proc. 448310/2014-7), and by the Center for Scientific Computing (NCC/GridUNESP) of Sao Paulo State.

**References:**

[1] D. Sheberla, S. Patra, Y. H. Wijsboom, S. Sharma, Y. Sheynin, A.-E. Haj-Yahia, A. H. Barak, O. Gidron and M. Bendikov, *Chem. Sci.*, **2015**, 6, 360–371.
[2] J. J. P. Stewart, *Journal of Molecular Modeling*, **2007**, 13, 1173–1213.
[3] J. J. P. Stewart, *J. Comput.-Aided Mol. Des.*, **1990**, 4, 1–103.

[4] J. J. P. Stewart, *MOPAC2012 : Molecular Orbital Package*, Stewart Computational Chemistry, **2012**.
[5] W. Yang and W. J. Mortier, *J. Am. Chem. Soc.*, **1986**, 108, 5708–5711.
[6] M. J. Frisch, G. W. Trucks, H. B. Schlegel, G. E. Scuseria, M. A. Robb, J. R. Cheeseman, G. Scalmani, V. Barone, B. Mennucci, G. A. Petersson and H. Nakatsuji, *Gaussian 09*, Gaussian, Inc., Wallingford CT, **2009**.
[7] R. K. Roy, S. Pal and K. Hirao, *The Journal of Chemical Physics*, **1999**, 110, 8236–8245.
[8] F. De Proft, C. Van Alsenoy, A. Peeters, W. Langenaeker and P. Geerlings, *J. Comput. Chem.*, **2002**, 23, 1198–1209.

# Molecular and Electronic Structure Elucidation of a New Class of Cannabisin. An Experimental and Theoretical study

Authors: Leonardo H. Morais, Leice M. R. de Novais, Virgínia C. da Silva, Renato G. Freitas.

*Address:* Laboratório Computacional de Materiais (LCM), Department of Chemistry, Federal University of Mato Grosso, 78060-900 Cuiabá, MT, Brazil

**Abstract:** The *Xylopia* genus belonging to the *Annonaceae* family is composed for approximately 160 species. The *Xylopia aromatica* (Lam.) Mart species aromatic is a typical plant of the savannah, known popularly as monkey pepper or monkey banana. After the application of several experimental techniques, cannabisin-b was isolated for the first time along plants found in Cerrado Bioma. This organic molecule is unpublished in the species *Xylopia aromatica*. Because of the potential medicinal properties [1], as well as the novel architectures, the total synthesis of several members of the lignanamide family has received considerable interest [2]. In this sense, theoretical calculation is used in order to probe the experimental data and obtain a molecular structure agreement. In the present work, we choose molecular dynamics (MD) [3] simulation and DFT [4,5] to compare the experimental data with PCM and explicit solvent at the structure, initially were performed geometry optimizations using GROMACS [6] with solvent methanol, soon after, we performed geometry optimizations and spectroscopies properties computations using Gaussian 09 [7] software suite. The computations were carried out using B3LYP [8,9] and 6-311++G (d,p) [10] basis set.

The MD simulations were carried out using the Optimized Potentials for Liquid Simulations (OPLS-AA) force field [11] along with organic parameter set extension within the GROMACS 5.1.4 program, as presented in Figure 1. The simple point charge (SPC) model was used to describe the methanol molecules.

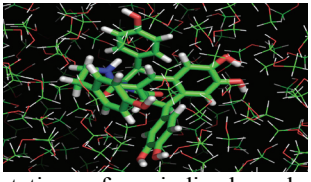

**Figure 1**. Snapshot presentation of periodic boundary condition simulation of cannabisin-b in methanol solvent.

After MD optimization, the cannabisin-b internal coordinates was submitted to infrared (IR) and nuclear magnetic resonance (NMR) computations, in order to compare to experimental data, as observed in Figure 2.

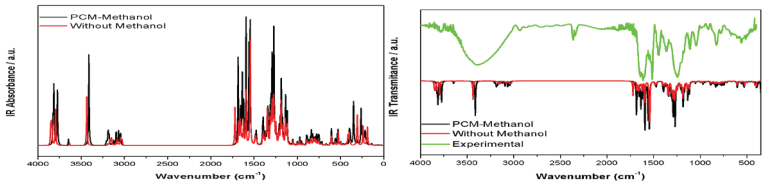


**Figure 2**. Theoretical IR spectra of cannabisin-b structure in PCM – methanol, without methanol and experimental IR data.

The values obtained using DFT display good agreement when compared for experimental, because the bands at theoretical computations are generally closer wavenumber and intensity to the experimental data.

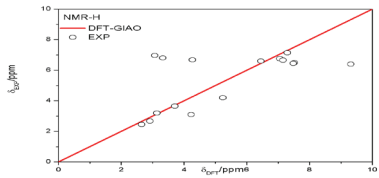


**Figure 3**. Correlation graphic between experimental and theoretical NMR $^{1}$H.

As can be seen from Figure 3, the theoretical $^{1}$H are in agreement to the experimental data. It is seen from the theoretical results, there is no remarkable difference between the results of the level of theory used in evaluating vibrational frequencies and experimental characterization.

**Key-words**: Cannabisin-b, MD, DFT
**Support:**This work has been supported by Capes CNPq and FAPEMAT (214599/2015). Authors thanks to CENAPAD Computing Center for affordable computational time and structure.

**References:**

[1] Xia, Yamu, et al. J. of Chemical Research 39.10 (2015).
[2] F. Bailly et al,.*Med*. Chem. Lett., ,**23**, 574 (2013).
[3] J. McCammon et al, Nature 267.5612(1977).
[4] Pierre Hohenberg and Walter Kohn. Physical Review 136.3B(1964).
[5] Walter Kohn and Lu Jeu Sham, Physical Review 140.4A(1965).
[6] Herman J. C. Berendsen et al, Computer Physics Communications 91.1-3 (1995)
[7] M. J. Frisch et al., Gaussian Inc., Wallingford CT, G09, Revision D.01(2009).
[8] A. D. Becke, J. Chem. Phys. 98, 5648 (1993).
[9] C. Lee, W. Yang, and R. G. Parr, Phys. Rev. B 37, 785 (1988).
[10] M. J. Frisch, J. A. Pople and J. S. Binkley, J. Chem. Phys. 80, 3265 (1984)
[11] W. L. Jorgensen et al, J. of the American Chemical Society 110.6 (1988).

# Quantum Theory of Atoms in Molecules charge-charge transfer-dipolar polarization classification of infrared intensities

Leonardo J. Duarte[1],Wagner E. Richter[2], Arnaldo F. Silva[1] and Roy E. Bruns[1]

[1]*Chemistry Institute, University of Campinas, CP 6154, Campinas, SP, Brazil. 13.083*
[2]*_Department of Chemical Engineering, Technological Federal University of Parana, Ponta Grossa, PR, 84016-210*

**Abstract:** Fundamental infrared intensities of gas-phase molecules are sensitive probes of changes in electronic structure accompanying small molecular distortions. Models containing charge, charge transfer and dipolar polarization effects are necessary for a successful classification of the C-H, C-F and C-Cl stretching and bending intensities. C-H stretching and in-plane bending vibrations involving $sp^3$ carbon atoms have small equilibrium charge contributions and are accurately modeled by the charge transfer-counterpolarization contribution and its interaction with equilibrium charge movement. Large C-F and C=O stretching intensities have dominant equilibrium charge movement contributions compared to their charge transfer-dipolar polarization ones and are accurately estimated by equilibrium charge and the interaction contribution. The C-F and C-Cl bending modes have charge and charge transfer-dipolar polarization contribution sums that are of similar size but opposite sign to their interaction values resulting in small intensities. Experimental in-plane C-H bends have small average intensities of 12.6±10.4 km $mol^{-1}$ owing to negligible charge contribuions and charge transfer-counterpolarization cancellations, whereas their average out-of-plane experimental intensities are much larger, 65.7±20.0 km $mol^{-1}$,as charge transfer is zero and only dipolar polarization takes place. The C-F bending intensities have large charge contributions but very small intensities. Their average experimental out-of-plane intensity of 9.9±12.6 km $mol^{-1}$ arises from the cancellation of large charge contributions by dipolar polarization contributions. The experimental average in-plane C-F bending intensities, 5.8±7.3 km $mol^{-1}$ is also small owing to charge and charge transfer-counterpolarization sums being cancelled by their interaction contributions. Models containing only atomic charges and their fluxes are incapable of describing electronic structure changes for simple molecular distortions that are of interest in classifying infrared intensities. One can expect dipolar polarization effects to also be important for larger distortions of chemical interest.

**Key-words**: Charge transfer , polarization, infrared intensities, QTAIM..

**Support:** A. F. S. and L. J. D. thank São Paulo's FAPESP for the award of postdoctoral grant number 2014/21241-9 and undergrad fellowship 2016/07411-4, and R. E. B. acknowledges FAPESP for funding through the award 2009/09678 and Brazil's CNPq for research fellowship, 304518/2014-0.

**References:**

1. R. L. A. Haiduke and R. E. Bruns, J. Phys. Chem. A, 2005, **109**, 2680.
2. R. F. W. Bader, *Atoms in Molecules. A Quantum Theory*. Clarendon Press, Oxford, 1990.
3. A. F. Silva, W. E. Richter, H. G. C. Meneses, R. E. Bruns, Physical Chemistry Chemical Physics 2014, **16**, 23224.

# Theoretical studies of PP5-$Mg^{2+}$ with potential inhibitors and H304A mutation

Authors: Letícia C. Assis[1], Tamiris M. de Assis[1], Daiana T. Mancini[1], Alexandre A. de Castro[1], Juliano B. Carregal[1],Teodorico C. Ramalho[1], Elaine F. F. da Cunha[1]

*Address: [1]Laboratory of Molecular Modeling, Department of Chemistry, Federal University of Lavras, CEP 37200-000, Lavras/MG*

**Abstract:** Serine/threonine protein phosphatase 5 (PP5) is a promising target for anticancer therapies and neurodegenerative diseases[1,2]. This enzyme is a member of the gene family of PPP phosphatases, which catalyze dephosphorylation reactions, a regulatory process in the signal transduction pathways that control various biological processes [2,3]. A strong inhibitor of PPP phosphatases is Cantharidin. This natural toxin acts on several cellular processes, such as DNA damage, cell cycle arrest and apoptosis [2,4]. However, the clinical application of this toxin is limited due to severe side effects in the gastrointestinal tract, kidney and ureter [4]. In this context, it is necessary to search for less toxic compounds than cantharidin, in order to aid in the future development of new compounds with important pharmacological properties for the PP5 inhibition. This work aims to study how the inhibition takes place between human PP5 and its inhibitors derived from cantharidin. Molecular dynamics techniques were employedin order to investigate the key interactions that occurin the active site and analyze the interference of the H304A mutation on the inhibition activity of ten compounds (Fig.1). The results obtained indicate that the inhibition activity of the cantharidin analogs takes place openly in the catalytic site and the most important residues, i.e., that contribute favorably to the interaction of the ligand within PP5, are Arg400, His304, Arg275, His244, Phe446 and Val429. In turn, theAsp271 and Asp274 residues disfavor such interactions. In addition, through the mutation, it was possible to evaluate the importance of the His304 residue interfering with the activity of these toxins, suggesting that the inhibitory potency of these compounds may be related to the

coordination mode with the metal and not only with the interaction in the PP5 active site.

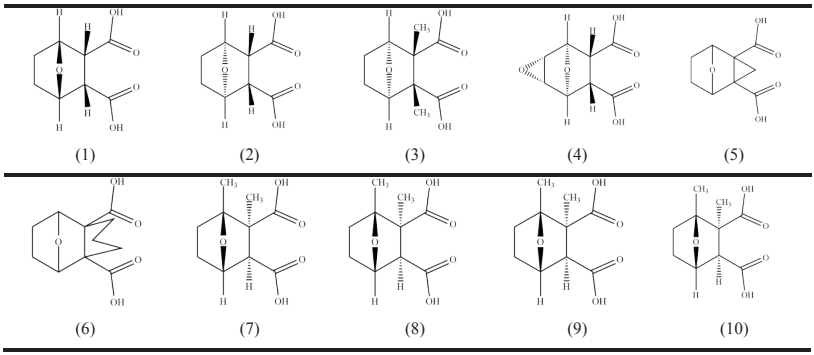


Figure 1: Chemical structures of the 10 analogous compounds of cantharidin.

**Key-words**: Serine/Threonine phosphatase 5, Cantharidin, Molecular Dynamics, H304A mutation
**Support:**This work has been supported by**CAPES, FAPEMIG, CNPq**.

**References:**

[1] L. Ji-Yuan, X. Chen, and Y. Zhang, Scientific reports, 5, (2015).
[2] M. R. Swingle, E. A. Salter, E. Wood, B.D'Arcy, C. Zivanov, K. Abney, A. Musiyenko, S. F. Rusin, A. Kettenbach, L. Yet, C. E. Schroeder, J. E. Golden, W.H. Dunham, A. Gingras, S. Banerjee, D. Forbes, A. Wierzbicki, R. E. Honkanen, Biochemical pharmacology,109. 14-26, (2016).
[3] R.Ribeiro, M.. Alberto, M. J.Ramos, P. A. Fernandes, Chemistry (Weinheim an der Bergstrasse, Germany), 19,42 14081–14089, (2013).
[4] I. Bertini, V. Calderone, M. Fragai, C. Luchinat, E. Talluri, 52, 15, 4838-4843, (2009).

# Effect of the Metal–Support Interaction on the Adsorption of NO on $Pd_4/\gamma\text{-}Al_2O_3$

Letícia M. Prates[1,PG*], Glaucio B. Ferreira[2,PQ], José W. de M. Carneiro[2,PQ], Wagner B. de Almeida[2,PQ], Maurício T. de M. Cruz[1,PQ]

*[1]Departamento de Química Geral e Inorgânica, Instituto de Química, Universidade do Estado do Rio de Janeiro (UERJ), Campus Maracanã, Rio de Janeiro (RJ), Brasil.*
*[2]Departamento de Química Inorgânica, Instituto de Química, Universidade Federal Fluminense (UFF), Campus do Valonguinho, Niterói (RJ), Brasil.*
**leticiamaiapr@gmail.com, cruzmtm@uerj.br*

**Introduction:** Strong metal−support interaction (SMSI)[1] is a term coined to describe an effect that hinders or even suppresses the chemisorption process in a catalyst, altering its efficiency. Nonetheless, it has been reported that the SMSI effect can be related to electronic and morphological contributions, which can favor or not the chemisorption process.[2-4] The $\gamma\text{-}Al_2O_3$ support, one of the most employed oxides in supported catalysts, displays a structure with octahedral and tetrahedral aluminum cations occupying the interstices between oxygen anions.[5] Due to the different coordination environments, these sites can influence in different manners the metal–support electronic flux, depending on where the metal atom sits.[6] However, despite of a large amount of research developed to understand the SMSI effect, the rationalization of its origin is still under debate. In this work, we performed DFT/B3LYP calculations to evaluate the nature of the metal–support interaction effect in a $Pd_4/\gamma\text{-}Al_2O_3$ catalyst model and its influence in the adsorption of a molecular prototype, the NO molecule.

**Key-words**: $\gamma\text{-}Al_2O_3$, palladium, NO, metal–support interaction, DFT

**Methodology:** A planar $Pd_4$ cluster was deposited and optimized on (110C) surface of a $\gamma\text{-}Al_2O_3$ model ($Al_{14}O_{24}H_6$). On the resulting $Pd_4/Al_{14}O_{24}H_6$ structure (Fig. 1), several adsorption modes were tested for NO molecule, allowing only this last to relax during optimization. The NO adsorption energies ($E_{ad}$) and the cohesion energy ($E_{coh}$) between palladium atoms were computed. The effect of metal-support interaction on NO adsorption was evaluated by means of two contributions: *electronic* ($\Delta E_{(E)} = E^{*}_{ad(NO_{(sp)}/Pd_4)} - E_{ad(NO/Pd_{4(sup)})}$) and *geometric* ($\Delta E_{(G)} = E_{ad(NO/Pd_4)} - E^{*}_{ad(NO_{(sp)}/Pd_4)}$). The DFT B3LYP methodology was employed using Gaussian 03 program. The electrons of $\gamma\text{-}Al_2O_3$, palladium clusters and were described by 6-31G(d,p), LANL2DZ and 6-311+G(d), respectively. All computed energies were corrected by the basis set superposition error (BSSE), calculated by the counterpoise method. The atomic charges were calculated by the Natural Bond Orbital (NBO) approach.

*NO adsorption energy on isolated $Pd_4$ in the same coordinates of $NO/Pd_{4(sup)}$.
(Obs: $Pd_{4(sup)} = Pd_4/Al_{14}O_{24}H_6$).

**Results and discussion:** $Pd_4$ adsorbs on $Al_{14}O_{24}H_6$ in a distorted arrangement (Fig. 1a,b). The Pd–alumina interaction leads to a reduction of 39.1 kcal.mol$^{-1}$ in the cohesion energy among palladium atoms, when comparing with the same distorted $Pd_4$ arrangement isolated. This decrease corresponds to an electronic contribution of 48.9%. Tab. 1 shows that as the NO coordination on palladium increases, the N–O distance elongates and the charge transfer to NO increases, which is relevant to the catalytic process. However, in the presence of support, these parameters are less modified, the adsorption energy decreases and the preferential adsorption mode changes from hollow (–52.0 kcal.mol$^{-1}$) to on-top (−25.4 kcal.mol$^{-1}$, in accordance with experimental result[7]). These results suggest the existence of SMSI effect. It can be observed that at the sites where the electronic contribution promoted by Pd–alumina interaction is higher, the decrease in the adsorption energy is greater. On Pd(2) is verified the lowest NO adsorption energy (–5.4 kcal.mol$^{-1}$) and an electronic effect of 57.0% (Fig. 1d). On Pd(3), however, the smallest decrease in the NO adsorption occurs and the electronic contribution is the lowest (2%, Fig. 1e). For the bridge mode, the metal–support interaction promotes the highest electronic effect (91.1%, Fig. 1f), an indicative that as the NO coordination increases, the electronic component becomes higher, even suppressing the mode (hollow) that could better favors the catalysis.

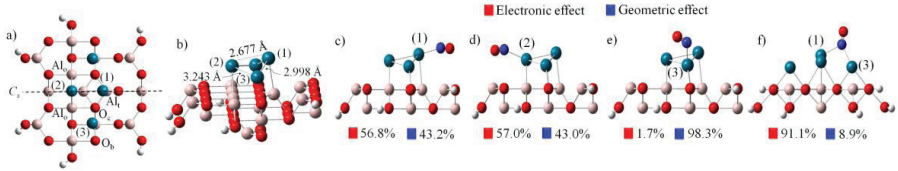


**Figure 1.** (a) Superior and (b) lateral views of $Pd_4/Al_{14}O_{24}H_6$ unit. (c–f) Lateral views of $NO/Pd_4/Al_{14}O_{24}H_6$ structures and electronic and geometric effects (%) involved in NO adsorption.

**Table 1.** Adsorption energy ($E_{ad}$, kcal.mol$^{-1}$), NBO charge density ($\bar{e}$) and bond distance (Å) for NO adsorbed on distorted isolated $Pd_4$ and $Pd_4/Al_{14}O_{24}H_6$.

| | Supported | | | | | Isolated | | | | |
|---|---|---|---|---|---|---|---|---|---|---|
| | On-top | | | Bridge | Hollow | On-top | | | Bridge | Hollow |
| Pd | (1) | (2) | (3) | (1)–(3) | (1)–(2) (3) | (1) | (2) | (3) | (1)–(3) | (1)–(2) (3) |
| N–O | 1.151 | 1.156 | 1.156 | 1.182 | convert | 1.158 | 1.165 | 1.157 | 1.185 | 1.205 |
| $q_{NO}$ | +0.070 | +0.011 | +0.072 | –0.106 | to | –0.012 | –0.019 | –0.032 | –0.236 | –0.410 |
| $E_{ad}$ | –17.55 | –5.37 | –25.36 | –14.47 | bridge | –26.81 | –25.78 | –31.93 | –42.75 | –51.98 |

**Conclusion:** The presence of γ-$Al_2O_3$ support decreases the cohesion energy between palladium atoms. The Pd–alumina interaction promotes an important electronic contribution, capable to weak the NO molecule adsorption. However, this contribution depends on the γ-alumina site at which the palladium atom interacts and also the adsorption mode of the adsorbate molecule.

**Support:** The authors would like to thank CNPq, CAPES and FAPERJ for the financial support.

**References:**

[1] S. J. Tauster, S. C. Fung, R. L. Garten, J. Am. Chem. Soc., 100, 170 (1978).
[2] L. M. Prates et al., J. Phys. Chem. C, 121, 14147 (2017).

[3] A. Bruix et al., J. Am. Chem. Soc., 134, 8968 (2012).
[4] S. D. Senanayake, J. A. Rodriguez, D. Stacchiola, Top. Catal., 56, 1488 (2013).
[5] M.-H. Lee et al., Chem. Phys. Lett., 265, 673 (1997).
[6] J. W. de M. Carneiro, M. T. de M. Cruz, J. Phys. Chem. A, 112, 8929 (2008).
[7] C.-B. Wang, T.-F. Yeh, H.-K. Lin, J. Hazard. Mater., 92, 241 (2002).

# Comparative study of the photochemical properties of silole, thiophene and furan

Letícia R. C. Corrêa[1], Mariana T. do Casal[1], Itamar Borges Jr.[2], Thiago Messias Cardozo[1].

*1. Instituto de Química, Universidade Federal do Rio de Janeiro (UFRJ). Centro Tecnológica, Bloco A, sala 408, Cidade Universitária, 21949-900, Rio de Janeiro, RJ, Brazil.*

*2. Instituto Militar de Engenharia. Praça General Tibúrcio 80, Praia Vermelha, 22290-270, Rio de Janeiro, RJ, Brazil*

leticiarccorrea@gmail.com

The development of new organics semiconductors materials has attracted a large interest due to its application in OLEDs, LCDs and photovoltaic cells. The use of these materials enables the manufacturing of thinner and more flexible displays, portable solar cells and have been used extensively in the manufacture of electronic products [1-3]. Studies indicate that silole-containing polymers could present increased efficiency [4,5]. Despite this, the photochemistry of the silole unit and its specific role in the photophysical mechanisms these materials undergo have not been thoroughly investigated.

In this work, a comparative study of the Potential Energy Surfaces (PESs) of silole, thiophene and furan along the ring puckering and ring opening coordinates are presented, which are usually involved in the deactivation mechanisms for five-membered rings. The surfaces were constructed with the Equation-of-Motion Coupled Cluster including simple and double excitations (EOM-CCSD) implemented in the MOLPRO package [6].

The optimized geometry, vertical excitation energies, and oscillator strength were determined with the 6-31G(d,p), cc-pVTZ and aug-cc-pVTZ basis sets. The calculated geometries are similar for the three basis sets and the first two states present wave functions of the same symmetry, oscillator forces and similar vertical excitations. For more excited states, the aug-cc-pVTZ base presents a significantly better description.

The PESs for the first ten states of silole along the ring puckering mechanism were constructed with the cc-pVTZ and aug-cc-pVTZ basis sets. The 6-31++G ** basis was used for the ring opening mechanism PES. In both mechanisms, we identified possible crossings between the surfaces involving the bright states, but no crossing involving the ground state were found, in contrast with those obtained for furan and thiophene.

In these preliminary studies it is not possible to relate the higher efficiency observed in polymers containing silole units *versus* those containing thiophene or furan, since the complete structure of the polymers constructed with these molecules is determinant to its properties and function. However, the results suggest that the silole

has a higher photostability compared to thiophene and furan, which is an advantage for its application in photovoltaic cells, OLEDs and similar materials.

**Key-words**: silole, photochemical and potential energy surface.

**Support:** This work has been supported by Professor Marco Antonio Chaer Nascimento (UFRJ) and Itamar Borges Junior (IME).

**References:**

[1] TANG, C. W.. Two-layer organic photovoltaic cell. **Appl. Phys. Lett.,** [s.l.], v. 48, n. 2, p.183-185, out. 1986.
[2] GÜNES, Serap; NEUGEBAUER, Helmut; SARICIFTCI, Niyazi Serdar. Conjugated Polymer-Based Organic Solar Cells.**Chemical Reviews,** [s.l.], v. 107, n. 4, p.1324-1338, abr. 2007.
[3] FU, Huiying; CHENG, Yuanrong. Electroluminescent and Photovoltaic Properties of Silole-Based Materials. Current Organic Chemistry, [s.l.], v. 16, n. 11, p.1423-1446, 1 maio 2012.
[4] Yamaguchi, S. *et al. Chem. - A Eur. J.* 2000, *6*, 1683–1692.
[5] Huang, S. et al. Macromolecular Chem and Phys 2017, 1.
[6] MOLPRO, version 2010, a package of ab initio programs, H.-J. Werner, P. J. Knowles, G.Knizia, F. R. Manby, M. Schütz, and others.

# Influência da oxigenação da cadeia carbônica na energia de dissociação C-C

Authors: Lisandra P. do Santos[1], Leonardo Baptista[1].

*Address: [1]Universidade do Estado do Rio de Janeiro, Faculdade de Tecnologia de Resende, Departamento de Química e Ambiental*

**Abstract:** Atualmente a forma mais utilizada para obtenção de energia em meios de transporte é a queima de combustíveis fósseis. Esse processo, no qual são utilizados combustíveis como o diesel e o biodiesel, gera um impacto ambiental devido a produção de gases poluentes que afetam o ozônio estratosférico e contribuem para o agravamento do efeito estufa. [1,2]

No presente estudo tem-se como objetivo identificar a influência da oxigenação da cadeia carbônica na reação de dissociação da ligação C-C das moléculas de etano, etanol e etanal, e correlacionar estas reações com processo de combustão.

Foram utilizados neste estudo os métodos multiconfiguracionais CASSCF e NEVPT2 e bases de cálculo 6-311G(d,p) e 6-311G(2df,2pd). Foram considerados dois espaços ativos: dois elétrons e dois orbitais e seis elétrons e seis orbitais. O cálculo das propriedades termodinâmicas e os coeficientes de velocidades foram calculados na faixa de temperatura de 298 a 200K. Os dados termodinâmicos foram obtidos através do software Orca versão 3.0.3 e os dados cinéticos foram obtidos através do software Multiwell versão 2014. [3,4]

A curva de energia de dissociação das moléculas de etano, etanol e etanal está apresentada na Figura 1 em função da metodologia.

Considerando os valores obtidos pode-ser perceber a diferença entre a energia de dissociação da ligação C-C entre as móleculas de etano, etanol e etanal. É perceptível que a reação de dissociação do etanol é favorecida em relação a reação de dissociação do etano e do etanal em nível CASSCF. Em nível NEVP2 muda-se o comportamento obtido em nível CASSF, a dissociação da ligação C-C é facilitada a medida que é aumentado o número de oxidação de um dos átomos de carbono.

As equações de Arrhenius para dissociação do etano, etanol e etanal, em nível NEVPT2(6,6)/6-311G(d,p) são respectivamente: $k(T) = 1{,}37x10^{17}exp(-4{,}05E4/T)$, $k(T)= 9{,}57x10^{12}exp(-4{,}14x10^{4}/T)$, e $k(T) = 2{,}37x10^{14}\ exp(-3{,}67x10^{4}/T)$.

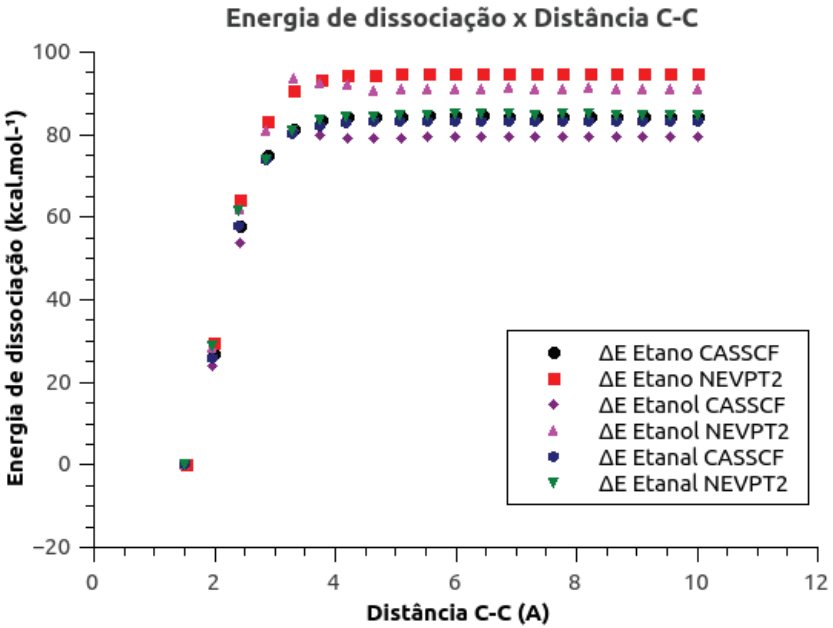


***Figura 1.*** Curva da energia de dissociação das moléculas de etano, etanol e etanal no método CASSCF(6,6) e base de cálculo 6-311G(d,p).

| | **Etano** | **Etanol** | **Etanal** |
|---|---|---|---|
| CASSCF (6,6) | 84,52 | 79,53 | 83,31 |
| NEVPT2 (6,6) | 94,51 | 91,19 | 84,91 |

***Tabela 1.*** Energia de dissociação em relação ao método com base de cálculo 6-311G(d,p) e em kcal.mol-[1].

**Key-words**: métodos multiconfiguracionais, energia de dissociação, biodisel
**Support:** FAPERJ, CNPq.
**References:**
[1] Correa, S. M.; Arbilla G. Atmos. Enviro. 2006, 40, 6821-6826
[2] Kohse-Höinghaus, Katharina Angewandte Chemie International Edition 2010, 49, 3572-3597
[3] R. Krishnan, J.S. Binkley, R. Seeger and J.A. Pople, J. Chem. Phys. 72, 650 (1980)
[4] John R. Barker, Int. J. Chem. Kinetics, 33, 232-45 (2001), John R. Barker, Int. J. Chem. Kinetics, 41, 748-763 (2009).

# Nonadiabatic dynamics of cycloparaphenylenes

Ljiljana Stojanovic[1], Rifaat Hilal[2], Felix Plasser[3], Thomas Niehaus[4], Mario Barbatti[1]

*[1]Aix Marseille Univ, CNRS, ICR, Marseille, France*
*[2]Chemistry Department, King Abdulaziz University, Jeddah, Saudi Arabia*
*[3I]nstitute of Theoretical Chemistry, Faculty of Chemistry, University of Vienna, Austria*
*[4]Université Claude Bernard Lyon 1, CNRS, Institut Lumière Matière, Lyon, France*

We implemented and applied the fewest switches surface hopping method based on time-dependent density functional tight binding (TD-DFTB) to study the gas-phase relaxation dynamics of two cycloparaphenylene molecules, [8]CPP and [10]CPP. TD-DFTB based on DFTB3 model provides a qualitatively correct description of excited-state dynamics, as compared to experimental and other theoretical results. According to the dynamics, both molecules remain in their excited states during 3 ps of dynamics. The long fluorescence lifetimes originate from the slow radiative relaxation from the $S_1$ state. The trend of increasing the fluorescence rate with the molecule size is explained by an increase of the energy gap and oscillator strength for the $S_1$-$S_0$ transition in the larger molecule. The analysis of the charge transfer and spatial localization properties of the $S_1$ states shows that these states have charge transfer characters. In the case of [8]CPP, the $S_1$ state is delocalized over the whole molecule, whereas in [10]CPP it comprises both localized and delocalized excitons. Even though the TD-DFTB method underestimates the excitation energies of the $S_1$ states, the charge-transfer character and the types of the excitations occurring during dynamics are well described, when compared to results of TD-DFTB with long-range corrected functional.

Cycloparaphenylenes, Surface hopping dynamics, TD-DFTB

# Validation of the chitin parameterization in the OPLS force field

Lourival Rodrigues de Sousa Neto, Roberto Ribeiro Faria, Erick Guimarães França,

Mirian Chaves Costa Silva, Eduardo de Faria Franca.

*Address: Federal University of Uberlândia, lorosone@hotmail.com.*

**Abstract:** The computational parameterization of the biopolymer chitin in the OPLS (Optimized Potentials for Liquid Simulations) force field is done, this work is essential for the theoretical study in what refers to the analysis of all the atoms present in the system, mainly to the atoms of hydrogen.

Chitin (CHT) is a very versatile biopolymer and most often used as an adsorbent decontaminant in water, Figure 1.

**Figure 1: a-** Three-dimensional representation of the chitin dimers and their respective van der Waals surfaces, with the nomenclature of the carbon atoms of the glycosidic chains, n being the degree of polymerization. **b-** Three-dimensional representation of 3 monomers of chitin used to perform the parameterization of this work.

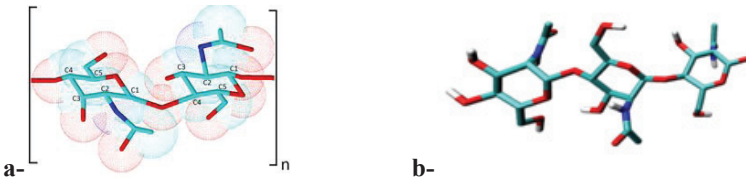


The CHT were parameterized previously in force field GROMOS54a7 in GROMACS computational package and obtained excellent results, but the present research group assembled the new parameters to simulate chitin also in the OPLS-AA, where the behavior of all the atoms of the system can be analyzed.

The determination of the chitin RESP (Restrained Electrostatic Potential) is fundamental for refined parametrization. Some charges obtained are shown in Figure 2. It was noticed that atoms of the same element had different charges, this is due to the chemical environment in which the atoms were immersed. During the procedure of obtaining the RESP were fixed in order to eliminate the errors of calculations. The quantum methodology used in the load calculations was 6-31G *.

**Figure 2:** Charge obtained for the chitin.

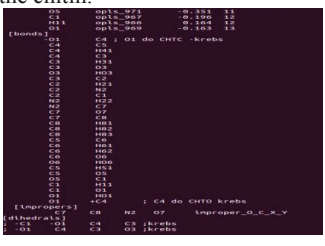

After finalization of the parameterization, a molecular dynamics simulation was performed as a way to validate the parameters inserted in the force field. The simulation time was 50 nanoseconds (ns) ou 50000 picoseconds (ps). For possible property predictions the root mean square deviation in structure of CHT was calculated, to analyze the distances between the atoms of CHT and the total energy of the system containing a chitin trimer in vacuo (Figures 3 and 4, respectively).

**Figure 3:** RMSD for CHT.

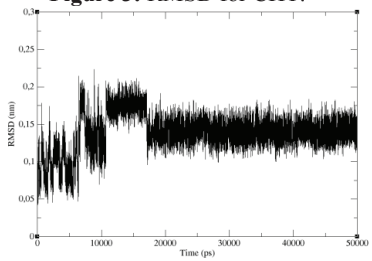


**Figure 4:** Table with total system energy data.

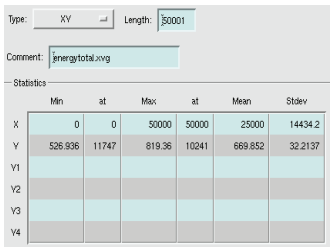


The state of the art of molecular dynamics validated the RESP obtained in the chitin parameterization performed for the OPLSAA force field, and the system and rmsd energy data show that the system converged to the termidamic equilibrium in time of approximately 16ns.

**Key-words**: parametrization; chitin; resp; oplsaa

**Support:** This work has been supported by FAPEMIG □ □ ...

**References:**

[1] M. Valiev, E.J. Bylaska, N. Govind, K. Kowalski, T.P. Straatsma, H.J.J. van Dam, D. Wang, J. Nieplocha, E. Apra, T.L. Windus, W.A. de Jong "NWChem: a comprehensive and scalable open-source solution for large scale molecular simulations" Comput. Phys. Commun. 181, 1477 (2010) doi:10.1016/j.cpc.2010.04.018

[2] FARIA, ROBERTO RIBEIRO ; GUERRA, RENAN FARIA ; DE SOUSA NETO, LOURIVAL RODRIGUES ; MOTTA, LUIZ FREDERICO ; FRANCA, EDUARDO DE FARIA . Computational study of polymorphic structures of α- and β- chitin and chitosan in aqueous solution. Journal of Molecular Graphics & Modelling JCR, 2016.

[3] HESS, B. et al. GROMACS 4: Algorithms for highly efficient, load-balanced, and scalable molecular simulation. Journal of Chemical Theory and Computation, v. 4, n. 3, p. 435-447, Mar 2008.

[4] PRONK, S. et al. GROMACS 4.5: a high-throughput and highly parallel open source molecular simulation toolkit. Bioinformatics, v. 29, n. 7, p. 845-854, Apr 1 2013.

# NMR J-Coupling Constants of Tl−Pt Bonded Metal Complexes in Aqueous Solution: Ab Initio Molecular Dynamics and Localized Orbital Analysis

Lucas C. Ducati,[†] Alex Marchenko,[‡] Jochen Autshcbach[‡]

[†]*Department of Fundamental Chemistry Institute of Chemistry, University of São Paulo, Av. Prof. Lineu Prestes 748, São Paulo, SP 05508-000, Brazil*

[‡]*Department of Chemistry University at Buffalo State, University of New York, Buffalo, New York 14260-3000, United States*

**Abstract:** The influence of solvent (water) coordination and dynamics on the electronic structure and nuclear magnetic resonance (NMR) indirect spin−spin coupling (J-coupling) constants in a series of Tl−Pt bonded complexes, $[(NC)_5Pt{-}Tl(CN)_n]^{n-}$, where n = 0, 1, 2, 3, and $[(NC)_5Pt{-}Tl{-}Pt(CN)_5]^{3-}$, is investigated using Kohn−Sham (KS) Car−Parrinello molecular dynamics (CPMD) and relativistic hybrid KS NMR calculations with and without coordination to water. Coordination of the Tl center by water molecules has a dramatic impact on $^1J$(Tl−Pt) and other J-coupling constants. It is shown that a previous computational study of the same complexes using static optimized structures and nonhybrid functionals was correct about the important role of the solvent but obtained reasonable agreement with experimental NMR data because of a cancellation of substantial errors. For example, the CPMD trajectories show that on average the inner coordination shell of Tl is not saturated, as previously assumed, which leads to poor agreement with experiment when the J-coupling constants are averaged over the CPMD trajectories using NMR calculations with nonhybrid functionals. The combination of CPMD with hybrid KS NMR calculations provides a much more realistic computational model that reproduces the large magnitudes of $^1J$(Tl−Pt) and the correct trends for other coupling constants. An analysis of $^1J$(Tl−Pt) in terms of localized orbitals shows that the presence of coordinating water molecules increases the capacity for covalent interactions between Tl and Pt. There is pronounced multicenter bonding along the metal−metal axis of the complexes.

**Keywords**: AIMD, CPMD, NMR, KS-DFT
**Support:** National Science Foundation (Grant Nos. CHE-1265833 and CHE-1560881), FAPESP (2014/21930-9); CNPq (202068/2015-3)

**Reference:** Ducati, L. C.; Marchenko, A.; Autschbach, J. *Inorg. Chem.* **2016**, *55* (22), 12011–12023.

# On the electronic origin of the high-efficiency of the PTB series donor polymers for organic photovoltaics

Lucas Modesto-Costa,[1] Itamar Borges Jr.,[1] Adélia J. A. Aquino[2], Hans Lischka[2]

[1]*Departamento de Química, Instituto Militar de Engenharia, Rio de Janeiro, Brazil*
[2]*Department of Chemistry and Biochemistry, Texas Tech University, Lubbock, USA*

**Abstract:** The recently synthetized poly-thienothiophene-benzodithiophene (PTB) polymer series is built from a sequence of alternating electron deficient thieno[3,4-b]thiophene (TT) and the electron rich benzodithiophene (BDT) moieties involving different substituents and side chains display remarkable properties as electron donors in organic solar cells of the bulk heterojunction type [1,2,3]. We studied the ground and the first four excited states of three different members of the PTB series, namely, PTB1 (no substituents and side chains), PTB6 (two o-n-propyl chains in BDT) and PTB7 (fluorine atom in TT and two o-iso-propyl side chain in BDT). The time-dependent density functional theory (TDDFT) with the B3LYP functional method was employed. We computed different types of bond length alternation (BLA) analysis of the ground and the first ($S_1$) excited states, natural population analysis (NPA) of all states, excitation energies and oscillator strengths. BLA in the ground state indicates that separation distance between oligomer units and between TT and BDT moieties in each unit are not much affected by the type of substituent. However, the same in not true in the $S_1$ state where the BLA showed the confinement of the exciton (electron-hole pair) in the middle of the chain and the quinoid nature of the excited state. The substituents in PTB7 decrease the difference between the C-C and C=C bond distances in the TT moiety in contrast with the corresponding negligible effect in PTB1 and PTB6. NPA charge shows a dipolar effect in the three cases, an experimental evidence of partial negative charge concentration on certain TT units and partial positive charge on the adjacent BDT that is more pronounced on the most efficient PTB7 polymer. This was also confirmed from charge difference plots of the four transitions.

**Key-words**: organic solar cell, pi-conjugated polymers, TDDFT
**Support:** CAPES, CNPq, Faperj, NSF (CHEM-1213263), Vienna Scientific Cluster, Robert A. Welch (D-0005)
**References:**

[1] Szarko, J. M.; Guo, J. C.; Rolczynski, B. S.; Chen, L. X.: J. Mater. Chem. 21, 7849 (2011).
[2] Borges, I; Aquino, Adélia J. A. ; Köhn, Andreas; Nieman, Reed; Hase, Willian L. ; Chen, Lin X. ; Lischka, Hans. The Journal of the American Chemical Society (JCAS), 135, 18252 (2013).
[3] Borges, I.; Uhl, E.; Modesto-Costa, L.; Aquino, A. J. A.; Lischka, H.: J. Phys. Chem. C 120, 21818 (2016).

# A Computational Study of The Wetting of Nanocrystalline Cellulose

Lucas N. Trentin, Munir S. Skaf

*Institute of Chemistry, University of Campinas, Barão Geraldo, 13083-852, Campinas - São Paulo, Brazil.*

**Abstract:** Sugarcane lignocellulosic biomass is a promising material, being the most available resource for biofuel generation [1]. Its recalcitrance to enzymatic hydrolysis is a key factor to overcome in order to have an economically viable conversion of plant biomass in fermentable sugars [2]. Molecular dynamics (MD) simulations have been used to model water nanodroplets on crystalline cellulose in order to study the hydrophilicity of cellulose faces. Cellulose builder [3] and Packmol [4] were used to create (010), (110), (1-10) and (100) cellulose Iβ faces packed with 3000 water molecules. Three 40ns independent MD simulations using CHARMM force field gave a droplet profile for each face, which was analyzed with LBADSA [5] plugin for ImageJ. It was found that (010) and (110) faces where completely wetted, whereas in (1-10) and (100) faces, contact angles close to 30º where observed, showing that even the so called "hydrophobic surfaces" exhibit some hydrophilic behavior. Full and partial wetting where associated with exposure of hydroxyl groups and axial aliphatic hydrogen atoms, respectively. In addition, the developing of a new software for contact angle determination and study of modified cellulose surfaces are planned to happen in the following months. These data can be useful for biotechnological applications.

**Key-words**: Crystalline Nanocellulose, Molecular Dynamics, Hydrophilicity, Contact Angle.

**Support:** This work has been supported by CNPq (144359/2017-0) and FAPESP (2013/08293-7).

**References:**

[1] S. P. S. Chundawat, G. T. Beckham, M. E. Himmel, B. E. Dale, Annu. Rev. Chem. Biomol. Eng., 2, 121 (2011).
[2] Y. H. P. Zhang, M. E. Himmel, J. R. Mielenz, Biotechnol. Adv. 24, 452 (2006).
[3] T. C. Gomes, M. S. Skaf, J. Comput. Chem. 33, 1338 (2012).
[4] L. Martínez, R. Andrade, E. G. Birgin, J. M. Martínez, J. Comput. Chem. 30, 2157 (2009).
[5] A. F. Stalder, T. Melchior, M. Müller, D. Sage, T. Blu, M. Unser, Colloids Surf., A 286, 92 (2010).

# Structural, electronic, elastic and vibrational properties of zinc sulfide nanotubes: a DFT approach

Lucas Pereira Mendes, Guilherme da Silva Lopes Fabris and Julio Ricardo Sambrano

*Modeling and Molecular Simulation Group - CDMF, São Paulo State University, P.O. Box 17033-360, Bauru, SP, Brazil*

**Abstract:** The discovery of graphene and its inorganic analogues has brought interest in possible structures generated by these 2D honeycomb-like systems, and it has increased considerably due to its great scientific and technological interest in material science, and its possible applications in nanotechnology, as for example, fullerenes, nanoscrolls and nanotubes. Nonetheless, in its pristine form, graphene is a zero gap semiconductor, and this brings restricted application in electronics. Today one of the most studied materials are nanotubes, this structure is formed by rolling up a 2D surface, in a specific direction that can be describe by the chiral indices n and m, which can form three possible conformation: armchair (n,n), zigzag (n,0) and chiral (n,m) type. This structure also has unique properties, which depend on the chirality, and besides being possible to apply this material in nanoelectronics it is also possible to use it as a nanofilter. These nanotubes also can be constructed by inorganic semiconductors like BN, GaN, ZnO, ZnS, among others, being the last one the focus of this study. Zinc sulfide (ZnS) is a II-IV semiconductor that has a band gap of ~3.6eV, and is mostly used in lasers, sensors and catalyst for photooxidation and photoreduction, being used as a nanocrystal. From its wurtzite phase it can be done a slab cut in the (0001) direction and with the hexagonal single layer of ZnS obtained it is possible to roll it up in a nanotube form (see Figure 1). In this work we study the structural, electronic, elastic and vibrational properties of zigzag and armchair ZnS nanotubes via periodic computational simulations based on density functional theory, implemented in CRYSTAL14 program, using the B3LYP functional and using a optimized all-electron basis set[1], being 86-411d31G[2] for the zinc atom and 86-311G*[3] for sulfur atom. Our results shows that this basis set and functional accurately describe the structural and electronic properties of the bulk ZnS. The lattice parameters a and c obtained (experimental values in parenthesis) were 3.83(3.83)Å and 6.25(6.26)Å, respectively; for the band gap it was obtained 3.95(3.77)eV. For the ZnS single layer the lattice parameter was 3.89Å and a band gap of 4.52eV. Our calculation shows that the band gap of the nanotubes independently of the chirality seems to be always around the 4.6eV. The results shows that simulations using the DFT method can accurately describe the structural, electronic, elastic and vibrational properties, and also being able to predict some properties still elusive.

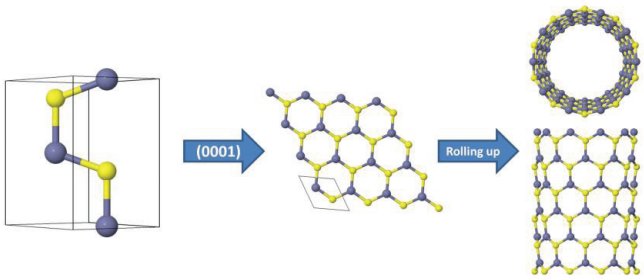


**Figure 1:** Graphical representation of the ZnS nanotube modelling.

**Key-words**: zinc sulfide, DFT, nanotubes
**Support:** This work was supported by the Brazilian funding agencies CNPq (grant no. 46126-4), CAPES (grant no. 787027/2013, 8881.068492/2014-01), and FAPESP (grant no. 2013/07296-2, 2016/07476-9, 2016/25500-4).
**References:**

[1] Y. Santana, C, Raubach, M. Ferrer et al, J. Appl. Phys. 110, 123507 (2011).
[2] A. Lichanot, E. AprÃ  and R. Dovesi, Phys. Stat. Sol. (b) 177, 157-163 (1993).
[3] J. E. Jaffe and A. C.Hess, Phys. Rev. B 48, 7903 (1993).

# Fully Anharmonic Resonance Raman Spectrum of Diatomics Through Vibrational CI Calculations

Authors: Gustavo J. Costa[a], Antonio C. Borin[b], Pedro A. M. Vazquez[c], Rogério Custodio[c], Luciano N. Vidal[a]

*Address:* [a]*Chemistry and Biology Department, UTFPR/Curitiba;* [b]*Department of Fundamental Chemistry, Institute of Chemistry, USP/São Paulo;* [c]*Chemistry Institute, Unicamp/Campinas.*

**Abstract:** Within the Born-Oppenheimer approximation, the pure vibrational Resonance Raman (RR) spectrum is obtained following three basic steps: (1) The Potential Energy Surface of the ground and one (or more) excited states must be calculated as well as the Electric Dipole Transition Moment Surface; (2) Vibrational energies and wavefunctions of those electronic states must be evaluated and (3) Building vibronic polarizabilities from the *sum over states* (current approach) or *time dependent* theory of the Raman effect. We present here a methodology to compute fully anharmonic RR spectrum of diatomic molecules where the potential energy curves (PEC) are evaluated using multiconfiguration *ab initio* wavefunctions and the vibrational problem is numerically solved using configuration interaction theory, where the matrix representation of the vibrational Hamiltonian is built using (hundreds/thousands of) harmonic oscillator basis sets. The potential energy contribution to that Hamiltonian matrix is numerically evaluated using the full PEC and cubic spline quadrature while the kinetic energy contribution is analytic. As an example, the RR differential cross sections of hydrogen molecule are presented in **Table 1**. The excitation laser wavelength is *109.12 nm*, corresponding to the CASSCF(124,2)/d-aug-cc-pVQZ wavelength of the electrically allowed $X^1\Sigma_g^+ \rightarrow B^1\Sigma_u^+$ transition. A pure vibrational half-width at half-maximum $\Gamma = 6.01966$ cm$^{-1}$, obtained after averaging the $B^1\Sigma_u^+$ fluorescence lifetimes over 25 rotovibronic states [1], was used to evaluate the RR polarizabilities. In general, the use of fully anharmonic wavefunctions results in a decrease of the predicted RR intensities of $H_2$. Such behavior is also observed at the Franck-Condon level. In addition, a slower convergence of RR cross sections is observed when anharmonic vibrational wavefunctions are used to compute the RR intensities. There is also a change in the relative intensities when anarmonicity is taken into account, with $1 \leftarrow 0$ transition being the strongest at the harmonic level while the anharmonic $3 \leftarrow 0$ transition being the strongest one. That change in the relative intensities is also observed in the RR spectrum of $O_2$, showing the importance of using anharmonic wavefunctions when evaluating the RR spectrum.

**Table 1**: Convergence of RR differential cross sections of $v_f \leftarrow v_i$transitions in $H_2$ molecule with respect to the number of intermediate vibrational states. These cross sections include Herzberg-Teller and thermal (T=300K) corrections.

| | $1 \leftarrow 0$ | | $2 \leftarrow 0$ | | $3 \leftarrow 0$ | |
|---|---|---|---|---|---|---|
| $N_{v_r}$ | Harm. | Anharm. | Harm. | Anharm. | Harm. | Anharm. |
| 2 | $8.3 \cdot 10^{-28}$ | $2.6 \cdot 10^{-28}$ | $9.6 \cdot 10^{-28}$ | $4.8 \cdot 10^{-28}$ | $8.7 \cdot 10^{-28}$ | $3.9 \cdot 10^{-28}$ |
| 14 | $1.2 \cdot 10^{-27}$ | $5.7 \cdot 10^{-29}$ | $1.1 \cdot 10^{-27}$ | $3.7 \cdot 10^{-28}$ | $8.8 \cdot 10^{-28}$ | $4.6 \cdot 10^{-28}$ |
| 26 | $1.2 \cdot 10^{-27}$ | $6.6 \cdot 10^{-29}$ | $1.1 \cdot 10^{-27}$ | $3.6 \cdot 10^{-28}$ | $8.8 \cdot 10^{-28}$ | $4.5 \cdot 10^{-28}$ |
| 38 | $1.2 \cdot 10^{-27}$ | $6.7 \cdot 10^{-29}$ | $1.1 \cdot 10^{-27}$ | $3.6 \cdot 10^{-28}$ | $8.8 \cdot 10^{-28}$ | $4.5 \cdot 10^{-28}$ |
| 54 | $1.2 \cdot 10^{-27}$ | $6.7 \cdot 10^{-29}$ | $1.1 \cdot 10^{-27}$ | $3.6 \cdot 10^{-28}$ | $8.8 \cdot 10^{-28}$ | $4.5 \cdot 10^{-28}$ |

**Key-words**: Vibronic Raman Spectroscopy; *Ab initio* methods; Anharmonicity.
**Support:** This work has been supported by CNPq.

**References:**

[1] A. Pardo, Spectrochimica Acta Part A: Molecular and Biomolecular Spectroscopy, 57, 1057 (2001).

# Spectroscopic Analysis of the $(C_{70})_2$ Dimer on Different Relative Configurations

Luciano Ribeiro[1], Rodrigo A. L. Silva[1], Daniel F. S. Machado[2], Valter H. Carvalho-Silva[1], Heibbe C. B. de Oliveira[2]

*Laboratório de Química Teórica e Estrutural de Anápolis, Universidade Estadual de Goiás, Anápolis, Brazil*[1]
*Laboratório de Estrutura Eletrônica e Dinâmica Molecular, Instituto de Química, Universidade de Brasília, Brasília, Brazil*[2]

**Abstract:** The present work is dedicated to study the spectroscopic property of the $(C_{70})_2$ dimers [1–3]. Based on this study, we built up the potential energy curves for the dimer formation. The spectroscopic constants were obtained by means of the Dunham's and Discrete Variable Representation methods [4,5]. For the full intermolecular potential representation, we employed the Rydberg analytical function [6]. As it is possible to modify the intermolecular interaction potential could be modified, as a result of the different faces that constitute the fullerenes, the spectroscopic properties of the $(C_{70})_2$ were examined for different intermolecular configurations. After running all calculations, it is possible to observe that the system's symmetry is reflected in both the potential energy curves and spectroscopic properties of the dimer. The small variations observed in the spectroscopic constants and in the dissociation energy values for the different configurations of the dimers can be attributed to the fact that the interaction between the monomer is most influenced by the hexagonal faces that make up the fullerene interacting units.

**Key-words**: $(C_{70})_2$ dimers, Spectroscopic properties, Dunham, DVR
**Support:**This work was financially supported by CAPES, PrP-UEG and FAPEG-GO.
**References:**
[1] R. Zhang, M. Murata, T. Aharen, A. Wakamiya, T. Shimoaka, T. Hasegawa, and Y. Murata, Nat. Chem. 8, 435 (2016).
[2] K. Nomura and S. Okada, Chem. Phys. Lett. 608, 351 (2014).
[3] M. Pagliai, G. Cardini, and R. Cammi, J. Phys. Chem. A 118, 5098 (2014).
[4] J. L. Dunham, Phys. Rev. 41, 721 (1932).
[5] J. J. S. Neto and L. S. Costa, Brazilian J. Phys. 28, 1 (1998).
[6] William F. Sheehan, J. Chem. Inf. Model. 53, 1689 (1965).

# Modelling the Polymer Electrolyte/Li-Metal Interface by Molecular Dynamics simulations

Mahsa Ebadi[a], Luciano T. Costa[b], C. Moyses Araujo[c], Daniel Brandell[a]

*a) Department of Chemistry – Angström Laboratory, Uppsala University Box 538, 75121 Uppsala, Sweden*
*b) Instituto de Química, Departamento de Físico-Química, Universidade Federal Fluminense, CEP 24020-141, Niterói-RJ, Brazil*
*c) Materials Theory Division, Department of Physics and Astronomy, Uppsala University, Box 516, 75120 Uppsala, Sweden*

**Abstract:** Solid polymer electrolytes are considered promising candidates for application in Li-metal batteries due to their comparatively high mechanical strength, which can prevent dendrite formation. In this study, we have performed Molecular Dynamics simulations to investigate structural and dynamical properties of a common polymer electrolyte, poly(ethylene oxide) (PEO) doped with LiTFSI salt in the presence of a Li metal surface. Both a physical (solid wall) and a chemical (slab) model of the Li (100) surface have been applied as show in Figure 1, and the results are also compared with a model of the bulk electrolyte.[1]

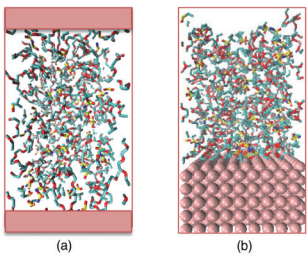


Figure 1. Schematic pictures of the equilibrated (a) Li walls and (b) Li slab models.

The average coordination numbers for oxygen atoms around the Li ions are ca. 6 for all investigated systems. However, the calculated Radial Distribution Functions (RDFs) for $Li^+$-$O_{PEO}$ and $Li^+$-$O_{TFSI}$ show sharper peaks for the Li slab model, indicating a more well-defined coordination sphere for $Li^+$ in this system. This is clearly a surface effect, since the RDF for $Li^+$ in the interface region exhibits sharper peaks than in the bulk region of the same system. The simulations also display a high accumulation of TFSI anions and $Li^+$ cations close to interface regions, in agreement with the literature.[2] This also leads to slower dynamics of the ionic transport in the systems, which have a Li-metal surface present, as seen from the calculated mean-square-displacement functions. The accumulation of ions close to the surface is thus likely to induce a polarization close to the electrodes.

**Key-words**: lithium ion battery, molecular dynamics, polymer electrolytes
**Support:** Swedish Energy Agency grant number 39036-1, the Carl Trygger Foundation, STandUP for Energy and the Swedish Research Council (VR) grant no. 2014-5984, Erasmus Mundo fellowship and FAPERJ.

**References:**

[1] M. Ebadi et al. Electrochimica Acta 234 (2017) 43–51.
[2] O. Borodin et al. Macromolecules. 36 (2003) 7873–7883.

# Molecular modeling in the inhibition of *M. tuberculosis* enzymes

Authors: Luis Mauricio S. Soares(*), Paulo Augusto Netz, Ícaro Ariel Simon, Vanessa Petry do Canto, Ricardo Fagundes da Rocha, Luis Andre Baptista

*Address: Universidade Federal do Rio Grande do Sul. Instituto de Química, Grupo de Química Teórica. Av. Bento Gonçalves, 9500. Bairro Agronomia. Porto Alegre/RS.*

**Abstract:** According to data from the World Health Organization (WHO), in the year 2015, occurred about 10.4 million of tuberculosis new cases; of these, 480 000 new cases of multidrug-resistant. Isoniazid (pyridine-4-carbohydrazide), a prodrug, used in tuberculosis treatment, has been known since 1952, as a potent agent against the *M. tuberculosis* bacillus; and is currently one of the main chemotherapeutics used to control this disease [1,2]. Among the *M. tuberculosis*'s mutant genes, about 75 to 85% of cases are related to the enzymes katG and inhA [3]. However studies have also found resistant strains of *M. tuberculosis*, with mutations in genes of the enzymes kasA (keto-acyl-synthase) and in ndh (NADH dehydrogenase) [4].

The present study aims to use computational methods to study of the interactions of isoniazid derivatives with enzymes of interest for the control of *M. tuberculosis* bacillus, focusing on resistant strains. Results of docking calculations carried out with the AutoDockVina program [5] using InhA and KatG enzymes as receptors are presented in this paper. The docking scores of about 104 docked molecules with different strains of the InhA and KatG enzymes were obtained and some of them are presented in the table below, compared with the reference isoniazid.

| **Enzyme** | **InhA** | | | **KatG** | | | |
|---|---|---|---|---|---|---|---|
| PDB's id | 4TRO* | 4DTI** | 2AQH** | 1SJ2* | 2CCD** | 4C50** | 4C51** |
| Ligands | Scores ($kcal.mol^{-1}$) | | | | | | |
| isoniazid | **-7.1** | -5.2 | -5.5 | -6.3 | -5.8 | -6.5 | -6.1 |
| 15 | **-10.9** | -8.1 | -8.8 | -7.6 | -7.1 | -8.6 | -7.3 |
| 19 | **-10.5** | -8.5 | -8.8 | -9.0 | -8.6 | -9.4 | -9.2 |
| 20R | **-9.8** | -7.5 | -7.1 | -7.7 | -6.9 | -6.9 | -7.5 |
| 23S | **-10.7** | -8.3 | -9.0 | -9.1 | -9.3 | -8.9 | -9.0 |
| 24R | **-10.5** | -8.6 | -8.3 | -9.2 | -8.9 | -8.4 | -8.6 |
| 25 | **-9.1** | -7.3 | -7.6 | -7.9 | -7.2 | -8.2 | -8.2 |

*native isoform, **mutant isoform

The location, conformation and interactions of the ligands in the receptors were analyzed and it was also possible to verify a good correlation between the poses of lower energy, and their fit in the regions already defined by the literature as binding sites in these enzymes.

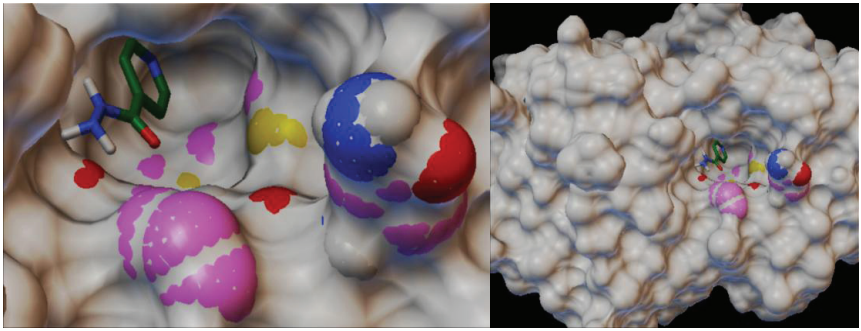

Figure 1 – Isonizid molecule fits to non-mutated Inha enzyme.

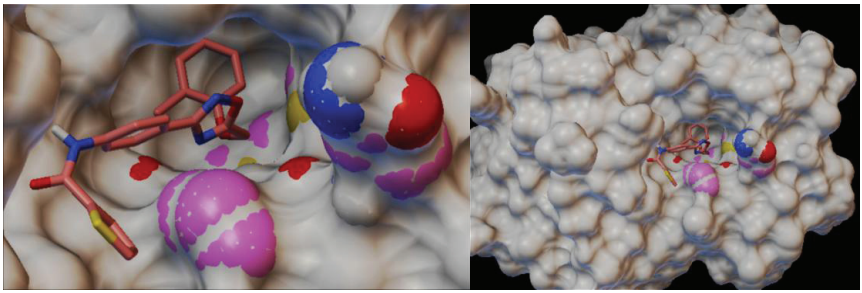

Figure 2 – Ligand 15, fits to same non-mutated Inha enzyme.

As second step of this study (already running), we expect to obtain, using molecular dynamics simulations, further insights regarding the interaction mechanisms of isoniazid-derived molecules, with different receptors, focusing InhA and KatG. Groups of molecules will also be selected and classified according to their topological characteristics, with aim of selecting molecules with larger pharmacological effect against *M. tuberculosis*.

**Key-words**: isoniazid, tuberculosis, Mycobacterium
**Support:** This work has been supported by Fundação de Amparo à Pesquisa do Rio Grande do Sul - FAPERGS, Universidade Federal do Rio Grande do Sul – UFRGS, Universidade Federal de Mato Grosso-UFMT.

**References:**

[1] Y. Zhang, A. Telenti, In: G.F. Hatfull, W.R.Jr. Jacobs, Washington, D.C ASM Press., p. 235-254 (2000).
[2] M.L.R. Rossetti et al. Revista Saúde Pública, v. 36, p. 525-532, 2002.
[3] N.L. Wengenack et al. Biochemistry. 37:15825-34. 1998.
[4] A. S. G. Lee, et al. Antimicrob. Agents Chemother. 45:2157–2159. 2001.
[5] O. Trott, A.J. Olson, J. Comp. Chem., v. 31, p. 455-461 (2010).

# Density Functional Calibration for Indirect Spin-Spin Coupling Constant Calculations

Luiz Felipe Guain Teixeira (PG), Lucas Colucci Ducati (PQ)

*Department of Fundamental Chemistry Institute of Chemistry, University of São Paulo, Av. Prof. Lineu Prestes 748, São Paulo, SP 05508-000, Brazil*

**Abstract:** The use of computational methods in order to determine NMR parameters can be challenging. Although Coupled Cluster and MCSCF calculations are the most accurate methods to evaluate magnetic properties, due to high computational cost they can be applied only for small molecular systems. On the other hand, DFT methods are the only ones that can treat properly "real systems" regularly, so that there is an interest to improve approximations to calculate coupling constants [1-3]. There is no "universal DFT" to evaluate all types of NMR coupling constants. Therefore, some benchmark studies have been reported in order to find the DFT with best accuracy for NMR properties – one of most recent evaluated the precision for 39 DFTs and compared with SOPPA *ab initio* methods [4]. In this work 26 DFTs are initially evaluated, changing the percentage of Hartree-Fock orbital exchange ($E_X^{HF}$) in order to obtain the best possible accuracy. The calibration set contains HF, CO, $H_2O$, $NH_3$, $BF_3$, $BHF_2$, $F_2O$, $PH_3$, $PF_3$, $CH_4$, $C_2H_2$, $C_2H_4$ and $C_2H_6$, and all systems are described by aug-pcJ-2 basis set. BHandH, B1B95 50% $E_X^{HF}$, B971 50% $E_X^{HF}$, B972 40% $E_X^{HF}$ and B98 50% $E_X^{HF}$ provided accurate results, so further investigation is done by optimizing geometries and performing vibrational corrections, and they are compared with SOPPA(CCSD) and SOPPA(CC2) levels of theory. New DFTs generated by combination of exchange and correlation potentials, changing $E_X^{HF}$, are evaluated to determine which approaches are better. Accurate ones are performed for geometries optimization, and compared with accuracy for every single coupling constant. Tests will be done to ensure if these functionals are good to describe spin-spin coupling in a variety of systems.

**Key-words**: DFT, NMR, Indirect Spin-Spin Coupling Constant

**Support:** This work has been supported by FAPESP and CNPq.

**References:**

[1] Helgaker, T.; Watson, M.; Handy, N. C. J. Chem. Phys. 2000, 113, 9402.
[2] Sychrovsky, V.; Grafenstein, J.; Cremer, D. J. Chem. Phys. 2000, 113, 3530-3547.
[3] Autschbach, J.; Ziegler, T. J. Chem. Phys. 2000, 113, 936-947.
[4] Kupka, T.; Nieradka, M.; Stachów, M.; Pluta, T.; Nowak, P.; Kjaer, H.; Kongsted, J.; Kaminsky, J. J. Phys. Chem. A 2012, 116, 3728

# Copper Acetylacetonate Intermolecular Interactions with Conjugated Polymers

Luiz F. A. Ferrão

*Instituto Tecnológico de Aeronáutica, ITA, São José dos Campos/SP*

**Abstract:** Hybrid propellants are of great interest in space propulsion for combining desirable characteristics of solid and liquid propulsion technologies: simplicity and operational readiness (from solid) with variable thrust and high performance (from liquid), minimizing the disadvantages associated with each one. However, a hybrid propulsion was always limited to the low rate of burning of its solid fuel, reducing its competitiveness for the transport of payload to the Earth's orbit. However, the use of paraffin has open new possibilities [1] and the application of paraffin particles agglutinated by a polymer is even more promising [2]. The latter does not exhibit excessive brittleness or melting observed in pure paraffin grains, but the high thermal degradation temperatures of the binder also reduces its propulsive performance. Thus, the improvement of the thermal degradation of the fuel is a central aspect in the development of hybrid propellants that are competitive to solid or liquid rocket engines. In this context, the present work considers adding a metal complex in the fuel to assist the thermal degradation of the polymeric binder. Specifically, a copper acetylacetonate complex ($cu(acac)_2$) was considered interacting with representative molecules of paraffin ($C_{12}H_{26}$) and fragments of hydroxyl-terminated polybutadiene ($C_{12}H_{14}$). The interaction enthalpies and free energies were computed, as well as the minimum energy paths to some dissociation channels, representing unimolecular elementary reactions which are possibly included in the thermal degradation mechanism. The stationary states and reaction paths were carried out using DFT method within M06 approximation [3] with DEF2-SVP basis set for all atoms [4]. The adsorption energies were refined by calculating the stationary states energies with CASPT2 method. The results indicate that the copper acetylacetonate complex changes the thermal degradation of the polymer acting as a catalyst and lowering the energy requirement of some dissociation channels.

**Key-words**: DFT, CASPT2, Hybrid Rocket, HTPB.
**Support:** This work has been supported by Conselho Nacional de Desenvolvimento Científico e Tecnológico (CNPq), process Nº 309051/2016-9.

**References:**

[1] M. A. Karabeyoglu, D. Altman, B. J. Cantwell, J. Propuls. Power, 18, 610 (2002).
[2] K. P. Cardoso, et al., J. Propuls. Power, 33, 448 (2017).
[3] Y. Zhao, D. G. Truhlar, Theor. Chem. Acc., 120, 215 (2008).
[4] F. Weigend, R. Ahlrichs, Phys. Chem. Chem. Phys., 7, 3297 (2005).

# The Selectivity of the *O*-/*N*-Nitroso Aldol Reactions

Luiz Henrique Medeiros da Costa and Prof. Miguel Angelo Fonseca de Souza

*Laboratório de Química Computacional, Instituto de Química, Universidade Federal do Rio Grande do Norte (UFRN), Natal, RN 59072-970, Brazil*

**Abstract:** Nitrosoarenes (Ar−N=O) and related species have a rich history in organic synthesis [1]. For example, the nitroso aldol (NA) reaction is one of the most powerful tools to introduce hydroxy or amino groups at the α-position of the carbonyl group [2]. Over the past few decades several experimental investigations (with several setups and conditions) have been performed to understand how to control selectivity of the *O*-/*N*-NA reactions [1]. This has occurred because, in light of the opposite behavior often exhibited by convectional chemistry, the greater electrophilicity of oxygen than that of nitrogen in some NA reactions is unclear until now. Lewis *et al.* reported the reaction of nitrosobenzene with 1-morpholin-1-ylcyclohexene followed by simple hydrolysis to give the hydroxyamino ketone (*N*-NA reaction) as the major product. Surprisingly, Yamamoto *et al*. found that the similar reaction of nitrosobenzene with 1-pyrrolidin-1-ylcyclohexene gave rise to the aminooxy ketone (*O*-NA reaction) almost exclusively [3]. Indeed, these are few computational studies exploring the control and origin of the selectivity of the *O*-/*N*-NA reaction [4,5]. In this context, we have performed a quantum mechanical computational study to understand the selectivity of these reactions of nitrosobenzene with enamines (1-morpholin-1- and 1-pyrrolidin-1-ylcyclohexene). For such, the DFT methods were used to obtain the energy profiles that included the energetic and structural characterization of the stationary minimum points (reagents, products and intermediates) and maximum (TS). All calculations were performed in benzene (PCM, implicit solvation model) with the Gaussian09 program. Three important mechanistic steps have been observed in the energy profiles. First, the enamine attack on the oxygen or nitrogen of the nitrosobenzene. After, the formed intermediate changes its conformation with a subsequent intramolecular proton transfer (prototropy). Then, from the results obtained has been possible to indentify that the stability of the intermediate and the prototropy are key points for understanding of the selectivity of this *O*-/*N*-NA reaction.

**Key-words**: *O*-/*N*-NA reaction, selectivity, DFT
**Support:** This work has been supported by UFRN and CENAPAD-UFC
**References:**
[1] Vancik, H. "**Aromatic C-Nitroso Compounds**" (2013), Springer, New York.
[2] P. Zuman, P. Shah, **Chem. Rev.,** 94, 1621 (1994).
[3] N. Momiyama. *et. al.*, **PNAS**, 101, 5374 (2004).
[4] P. Ha-Yeon, K. N. Houk, **J. Am. Chem. Soc.**, 126, 13912 (2004).
[5] M. Akakura, M. Kawasaki, H. Yamamoto, **Eur. J. Org. Chem.**, 4245 (2008).

# Theoretical-experimental study of asphaltene properties

Lyzette G.M. de Moura, Jaldyr J. G. Varela Jr, Auro A. Tanaka

*Laboratório de Química Quântica Computacional, Universidade Federal do Maranhão, Cidade Universitária Dom Delgado, Avenida dos Portugueses, 1966, Vila Bacanga, São Luís, Maranhão, CEP 65065-545*

Asphaltenes are structures mainly constituted by polycondensed aromatic rings, also presenting aliphatic lateral chains, some functional groups containing oxygen, nitrogen, and sulfur, in addition to trace quantities of metals as vanadium and nickel. The heteroatoms (N, O, and S) are strongly involved in the interactions (hydrogen bond, charge transfer, etc.) responsible for the asphaltene self-association [1-3]. This work aim to investigate a serie of properties (thermodynamics, structurals, and electronics) of asphaltenes and the intermolecular interactions of this fraction in the crude oil medium, such as, energy bonding, charge distribution, HOMO-LUMO gap, π-π interaction, vibration frequency, heat of formation, enthalpy, and free energy, focusing on the determination of characteristics such as molar mass and volume, based on the density functional theory, DFT. This will make possible to propose stable structural conformations that will be validate comparing data from literature and experimental results of characterization of asphaltenes from Brazilian crude oils. Preliminary experimental data obtained from LDI-MS provided a molar mass value of approximately 760 Da (n-heptane insoluble asphaltenes) and results from RMN indicated the presence of nitro group ($-NO_2$) and aromatic rings, information that conducted to the minima molecular formula $C_{51}H_{100}NO_2$. These data were used to propose two kinds of structures (an island and an archipelago) that are being evaluated and optimized employing the functional B3LYP; the basis set 6-311++G(d,p), LANL2TZ(f) and aug-cc-pVDZ will be applied to the determination of thermodynamics, structurals, and electronics parameters.

**Key-words**: asphaltenes, DFT, thermodynamic properties
**Support:** This work has been supported by FAPEMA/CNPq
**References:**
[1] P.A. Pantoja, M.A. Mendes, C.A.O. Nascimento, J. Pet. Sci. Eng. 109, 198 (2013).
[2] A.M. Mckenna, A.G. Marshall, R.P. Rodgers, Energy Fuels 27, 1257 (2013).
[3] O.C. Mullins, An. Rev. Anal. Chem. 4, 393 (2011).

# First-principle calculations and ab initio direct dynamics study on the molecular mechanism of the 1,3-dipolar cycloaddition reactions

M. Z. Jimenez[1] and F. A. La Porta[1*]

[1]*Laboratório de Nanotecnologia e Química Computacional, Universidade Tecnológica Federal do Paraná, Londrina, 86036-370, Brazil*
**felipelaporta@utfpr.edu.br*

**Abstract:** In this work, we reported a systematic investigation by means the theoretical calculations on the regioselectivity and chemical reactivity for a series of the four 1,3-dipolar cycloaddition reactions was studied here using global and local reactivity based on molecular orbital calculations, as well as, also evaluated the thermal effects along the course of the reaction. Here we show that the HOMO energies are, in principle, insufficient to describe the behavior of these chemical reactions at the molecular level, i.e., when there is, for example, the presence of heteroatoms along the pathway of the chemical reaction. By using the frontier effective-for-reaction molecular orbital (FERMO) concept [1-3], the reactions that are driven by HOMO, and those that are not, can be better explained, independent of the calculation method used, because both HF and Kohn-Sham methodologies lead to the same FERMO. On the basis of the localization and the composition of the orbitals can reveal a frontier molecular orbital close to the HOMO energy with a large contribution in atoms present at the active site (APAS), i.e., this special orbital is FERMO. Moreover, the 1,3-dipolar cycloaddition reactions were also studied with the first-principle ADMP molecular dynamics technique at 400 K with the DFT method at level B3LYP with the basis set 6-31 g (d, p) [3]. All calculations were carried out with the Gaussian 09 package [4]. In line with current and previous studies, we find that our approach is adequate to describe qualitative and quantitative concepts on the 1,3-dipolar cycloaddition reactions in light of the FERMO concept and may provide an in-depth understanding of these important reactions.

**Acknowledgment**

This work has been supported by NanoQC, CAPES, CNPq and FundaçãoAraucária.

**References:**

[1] R. R. Da Silva, et al. J. Phys. Chem. A 2006, 110, 1031□1040

[2] R. R. Da Silva, et al. J. Braz. Chem. Soc. 2006, 17, 233□236.

[3] F. A. La Porta, et al. J. Phys. Chem. A 2011, 115, 824□833.

[4] M. Frisch, et al. Gaussian 09, Revision B.01, Gaussian Inc.: Wallingford, CT, 2010.

# Estados eletrônicos de mais baixa energia da molécula $CI^{2+}$

Maiara Oliveira Passos e Tiago Vinicius Alves

*Instituto de Química, Universidade Federal da Bahia -Salvador, Bahia, Brasil*

**Resumo:** O estudo das propriedades energéticas, estruturais e espectroscópicas de sistemas diatômicos dicatiônicos têm sido o alvo de inúmeros estudos teóricos e experimentais [1-3]. Dentro deste contexto e, motivados pelas investigações recentes realizadas no nosso grupo de pesquisa [3], realizamos uma ampla exploração dos estados de mais baixa energia que se correlacionam com os dois primeiros canais de dissociação, $C^+(^2P_u) + I^+ (^3P_g)$ e $C^+(^2P_u) + I^+(^1D_g)$. Para isto, utilizamos o estado-da-arte em termos de métodos de estrutura eletrônica (SA-CASSCF/MRCI), juntamente com um conjunto de bases consistente na correlação do tipo aug-cc-pV5Z, para o carbono, e aug-cc-pV5Z-PP, para o iodo. Numa primeira exploração, o estado fundamental, $X\ ^2\Sigma^+$, apresenta uma distância internuclear de equilíbrio de 1.8545 Å e uma frequência vibracional harmônica de 885.69 $cm^{-1}$. O primeiro estado excitado, $1\ ^2\Pi$, encontra-se a 4649.4 $cm^{-1}$ do estado fundamental e com uma distância de equilíbrio significativamente maior ($R_e$ = 2.1624 Å). O próximo estado excitado, $1\ ^4\Sigma^+$ ($R_e$ = 2.0484 Å e $w_e$ = 516.77 $cm^{-1}$), encontra-se localizado a 16314.12 $cm^{-1}$.

Tabela 1. Parâmetros espectroscópicos para a molécula $CI^{2+}$. $T_e$, $\omega_e$, $\omega_e x_e$, $\omega_e y_e$, em $cm^{-1}$, e $R_e$, em Å

| Estados | $T_e$ | $R_e$ | $\omega_e$ | $\omega_e x_e$ | $\omega_e y_e$ |
|---|---|---|---|---|---|
| $X\ ^2\Sigma^+$ | | 1.8545 | 885.69 | 6.1228 | -0.0400 |
| $1\ ^2\Pi$ | 4649.4 | 2.1624 | 514.77 | 3.5697 | -0.1325 |
| $1\ ^4\Sigma^+$ | 16314.12 | 2.0484 | 516.77 | -1.5653 | -1.4960 |

**Palavras-chave**: Diatômica, MRCI.

**Suporte:** Esse trabalho teve suporte do CNPq.

**Referências:**

[1] M. Tsuji, K. Shinohara, T. Mizuguchi, Y. Nishimura,*Can. J. Phys*. 61 (1983) 251.
[2] C. Proctor, C. Porter, T. Ast, J. Beynon, *Int. J. Mass Spectrom.* 41 (1982) 251.
[3] I. A. Lins, A. R. Belinassi, F. R. Ornellas, T. V. Alves, Chem. Phys. Lett., 682, 108 (2017).

# Theoretical study of the methane decomposition catalyzed by niobium doped nickel oxide: thermodynamic profile and reaction mechanism

Authors: Maíra dos Santos Pires[(1)], Lívia Clara Tavares Lacerda[(1)], Telles Cardoso Silva[(1)], Silviana Corrêa[(1)], Francisco Guilherme Esteves Nogueira[(2)], Alexandre Alves de Castro[(1)], Teodorico de Castro Ramalho[(1)].

*Address: [(1)] Laboratory of Molecular Modeling, Department of Chemistry, Federal University of Lavras, CEP 37200-000, Lavras-MG, Brazil.*
*[(2)] Department of Chemistry, University of São Paulo, Institute of Chemistry of São Carlos, São Carlos Campus. CEP 13566-590, São Carlos-SP, Brazil.*

**Abstract:**
The formation of carbon nanofibers (CNF) and carbon nanotubes (CNT) can be attributed to the ability of NiO to decompose hydrocarbons, mainly methane ($CH_4$). This process includes the activation and the $CH_4$ decomposition in the crystallographic Ni (100) and Ni (110) planes, and the CNF germination in the Ni (111) plane [1]. According to experimental studies, the addition of $Nb_2O_5$ in these catalysts can increase the intensity of the active planes, favoring the $CH_4$ decomposition [2]. In this context, the goal of this work is to investigate, through theoretical calculations, the properties of the material after doping with Nb. All calculations were performed using the ADF-BAND package, with application of the DFT method at the GGA-PBE level and TZP basis set. The structures of the pure and niobium doped NiO catalysts were indexed in the (100), (110) and (111) planes. The addition of Nb conferred greater stability to the compound in all analyzed planes. This variation was of 186.15, 186.20 and 167.70 kcal/mol to lower energy values, in the (100), (110) and (111) planes, respectively. For the adsorption study, the methane molecule was optimized in contact with the (111) plane of the NiO and NiO/Nb catalysts at different distances. The methane adsorption begins to take place on the surfaces at a distance of approximately 4 Å and reaches the minimum energy at 3 Å. However, on the Nb doped catalyst, the equilibrium geometry occurs at an adsorption energy of 9.92 kcal/mol larger than on pure NiO. As for the proposed mechanism, the study suggests that the carbon deposition on the catalyst starts with adsorption, followed by a series of steps of methane dissociation on the metal surface, leading to the formation of several adsorbed species and, finally, carbon and hydrogen. From now on, it takes place the growth of the crystalline carbon. The potential energy surface of the dissociation catalyzed by NiO, in black, and by NiO/Nb, in red, is then obtained.

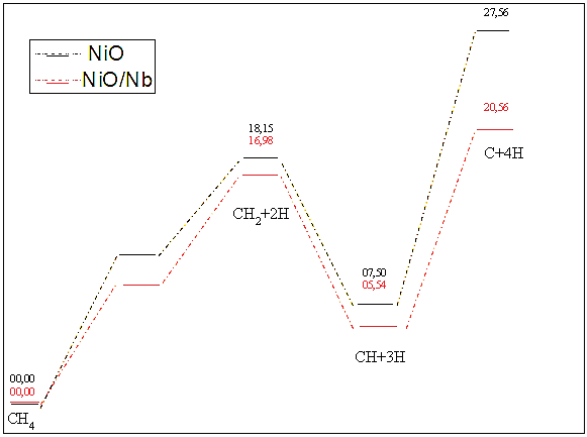


It is found that the $CH_4$ dissociation into carbon and hydrogen by the modified surface is favored thermodynamically with respect to the pure catalyst at all stages. This behavior may be related to the existence of a synergistic effect between Ni and Nb, which results in improved catalytic performance of the modified structure throughout the dissociation. Thus, the theoretical results indicate that the modification of the NiO structure caused by the presence of Nb can bring about improvements in the activity of this material in methane decomposition reactions and subsequent formation of CNF and CNT.

**Key-words**: *DFT*, *Nickel oxide, Methane decomposition, CNF, CNT.*
**Support:** This work has been supported by FAPEMIG and FAPESP.
**References:**
[1] K. P. De Jong; J. W. Geus Catal. Rev.-Sci Eng. **2000**, 42, 481
[2] Li, J. Z.; Lu, G. X.; Li, K. Chemistry Latters **2004**, *33*, 652.

# DFT Calculations of Spectroscopic Properties for Zn (II) -Kaempferol Complexes

Malucia M. Soeiro, Leonardo A. De Souza, Wagner B. De Almeida

*Departamento de Química Inorgânica, Instituto de Química, Universidade Federal Fluminense, Campus do Valonguinho, Centro, Niterói, RJ 24020-141, Brazil.*

**Abstract:** The coordination of Zn(II) ion with the flavonoid kaempferol were found to improve the anticancer effects compared to the free kaempferol and, therefore, a theoretical study of structural and spectroscopic properties of Zn(II)-kaempferol complex can be relevant as a starting point for the investigation of the mechanism of action at a molecular level [1,2]. Recently, our group [3] through DFT calculations studied the $^{1}$H NMR chemical shifts for three polyphenols in order to assess the conformation adopted by these molecules in solution. We showed that a rotation of the B ring (Figure 1) through the inter-ring dihedral angles, causing a deviation from the planar configuration predicted by theoretical gas phase full geometry optimization, is essential to reach a good agreement with experimental $^{1}$H NMR spectra measured in solution (DMSO solvent). Here, we report DFT calculations of spectroscopic properties ($^{1}$H NMR, IR and UV-Vis spectra) of distinct Zn(II)-kaempferol complexes. We compared our theoretical results with experimental data in solution just published. As $^{1}$H NMR chemical shifts of the kaempferol molecule are very sensitive to the molecular chemical environment due to the presence of the metal (Figure 1), the best match between experimental and theoretical $^{1}$H NMR profile can lead to information on the Zn(II)-Kaempferol complex molecular structure in solution, which is difficult to achieve on experimental basis only. This is valuable information for futures studies involving structure-activity relationship and interaction mechanism with DNA.

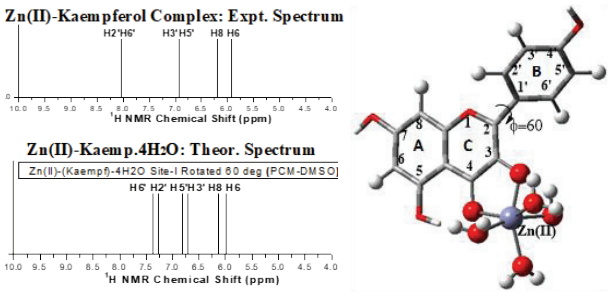


**Figure 1.** B3LYP/6-31G(d,p)-LANL2DZ optimized Zn(II)-kaempferol complex structures leading to the best agreement with experimental $^{1}$H NMR spectra in DMSO, with the B ring rotated 60°.

**Key-words**: **Flavonoids, Anticancer Drugs, DFT calculations, $^{1}$H NMR spectra**.
**Support:** This work has been supported by CAPES and CNPQ.

**References:**

[1] L. -V. Tu, J. Pi, H. Jin, J. -Y. Cai, S. -P. Deng, Bioorg. Med. Chem. Lett., 26, 2730 (2016).
[2] Y. Wei, M. Guo, Biol. Trace Elem. Res., 161, 223 (2014).
[3] L. A. De Souza, W. M. G. Tavares, A. P. M. Lopes, M. M. Soeiro, W. B. De Almeida, Chem. Phys. Lett. 676, 46 (2017).

# Thermochemistry calculations of farnesane biofuel

Marcelo A. P. Pontes[1], Hellen C. R. Rodrigues[1,2],

Francisco B. C. Machado[1], Luiz F. A. Ferrão[1], Orlando Roberto-Neto[3].

[1]*Instituto Tecnológico de Aeronáutica, ITA, São José dos Campos/SP,*
[2]*Escola de Engenharia de Lorena, Universidade de São Paulo, EEL-USP, Lorena/SP,*
[3]*Instituto de Estudos Avançados, IEAv, São José dos Campos/SP*

**Abstract:** With the increasing worldwide concern about the use of fossil fuels, it is necessary to develop less polluting and more efficient fuels. Farnesane (2,6,10-trimethyldodecane - $C_{15}H_{32}$) is a promising renewable fuel for use in aerospace engines, due to the smaller amount of nitrogen oxides and soot produced [1,2]. In this work, we have carried out a study of the hydrogen abstraction reaction by a hydrogen atom in *n*-dodecane, 2-methyldodecane, 4-methyldodecane and farnesane molecules (Figure 1). The stationary states (reactants, saddle points and products) of the hydrogen abstraction reactions were optimized to obtain the thermochemical properties. The DFT method within the M06-2X approximation [3] and Truhlar´s may-cc-pVTZ basis set [4] were used, and all calculations were carried out using the Gaussian09 code [5].

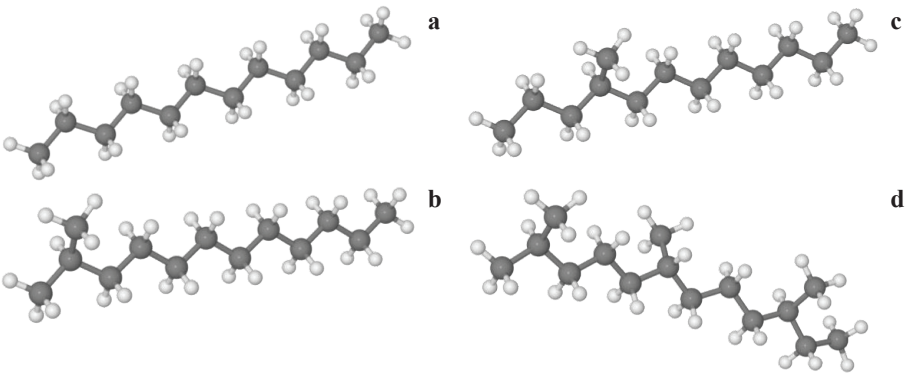


Fig. 1. *n*-dodecane (a), 2-methyldodecane (b), 4-methyldodecane (c) and farnesane (d) molecules.

Figure 2 shows the adiabatic barriers for the abstraction reactions of farnesane, presenting values around 6 kcal.mol$^{-1}$ for tertiary carbons, followed by secondary and primary carbons with values around 8 and 10 kcal.mol$^{-1}$, respectively. Farnesane presents the highest reaction enthalpy around -9 kcal.mol$^{-1}$, followed by 2-methyldodecane, 4-methyldodecane and *n*-dodecane molecules.

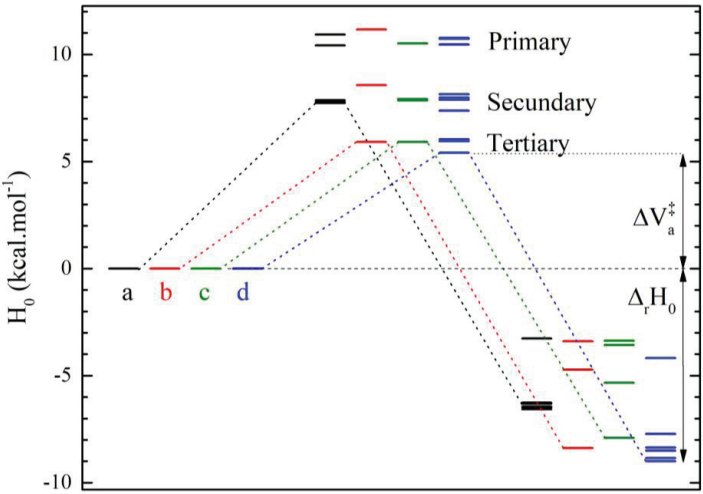


Fig. 2. Energy diagram of the hydrogen abstraction reaction of the *n*-dodecane (a), 2-methyldodecane (b), 4-methyldodecane (c) and farnesane (d) molecules.

In conclusion, this work showed a comparison between the thermochemical properties for some $C_{12}$-chain molecules. The inclusion of methyl radical in the carbon chain influences the reduction of the reaction barriers and increase the enthalpy of reactions. The methyl positioning allows the choice of the formed radical product, where the formation of soot formation precursors can be avoided.

**Key-words**: Farnesane, Hydrogen Abstraction, Thermochemistry, DFT.

**Support:** This work was supported by the COMAER PROPHIPER 14-X project and Brazilian agencies FAPESP, CNPq and CAPES.

**References:**

[1] F. Millo, et al., Fuel, 138, 134 (2014).
[2] P. Oβwald, et al. Fuel, 187, 43 (2017).
[3] Y. Zhao, D. G. Truhlar, Theor. Chem. Acc., 120, 1–3, 215 (2008).
[4] E. Papajak, D. G. Truhlar, J. Chem. Theory Comput., 7, 1, 10 (2011).
[5] M. J. Frisch, et al. Gaussian 09, Wallingford CT Gaussian, Inc., (2009)

# Cd(II)-Cd(II) Metal-Substitued Phosphotriesterase: Theoretical Analysis of A New Enzymatic Mechanisms to Paraoxon Phosphate Triester Hydrolysis

Marcelo Andrade Chagas[a], Eufrásia de Sousa Pereira[a], Júlio C. S. Da Silva[b], Willian Ricardo Rocha[a]

[a]*Departamento de Química, Instituto de Ciências Exatas (ICEx), Universidade Federal de Minas Gerais (UFMG), Campus Universitário Pampulha, Belo Horizonte, MG, 31270-901, Brasil.*
[b]*Instituto de Química e Biotecnologia, Universidade Federal de Alagoas (UFAL), Campus A.C. Simões, Maceió, AL, 57072-900, Brasil.*

**Abstract:** Among the numerous phosphates, triesteres are employed widely as agricultural insecticides and chemical warfare nerve agents. Unfortunately, the extreme toxicity of phosphotriesters makes the experimentations of the chemical destruction for the purposes of chemical defense extremely difficult. Therefore, there is great interest in developing bioremediation technologies to facility the degradation of organophosphate contaminants including the disposal chemical weapons. The enzyme PTE from *Pseudomonas diminuta* is particularly attractive as a biocatalyst because a large number of phosphotriesters can be hydrolyzed. This enzyme has in its native form a active site containing divalent zinc metal cations. The two native $Zn^{2+}$ ions can be substituted with either $Cd^{2+}$, $Co^{2+}$, $Ni^{2+}$, or $Mn^{2+}$ with the restoration of the full catalytic activity [1]. The remarkable enhancement of the hydroysis of organophosphates catayzed by the wild-type PTE can be exemplified with paraoxon (diethyl 4-nitrophenyl phosphate) as the best substrate. Hong and Raushel determined the kinetic rate constant for the hydrolysis of paraoxon by wild-type PTE is $k_{cat}$ = 2100 $s^{-1}$ at 298 K, wich can be translated into a free-energy barrier of 12.9 $kcalmol^{-1}$. The alkaline hydrolysis of paraoxon in aqueous solution takes place with a second-order rate constant of $7.5x10^{-2}$ $M^{-1}s^{-1}$ at 298 K with a free-energy barrier of 18.9 $kcalmol^{-1}$ [2]. Several theoretical analyses have been conducted to elucidate the mechanism of phosphotriester hydroysis in the PTE active site, although, for different reasons, none of them offers a complete picture of the process [2]. In the present work, we investigate the PTE/Cd(II)Cd(II) system, in order to support a more detailed study of the hydrolysis. A new mechanism of organophosphate paraoxon triester is proposed in which the nucleophile is formed in situ through the activation of a water molecule present in the active site of the enzyme. .Thus, the utility of a bridging μ-hydroxo as the specific nucleophile in binuclear enzyme centers has been questioned. We have in all calculations employed DFT to model the enzymes' active sites based on their high resolution crystal structure obtained from PDB (1JGM) for PTE/Cd(II)-Cd(II). The five amino acids that is directly

coordinated to the two metal ions are His55, His57, His201, His230 and Asp301. The metals are bridged by a carboxylated lysine (Lys169) and a μ-hydroxo ion. The two metal ions are designated as α and β. The β metal is more solvent-exposed and coordinated by two waters molecules. The active site were modeled as cluster structure, in which the histidines were modeled as methylimidazoles, Lys169 as carboxylated methylamine and Asp301 as acetate. We optimized the active site model with and without constraining coordinates of the ligands' methyl carbon atoms. So, geometries of all reactant complexes, transition states, intermediates and product complexes involved in this study were fully optimized by using density functional theory (DFT). We used functional B3LYP and standard basis set 6-31+G(d) for C, H, O and N atoms and LANL2DZ for Cd valence electrons. Cd core electrons were treated with LANL2DZ pseudo potential. All calculations were done in gas phase. In addition, the solvent effect was modeled by PCM and SMD continuum models, with dielectric constants ε = 4 (standard protein cavity medium value) and ε = 80 (standard aqueous medium value) using the standard bases set 6-31+G(d) and 6-311++G(2d,2p) using optimized geometries in single-point energies calculations to roughly estimate solvation energies in aqueous solution. All calculations were completed using the Gaussian 09 program package. The most system study is with Zn(II)-Zn(II) metal-substituted phosphotriesterase. Thus, the more elaborated mechanism concerning a proton relay from the μ-hydroxo bridge nucleophile to Asp301 then to His254 and finally to Asp233 has been proposed. In the one this simulations studies reported a energy barrier of 18.3 $kcalmol^{-1}$, and the value derived from the experimental rate constant is 12.8 $kcalmol^{-1}$ for the wild-type PTE. In this work we proposed that only the P=O oxygen is bound to one zinc ion, $Zn(II)_{\beta}$, more exposed to the solvent in the product complex. In contrast to all above theories, Jackson *et al.* claimed that the u-hydroxo bridge is not a nucleophile but acts a base for freely exchangeable nucleophilic water molecule. However, the efficiency by the hydrolysis verification by Cd(II)-Cd(II) enzyme type with the pseudo-first-order rate constant $V_{max}$=12900 $s^{-1}$, $k_{cat}$=2500 $s^{-1}$ and reported a energy barrier of 11.8 $kcalmol^{-1}$. Our structural studies model with $Cd^{2+}$ containing *pd*PTE active site includes the coordinated water molecules which are stabilized by several hydrogen bonding interactions. In the present study we propose that the nucleofilic hydroxide ion is generated by a proton transfer from the coordinated water molecule to the bridged μ-hydroxo ion and formation the nucleophile $OH^-$ in situ. The free-energy barrier obtained is 10,8 $kcalmol^{-1}$ is in excellent agreement with experimental value reported above. More details of the mechanism and the theoretical methodology will be presented.

**Key-words**: Organophosphates, Phosphate Triesters, Paraoxon, Reaction Mechanisms.
**Support:** This work has been supported by CNPq, FAPEMIG, INCT Catálise.

**References:**

[1] Bigley, A. N., Raushel, F. M., *Biochimica et Biophysica Acta*, 1834, 443, (2013).
[2] López-Canut, V., Ruiz-Pernía, J. J., Castillo, R., Molimer, V., Tuñón, I., *Chem. Eur. J.*, 18, 9612, (2012).

# Molecular orbital analysis of the halogen dependence of nuclear magnetic shielding in $PX_3$ and $POX_3$ (X = F, Cl, Br, I)

Marcelo Mota Reginato (PG) and Lucas Colucci Ducati (PQ)

*Department of Fundamental Chemistry Institute of Chemistry, University of São Paulo, Av. Prof. Lineu Prestes 748, São Paulo, SP 05508-000, Brazil*

**Abstract:** Nuclear magnetic resonance (NMR) spectroscopy analyzes the magnetic properties of an active nucleus for physical and chemical determination. Important information about chemical bonding and molecular structure are provided by chemical shifts (δ) and spin-spin coupling parameters.[1,2] The chemical shift (δ) trends for halogen (X) in different nuclei ($^{125}$Te, $^{13}$C, $^{139}$La, $^{31}$P, etc.) have been investigated experimentally and theoretically.[2] Chemical shift behaves quite differently among some isotopes, i.e., for $^{13}$C ($CX_4$) it decreases strongly along the series (X=F, Cl, Br, I), namely normal halogen dependence (NHD); on the other hand, $^{139}$La ($LaX_3$) chemical shift increases strongly, showing an inverse halogen dependence (IHD).[3-5] $PX_3$ series shows an IHD while its oxide form, $POX_3$, presents NHD. The halogen dependence on $^{31}$P was investigated by density functional theory (DFT) calculations and natural localized molecular orbitals (NLMO)[6] using the Amsterdam density functional (ADF, v. 2014) software. Geometry optimization and $^{31}$P NMR shielding tensor calculations were performed using PBE0 hybrid functional and TZ2P basis set.[7-9] The shielding tensors were decomposed into paramagnetic ($\sigma_{para}$), diamagnetic ($\sigma_{dia}$) and spin-orbit ($\sigma_{so}$) contributions and their principal components were obtained. Only $\sigma_{para}$ and $\sigma_{so}$ contributions change along the series, in which the magnitude of $\sigma_{para}$ component is always larger than the $\sigma_{so}$. The negative $\sigma_{para}$ tensor has the largest changes in comparison with the positive $\sigma_{so}$ one, explaining IDH for $PX_3$ series. The $\sigma_{para}$ decomposition component showed that σP-X and LP-P NLMOs have the largest contribution. These two orbitals correspond to about 70% of the $\sigma_{para}$ total value. For the $POX_3$ series, the positive $\sigma_{so}$ tensor has the largest variation, leading to NDH for these oxide phosphines. The σP-X, σP-O, $CR_2$-P, $\sigma^*$P-X and $\sigma^*$P-O NLMOs have the largest contribution to $\sigma_{so}$ tensor. The $\sigma_{so}$ tensor increase may be understood as interaction between the SO coupling of the heavy atom (HA) and the spin-dependent fermi contact (FC) and spin-dipolar (SD) mechanisms. The induced spin polarization can be transmitted through a covalent bond from an HA (halide) to an LA (neighboring phosphorus) nucleus, resembling the transmission mechanism of the FC term in indirect spin–spin coupling constants (FC/FC mechanism).[10,11] The *s* and *p* character of the σP-X bond influences the components $\sigma_{para}$ and $\sigma_{so}$. The $PX_3$ series shows an increase of *p*-character and subsequent decrease of *s*-character in both P and X atoms of the σP-X bond, whereas in the $POX_3$ series the *s*- and *p*-character are almost constant, with values of 40 and 60% respectively. This result may be one evidence among others that NDH and IDH effects are associated mainly with *s*- and *p*-character, respectively.

**Key-words**: DFT, NMR, shielding tensor, localized molecular orbitals
**Support:** This work has been supported by FAFESP and CAPES.
**References:**

[1] M. Kaupp M. Buhl, V. G. Malkin, “Calculation of NMR and EPR Parameters, Theory and Aplications” (2004) Wiley-VCH, Darmstadt.
[2] P. Tahtinen, A. Bagno, A. Koch, K. Pihlaja, Eur. J. Org. Chem. 1, 4921, (2004).
[3] M. Kaupp, O. L. Malkina, P. Pyykkö, Chem. Eur. J 4, 118-126, (1998).
[4] Y. Nomura, Y. Takeuchi, N. Nakagawa, Tetrahedron Lett. 8, 639-642, (1969).
[5] I. Morishima, K. Endo, T. Yonezawa, Chem. Phys. 59, -3356-3364, (1973).
[6] A. Reed, F. Weinhold, J. Chem. Phys. 83, 4, 1736-1740, (1985).
[7] E. J. Baerends, T. Ziegler, J. Autschbach, et. al. Amsterdam Density Functional (ADF), SCM, Theoretical Chemistry, Vrije Universiteit, Amsterdam, The Netherlands (2014) URL *http://www.scm.com*
[8] J. P. Perdew, Phys Rev, B, 33, 8822-88-24, (1986).
[9] E. Van Lenthe, E. J. Baerends, J. Comp. Chem. 24, 9, 1142-1156, (2003).
[10] M. Kaupp, O. L. Malkina, V. G. Malkin and P. Pyykkö, Chem. Eur. J., 4, 118–126 (1998).
[11] M. Hyvärinen, J. Vaara, A. Goldammer, B. Kutzky, K. Hegetschweiler, M. Kaupp and M. Straka, J. Am. Chem. Soc., 131, 11909–11918, 2009.

# Gas Storage in MOFs: A Friendly Strategy to Predict the Ability of Molecule Insertion

Marcia K. D. Belarmino (PG), Arturo Gamonal (PQ), Gustavo L. C. Moura (PQ), Severino A. Jr (PQ), and Nathalia B. D. Lima (PQ)

*Departamento de Química Fundamental, Universidade Federal de Pernambuco, 50740-540, Recife (PE), Brasil.*

**Abstract:** Metal-Organic Frameworks (MOFs) are materials often employed in applications such as: gas storage[1], nuclear fuel reprocessing plants[2], environmental remediation[3], sensors[4], and catalysis[5]. In this sense, the prediction of chemical properties of reactions involving this class of materials can be difficult. Hence, we advance a friendly strategy to predict the ability of inserting gas molecules in the pores of a set of MOFs, which structures can be found in the Cambridge Structural Database System (CSDS). All MOFs chosen have been reported to be capable of storing gas molecules[6–10]. The methodology employed was the full optimization of geometry of all species involved in the insertion reactions of the type: gas + MOF→ gas@MOF, where the gas molecules can be $H_2$, $CO_2$, $N_2$, or $C_2H_2$, and the MOF systems can be Zn(bpb)[9], MOF-646[7], DUT-10(Zn)[6], ZIF-71[8], or Zn(dcpa)[10]. Subsequently, we calculate the enthalpy of reaction, $\Delta_rH$, for all cases considered in our study. The semiempirical method used was the PM6[11], where the calculations were performed by using the quantum chemical software MOPAC 2016[12]. Table 1 shows the $\Delta_rH$ values for all insertion reactions of gas molecule into the pore of each MOF considered, which has been reported to be able to store it.

**Table 1.** PM6 values of $\Delta_rH$ at 298K of the insertion reactions of gas molecules in MOFs: gas + MOF→ gas@MOF. The CSD code of the MOFs can be found in the Cambridge Structural Database System (CSDS).

| CSD Code | System Gas@MOF | $\Delta_rH$ (kcal/mol) | Diameter of the pore (Å) |
|---|---|---|---|
| SUTBEP | $CO_2$@Zn(bpb) | -517 | 9.9 |
| | $C_2H_2$@Zn(bpb) | -340 | |
| VAGTUU | $H_2$@MOF-646 | -200 | 5.3 |
| XAFFAN | $CO_2$@DUT-10(Zn) | -157 | 13.6 |
| | $H_2$@DUT-10(Zn) | -54 | |
| | $N_2$@DUT-10(Zn) | -71 | |
| GITVIP01 | $CO_2$@ZIF-71 | -11 | 17.0 |
| DEYVUA | $CO_2$@Zn(dcpa) | -3 | 4.7 |
| | $H_2$@Zn(dcpa) | -3 | |
| | $N_2$@Zn(dcpa) | -4 | |

From table 1 we verify that the $\Delta_r H$ values calculated by semiempirical PM6 method are consistent with the experimental ability of the MOFs to store gas molecules. For example, the $\Delta_r H$ value for the storage of $CO_2$, and $C_2H_2$ gas molecules in Zn(bpb) MOF, leading to systems $CO_2$@Zn(bpb), and $C_2H_2$@Zn(bpb), are -517 kJ.mol$^{-1}$, and -340 kJ.mol$^{-1}$, respectively. Further, we verify that the diameter of the pore, seemingly, is not the main factor for the success of a gas molecule be stored, at least for the set of systems studied. For example, the $\Delta_r H$ value for the storage of $CO_2$ in the pore of the ZIF-71 (with diameter of 17.0 Å) is -11 Kcal.mol$^{-1}$, and for storage of the same molecule in the pore of the Zn(dcpa) (with diameter of 4.7 Å) is only -3 Kcal.mol$^{-1}$. In summary, the PM6 semiempirical method, available for free at MOPAC 2016, can be considered a friendly strategy to predict the ability of gas molecules insertion in pores of MOFs.

**Key-words**: MOF, semiempirical, MOPAC, gas storage.
**Support:** This work has been supported by CNPq, CAPES, and FACEPE (PRONEX).
**References:**
[1] D. Alezi, Y. Belmabkhout, M. Suyetin, P.M. Bhatt, L.J. Weseliński, V. Solovyeva, K. Adil, I. Spanopoulos, P.N. Trikalitis, A.H. Emwas, M. Eddaoudi, , J. Am. Chem. Soc., 137, 13308 (2015).
[2] J. Liu, P.K. Thallapally, D. Strachan, Langmuir., 28, 11584 (2012).
[3] M.O. Rodrigues, M. V. de Paula, K.A. Wanderley, I.B. Vasconcelos, S. Alves, T.A. Soares, Int. J. Quantum Chem., 112, 3346 (2012).
[4] F.-Y. Yi, D. Chen, M.-K. Wu, L. Han, H.-L. Jiang, Chemical Sensors Based on Metal-Organic Frameworks, Chempluschem., 81, 675 (2016).
[5] Y.-B. Huang, J. Liang, X.-S. Wang, R. Cao, Chem. Soc. Rev., 46, 126 (2017).
[6] R. Grünker, I. Senkovska, R. Biedermann, N. Klein, A. Klausch, I.A. Baburin, U. Mueller, S. Kaskel, Eur. J. Inorg. Chem., 2, 3835 (2010).
[7] S. Barman, H. Furukawa, O. Blacque, K. Venkatesan, O.M. Yaghi, H. Berke, Chem. Commun., 46, 7981 (2010).
[8] R. Banerjee, A. Phan, B. Wang, C. Knobler, H. Furukawa, M. O'Keeffe, O.M. Yaghi, Science., 319, 939 (2008).
[9] S. Galli, N. Masciocchi, V. Colombo, A. Maspero, G. Palmisano, F.J. López-Garzón, M. Domingo-Garcia, I. Fernández-Morales, E. Barea, J.A.R. Navarro, Chem. Mater., 22, 1664 (2010).
[10] B. Liu, Y. Li, L. Hou, G. Yang, Y.-Y. Wang, Q.-Z. Shi, J. Mater. Chem. A., 1, 6535 (2013).
[11] J.J.P. Stewart, J. Mol. Model., 13, 1173 (2007).
[12] J.J.P. Stewart, MOPAC2016 (Molecular Orbital PACkage). http://openmopac.net/MOPAC2016.html (accessed July 29, 2017).

# Explicitly Correlated Calculations in the CNO System

Marcio O. Alves[1], Cayo E. M. Gonçalves[3], Breno R. L. Galvão[2], João P. Braga[3]

[1]*Departamento de Controle Ambiental e Química, Centro Federal de Educação Tecnológica de Minas Gerais, CEFET-MG, Av. Dr. Antônio Chagas Diniz 665, Contagem, MG, Brazil*

[2]*Departamento de Química, Centro Federal de Educação Tecnológica de Minas Gerais, CEFET-MG, Av. Amazonas 5253, Belo Horizonte, MG, Brazil*

[3]*Departamento de Química, Universidade Federal de Minas Gerais, Av. Antônio Carlos 6627, Belo Horizonte, MG, Brazil*

**Abstract:** The $CNO$ role in the atmospheric and combustion chemistry, and its spectroscopic complexity has led to several theoretical and experimental studies in the recent years [1-3]. It is related to some important reactions, involving essential chemical species to several processes such as combustions of nitrogen containing compounds.

It has three linear important species (namely $NCO$, $CNO$ and $CON$) in the $^2\Pi$ symmetry, which are Renner-Teller molecules. The $NCO$ is the ground state and is known to be the main product of the $CN + O_2$ reaction [4].

The literature reports several results for the $CNO$ system [5-9], but with the ever-evolving capacity of the computational and experimental techniques these results become inaccurate. For that, we report geometries, frequencies and spin orbit couplings in the state-of-art Explicitly Correlated Multi Reference Configuration Interaction (MRCI-F12). The calculations were carried out in the MOLPRO package, using the MRCI-F12 (including the Davidson correction) and the vqz-F12 basis set. Table 1 lists the preliminary results for the optimized geometries and energies.

Table 1 – Optimized geometries with bond lengths in bohr and energies in ev. Energies are relative to the three isolated atoms.

| Species | $R_{CN}$ | $R_{NO}$ | $R_{CO}$ | ε |
|---|---|---|---|---|
| NCO | 2.311 | 4.536 | 2.225 | −13,629 |
| CNO | 2.287 | 2.297 | 4.584 | −10,921 |
| CON | 4.743 | 2.505 | 2.238 | −8,415 |

The frequencies and spin-orbit splitting calculations are still being carried. Investigations of the explicitly correlation importance to the properties will be evaluated. Since there is few information in configurations that differ from the linear and there is no potential energy surface (PES) to this system in such high accurate level of theory, we intend to develop two PES (A' and A'' symmetries).

**Keywords:** Explicitly Correlated, Spin-Orbit Coupling, CNO, MRCI-F12

**Support:** This work has been supported by FAPEMIG and CNPq

**References:**

[1] N. Lamoureux *et al.*, Journal of Physical Chemistry A **115** (2011) 5346.
[2] S. S. Prasad, and W. T. Huntress, Monthly Notices of the Royal Astronomical Society **185** (1978) 741.
[3] R. Prasad, Journal of Chemical Physics **120** (2004) 10089.
[4] K. J. Schmatjko, and J. Wolfrum, Berichte Der Bunsen-Gesellschaft-Physical Chemistry Chemical Physics **82** (1978) 419.
[5] S. Andersson, N. Markovic, and G. Nyman, Journal of Physical Chemistry A **107** (2003) 5439.
[6] O. Yazidi, H. Gritli, and G. Chambaud, Molecular Physics **103** (2005) 3321.
[7] C. Leonard, H. Gritli, and G. Chambaud, Journal of Molecular Spectroscopy **243** (2007) 90.
[8] C. Leonard, and G. Chambaud, Chemical Physics Letters **458** (2008) 24.
[9] C. Leonard, H. Gritli, and G. Chambaud, Journal of Chemical Physics **133**, 124318 (2010)

# Title: Computational studies of potential inhibitors to the protein aurora b kinase

Authors: Marco Antônio de Mecenas Filho; Elaine Fontes Ferreira da Cunha.

*Address: Universidade Federal de Lavras, Av. Doutor Sylvio Menicucci, 1001 - Kennedy, Lavras - MG, 37200-000.*

**Abstract:**

Cancer is a neoplastic disease caused by the uncontrolled growth of malignant cells affecting vital organs. An important target for the treatment of this disease is the aurora B kinase protein. The drugs used in the strives against cancer have high toxicity, resistance and low bioavailability, so it is necessary to study the discovery of new compounds against cancer [1-3]. For this, a molecular docking study (*docking*) was performed between potential inhibitors [4](Figure 1) and the protein active site, aiming to obtain the best conformation of each compound [5]. These conformations were used in the QSAR (Quantitative structure-activity relationships) study relating the structures of potential inhibitors with biological activity [6]. The molecular interaction field (MIFs) steric is based on the parameter AMBER FF99 of Van Der Waals And calculated according to the potential 6-12 de Lennard-Jones between the molecules and a carbon probe $sp^3$. The MIFs steric is based in the punctual charge model and calculated by the Coulomb interaction between positively charged probes and the atoms of the molecules [7]. Partial Least Squares (PLS) method was used to obtain the best QSAR models. It correlates to experimental binding affinities with the contribution of molecular fields [8].

Figure 1. General formulas of potential inhibitors

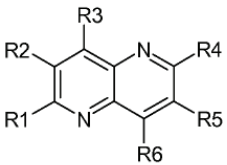


The results show through molecular anchorage studies was evaluated the mode of interaction of potential inhibitors On the active site of the aurora B kinase protein, in which it can be observed that there is a tendency between the biological activity and the interactions performed. The analysis of MIF results (Figure 2) showed that compounds with functional groups with high electron density such as pyrazole and with volumes close to cyclopopil are present in favorable regions.

Figure 2. Electrostatic and steric fields

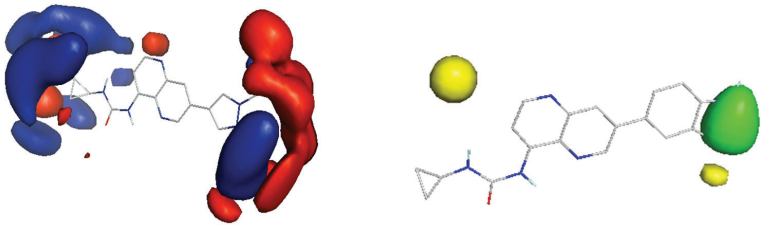

The theoretical results reinforce the experimental, noting that these compounds can be used as a starting point for the development of novel anticancer compounds.

**Key-words**: Cancer. Aurora B kinase. Molecular docking. QSAR-3D
**Support:** This work has been supported by National Council for Scientific and Technological Development (CNPq), Federal University of Lavras (UFLA) and Chemistry department.

**References:**

[1] SILVA, L. L. et al. Investigação eletroquímica e calorimétrica de novos agentes antitumorais biscatiônicos com DNA. Química Nova, v. 35, n.7, p. 1318-1324, 2012.

[2] HANAHAN, D.; WEINBERG, R. A. Hallmarks of cancer: the next generation. **cell**, v. 144, n. 5, p. 646-674, 2011.

[3] SMITH, S. L. et al. Overexpression of aurora B kinase (AURKB) in primary non-small cell lung carcinoma is frequent, generally driven from one allele, and correlates with the level of genetic instability. **British journal of cancer**, v. *93,* n.6, p. 719-729. 2005.

[4] SCHUSTER, T. et al. Novel naphthyridine derivatives and the use thereof as kinase inhibitors. WO 2011/064250 A1, 3 de junho de 2013.

[5] THOMSEN, R.; CHRISTENSEN, M. H. MolDock: a new technique for high-accuracy molecular docking. Journal of medicinal chemistry, v.49, n.11, p. 3315-3321. 2004.

[6] CRAMER, R. D.; PATTERSON, D. E.; BUNCE, J. D. Comparative molecular field analysis (CoMFA). 1. Effect of shape on binding of steroids to carrier proteins. **Journal of the American Chemical Society**, v. 110, n. 18, p. 5959-5967, 1988.

[7] TOSCO, P.; BALLE, T. Open3DQSAR: a new open-source software aimed at high-throughput chemometric analysis of molecular interaction fields**. Journal of molecular modeling**, Vol. 17, p.201-208, 2011

[8] CALDAS, G. B.; RAMALHO, T. C.; CUNHA, E. F. da. Application of 4DQSAR studies to a series of benzothiophene analogs. **Journal of Molecular Modeling,** Amsterdam, v. 20, n. 10, p. 1-10, 2014.

# Molecular dynamic study on graphene-based chemical sensors: adsorption studies and substrate effect

Authors: Marco A. E. Maria [a,b] , Augusto Batagin-Neto [c]

[a] *Faculdade de Engenharia de Sorocaba - Facens, Sorocaba, São Paulo.*
[b] *Universidade Federal de São Carlos - UFSCar, Sorocaba, São Paulo.*
[c] *Universidade Estadual Paulista (Unesp),Câmpus Experimental de Itapeva, SãoPaulo*

The monitoring and control of gas concentration have an essential role in several technological areas [1-3]. In this context, graphene-based materials have been considered interesting candidates for applications in chemical sensors. Besides of presenting unique electrical, mechanical and structural properties, these compounds have also shown high sensitivity for the detection of toxic gases [4-6]. However, some recent studies suggest that the sensory properties of graphene are not intrinsic, but they are associated with the presence of defects in the substrate on which it is deposited [7], suggesting that electrostatic graphene/substrate interactions may be relevant for the formation of adsorption centers. In this context, in the present work we carried out a series of adsorption studies of dimethyl methylphosphonate (DMMP) molecules on the surface of graphene nanosheets in the presence of a silica substrate. The simulations were carried out via molecular dynamic calculations (MD) considering systems composed of a two dimensional graphene nanosheet, 1000 DMMP molecules and a silica substrate. Classical force fields were employed to the system and NPT and NVT ensembles were considered at 300 K and 1.0 atm, considering a 90 A x 90 A x 90 A simulation box. The calculations were implemented with the aid of LAMMPS computational package [8]. As shown in Figure 1 the results indicate that the presence of silica substrate intensify the interaction between the graphene nanosheet and the analyte (DMMP), suggesting that specific interactions between the nanosheets and the substrate are indeed relevant to improve the sensory properties of graphene.

***Figure 1**. Radial distribution function for the carbono(C) belonging to graphene and phosphorus and the phosphorus (P) of the DMMP molecule.*

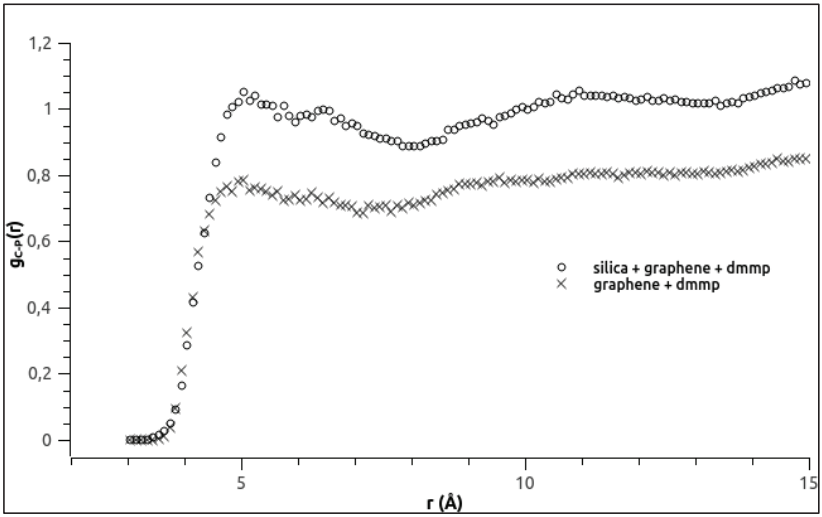


**Key-words**: dimethyl methylphosphonate, grapheme, silica, molecular dynamics
**Support:** This work has been supported by CNPq (proc. 448310/2014-7)

**References:**

[1] Liu, X.; Cheng, S.; Liu, H.; Hu, S.; Zhang, D.; Ning, H. ;Sensors 2012, 12, 9635.
[2] Chen, Z.; Lu, C. ;Sens. Lett. 2005, 3, 274.
[3] Batzill, M. ;Sensors 2006, 6, 1345.
[4] Yuan, W.; Shi, G. ;J. Mater. Chem. A 2013, 1, 10078.
[5] Wang, Y.; Yeow, J. T. W. ;J. Sens. 2009, 2009, 1.
[6] Zhang, Y.-H.; Chen, Y.-B.; Zhou, K.-G.; Liu, C.-H.; Zeng, J.; Zhang, H.-L.; Peng, Y. ;Nanotechnology 2009, 20, 185504.
[7] Kumar, B.; Min, K.; Bashirzadeh, M.; Farimani, A. B.; Bae, M.-H.; Estrada, D.; Kim, Y. D.; Yasaei, P.; Park, Y. D.; Pop, E.; Aluru, N. R.; Salehi-Khojin, A. ;Nano Lett. 2013, 13, 1962.
[8] S. Plimpton, Fast Parallel Algorithms for Short-Range Molecular Dynamics, J Comp Phys, 117, 1-19 (1995).

# Estados Excitados e Fotoquímica da Desoxirribose

Marcos Paulo de Oliveira, Clarissa Oliveira da Silva, Márcio Soares Pereira

*DEQUIM- Universidade Federal Rural do Rio de Janeiro, BR 465 km 07, Seropédica, RJ, CEP: 23890-000.*

**Abstract:** A investigação da desoxirribose é de grande relevância, uma vez que essa molécula faz parte da composição da estrutura do DNA. O estudo computacional de carboidratos é uma maneira interessante de se entender o comportamento dessas moléculas frente a pertubações no estado fundamental. Apesar da grande quantidade de publicações de propriedades dos estados excitados de compostos orgânicos, ainda são poucos os estudos envolvendo carboidratos, o que dificulta a compreensão das suas propriedades fotoquímicas[1]. Para este trabalho foram selecionadas as quatro geometrias mais estáveis da desoxirribose[2] e analisadas suas energias de excitação, suas geometrias mais estáveis e possíveis caminhos de reação via interseção cônica. Neste estudo foi utilizado o método time-dependent density functional theory (TDDFT), e o método complete active space self-consistent field (CASSCF) para cálculos de otimização de geometria no estado excitado e interseção cônica. Os cálculos foram realizados com o software GAMESS[3]. Foram identificados dois possíveis canais de reação no estado excitado S1 a partir da região de Franck-Condon. O primeiro canal envolve a abertura do anel enquanto o segundo canal envolve o destacamento de um átomo de hidrogênio. Estão em curso investigações das conexões destes canais de reação com interseções cônicas entre o estado excitado S1 e o estado fundamental S0. Os dados obtidos ajudam a compreender as reações fotoquímicas e são de grande importância para o estudo dos carboidratos que formam a estrutura da hélice do DNA, e como ela pode ser afetada por radiação eletromagnética, o que pode sugerir mecanismos de sua deterioração envolvidos no câncer.

**Key-words**: Desoxirribose, Carboidratos, Fotoquímica, Estado Excitado
**Support:**CNPq

**References:**

[1] TUNA, Deniz; SOBOLEWSKI, Andrzej L.; DOMCKE, Wolfgang.Physical Chemistry Chemical Physics, v. 16, n. 1, p. 38-47, 2014.

[2] ALVES, Leandro Guilherme. Automatizaçãodo processo de obtenção das conformações mais estáveis para pentoses por métodos ab initio.Dissertação (Mestrado) –ICE-UFRRJ Seropédica, 2014.

[3] "General Atomic and Molecular Electronic Structure System" M.W.Schmidt, K.K.Baldridge, J.A.Boatz, S.T.Elbert, M.S.Gordon, J.H.Jensen, S.Koseki, N.Matsunaga, K.A.Nguyen, S.Su, T.L.Windus, M.Dupuis, J.A.Montgomery J. Comput. Chem., 14, 1347-1363(1993).

# Structure and bonding in triorganotin halides complexes: a perspective by Energy Decomposition Analysis

Marcus V. J. Rocha[1], Matheus R. M. Signorelli[1], Teodorico C. Ramalho[2], Luciano T. Costa[1].

[1]*Departamento de Físico Química, Instituto de Química, Universidade Federal Fluminense, Outeiro de São João Batista, s/n, CEP 24020-141, Niterói/RJ*
[2]*Departamento de Química, Campus Universitário, CEP 37200-000, Lavras/MG*

**Abstract:** In the recent years, organotin compounds have been shown a wide variety of active components for biological systems such as fungicidal and bactericides. [1-5] They are also very promising antitumor agents against various type of cancer. Also, they are used in organic synthesis as catalysts. [1-5] This interest is due to their structure and chemical properties, which depends mainly on the number of Sn-C bonds and the electronic properties of X ligands, such as halogens. For instance, the formation of intermediate cation $R_nSn^+$ in the biological systems, like ATP-Synthase inhibition is one of the steps to determinate the biological activity. [6-7] Therefore, the study on the Sn-X chemical bond becomes interesting for understanding how the cation is formed and in which alkyl ligands are more favourable, and what the major electronic structural differences among them. In this context, we studied the nature of the Sn-Cl bond in some organotin halides and their dissociation based on energy decomposition analysis (EDA) and Kohn-Sham orbitals. All the geometries were optimized by ORCA package using relativistic Density Functional Theory (DFT) at ZORA-TPSSh/LANL08(d) for Sn and QZVP for C, H and Cl atoms. The interaction energy $\Delta E_{int}$ is further analysed in the conceptual framework provided by the Kohn–Sham molecular orbital method, using a quantitative energy decomposition scheme.[8] These calculations were performed by ADF 2017 package, at ZORA-TPSSh/QZ4P level of theory, applying the $C_{3V}$ symmetry. We are interested how easy the dissociation on Sn-Cl is in the four models. This is important for the applications of the organotin compounds, mainly as fungicides, in which the cation is the most responsible for the action mechanism in the biological systems. The σ orbital term is the dominant contributor to the stabilization of the Sn-Cl bond. From the gross populations of the fragment molecular orbitals (FMOs), we observe σ-donation from one p orbital of chlorine (P=1,79e) to the cation fragment anti-bonding orbital (see fig. 1) The energy of σ bond decreases from methyl to butyl and increases for phenyl whereas the π bond energy for $Ph_3SnCl$ is much smaller than others. This term is determinant for the $\Delta E_{OI}$ to be lower for $Ph_3SnCl$. A strong contribution of π orbitals from conjugated system of the $Ph_3SnCl$ is noticed. Despite of $\Delta E_{Pauli}$ is larger compared to other complexes, the contribution of π orbitals from conjugated system favours the stability of the Sn-Cl bond. Also, the decreasing of the

contribution of chlorine p orbitals for the HOMO, from methyl to phenyl ligands (72% to 50%) has to be taken into account. On the other hand, the contribution of the p orbitals from Sn for the LUMO increases from methyl to phenyl ligands (up to around 70%).

Table 1. Analysis of Sn-Cl bond between $R_3Sn^+$ and $Cl^-$ in triorganotin complexes [a]

| EDA (kcal/mol$^{-1}$) | $Me_3SnCl$ | $Et_3SnCl$ | $Bu_3SnCl$ | $Ph_3SnCl$ |
|---|---|---|---|---|
| $\Delta V_{elstat}$ | -204,39 | -197,99 | -193,03 | -201,28 |
| $\Delta E_{Pauli}$ | 118,77 | 120,72 | 123,64 | 124,64 |
| $\Delta E_{OI}$ [b] | -85,94 | -86,49 | -89,11 | -94,05 |
| $\Delta E_{A1}$ | -65,79 | -66,15 | -68,42 | -67,74 |
| $\Delta E_{A2}$ | -0,05 | -0,09 | -0,13 | -1,80 |
| $\Delta E_{E1:2}$ | -17,94 | -17,80 | -18,13 | -23,12 |
| $\Delta E_{Int}$ | -171,56 | -163,76 | -158,5 | -170,69 |

[a]Computed at ZORA-TPSSh/QZ4P [b]Included Metahybrid correction

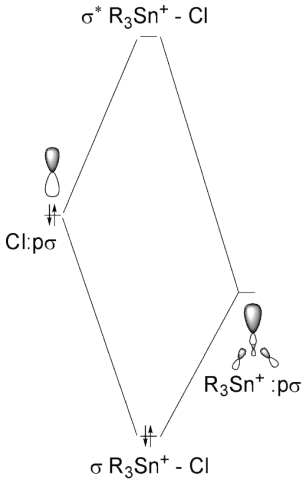


Figure 1. Orbital interaction diagram for $Me_3SnCl$

**Key-words**: organotin compounds, energy decomposition analysis, DFT

**Support:** This work has been supported by CAPES

**References:**

[1] S. Zhang, W. Wang, Q.Liu, X. Zheng, L. Tian, Main Group Met. Chem., 39, 87 (2016).
[2] Z. Shariatinia, E. Asadi, M. Yousefi, M. Sohrabi, J. Organometal. Chem., 715, 82 (2012).
[3] M. Sirajuddin, M. Tariq, S. Ali, J. Organometal. Chem., 779, 30 (2015).
[4] M. Shah, S. Ali, M. Tariq, N. Khalid, F. Ahmad, M. A. Khan. Fuel 118, 392 (2014).
[5] M. Sirajuddin, S. Ali, Cur. Pharm. Design, 22, 6665 (2016).
[6] T. C. Ramalho, M. V. J. Rocha, E. F. F. Cunha, L. C. A. Oliveira, K. T. G. Carvalho, J. Biomol. Struc. Dyn., 28, 227 (2010).
[7] M. V. J. Rocha, T. C. Ramalho, M. S. Caetano, E. F. F. Cunha, J. Biomol. Struc. Dyn., 31, 1175 (2013).
[8] L. P. Wolters, F. M. Bickelhaupt, WIREs. Comput. Mol. Sci., 5, 324 (2015).

# Sudden Changes in Atomistic Mechanisms for the $Cl^- + CH_3I$ $S_N2$ Reaction with Increasing Collision Energy

Maria Carolina Nicola Barbosa Muniz,[1] Subha Pratihar,[2] William L. Hase,[2]
Itamar Borges Jr.[1]

[1]*Departamento de Química, Instituto Militar de Engenharia, Rio de Janeiro, RJ, Brazil.*
[2]*Department of Chemistry and Biochemistry, Texas Tech University, Lubbock, USA*

**Abstract:** Studies have shown that the gas-phase $X^- + CH_3Y \rightarrow XCH_3 + Y^-$ $S_N2$ nucleophilic substitution may occur via direct mechanisms as well as many indirect mechanisms, including pre- and/or post-reaction complex formation, central barrier recrossing and roundabout mechanisms [1-4]. For the $Cl^- + CH_3I \rightarrow ClCH_3 + I^-$ reaction, there is a sudden change from predominantly indirect to direct mechanisms as the collision energy is increased [3]. However, there is some uncertainty regarding when the change occurs. Experiments show that for a collision energy of 0.39 eV the $Cl^- + CH_3I$ $S_N2$ reaction occurs by an indirect mechanism, but at 0.70 eV it occurs by a direct one [1]. On the other hand, direct dynamics simulations employing the MP2 and DFT/BhandH theories and the ECP/d basis set indicate that the reaction mechanisms are predominantly direct at 0.39 eV collision energy, but indirect at 0.20 eV [3]. In this work, the transition from indirect to direct mechanism was studied for collision energies of 0.15, 0.20, 0.25, 0.30, 0.35 and 0.40 eV through BHandH/ECP/d direct dynamics simulations. Impact parameters of 0 and 1 Å were investigated and the trajectories were integrated for 15 ps. For these collision energies, the only direct mechanism found was the direct rebound (DR). Direct stripping only occurs for higher collision energies. Regarding the indirect mechanisms, the same mechanisms found on previous simulations were observed for these collision energies, namely, pre- and/or post-reaction complex formation, central barrier recrossing and roundabout. Furthermore, indirect reactions also occurred by combinations of the three aforementioned mechanisms.

**Key-words**: direct dynamics, nucleophilic substitution, reaction mechanisms, density functional theory
**Support:** Capes, Robert A. Welch Foundation Grant No. D-0005.
**References:**
[1] J. Mikosch, S. Trippel, C. Eichhorn, R. Otto, U. Lourderaj, J.-X. Zhang, W. L. Hase, M. Weidemüller, R. Wester, Science 319, 183 (2008).
[2] J.-X. Zhang, J. Mikosch, S. Trippel, R. Otto, M. Weidemüller, R. Wester, W. L. Hase, J. Phys. Chem. Lett. 1, 2747 (2010).
[3] J.-X. Zhang, U. Lourderaj, R. Sun, J. Mikosch, R. Wester, W. L. Hase, J. Chem. Phys., 138, 114309 (2013).
[4] J. Xie, W. L. Hase, Science, 352, 32 (2016)

# Development of a Composite Method Based Exclusively on The Density Functional Theory

Authors: Toretti Caldeira, Mariana; Custodio, Rogério.

*Address: marytoretti@gmail.com; rogerct@unicamp.br*

**Abstract:** Composite methods tend to combine different ab initio calculations with different basis functions at different level of electron correlation effects, in addition to other important effects[1-4]. On the other side, Density Functional Theory (DFT) has been widely used for the calculation of different properties in large molecular systems containing hundreds of atoms. One of the great difficulty in choosing the appropriate DFT method is the diversity of the exchange-correlation functional.[5-6]

The most used functional in the literature is the B3LYP hybrid functional, which includes semi-empirical parameters optimized from thermochemical properties, such as atomization energy, ionization potential and proton affinity.[7]

A thermochemical property not well described by the B3LYP functional is the enthalpy of formation. In this work, basis functions, exchange-correlation parameters of the functional and atomization energies were optimized to achieve results close to the experimental values. The theoretical method combines the principles of the composite method, but considering additional corrections takin the B3LYP/6-31G(2df,p) calculations as reference ($E_{ref}$). The fundamental corrections considered in this work are:

$$E_{new} = E_{ref} + \Delta E_{xc} + E_{SO} + E_{ZPE} + E_{therm} + E_{HLC}$$

Where the corrections are: $\Delta E_{xc}$ for the exchange-correlation, $E_{SO}$ for spin-orbit, $E_{ZPE}$ for zero point energy, $E_{therm}$ for thermal and $E_{HLC}$ for a "higher level correction" which take into account the number of valence α and β electrons.

Three different methods were teste: a) the first one considered only the optimization of the exchange-correlation functional, b) the second method, in addition to the exchange-correlation parameters, considered the optimization of the basis functions of the atoms: aluminum, bromine, fluorine, phosphorus, nitrogen, carbon, chlorine, sulfur and oxygen, c) the third and fourth methods are direct use of the adjusted parameters from (a) and (b)

as original parameters yielding two different functionals. An additional adaptation of the experimental atomization energies of the elements used in the calculation of the enthalpies of formation was also tested in all cases. This adjustment proved to be necessary to achieve a remarkable accuracy.

The second composite method is the best alternative with the optimization of 10 basis set and the exchange-correlation functional, achieving a mean absolute error of less than 2 kcal $mol^{-1}$ for a set of 254 enthalpies of formation of compounds in gas phase. The direct use of the parameterization in two original functionals present a quantitative behavior not far from methods (a) and (b), indicating that they can be considered as acceptable to provide reliable enthalpies of formation. All the attempts made in this work provide significantly better enthalpies of formation regarding the original B3LYP functional.

**Key-words**: **Composite Method, DFT, B3LYP, Enthalpy of formation.**

**Support:** This work has been supported by FAPESP, CNPq, FAEPEX-UNICAMP and CENAPAD - SP

**References:**

1. Dorofeeva, O. V., Kolesnikova, I. N., Marochkin, I. I. & Ryzhova, O. N. Assessment of gaussian-4 theory for the computation of enthalpies of formation of large organic molecules. *Struct. Chem.* **22,** 1303–1314 (2011).
2. Curtiss, L. A., Redfern, P. C. & Raghavachari, K. Gaussian-4 theory. *J. Chem. Phys.* **126,** (2007).
3. Baboul, A. G., Curtiss, L. A., Redfern, P. C. & Raghavachari, K. Gaussian-3 theory using density functional geometries and zero-point energies. *J. Chem. Phys.* **110,** 7650–7657 (1999).
4. Pople, J. A., Head-Gordon, M., Fox, D. J., Raghavachari, K. & Curtiss, L. A. Gaussian-1 theory: A general procedure for prediction of molecular energies. *J. Chem. Phys.* **90,** 5622 (1989).
5. Cramer, C. J. *Essentials of computational chemistry: theories and models*. (2002).
6. Jensen, F. *Introduction to Computational chemistry*. (2006).
7. Lu, L.; Hu, H.; Wang, B. An improved B3LYP method in the calculation of organic thermochemistry and reactivity. *Comput. Theor. Chem.* **1015,** 64–71 (2013).

# Reactions of hypergolic pair $N_2H_4$ and $NO_2$

Marina Pelegrini[a], Marcelo A. P. Pontes[b], Luiz F. A. Ferrão[b], Orlando Roberto-Neto[c], Francisco B. C. Machado[b]

[a]*Divisão de Ensino, Academia da Força Aérea, Pirassununga – SP, Brazil,* [b]*Departamento de Química, Instituto Tecnológico de Aeronáutica, São José dos Campos-SP, Brazil,* [c]*Instituto de Estudos Avançados, Departamento de Ciências e Tecnologia Aeroespacial, São José dos Campos- SP, Brazil*

**Abstract:** Hydrazine ($N_2H_4$) and nitrogen tetroxide ($N_2O_4$) are well known by their energetic power especially when they are combined as a hypergolic pair, an auto ignition system. These molecules are widely utilized in aerospace applications such as rocket fuel and satellite thrusters [1]. The high reactivity of the hypergolic system was attributed to the high effectiveness of nitrogen dioxide in hydrogen abstraction of hydrazine [2]. In this work, the reactions between hydrazine and nitrogen oxide have been studied using DFT theory, with B3LYP and M062-X functionals and 6-311++G(d,p) atomic basis set. Every interaction sites have been studied and the energy diagram of the possible reactions indicates that interactions "hydrogen bond" like play crucial role in the reactions exothermicities through the intermediate species formation. The intermediate species are characterized by relative very low vibrational frequencies, indicating their low stabilities, and the higher the first frequency vibrational of the intermediate, more exothermic will be its formation. The reactants, transitions states, intermediate species and the final products $N_2H_3$ and HONO*cis*, HONO*trans* and $HNO_2$ were optimized and IRC calculations were performed to confirm the connection between reactants and intermediate species. Reactions of hydrazine with $NO_2$ and other molecules N-O containing had been studied by DFT calculations by Lai et al. [3,4], but the steps reaction and molecular structures are somewhat different here. In this work, two different transition states connect with an intermediate species so close in geometry with the products $N_2H_3$+$HNO_2$, by means of barrier heights around 5 and 7 kcal.mol$^{-1}$. Two different transition states connect with two intermediate species that are so close in geometry with the products $N_2H_3$+HONO*cis*, by means of barrier heights around 3 and 7 kcal.mol$^{-1}$. And one transition state connects with an intermediate species with barrier height like to 7 kcal.mol$^{-1}$. Every intermediate species are exothermic relative to reactants.

**Key-words**: propellant, transition state, DFT

**Support:** This work has been supported by CNPq/FAPESP

**References:**

[1] J. C. Leary, R. F. Conde, G. Dakermanji et al. Space Sci. Rev. 131, 187 (2007).
[2] R. F. Sawyer, I. Glassman, Proc. Combust. Inst., 11, 861 (1967).
[3] J. Tomasi, B. Mennucci, R. Cammi, Chem. Rev. 105, 2999 (2005).
[4] K. –Y. Lai, R. S. Zhu, M. C. Lin, Advances in Quantum Chemistry, 69, 253 (2014).

# Estudo de Propriedade-Estrutura para Cadeias Orgânicas Conjugadas Ramificadas via Análise de Componente Principal

Marina Pinheiro Dourado, Arthur Akira Mamiya e Demétrio A. da Silva Filho

*Instituto de Física - Universidade de Brasília - Brasília (DF) - Brasil*

**Abstract:** Comumente, associa-se condutividade elétrica aos metais; enquanto propriedade isolante aos polímeros. Com os trabalhos de Hideki Shirakawa *et al* [1,2], notou-se que, em poliacetileno, a condutividade pode aumentar em até 10 ordens de grandeza. Para que um polímero orgânico adquira a capacidade de conduzir eletricidade é preciso que possua cadeia conjugada (a alternância entre ligações simples e duplas faz com que os elétrons π se desloquem ao longo da cadeia [3]). Em seguida, essa estrutura é submetida a uma dopagem, uma perturbação em que a estrutura ou receba elétrons ou os perca. Nesse trabalho, os cálculos *ab initio* foram feitos com estruturas de trans-poliacetileno com tamanhos diferentes e a dopagem utilizada será através de ramificações ao longo da cadeia. Primeiramente, as cadeias lineares são obtidas por meio de um script em *Python* e são otimizadas no *Gaussian 09* [4] com o método DFT, funcional B3LYP e a função de base 6-31G. Com os resultados, outro programa é feito em que são extraídas apenas as posições dos átomos de carbono e são calculados o BLA (do inglês, *Bond Length Alternation*) para cada cadeia. O BLA é um parâmetro que está relacionado à polarizabilidade e é definido pela subtração entre a média do comprimento das ligações pares e a média do comprimento das ligações ímpares [5]. A montagem das cadeias ramificadas foi feita manualmente no *GaussView* [6], usando as cadeias lineares já otimizadas. Os casos estudados consistem em duas ramificações ao longo da cadeia: $C_3H_4$ no último carbono e $C_4H_5$ no penúltimo carbono [7]; $C_3H_4$ no último carbono e $C_4H_5$ no primeiro carbono; $C_3H_4$ no último carbono e $C_4H_5$ a 3 carbonos de distância do último; $C_3H_4$ no último carbono e $C_4H_5$ no meio da cadeia. Por fim, otimiza-se cada cadeia ramificada e é preciso redefinir parâmetro BLA usando o método estatístico PCA (do inglês, *Principal Components Analysis*), procedimento que permitirá determinar quais as ligações de maior relevância para o valor de BLA. Para isso, calcula-se a matriz covariância usando 5 ligações de cada molécula de mesma natureza e, posteriormente, seus autovalores e autovetores. A correção do BLA com PCA é definida como o somatório do produto entre o comprimento da ligação e coeficiente do maior autovetor (primeiro componente principal) [5]. Para as cadeias lineares, foram utilizados os seguintes poliacetilenos: $C_6H_8$, $C_{10}H_{12}$, $C_{12}H_{14}$, $C_{14}H_{16}$, $C_{20}H_{22}$, $C_{24}H_{26}$ e $C_{30}H_{32}$. Dos resultados obtidos, nota-se que quanto maior a quantidade de carbono na cadeia, maior o BLA e, portanto, maior polarizabilidade. Ou seja, maior será a capacidade da molécula atrair elétrons. Nos casos de cadeia ramificada, os pesos de cada ligação mostram que para o parâmetro PCA são favorecidas as ligações das

ramificações e suas redondezas e os valores de $BLA_{PCA}$ aumentam. Outra propriedade analisada em todas as cadeias foi a energia dos orbitais HOMO e LUMO, mais precisamente, a diferença entre eles denominada de energia gap. Semelhante ao modelo de bandas proposto para semicondutores inorgânicos, é possível explicar a condutividade elétrica dos polímeros [8] através da largura da faixa de energia gap, região inacessível aos elétrons e que separa as bandas de valência e condução. Com os resultados, nota-se que a energia gap será maior na cadeia linear e essa propriedade diminui à medida que aumenta o tamanho da cadeia e diminui a distância entre as ramificações. Nesse trabalho, ao analisar o parâmetro estrutural BLA de estruturas de trans-poliacetileno e as energias gap, nota-se que quanto maior o tamanho da cadeia e a presença de ramificações, maior será a capacidade da molécula atrair elétrons e conduzir corrente elétrica. Além disso, ao calcular o PCA dos polímeros ramificados, percebe-se que essa propriedade depende da posição das ramificações. O estudo foi baseado em ramificações covalentes, se fossem analisadas o trans-poliacetileno com compostos iônicos, teria-se estruturas mais estáveis e com maior condutividade elétrica [9].

**Key-words**: Poliacetileno, BLA, PCA, propriedades eletrônicas.

**References:**

[1] H. Shirakawa, T. Ito, S. Ikeda. “Electrical Properties of Polyacetylene with Various Cis-Trans Compositions” (1978). Macromolecular Chemistry and Physics, 179.

[2] H. Shirakawa. “The Discovery of Polyacetylene Film: The Dawning of an Era of Conducting Polymers (Nobel Lecture)” (2001). Angewandte Chemie International, 40.

[3] V. Costa, A. Freire, J. Silva. “Polímeros Condutores” (1986). Boletim Sociedade Portuguesa de Química, 24.

[4] M.J. Frisch et al. Gaussian 09, Revision A.02. In., Series Gaussian, Inc., Wallingford CT; 2009.

[5] C.A.M.M. Neto. “Uso da Técnica de Analise de Componentes Principais na Redefinição do Parâmetro BLA” (2016). Dissertação (Mestrado em Física) - Instituto de Física, Universidade de Brasília, Brasília.

[6] R. Dennington, T. Keith, J. Millam. GaussView, Version 4.1 In., Series GaussView, Version 4.1. Shawnee Mission KS:Semichem Inc.; 2003.

[7] G. M. E Silva, P. H. Acioli, Y. Ono. “Charge Propagation on Branching off Conjugated Polymers” (1998). Journal of the Physical Society of Japan. volume 67, número 11.

[8] R. Faez et al. “Polímeros Condutores” (2000). Química Nova na Escola, 11.

[9] J. Wu et al. “Branched 1,2,3-Triazolium-Functionalized Polyacetylene with Enhanced Conductivity” (2016). Macromolecular Journals.

# Zn(II)-Zn(II) and Cd(II)-Cd(II) Metal-Substituted Phosphotriesterase (pdPTE): Theoretical Analysis of the Structure the Active Site and Interaction with Phosphate Triester Paraoxon

Marina P. B. Godinho, Marcelo Andrade Chagas, Willian Ricardo Rocha

*Departamento de Química, Instituto de Ciências Exatas (ICEx), Universidade Federal de Minas Gerais. Campus Universitário Pampulha, Belo Horizonte, MG, 31270-901, Brasil*

**Abstract:** Phosphotriesterases (PTEs) are enzymes with an active site that contains a binuclear metal center composed of ions such as $Zn^{2+}$, $Cd^{2+}$, $Co^{2+}$, $Mn^{2+}$. These enzymes catalyze the hydrolysis of a vast array of organophosphate triesters, which are chemical species frequently used as insecticides and agricultural pesticides and as chemical warfare nerve agents. [1] Since there is great interest in developing technologies to facilitate degradation of organophosphate contaminants, the study of such enzymes is relevant. [2] In the present work, we investigate the structural properties of PTE/Zn(II)-Zn(II) and PTE/Cd(II)-Cd(II) and how they are influenced by the presence of the substrate Paraoxon, as well as substrate-enzyme interaction, in order to support a more detailed study of the hydrolysis mechanism of organophosphate triesters catalyzed by these enzymes. To this end, we have employed DFT to model the enzymes' active sites based on their crystal structures (PDB codes 1HZY and 1JGM for PTE/Zn(II)-Zn(II) and PTE/Cd(II)-Cd(II), respectively), where the first shell ligands are His55, His57, His201 e His230, Lys169 e Asp301. For the PTE/Zn(II)-Zn(II) system there is one water molecule coordinated to the active site metal ion most exposed to the solvent and for the PTE/Cd(II)-Cd(II) system there are two. The active sites were modeled as cluster structures, in which the His were modeled as methylimidazoles, Lys169 as carboxylated methylamine and Asp301 as acetate. We used functionals B3LYP, X3LYP, TPSSh and M06 and bassets 6-31+G(d) and 6-311++G(d,p) for C, H, O and N atoms and LANL2DZ for Zn and Cd valence electrons. Zn and Cd core electrons were treated with LANL2DZ pseudo potential. We optimized the active site model with and without constraining coordinates of the ligands' methyl carbon atoms. We also used the ONIOM approach in which the active site was treated with DFT while the remainder of the protein was treated at molecular mechanics level for PTE/Cd(II)-Cd(II). Excluding the ONIOM calculation, all calculations were done both for gas and solvated phases. The solvent effect was modeled by IEFPCM, with dielectric constants $\varepsilon = 4$ (standard protein cavity medium value) and $\varepsilon = 80$ (standard aqueous medium value). The influence of the substrate on the enzymes' structural properties was evaluated by a potential surface scan using DFT optimizations at theory level B3LYP, with pseudo potential and basset LANL2DZ for Zn and Cd atoms and basset 6-31G(d,p) for C, H, O,

N and P atoms. System energy, structural data and atom charges were evaluated as a function of the enzyme-substrate distance. Atom charges were calculated by Mulliken and CHELPG methods. Substrate-enzyme interaction was investigated by molecular conformational analysis, which was performed by employing DFT at theory level B3LYP 6-31G+(d) to calculate system energy values for different substrate geometries as it interacts with the enzyme. The resulting conformation was then used in a potential surface scan analogous to the prementioned one. Active site model adequacy was evaluated by RMSD comparison with the crystal structure. Taking into account computational cost, adequacy, and information available in the literature, we chose as best, for both systems, the model optimized at gas phase at theory level B3LYP 6-31G+(d) with the fixed atoms constraint. We found that applying fixed atom constraints did not result in significant change of RMSD for bond lengths. However, the overall RMSD for relevant angles of the constrained system was 6.30, while for the unconstrained system it was 16.61. Our results indicated that constraining the system emulates the effect of the enzyme structure external to the active site that is not modeled in the cluster structure. Based on our active site model, for the Zn system, the distance between the water hydrogen and the bridging hydroxyl oxygen in the active site was found to be 1.845 Å while its distance to the water oxygen was found to be 0.987 Å. For one of the water molecules in the Cd system, theses distances were found to be 1.504 Å and 1.035 Å, respectively. This suggests that these water molecules are not very labile and could thus participate in the hydrolysis mechanism. From the potential surface scan, we found that for PTE/Zn(II)-Zn(II), system energy increases as the distance enzyme-substrate decreases. Contrastingly, for PTE/Cd(II)-Cd(II) we have observed an energy decrease as this distance decreases. It is therefore suggested that PTE/Cd(II)-Cd(II) catalysis is favorable over the Zn enzyme. Furthermore, for PTE/Cd(II)-Cd(II), we observed a significant decrease of distance between the water hydrogen and the hydroxyl oxygen as the substrate approaches de enzyme. At r = 4 Å, this distance is 1.66 Å, whereas at r = 2.2 Å, the distance is 1.61 Å and the hydrogen is acidic, since its charge is positive. We could not conclude the conformational analysis for the abstract submission date, but believe that it will be finished for the poster presentation. We also intend to compare the result with molecular docking. From our study, in addition to modeling the active site, which is fundamental for a more detailed mechanism investigation, we were able to analyze structural properties that support a hydrolysis catalysis mechanism in which there is participation of the coordinated water molecule.

**Key-words**: Organophosphates, Phosphate Triesters, Reaction Mechanisms
**Support:** This work has been supported by CNPq, FAPEMIG, INCT Catálise
**References:**

[1] S. L. Chen, W. H. Fang, F. Himo. “Theoretical Study of the Phosphotriesterase Reaction Mechanism”. J. Phys. Chem. B, Vol. 111, No. 6, 2007.
[2] K. Y. Wong, J. Gao. “The Reaction Mechanism of Paraoxon Hydrolysis by Phosphotriesterase from Combined QM/MM Simulations”. Biochemistry, Vol. 46, No. 46, 2007.

# Theoretical calculations on the OSiS molecule and its interstellar relevance

Authors: Mateus A. M. Paiva and Breno R. L. Galvão

*Address: Departamento de Química, Centro Federal de Educação Tecnológica de Minas Gerais, CEFET-MG, Av. Amazonas 5253, (30421-169) Belo Horizonte, Minas Gerais, Brazil.*

**Abstract:**

One of the most abundant elements in the universe is silicon, and several studies have already been performed on their silicate forms. Nevertheless, few species with the SiO bond have been detected in the interstellar space [1][2]. Recently, spectroscopic techniques have detected SiS in some interstellar clouds, and SiO in minor amounts. These two diatomic molecules can be related to a depletion of silicon atoms in interstellar clouds, a fact that needs explanation and possibly is linked to formation of derivative compounds like OSiS and SiOS [1][3].

OSiS was first observed in 1981, consisting of silicon bound to one atom of oxygen and sulfur. This molecule is very little studied and can present information to create a mechanism for explaining how SiS exists in the interstellar environment and if it can evolve to SiO. Some recent publications have shown that OSiS molecule may be observed in interstellar clouds and may be a target for promising studies on stability patterns and chemical kinetics of formation of molecules in space [4] [5].

The goal of this work is to perform a theoretical study of OSiS molecule and its isomers, analysing its stability and kinetics of formation in space. For this purpose, we performed calculations in the MOLPRO package at CASSCF and MRCI level with quadruple zetta Dunning-type basis set.

The first results confirm the existence of the linear OSiS molecule as a global minimum, with inter-atomic distances for the singlet state of 1.508 and 1.907 angstrom for silicon-bound oxygen and sulfur respectively. These distances are close to the values found in the literature employing less accurate methods [4][5]. Several singlet excited eletronic states were also calculated and analysed.

The results for the triplet state showed transition states for both SiS+O reation (250 kJ . $mol^{-1}$) and SiO+S (50 kJ . $mol^{-1}$) and a non linear SSiO structure, with SiO bond length of 1.531 angstrom SiS of 2.136 angstrom and angle of 120.9 degrees. The calculations showed that the triplet state is the most probable path for the S+SiO → SSi + O reation. We have verified the existence of a singlet-triplet crossing that may be relevant for the dynamics, and futher calculations are being performed.

Calculations for the constitutional isomers were also performed showing stability patterns for the SiOS molecule with oxygen between silicon and sulfur atom. In the case of these isomers the molecules are not as stable as OSiS, but are possible to form at more energetic conditions.

**Key-words**: Interstellar, SSiO, silicon, ab initio.
**Support:** This work has been supported by FAPEMIG and CNPq

**References:**

[1] U. Haris, V. S. Parvathi, S. B. Gudennavar, S. G. Bubbly, J. Murthy, x U. J. Murthy. Silicon depletion in the interstellar medium. *The Astronomical Journal*, *151*(6), 143. (2016)
[2] S. T. Zeegers, E. Costantini, C. P. de Vries, A. G. G. M. Tielens, H. Chihara, F. de Groot, S. Zeidler. Absorption and scattering by interstellar dust in the silicon K-edge of GX 5-1. *Astronomy & Astrophysics*, *599*, A117. (2017)
[3] J. L. Edwards, L. M. Ziurys. Sulfur-and silicon-bearing molecules in planetary nebulae: The case of M2-48. *The Astrophysical Journal Letters*, *794*(2), L27. (2014)
[4] S. Thorwirth, L. A. Mück, J. Gauss, F. Tamassia, V. Lattanzi, M. C McCarthy. Silicon Oxysulfide, OSiS: Rotational Spectrum, Quantum-Chemical Calculations, and Equilibrium Structure. *The journal of physical chemistry letters*, *2*(11), 1228-1231 (2011).
[5] Y. T. Liu, X. Wang, X. Y. Liu, X. P. Li, Y. Q Ji. Theoretical studies on structure, isomerization, and stability of [Si, O, S]. *Chemical Research in Chinese Universities*, *29*(2), 351-354. (2013).

# Comparing structure and dynamics of solvation of different iron oxide phases for enhanced MR imaging

Mateus A. Gonçalves (PG)[a], Mozarte Santos Santana (PG)[a], Lizandro S. Santos[b], Fernando C. Peixoto[b], Teodorico C. Ramalho (PQ)[a]

[a]*Departamento de Química, Universidade Federal de Lavras, Lavras, Minas Gerais, Brasil.*
[b]*Department of Chemical and Petroleum Engineering, Federal University Fluminense, Niterói, Rio de Janeiro, Brasil.*

**Abstract:** Cancer is a global epidemic that significantly affects all ages and socioeconomic groups[1]. One of the great difficulties of cancer is its diagnosis, mainly in the initial phase. Currently, the most used and effective technique for cancer diagnosis is Magnetic Resonance Imaging (MRI)[2]. For a better visualization of MRI images, it is necessary to use contrast agents (CAs). The CAs are paramagnetic compounds which increase image contrast by preferentially influencing $T_1$ and/or $T_2$ relaxation times of water molecules in the vicinity of their compounds[3]. Currently, the CAs most used as MRI probes are gadolinium ($Gd^{3+}$) complexes; despite being very effective, they are very toxic to the body, even in small concentrations. Thus, less toxic and more efficient CAs able to substitute $Gd^{3+}$ complexes have been studied. The SPIONs (superparamagnetic iron oxide nanoparticles) have been investigated as novel contrast agents in MRI, due to a combination of favorable superparamagnetic properties[4]. Following this line, the aim of this study is to analyze water coordinates in the face 100 of different phases of iron oxides (δ-FeOOH, α-FeOOH, $Fe_2O_3$, $Fe_3O_4$), in order to replace $Gd^{3+}$ complexes. For this purpose, calculations of molecular dynamics (MD) with the FEOCH force field, were performed and the main conformations were selected using the OWSCA method[5] for subsequent quantum calculations of the hyperfine coupling constant ($A_{iso}$). The $A_{iso}$ calculations were performed using the Gaussian 09 program[6]; functional PBE1PBE with the basis set aug-cc-pVTZ-J was used for oxygen and hydrogen atoms, and Lanl2dz for iron atoms for all structures. The results show a large increase in $A_{iso}$ values. This increase in $A_{iso}$ values was mainly due to the H bonds between water molecules and between water molecules and the oxides; this fact was proven by QTAIM and NCI calculations. At last, we strongly affirm that all the iron oxides studied are great candidates as promising ACs in MRI.

**Key-words**: MRI, Contrast Agents, Iron Oxide, SPIONs, OWSCA

**Support:** The authors thank the Brazilian agencies FAPEMIG, CAPES, and CNPq for the financial support of this research the UFLA and UFF for infrastructure and encouragement in this work.

**References:**

[1] V. L. De Almeida, A. Leitão, C. Barrett, C. Alberto and C. Luis, *Quim. Nova*, **2005**, 28, 118–129.
[2] J. Y. et al LI, Spectrochim. Acta Part A Mol. Biomol. Spectrosc. **2013**, 102, 66–70.
[3] S. J. Dorazio and J. R. Morrow, *Eur. J. Inorg. Chem.* **2012**, 2006–2014.
[4] S. Yoffe, T. Leshuk, P. Everett and F. Gu, *Current Pharmaceutical Design*. **2013**, 19, 493–509.
[4] M. A. Gonçalves, F. C. Peixoto, E. F. F. da Cunha and T. C. Ramalho, *Chem. Phys. Lett.,* **2014**, 609, 88–92.
[5] Frisch MJ, Trucks GW, Schlegel HB et al, Gaussian 09